Life history of rays (Batoidea), intrinsic sensitivity to fishing, and implications for conservation and management

A thesis submitted by

Ellen Barrowclift-Mahon

for the award of Doctor of Philosophy (PhD)



School of Natural and Environmental Sciences

Newcastle University

August 2024

Abstract

Rays (Superorder Batoidea) are overfished through targeted and incidental catch in industrial and small-scale fisheries. Rays are important components of healthy marine ecosystems and as sources of income and protein for global fishing communities, particularly in small-scale fisheries. The interlinked need to conserve these species and support the livelihoods dependent on fisheries is a major global challenge. This thesis aims to investigate the intrinsic sensitivity of rays to fishing mortality to inform species status and fisheries stock assessments. The thesis first investigates the biological traits and indicators of fishing exposure that best predict species extinction risk in pelagic rays (Families Myliobatidae, Aetobatidae, Rhinopteridae, and Mobulidae, and *Pteroplatytrygon violacea*) using ordinal regression models. The analyses revealed that species with larger geographic ranges and greater exposure to small-scale fishing pressure in tropical, coastal waters were more likely to be threatened. Thereby, highlighting the need for coordinated, transnational management action, with focus on small-scale fisheries. Next, the thesis investigates global patterns in the intrinsic sensitivity of 85 ray species using a multi-model, information-theoretic approach. It was found that tropical rays (Orders Torpediniformes, Rhinopristiformes, and Myliobatiformes) were more intrinsically sensitive (lower maximum intrinsic rate of population increase, r_{max}) to overfishing compared to temperate skates (Order Rajiformes). This result contrasts the expectation from metabolic theory that species in warmer waters have faster metabolism and life histories (grow faster, mature earlier, have shorter generation times, and higher r_{max}) and therefore are more resilient to fishing. It was found that the larger absolute offspring size of live-bearing, tropical rays likely explained the lower r_{max} compared to egg-laying skates with relatively small but more numerous offspring. For many ray species, the life history data needed to inform demographic and stock assessment models are lacking. To fill this data gap for two Endangered devil rays, Mobula mobular and M. thurstoni, age estimates were generated using caudal vertebrae of individuals caught in small-scale fisheries in Indonesia and Pakistan. A Bayesian approach was used to calculate key life history parameters using the resulting age-at-length dataset. The results indicated that both species have relatively low somatic and population growth rates and that calculated fishing mortalities are likely unsustainable. In summary, the thesis provides an approach for assessment of data-poor species and presents new information highlighting the nuanced complexities of species vulnerability to fishing. The results inform much needed conservation and management actions to prevent further ray species extirpation and extinction.

Acknowledgements

I would first like to thank my primary supervisor, Prof. Per Berggren, for the continued support and guidance from undergraduate to this PhD thesis. I am truly grateful for all the exciting research I have been involved with and the opportunities that have arisen. I would further like to thank external supervisors and mentors Prof. Nick Dulvy, Prof. Rus Hoelzel, Dr Andrew Temple, and my second supervisor Prof. John Bythell as well as Dr Jennifer Bigman and Dr Sebastián Pardo for their valuable insight. I would also like to thank the examiners Dr Theresa Rueger and Dr Alec Moore for constructive discussions and suggestions. This thesis has greatly benefitted from the additional perspectives and support.

The project would not have been possible without the support and expertise of the following collaborators: Dr Alexander Khan at Padjadjaran University in Indonesia, Shoaib Abdul Razzaque and Umair Shahid at WWF Pakistan, Dr Nina Wambiji at Kenya Marine & Fisheries Research Institute, Dr Sammy Wambua at Pwani University in Kenya, and Dr Kolobe Mmonwa at KwaZulu-Natal Sharks Board in South Africa. I would also like to thank further colleagues at these institutions who facilitated data collection as well as further members of the research community who were open to collaboration even if data collection was not ultimately possible. I would also like to thank the fishers, traders, and local government officials at landing sites for supporting data and sample collection.

I would like to extend my gratitude to Dr Samuel Logan, Dr Darroch Hall, Dr Gavin Horsburgh, and Peter McParlin for the unwavering assistance when conducting laboratory work for this thesis. I would also like to thank members of the Marine MEGAfauna Lab for their assistance and collaboration throughout this PhD.

I am grateful to the NERC IAPETUS2 Doctoral Training Partnership PhD studentship that provided the opportunity to conduct this research as well as the Save Our Seas Foundation and Banyan Tree Global Foundation for supporting the project.

A final special thanks to my wonderful family and Max for their endless support throughout this PhD.

Contents

Figure list	iv
Table list	ix
List of publications	xii
Thesis overview	1
Background and rationale	1
Problem statement	2
Thesis outline	3
Chapter 1. Species trait and threat indicators of extinction risk for pelagic rays	4
1.1 Abstract	4
1.2 Introduction	4
1.3 Methods	9
1.3.1 Species trait data	9
1.3.2 Indices of threats and threat exposure	10
1.3.3 Ordinal regression models	10
1.4 Results	12
1.5 Discussion	16
Chapter 2. Global patterns of intrinsic sensitivity to fishing in rays	20
2.1 Abstract	20
2.2 Introduction	20
2.3 Methods	23
2.3.1 Collation of life history trait data and estimation of r _{max}	23
2.3.2 Body mass, depth, and temperature-at-depth data	24
$2.3.3$ How does r_{max} vary with body mass, temperature, and depth?	25
2.4 Results	31
2.5 Discussion	40

Chapter 3. Does offspring size resolve a latitudinal population growth rate para	idox in
rays and skates?	48
3.1 Abstract	48
3.2 Introduction	48
3.3 Methods	51
3.3.1 Source of life history data and calculation of r _{max}	51
3.3.2 Calculation of environmental temperature-at-depth	52
3.3.3 Statistical analyses	53
3.4 Results	54
3.5 Discussion	66
Chapter 4. Age, growth, and intrinsic sensitivity of Endangered Spinetail (A	1obula
mobular) and Bentfin devil rays (M. thurstoni) in the Indian Ocean	71
4.1 Abstract	71
4.2 Introduction	71
4.3 Methods	74
4.3.1 Sample collection and species identification	74
4.3.2 Disc width-weight relationship	76
4.3.3 Age estimation using caudal vertebrae	78
4.3.4 Estimating growth	81
4.3.5 Estimation of maximum intrinsic rate of population increase	84
4.3.6 Estimation of total mortality, fishing mortality, and the exploitation ratio	85
4.4 Results	86
4.4.1 Disc width-weight relationship	86
4.4.2 Age estimation using caudal vertebrae	89
4.4.3 Estimating growth	90
4.4.4 Estimation of maximum intrinsic rate of population increase	93

4.4.5 Estimation of total mortality, fishing mortality, and the exploitation ratio	94
4.5 Discussion	96
Chapter 5. Thesis conclusions	106
5.1 Overview	106
5.2 Administrative challenges faced and recommendations for biological sampling	108
5.3 Future research directions to inform conservation and management	111
5.4 Conclusion	114
References	115

Figure list

catch FAO (2010-2021) by reporting country (countries reporting the highest catches shown in the
legend); b) Sea Around Us (2010-2019) discarded and landed catch by country (countries reporting the highest catches shown in the legend); c) Sea Around Us total catch by species; and d) Sea Around Us
total catch by fishing sector. FAO nominal catch data were obtained using FishStatJ software (Version 4.03.06) (FAO, 2023) from the 'Global Capture Production' dataset to record total retained catch (for all fishing sectors but excludes discards) reported for any relevant taxa. Downloaded global Sea Around Us catch reconstruction data for relevant taxa (reports by fishing sector and discard data) (Pauly &
Zeller, 2015)
Figure 1.2 Available annual total fisheries catch (tonnes) statistics from the Indian Ocean Tun. Commission RFMO (2010-2022) by reporting country, with the percentage of total catch reported a artisanal indicated (remainder reported as industrial). IOTC Nominal retained catch data for all specie from the IOTC website (https://iotc.org/data/datasets) (reports by fishing sector)
Figure 1.3 Mean effect (\pm 95% confidence intervals) of SSF pressure, species range (number of countries a species occurs in), median depth, maximum size, and generation length on threat status (IUCN RecList) for top 9 models with Δ AIC <2 (n =38). The Relative Variable Importance (RVI) is shown for each variable included in the top models. Effect sizes can be considered significant when confidence intervals do not overlap zero.
Figure 1.4. The effect of a) species range (number of countries a species occurs in), b) SSF pressure and c) median depth (m) on the probability a pelagic ray species (n =38) is listed as Critically Endangered (CR, red) Endangered (EN, orange), Vulnerable (VU, yellow), Near Threatened (NT, light green), of Least Concern (LC, dark green) from the top (a and b) and third (c) ordinal regression models. The percentage of species threatened (CR, EN, and VU) is indicated at the end of each bar
Figure 1.5. a) Species geographic range (number of countries a species occurs in), b) small-scale fishing (SSF) pressure, and c) median depth (m) for threatened (IUCN Red List statuses of Critically Endangered, Endangered, and Vulnerable) (n =32) and not threatened (Near Threatened and Leas Concern) (n =6) pelagic ray species with black dots showing the median (\pm standard error and outliers)

and 97.5% quantiles. A single phylogenetic tree from the possible distribution of trees from Stein, Mull,
et al., (2018) is displayed
Figure 2.2 Phylogeny, maximum intrinsic rate of population increase (r_{max}), maximum weight (kg), median depth (m) and median temperature (°C) in log10 space for 85 ray and skate species. Solid lines show median values for Myliobatiformes (n =32), Rhinopristiformes (n =16), Torpediniformes (n =5) and Rajiformes (n =32). A single phylogenetic tree from the possible distribution of trees from Stein, Mull et al., (2018) is displayed
Figure 2.3 Coefficient estimates for the six models of $ln(r_{max})$ with AICc values < 2. Error bars show 95% confidence intervals. Effect sizes were considered significant when confidence intervals do not overlap zero. Shaded area shows the expected effect sizes for body mass (-0.33 to -0.25) and temperature (-1.0 to -0.6) based on metabolic theory.
Figure 2.4 Relationship between maximum intrinsic rate of population increase (r_{max}) and a) temperature (°C) and b) depth (m) in log10 space for 53 ray (Orders Myliobatiformes, Rhinopristiformes, and Torpediniformes) and 32 skate (Order Rajiformes) species. a) Median depth (m) is shown by the point size, with a linear model fitted to ray (red) and skate (blue) points. b) Median temperature (°C) and maximum weight (kg) is shown by the point colours and size, respectively, with a linear model fitted to ray (circular) and skate (triangular) data points. The grey band around the fitted models show the confidence intervals.
Figure 2.5 Relationship between maximum intrinsic rate of population increase (r_{max}) and body mass in log10 space for 85 ray species. Fitted lines show predicted relationships based on the top-ranked models: a) $\ln(r_{max}) \sim \ln(M) + (1/k_BT)$ and b) $\ln(r_{max}) \sim \ln(M) + \text{depth}$. Predicted allometric changes of r_{max} across a) median temperatures (6, 10, 20 °C) and b) median depths (10, 500, 1000 m). Median temperature and depth are shown by the point colour and size, respectively
Figure 2.6 Relationship between maximum intrinsic rate of population increase (r_{max}) and body mass in log10 space for 53 ray species (Orders Myliobatiformes, Rhinopristiformes, and Torpediniformes) and 32 skate species (Order Rajiformes). Fitted lines show predicted relationships based on the top-ranked model: $\ln(r_{max}) \sim \ln(M)$ + temperature-depth index + Order. Predicted allometric changes of r_{max} across constant temperature-depth index (PC1 = 1) for ray (red) and skate (blue) data points
Figure 3.1 Coefficient plot showing the effect sizes for offspring body mass ($M_{offspring}$), adult body mass (M), and inverse temperature ($1/k_BT$) on r_{max} in the top three models. Error bars show the 95% confidence intervals and effect sizes are considered significant when confidence intervals do not overlap zero. The grey boxes show the expected effect size for adult body mass (-0.33 to -0.25) and temperature (-1.0 to -0.01) and the property of the size of
0.6) based on metabolic theory

Figure 3.2 Relationship between maximum intrinsic rate of population increase (max) and a) offspring
body mass (g) and b) adult body mass (g) in $log10$ space for 85 ray ($n=53$, red points) and skate ($n=32$)
blue points) species. Fitted lines show the predicted relationships for the top model: $\ln(r_{\text{max}}) \sim \ln(M)$
$\ln(M_{offspring}) + 1/k_BT$, where M is adult body mass, $M_{offspring}$ is offspring body mass, and $1/k_BT$ is inverse temperature, across (a) three temperatures (6, 10, 20°C) with fixed median adult body mass and (b) three median offspring body masses (small, skates; medium, all species; large; rays) with fixed temperature
(10°C). (a) Adult body mass (g) and (b) offspring body mass (g) are shown by the point size. Fitting the
top model across different median adult weights (e.g. small, skates; medium, all species; large; rays
does not change the fitted relationship.
Figure 3.3 Relationship between offspring body mass (g) and a) adult body mass (g) and b) median annual fecundity in $log10$ space for 85 species of ray ($n=53$, red points) and skate ($n=32$, blue points) (a) Median annual fecundity and (b) adult body mass (g) are shown by the point size
Figure 3.4 Phylogeny, maximum intrinsic rate of population increase (r_{max}), adult and offspring body mass (g), and adult:offspring size ratio in log10 space for 85 ray (n =53, red points) and skate (n =32 blue points) species. Solid lines show median values. Uncertainty in r_{max} estimate shown with 2.5% and 97.5% quantiles. Phylogenetic tree from Stein, Mull et al., (2018) (available on Vertlife.org) with binomial nomenclature updated to reflect current taxonomic nomenclature
Figure 3.5 Relationship between temperature (°C) and a) offspring body mass (g) and b) adult body mass (g) in log space for 85 ray (n =53, indicated by red points) and skate (n =32, indicated by blue points) species. Median depth of occurrence (m) is shown by the point size, with a linear model fitted to ray and skate data points. The grey bands around the fitted models show the confidence intervals.
Figure 3.6 Relationship between adult:offspring size ratio (g) and adult body mass (g) in $\log 10$ space for 85 ray (n =53, indicated by red points) and skate (n =32, indicated by blue points) species. The gree bands around the fitted models show the confidence intervals and grey dashed lines show adult:offspring size ratios of 1 to 4 where offspring size is 10 to 0.01% of adult body mass, respectively
Figure 4.1 Sampling locations for <i>Mobula mobular</i> , <i>M. thurstoni</i> , and <i>M. tarapacana</i> across the Indian Ocean (<i>n</i> =195)
Figure 4.2 The two main species sampled in this study: a) Spinetail devil ray (<i>Mobula mobular</i>) and b Bentfin devil ray (<i>M. thurstoni</i>)
Figure 4.3 Preparation of <i>Mobula</i> spp. vertebrae sections for age determination including: a) portion of the vertebral column where caudal vertebrae samples were taken; b) embedded vertebrae centra in an epoxy resin in silicon moulds; c) longitudinal sectioning of set vertebrae centra using a Buehler IsoMe Low-Speed Diamond Blade Saw fit with two 4 inch blades and a 3.5 inch 0.5mm plastic separator; and d) imaging of vertebrae sections for age determination using an Optika dissecting microscope with a

fitted camera, illuminated from above using reflected light and from either side using a double-armed
fibre optic light source
Figure 4.4 Images of a) <i>Mobula mobular</i> and b) <i>M. thurstoni</i> vertebrae sections for age determination
using an Optika dissecting microscope with a fitted camera, illuminated from above using reflected light
and from either side using a double-armed fibre optic light source, and enhanced in Adobe Photoshop
Elements 2021 Photo Editor (Version: 19.0), annotated with birth line and annual growth bands. The
imaged sections are from a) a male M. mobular aged as 8 years and b) a male M. thurstoni aged as 5
years caught in a small-scale gillnet fishery in Cilacap, Central Java, Indonesia between September-
October 2020
Figure 4.5 Disc width (cm) frequency distribution for a) Spinetail devil ray (M . $mobular$) ($n=103$) and
b) Bentfin devil ray ($M.\ thurstoni$) (n =89) sampled from Indonesia (n =112), Kenya (n =43), and Pakistan
(n=37) with known female (orange dashed) and male (green dashed) minimum size at maturity;
$minimum\ offspring\ size\ and\ maximum\ size\ (black\ dotted\ lines)\ for\ each\ species\ indicated\ (IUCN,\ 2023).$
Figure 4.6 Natural log-transformed disc width (cm) and weight (kg) Bayesian linear relationship (with
95% credible intervals) for female (orange) and male (green) a) Spinetail devil ray ($M.\ mobular$)
(<i>n</i> =101) and b) Bentfin devil ray (<i>M. thurstoni</i>) (<i>n</i> =76)
Figure 4.7 Bland-Altman analyses of agreement, precision, and bias in age estimates (year \pm 0.5) within
and between readers for 1) Spinetail devil ray ($M.\ mobular$) ($n=79$) and 2) Bentfin devil ray ($M.\ mobular$)
thurstoni) ($n=59$). Plots show the relationship between: vertebrae age band counts for a) reader 1 and c)
reader 2 and between e) mean vertebrae age band counts from readers 1 and 2. b) Bland-Altman plots
display bias and precision between vertebrae age band counts for b) reader 1 and d) reader 2 and between
f) mean vertebrae age band counts from readers 1 and 2
Figure 4.8 Bayesian von Bertalanffy (purples), Gompertz (blues), and logistic (reds) growth curves
describing the disc width and age (nearest year) relationship for a) combined female $(n=41)$ and male
$(n=38)$ Spinetail devil ray $(M.\ mobular)$ $(n=79)$ and b) combined female $(n=29)$ and male $(n=30)$ Bentfin
devil ray ($M.\ thurstoni$) ($n=59$) length-at-age data from individuals sampled in Indonesia (circles) and
Pakistan (triangles). The top model for each species is shown with a solid line with 95% credible
intervals shown with solid black lines. Remaining models are shown with dashed lines. Dotted lines
show the asymptotic size (DW_∞) estimate for the top model, the maximum observed size for the species
(black) and the maximum observed size in this study (brown)
Figure 4.9 Comparison between length-at-age estimates determined from Bayesian (purple) and
frequentist (green) von Bertalanffy growth models, with 95% credible intervals and 95% confidence

intervals, respectively, for combined female $(n=41)$ and male $(n=38)$ Spinetail devil ray $(M. mobular)$ $(n=79)$
Figure 4.10 Posterior (black lines) and prior (red lines) distributions for von Bertalanffy growth parameters (k, DW_{∞}) , and DW_{0} , the hyperprior $kappa$, and the error term (σ^{2}) for three Bayesian models (von Bertalanffy, Gompertz, and Logistic) with strong and weaker priors fitted to a) Spinetail devil ray (<i>Mobula mobular</i>) and b) Bentfin devil ray (<i>M. thurstoni</i>) disc width-at-age data. Dashed lines show mean values and mean k and DW_{∞} , indicated on each plot.
Figure 4.11 Posterior distribution for von Bertalanffy growth parameters a) k and b) DW_{∞} for Bayesian models with strong priors fitted to Indian Ocean M . $mobular$ disc width-at-age data from this study using samples from Indonesia (blue) and Pakistan (black) and previous studies using samples from Mexico (red) (Cuevas-Zimbrón et al. 2013; Pardo, Kindsvater, Cuevas-Zimbrón, et al., 2016)
Figure 4.12 Bayesian logistic regression with strong priors describing the relationship between a) age $(n=56)$ and b) disc width $(n=73)$ and maturity status for M. mobular with 95% Credible Intervals. Age and disc width at 50% maturity (with 95% Credible Intervals) are shown with dashed lines
Figure 4.13 Distribution of estimated maximum intrinsic population growth rate (r_{max}) and exploitation ratio (E) for M . mobular (a and b, respectively) and M . thurstoni (c and d, respectively). Dashed lines show median values
Figure 4.14 Chapman-Robson catch curve for a) Spinetail devil ray ($Mobula\ mobular$) (n =103) and b) Bentfin devil ray ($M.\ thurstoni$) (n =89) from Indian Ocean small-scale fisheries. Age class for full recruitment to the fishery was 3 and 2 years, respectively, and catch curve regression lines between ages 4 to 18 and 3 to 13, respectively. Total mortality Z indicated
Figure 5.1 Timeline (October 2019 – 2023) of administrative tasks and challenges encountered during biological sampling (vertebrae and muscle tissue - genetic resources) of Indian Ocean <i>Mobula</i> spp. (listed on CITES Appendix II) from fisheries catch through a network of international Project Collaborators (PCs) in order to investigate life history and population structure. A conservative estimate
of 720 emails were sent over the four-year duration, with the estimated number of emails sent for each step of the process indicated by envelope icons. From eight initial PCs, biological samples were eventually received from four PCs and countries (Indonesia, Kenya, Pakistan, and South Africa). Acronyms include MoU (Memorandum of Understanding), MTA (Material Transfer Agreement), PIC
(Prior Informed Consent), and MAT (Mutually Agreed Terms)

Table list

Table 1.1 Comparison of 24 of 48 candidate models with Δ AIC <10 using Akaike Information Criteria (AIC), difference in AIC from the top model (Δ AIC), and Akaike weights. Models are ordered by ascending AIC, with the top model shown in bold and models with AIC <2 shown in grey
Table 2.1 The 24 models examined with associated hypotheses for how maximum intrinsic rate of copulation increase (r_{max}) varies with body mass M , inverse temperature (1/ k_BT). depth and a composite temperature-depth index. The expected model from metabolic scaling theory is highlighted in grey. Note, Order was categorical for rays (Orders Myliobatiformes, Rhinopristiformes, and Torpediniformes) and skates (Order Rajiformes)
Γable 2.2 Corrected Akaike Information Criteria (Δ AICc) for the 24 models tested for how r_{max} varies with inverse temperature (1/ k_BT), depth, adult body mass (M), the temperature-depth index, and Order, with 20 different phylogenetic trees obtained from Stein, Mull $et~al.$ (2018). The model with the lowest Δ AICc value in each iteration is highlighted in grey.
Γable 2.3 Comparison of $\ln(r_{\text{max}})$ models re-ran with data points for eight larger-bodied rays (body mass $M \ge 290 \text{ kg}$) removed, using corrected Akaike Information Criteria (AICc), number of parameters (n), negative log-likelihood (-LL), adjusted R^2 (Adj. R^2) and Akaike weights. The model with the lowest ΔAICc value is marked in bold and models with ΔAICc ≤ 2 are highlighted in grey. Models are ordered by ascending AICc, with the top model first
Table 2.4 Comparison of r_{max} models using corrected Akaike Information Criteria (AICc), number of parameters (n), negative log-likelihood (-LL), adjusted R^2 (Adj. R^2), and Akaike weights. Models are ordered by ascending AICc, with the top model highlighted in bold and models with Δ AICc < 2 nighlighted in grey.
Table 2.5 Coefficient estimates (95% confidence intervals estimated from standard errors shown in brackets) for all models of $\ln(r_{\text{max}})$. The model with the lowest ΔAICc value is marked in bold and the models with $\Delta \text{AIC} < 2$ are highlighted in grey. Pagel's λ indicates the strength of the phylogenetic signal.
Γable 3.1 All 30 models tested with associated hypotheses for how maximum intrinsic rate of population ncrease (r_{max}) varies with adult body mass M , offspring body mass $M_{\text{offspring}}$, inverse temperature $1/k_BT$, depth, and a temperature-depth index (PC1 axis from Principle Components Analysis of collapsed temperature and depth data in Barrowclift et al. (2023). Comparison of 30 ln(r_{max}) models using

for rays (Orders Myliobatiformes, Rhinopristiformes, and Torpediniformes) and skates (Order Rajiformes).
Table 3.2 The 14 models examined with associated hypotheses for how maximum intrinsic rate of population increase (r_{max}) varies with adult body mass M , inverse temperature $1/k_BT$, depth. Comparison of models using corrected Akaike Information Criteria (AICc), number of parameters (n), negative log-likelihood (-LL), adjusted R^2 , difference in AICc from the top model (Δ AICc), and Akaike weights. Models are ordered by ascending AICc, with models with AICc < 2 shown in bold
Table 3.3 Comparison of 14 $\ln(r_{\text{max}})$ models fitted with 10 different phylogenetic trees obtained from Stein, Mull et al., (2018) (available on Vertlife.org) using corrected Akaike Information Criteria (AICc). The model with lowest AICc for each iteration is shown in bold.
Table 3.4 Comparison of 14 $\ln(r_{\text{max}})$ models fitted without data for two manta ray species (<i>Mobula alfredi</i> and <i>M. birostris</i>) with largest offspring sizes using corrected Akaike Information Criteria (AICc) number of parameters (n), negative log-likelihood (-LL), R^2 , adjusted R^2 (Adj. R^2), difference in AICc from the top model (Δ AICc), and Akaike weights. Models are ordered by ascending AICc, with models with AICc < 2 shown in bold.
Table 3.5 Coefficient estimates (95% confidence intervals estimated from standard errors shown in brackets) for all models of $ln(r_{max})$. The model with the lowest $\Delta AICc$ value is marked in bold and models with $\Delta AICc < 2$ are highlighted in grey. Pagel's λ indicates the strength of the phylogenetic signal.
Table 4.1 Strong and weaker priors used for each parameter in Bayesian length-weight regression growth models, and length-maturity regression models for <i>Mobula mobular</i> $(n=79)$ and <i>M. thurston</i> $(n=59)$
Table 4.2 Age frequency for sampled <i>Mobula mobular</i> (<i>n</i> =79) and <i>M. thurstoni</i> (<i>n</i> =59) by location, sex and month.
Table 4.3 Mean estimates (95% Credible Intervals) of Bayesian length-weight regression, growth models, and length-maturity regression models using strong and weaker priors for <i>Mobula mobular</i> $(n=79)$ and M . thurstoni $(n=59)$.
Table 4.4 Estimates of ageing agreement, precision, and bias in age reads for <i>Mobula mobular</i> (n =79) and <i>M. thurstoni</i> (n =59) within and between two readers: Average Percent Error (APE), Coefficient of Variation (CV), Percent Agreement (PA), PA ±1 year, and Bland-Altman Limits of Agreement (LOA)

Table 4.5 'Leave One Out' cross validation Information Criterion (LOOIC) and LOOIC	standard error
(se) for growth model analyses for Mobula mobular and M. thurstoni. The best model w	vith the lowest
LOOIC and largest weight for each species is shown in bold	91

List of publications

Some of the work described in this thesis has been presented in the following publications:

Publications:

Thesis Chapter 2

Barrowclift, E., Gravel, S.M., Pardo, S.A., Bigman, J.S., Berggren, P., Dulvy, N.K., 2023. Tropical rays are intrinsically more sensitive to overfishing than the temperate skates. Biological Conservation: https://doi.org/10.1016/j.biocon.2023.110003.

Thesis Chapter 3

Barrowclift, E., Bigman, J.S., Digel, E.D., Berggren, P., Dulvy, N.K., 2024. Offspring size resolves a latitudinal population growth rate paradox in rays and skates. bioRxiv preprint available: https://doi.org/10.1101/2024.01.02.573919.

Data/code availability:

The following dataset was compiled to support analyses in Thesis Chapters 2 and 3 and made publicly available at FigShare (https://doi.org/10.6084/m9.figshare.20182109). The code to reproduce the analyses of these chapters in R are available at Github (https://github.com/EBarrowclift/batoid-rmax-scaling and https://github.com/EBarrowclift/batoid-rmax-offspring-379 scaling).

Thesis overview

Background and rationale

Over one-third of rays (Class Chondrichthyes, Superorder Batoidea), along with their close cartilaginous relatives sharks, are threatened with extinction by overfishing (Dulvy et al., 2014, 2021). Increased fishing mortality is the primary cause of declining ray and shark populations across marine ecosystems, including open ocean (Pacoureau et al., 2021), coral reefs (Sherman et al., 2023), and deep seas (Finucci et al., 2024). Rays, like sharks, play important roles in marine ecosystems as mesopredators (Navia et al., 2017; Vaudo & Heithaus, 2011; Dean et al., 2017), bioturbators (O'Shea et al., 2011; Takeuchi & Tamaki, 2014; Kiszka et al., 2015), and by providing energetic links across trophic levels and habitats (Martins et al., 2018; Sheaves, 2009; Ajemian & Powers, 2014). The decline of rays and sharks can therefore have complex ecosystem effects such as through predator-prey interactions and competition (Valinassab et al., 2006; Ward & Myers, 2005; Sherman et al., 2020). Rays are commercially valued as food and traditional medicines, primarily harvested for meat and fins (shark-like rays including wedgefishes, guitarfishes, and sawfishes) but are also utilised for other products such as gill plates (Mobula spp. used for traditional medicines in Asia), skin (used as leather), cartilage (medicinal), and liver oil (pharmaceutical) (Dulvy et al., 2017; O'Malley et al., 2017; Dent & Clarke, 2015). In addition to target fisheries (Sheaves, 2009; Ajemian & Powers, 2014; Martins et al., 2018), the commercial value means that rays are often retained as valuable bycatch in non-target fisheries (Gupta et al., 2020; Barrowclift et al., 2017; Haque et al., 2021). Therefore, declining ray populations also have implications for livelihood and food security, particularly where caught in small-scale fisheries (SSF) in developing countries (Catarci, 2004; Temple et al., 2024; Moore et al., 2019).

SSF catch has typically been understudied relative to industrial fisheries (Zeller et al., 2006; Berkes et al., 2001). It is difficult to accurately determine SSF contribution to global catch from official statistics, with SSF landings aggregated with industrial fisheries in national reporting to the FAO (Chuenpagdee et al., 2006; Salas et al., 2007; Béné, 2006). However, reconstruction of SSF catch data have been estimated to contribute up to one third of global marine fisheries catch (Belhabib et al., 2018; Chuenpagdee et al., 2006; Alfaro-Shigueto et al., 2010), employ over 75% of the world's fishers, and provide an important source of protein for millions of people, primarily in developing countries (Béné, 2006; Béné et al., 2012; Berkes et al., 2001; McGoodwin, 2001). Small-scale fishers have less capacity to adapt to declining catches,

exacerbating concerns for the consequences for income and food security (Cinner et al., 2009; Allison et al., 2009; Béné, 2009; Short et al., 2021). As well as underreporting of ray and shark catch in official statistics (Clarke, McAllister, et al., 2006; Worm et al., 2013), catch is often aggregated at a low taxonomic resolution (Catarci, 2004) and ray catch is particularly underestimated as shark-like rays are often grouped with sharks (Last et al., 2016), making it difficult to get a clear picture of species catch composition. Therefore, improved data collection, further research, and evidence-based management efforts need to be prioritised for SSF (Smith et al., 2021; Belhabib et al., 2018) to improve conservation and management of rays.

Rays and sharks are particularly vulnerable to overfishing due to their typical life history strategies resulting in slow growth, late maturity, low fecundity, and long lifespans (Hutchings et al., 2012; Cortés, 2000). However, there is considerable diversity in their life history, both among (Conrath & Musick, 2012; Cortés, 2000) and within species (Trinnie et al., 2014; Jacobsen & Bennett, 2010; Lombardi-Carlson et al., 2003). Life history data, alongside fisheries exploitation data, are used in fisheries stock assessments (Cortés, Brooks and Gedamke, 2012), demographic modelling (Cortés, 2002; Smith et al., 2008), setting fishing limit reference points (Zhou et al., 2021), predicting rebound potential (Smith et al., 1998), and fisheries exploitation risk assessment (Hobday et al., 2011). Understanding species' life history is therefore key to informing sustainable fisheries management and conservation actions (Kindsvater et al., 2016). Rays are capable of supporting sustainable fishing with enforced science-based limits (Dulvy et al., 2017; Simpfendorfer & Dulvy, 2017). Whilst some data gaps in ray biology and ecology have been filled, as demonstrated by a reduction in species listed as Data Deficient on the IUCN Red List (Dulvy et al., 2014; 2021), data paucity still limits status assessments for many species. Data-poor approaches using available understanding of life history traits (Cortés & Brooks, 2018; Kindsvater et al., 2016) as well as generation of species- and population-specific life history data (Salvador et al., 2022) are therefore needed to facilitate management to prevent further species extirpation and extinction.

Problem statement

The interlinked ecological and socio-economic importance of rays presents a major global challenge of balancing the need for healthy marine ecosystems and food security. Rays are the most diverse group of chondrichthyans (Aschliman et al., 2012); therefore, understanding differences in species vulnerability to fishing is important for prioritising and tailoring global conservation and management efforts. Many rays are lacking basic life history information that

is crucial for assessing fisheries sustainability, setting fishing limits, and predicting rebound potentials.

This thesis aims to investigate predictors of extinction risk and global patterns in intrinsic sensitivity of rays as well as address data gaps in life history parameters for some of the potentially least productive and highly threatened species: devil rays (*Mobula* spp.).

Thesis outline

The objective of Chapter 1 is to investigate which indicators of intrinsic sensitivity (species biological traits of body size and generation length) and extrinsic exposure to fishing (number of countries within a species' geographic range, depth occurrence, small-scale and industrial fishing pressure) that best predict the threat of extinction (defined as IUCN Red List of Threatened Species statuses of Vulnerable, Endangered, and Critically Endangered) for rays with a pelagic lifestyle.

In Chapter 2, the first objective is to calculate the maximum intrinsic rate of population increase (r_{max}) as an indicator of intrinsic sensitivity for ray species where sufficient life history data were available. The second objective of Chapter 2 is to examine how these r_{max} estimates vary with body mass, temperature, and depth whilst accounting for phylogenetic relationships to inform the understanding of geographic patterns in extinction risk and setting the foundations for predicting extinction risk for data-poor species.

The objective of Chapter 3 is to further investigate observed differences in r_{max} between rays with different life history strategies (live-bearers and egg-layers) using offspring size to explore global patterns in life histories and implications for species vulnerabilities.

In Chapter 4, the objectives are to determine key life history parameters, including age, growth, age at maturity, and r_{max} , and to estimate fishing mortality for two species of Endangered devil rays ($Mobula\ mobular\$ and $M.\ thurstoni$) to inform status assessment of the two species in the Indian Ocean.

Finally, a reflection of the key findings of this thesis is provided in Chapter 5 along with recommendations for future international collaborative research efforts to inform conservation and management of rays.

Chapter 1. Species trait and threat indicators of extinction risk for pelagic rays

1.1 Abstract

Overfishing is the primary driver of ray (Superorder Batoidea) decline, with species facing a higher threat in tropical, coastal waters. This study uses ordinal logistic regression models to investigate which key indicators of intrinsic sensitivity (species biological traits of body size and generation length) and extrinsic exposure to fishing (number of countries within a species' geographic range, depth occurrence, small-scale and industrial fishing pressure) best predict threat of extinction (defined as IUCN Red List of Threatened Species statuses Vulnerable, Endangered, and Critically Endangered) for 38 pelagic and bentho-pelagic rays (Families Myliobatidae, Aetobatidae, Rhinopteridae, and Mobulidae, and Pteroplatytrygon violacea). The top model is then used to predict the probability of extinction for two Data Deficient species. Species with larger geographic range, greater exposure to small-scale fishing pressure, and occurring at shallower depths had a higher probability of being threatened with extinction. Small-scale fishing pressure was more important in predicting extinction risk than industrial fishing pressure for pelagic rays. Indicators of species intrinsic sensitivity were less important than indicators of extrinsic exposure to fishing in determining extinction risk, in contrast to chondrichthyans more broadly. Many pelagic ray species are already threatened by overfishing; well-enforced, science-based fisheries management is needed across nations to prevent further decline, species extirpation and extinction, and to ensure sustainable fisheries.

1.2 Introduction

Approximately 35% of rays (Superorder Batoidea) are threatened with extinction (IUCN, 2024). Fishing is the primary driver of extinction risk in rays, impacting 100% of threatened species (IUCN, 2024), which are caught in industrial and small-scale fisheries (SSF) worldwide. The vulnerability of a species to fishing and other threats depends on a combination of its intrinsic sensitivity (i.e. biological traits that determine resilience) and extrinsic exposure to the threat. In the case of fisheries, intrinsic sensitivity is the result of those biological traits that determine population growth rates (Dulvy & Kindsvater, 2017; Juan-Jordá et al., 2015; Cortés, 2016), and extrinsic exposure is primarily a combination of susceptibility to being caught (encounterability e.g. geographic range and depth overlap, and gear selectivity), fishing effort, and fishing power (gear coverage and efficiency) (Hobday et al., 2011; Gallagher et al., 2012; Cortés et al., 2015). Extrinsic exposure may also be influenced by the social and

economic drivers of ray catch (Booth et al., 2019; Barrowclift et al., 2017; Temple, Berggren, et al., 2024), though these drivers are poorly quantified at larger geographic scales. Understanding both the traits that determine intrinsic sensitivity and predictors of exposure has been shown to provide useful insights for species' extinction risk assessment, population trends, and management at broad taxonomic scales, including for sharks and rays (Sherman et al., 2023; Walls & Dulvy, 2020; Dulvy et al., 2021). Yet, these relationships may differ at higher taxonomic resolutions where differences in species' biology and ecology may play a greater moderating role.

Pelagic rays, defined here as rays exhibiting pelagic and bentho-pelagic lifestyles, that are considered aquilopelagic ecomorphotype based on their similar morphology, habitat, and behaviour (Compagno, 1990). These rays occupy both oceanic and inshore/shelf areas with wing-like, expanded pectoral fins for active propulsion (Last et al., 2016). The pelagic lifestyle of these rays may affect their susceptibility to being caught in fisheries, particularly those using drift gillnets. Some species are also wide-ranging (Notarbartolo di Sciara, 1988; DeGroot et al., 2021; Ajemian & Powers, 2014), which increases their exposure to different management regimes or in many instances a lack of appropriately enforced management (Dulvy et al., 2017). Some pelagic ray species are also known to form large aggregations (Bassos-Hull et al., 2014; Couturier et al., 2018; Kelaher et al., 2023), which likely increases their fisheries susceptibility. Pelagic rays are some of the most threatened elasmobranchs (sharks and rays), with 80% of assessed species threatened with extinction (IUCN, 2024; Dulvy et al., 2021). This is much higher than the threat of extinction (around one-third) for rays and sharks (Class Chondrichthyes) more broadly (IUCN, 2024; Dulvy et al., 2021). Here, we include four families of rays within the Order Myliobatiformes (39 species assessed on the International Union for Conservation of Nature (IUCN) Red List of Threatened Species): eagle rays (Myliobatidae, n=18), pelagic eagle rays (Aetobatidae, n=5), cownose rays (Rhinopteridae, n=7) and Devil rays (Mobulidae, n=9). These rays are durophagous, feeding on hard-shelled prey, except for devil rays (Aschliman, 2014). Additionally, planktivorous the pelagic (Pteroplatytrygon violacea) (Family Dasyatidae) was included as a truly pelagic species. Of these 40 species, 32 are threatened with extinction (IUCN Red List Categories of Vulnerable, Endangered, and Critically Endangered) and two species (Aetomylaeus asperrimus and Rhinoptera neglecta) are classed as Data Deficient. The majority of these species (n=34) show decreasing population trends according to the IUCN Red List.

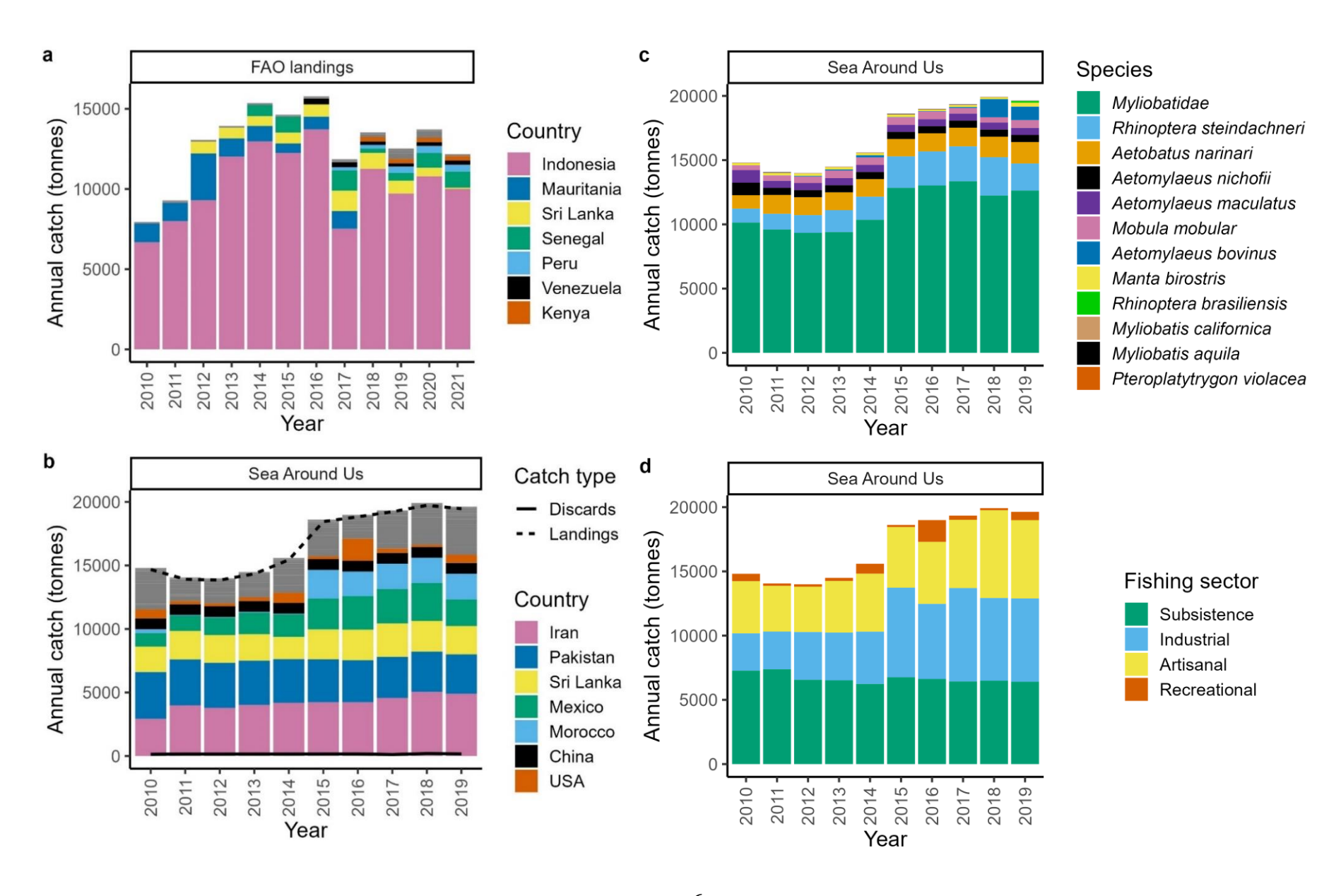


Figure 1.1 Available annual total fisheries catch (tonnes) statistics from different sources: a) FAO landed catch FAO (2010-2021) by reporting country (countries reporting the highest catches shown in the legend); b) Sea Around Us (2010-2019) discarded and landed catch by country (countries reporting the highest catches shown in the legend); c) Sea Around Us total catch by species; and d) Sea Around Us total catch by fishing sector. FAO nominal catch data were obtained using FishStatJ software (Version 4.03.06) (FAO, 2023) from the 'Global Capture Production' dataset to record total retained catch (for all fishing sectors but excludes discards) reported for any relevant taxa. Downloaded global Sea Around Us catch reconstruction data for relevant taxa (reports by fishing sector and discard data) (Pauly & Zeller, 2015).

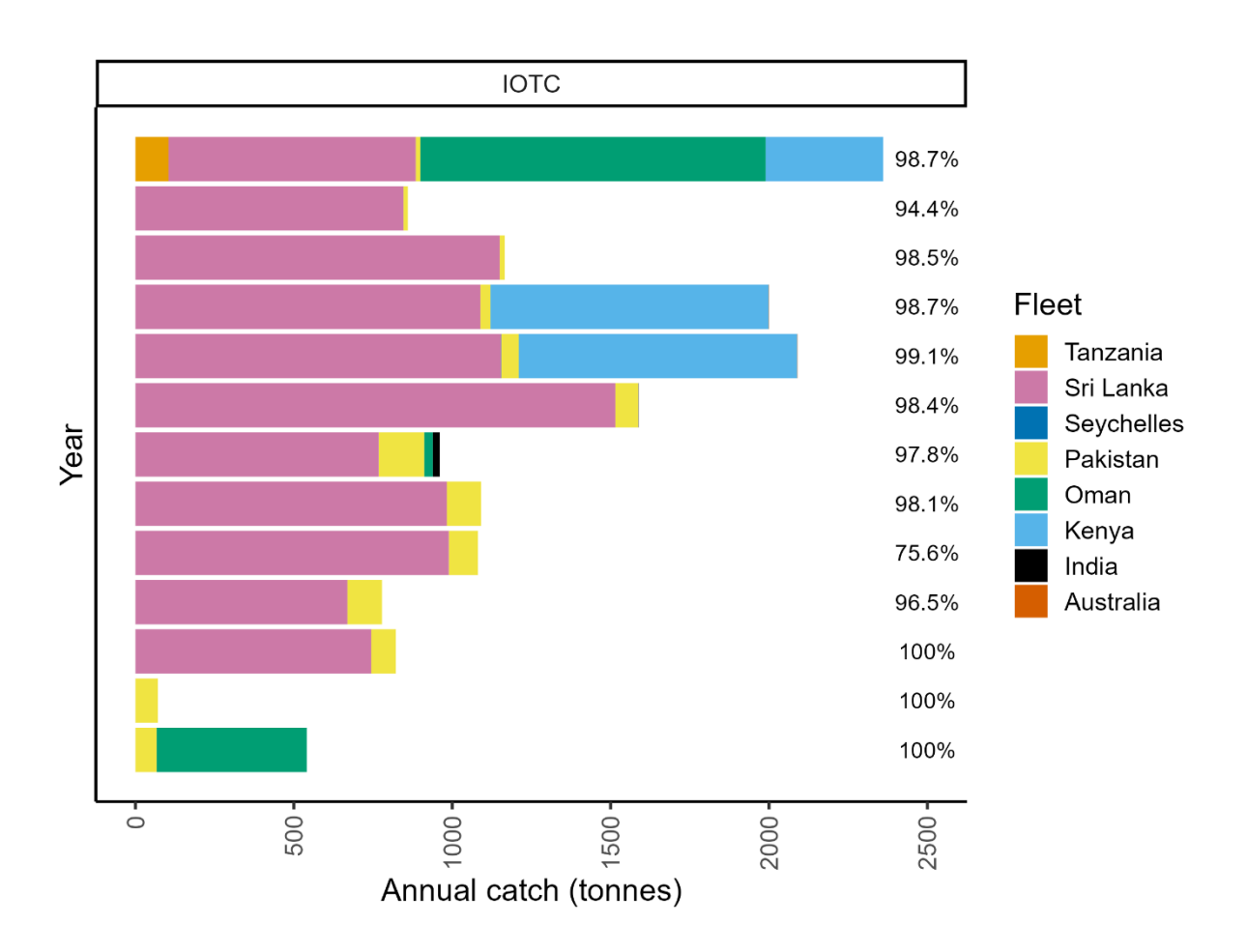


Figure 1.2 Available annual total fisheries catch (tonnes) statistics from the Indian Ocean Tuna Commission RFMO (2010-2022) by reporting country, with the percentage of total catch reported as artisanal indicated (remainder reported as industrial). IOTC Nominal retained catch data for all species from the IOTC website (https://iotc.org/data/datasets) (reports by fishing sector).

Available fisheries landings data reported in the Food and Agriculture Organisation of the United Nations (FAO) statistics indicates a mean total (retained) catch of approximately 14,000 tonnes per annum from 18 countries for pelagic ray taxa (2013-2019) (Figure 1.1) (FAO, 2023). This excludes an aggregated grouping of 'rays, stingrays, mantas' of approximately 138,000 tonnes from 71 countries, which likely also includes a substantial volume of relevant pelagic ray species. Available catch data from Regional Fisheries Management Organisation (RFMO) statistics are limited, mainly reported by the Indian Ocean Tuna Commission, which provides an additional indication of the breakdown by fishing sector (primarily small-scale, reported as artisanal) (Figure 1.2). These catch statistics are likely severely underreported (Mucientes et al., 2022; Clarke, McAllister, et al., 2006; Pauly & Zeller, 2016). Sea Around Us data, which aim to address underreporting by reconstructing catch data from additional sources, indicates a 35% higher mean total catch of approximately 19,000 tonnes per annum from 30 countries compared with the FAO statistics and provides a further indication of the breakdown by fishing sector and discarded catch (Figure 1.1) (Pauly & Zeller, 2015). Countries reporting the highest catches of pelagic rays include Indonesia, Sri Lanka, Mauritiana, Pakistan, and Iran, all of which have large industrial and/or small-scale gillnet fleets (Zeller et al., 2023).

Only Mobulidae species are listed on Appendix II of the Convention on International Trade in Endangered Species of Wild Fauna and Flora (CITES) and Appendices I and II of the Convention on the Conservation of Migratory Species of Wild Animals (CMS). These listings were driven by the observed decline in fisheries catch, exacerbated by international trade of their gill plates, and the conservative life history of devil rays that produce a single pup every 1-7 years (Couturier et al., 2012; O'Malley et al., 2017). Concern over fisheries sustainability has also led to the majority of RFMOs protecting devil rays and for some national protective legislation for these species. However, most pelagic ray species are largely unprotected and unmanaged in global fisheries.

Here, indicators of species traits (maximum size and generation length as indices of intrinsic sensitivity), extrinsic fishing threat (small-scale and industrial fishing pressure), and threat of fishing exposure (median depth of occurrence and number of countries within a species' geographic range) are explored to investigate which best predict extinction risk (IUCN Red List status) for pelagic rays.

1.3 Methods

Sources of species trait data, threats and threat exposure indicators, including fisheries catch data are outlined, followed by the statistical approach used.

1.3.1 Species trait data

The IUCN Red List of Threatened Species, herein referred to as the IUCN Red List, is widely used to assess species extinction risk including for sharks and rays, which were recently globally reassessed (Dulvy et al., 2021). The IUCN Red List status of the 40 assessed pelagic ray species (as defined in the introduction) was assigned an ordinal value from 1-5 (1 being Least Concern, 5 being Critically Endangered), with two Data Deficient Species unassigned. Whilst there are potentially further species that could be considered bentho-pelagic, such as those considered to occupy 'Marine Oceanic' or 'Marine Neritic – Pelagic' habitat types on the IUCN Red List, species with similar morphology, habitat, and behaviour (aquilopelagic ecomorphotype) were chosen to see how biological traits and indicators of extrinsic exposure to fishing affected the threat of extinction.

Maximum disc width data (straight line length measurement between the wing tips in cm), as the most appropriate length measurement for the body shape of Myliobatiformes, were sourced from Rays of the World (Last *et al.*, 2016). Generation length (GL, years) data were sourced from IUCN Red List Assessments where available (n=6), which are calculated as the mid-point between female age at maturity (at which 50% of the female population are mature, α_{mat}) and maximum age (α_{max}) (Dulvy et al., 2021) with GL = α_{mat} + ([$\alpha_{max} - \alpha_{mat}$]z). This is a simple measure of generation length based on a conservative mortality rate z of 0.5 to account for systematic underestimation in chondrichthyan ages (Harry, 2018; Dulvy et al., 2021). A lower mortality rate would result in a faster generation length and vice versa. Generation lengths for the majority of species (n=31) were inferred from similar species with a similar body shape and adjusted for maximum body size (as specified in the relevant IUCN Red List assessment) due to a lack of age data. *Aetobatus* spp., *Rhinoptera* spp., and *Mobula* spp. were inferred from species within the same genus (two species with age data in each genus) and *Aetomylaeus* and *Myliobatis* spp. were inferred from two eagle ray species (Family Myliobatidae) with age data (Bat Ray, *Myliobatis californicus* and Duckbill eagle ray, *Aetomylaeus bovinus*).

1.3.2 Indices of threats and threat exposure

Median depth of occurrence was calculated as the median of the minimum and maximum depth (m) as reported in the IUCN Red List. Whilst this may mean that single deepwater records could bias the estimate, median depth was used to be representative of relative depth ranges of each species. Species geographic range was indexed by the number of countries' Exclusive Economic Zones that overlapped with the species range, sourced from the IUCN Red List.

Industrial and small-scale fisheries total annual catch data in tonnes were sourced from Sea Around Us for 2019 for available countries (Pauly & Zeller, 2015). These catch data were used to calculate a measure of relative fishing pressure for each country by dividing catch by the country's coastline length, given that fishing pressure is exerted from the coastline outwards, particularly for SSF. This was done for both industrial and SSF catch. Then for each species, fisheries catch was totalled across countries for which species geographic range overlaps (i.e. the same countries that are totalled to provide an index of species geographic range) and was divided by the total length of those countries coastlines to get proxies for the industrial and SSF fishing pressures that each species are exposed to. This means that for the same fisheries catch biomass, a greater coastline length would result in lower relative fishing pressure, whilst for the same coastline length, higher catch biomass would result in higher relative fishing pressure.

1.3.3 Ordinal regression models

Ordinal logistic regression models were used to explore which species traits (maximum size and generation length), threats (industrial and small-scale fishing pressure), and threat exposure (median depth and number of countries) indicators best predict extinction risk (IUCN Red List status) for the 38 assessed pelagic ray species (excluding the two Data Deficient species), using the R package *ordinal* (Christensen, 2023). All explanatory variables were log-transformed and normalised (scaled and centred) prior to analyses. All variables were tested for correlation with no variables correlated above a threshold of 0.7 in which collinearity severely distorts model estimation included in the same models (Dormann et al., 2013). Industrial and small-scale fishing pressure were positively correlated >0.7 and therefore were not included in the same models. The 48 candidate models for how extinction risk may vary with different species trait and threat indices were fit. Variance-inflation factors (VIF) were estimated for all coefficients in the models using the *car* package (Fox & Weisberg, 2019), with no VIF value greater than two indicating that all models were robust to collinearity.

Akaike Information Criterion (AIC) was used to compare candidate models, with the top model being the most parsimonious (fewest variables) with an AIC value within 2 units of the lowest AIC (Burnham & Anderson, 2002; Arnold, 2010). To account for model uncertainty, model averaging for models with Δ AIC <2 was used to calculate a weighted multi-model average of each explanatory variable. These Relative Variable Importance values were calculated from the sum of the AIC (Akaike) weights of models that included the explanatory variable. The top model was then used to predict the probability of being threatened (IUCN Red List statuses of Critically Endangered, Endangered, and Vulnerable) for the two Data Deficient species. All analyses were run in R version 4.1.2 (R Core Team, 2021) in RStudio (RStudio Team, 2021).

Table 1.1 Comparison of 24 of 48 candidate models with Δ AIC <10 using Akaike Information Criteria (AIC), difference in AIC from the top model (Δ AIC), and Akaike weights. Models are ordered by ascending AIC, with the top model shown in bold and models with AIC <2 shown in grey.

Model	AIC	ΔΑΙС	Weights
Species Range + SSF Pressure	99.97	0	0.128
Median Depth + Species Range + SSF Pressure	100.1	0.13	0.120
Median Depth + Species Range	100.91	0.94	0.080
Generation Length + Median Depth + Species Range	101.02	1.05	0.076
Generation Length + Median Depth + Species Range + SSF Pressure	101.22	1.25	0.069
Maximum Size + Median Depth + Species Range	101.71	1.74	0.054
Maximum Size + Median Depth + Species Range + SSF Pressure	101.72	1.75	0.053
Generation Length + Species Range + SSF Pressure	101.82	1.85	0.051
Maximum Size + Species Range + SSF Pressure	101.9	1.93	0.049
Median Depth + Species Range + Industrial Pressure	102.21	2.24	0.042
Species Range	102.71	2.74	0.033
Generation Length + Median Depth + Species Range + Industrial Pressure	102.72	2.75	0.032
Maximum Size + Generation Length + Median Depth + Species Range	102.91	2.94	0.029
Species Range + Industrial Pressure	102.95	2.98	0.029
Maximum Size + Generation Length + Median Depth + Species Range + SSF Pressure	103.21	3.24	0.025
Maximum Size + Generation Length + Species Range + SSF Pressure	103.41	3.44	0.023
Maximum Size + Median Depth + Species Range + Industrial Pressure	103.47	3.5	0.022
Generation Length + Species Range	104.16	4.19	0.016
Generation Length + Species Range + Industrial Pressure	104.59	4.62	0.013
Maximum Size + Generation Length + Median Depth + Species			
Range + Industrial Pressure	104.68	4.71	0.012
Maximum Size + Species Range	104.71	4.74	0.012
Maximum Size + Species Range + Industrial Pressure	104.89	4.92	0.011
Maximum Size + Generation Length + Species Range	105.66	5.69	0.007
Maximum Size + Generation Length + Species Range + Industrial Pressure	105.95	5.98	0.006

1.4 Results

Nine out of the 48 constructed models had $\Delta AIC < 2$, with two of these models consisting of two explanatory variables (most parsimonious), providing good support for best predicting extinction risk (IUCN Red List status) in pelagic rays (Table 1.1). The top model ($\Delta AIC=0$) with the greatest amount of support (Akaike weights) included species geographic range (number of countries a species occurs in) and SSF pressure (Table 1.1). The third model ($\Delta AIC=0.94$), which included species range and median depth received approximately 63% of the support of the top model (based on Akaike weights) (Table 1.1). Species range had the greatest Relative Variable Importance of the explanatory variables in models with $\Delta AIC < 2$, followed by SSF pressure, and median depth (Figure 1.3). Additional models with $\Delta AIC < 2$ included additional variables (were more complex) without an improvement in ΔAIC and can therefore be considered uninformative (Burnham & Anderson, 2002; Arnold, 2010). Species trait data including maximum size and generation length were not in top-ranking models and had the lowest Relative Variable Importance (Figure 1.3). Industrial fishing pressure was not in any models with $\Delta AIC < 2$.

The effect of species range was positive across models indicating that the probability of being threatened increased with the number of countries a species occurs in (Figure 1.3; Figure 1.4). The effect size of species range was considered significant as the 95% confidence intervals did not overlap zero (Figure 1.3). SSF pressure was also positive suggesting that species facing higher SSF pressure were also more likely to be threatened (Figure 1.3; Figure 1.4). Median depth was generally negative suggesting that the probability of a species being threatened increased for shallower water species (lower median depth) (Figure 1.3; Figure 1.4).

Data Deficient pelagic ray species would therefore be expected to have a greater risk of being threatened with extinction if they had a greater species range and were exposed to higher fishing pressure across that range. Based on the top-ranked model, the two Data Deficient Species (*Aetomylaeus asperrimus* and *Rhinoptera neglecta*) have an approximately 10% probability of being threatened (IUCN Red List statuses of Critically Endangered, Endangered, and Vulnerable). Both species only occurred in three and two countries, respectively, and were exposed to relatively low SSF pressure despite occurring in relatively shallow waters (median depth of 25 metres). This is in line with IUCN Red List assessments of similar species including *Aetomylaeus caeruleofasciatus*, which is classified as Least Concern due to no reported decline across its main distribution in Australian waters (Figure 1.5). Similarly, *Rhinoptera*

steindachneri is classified as Near Threatened despite high fishing pressure across some of its range due the northern range population being considered stable. However, an estimated 10% probability of being threatened may be unrealistically low, given 70% of assessed species (n=7) within both the *Aetomylaeus* and *Rhinoptera* genera are classified as threatened on the IUCN Red List (n=5), due to high fisheries exploitation and likely low productivity limiting their resilience to this pressure.

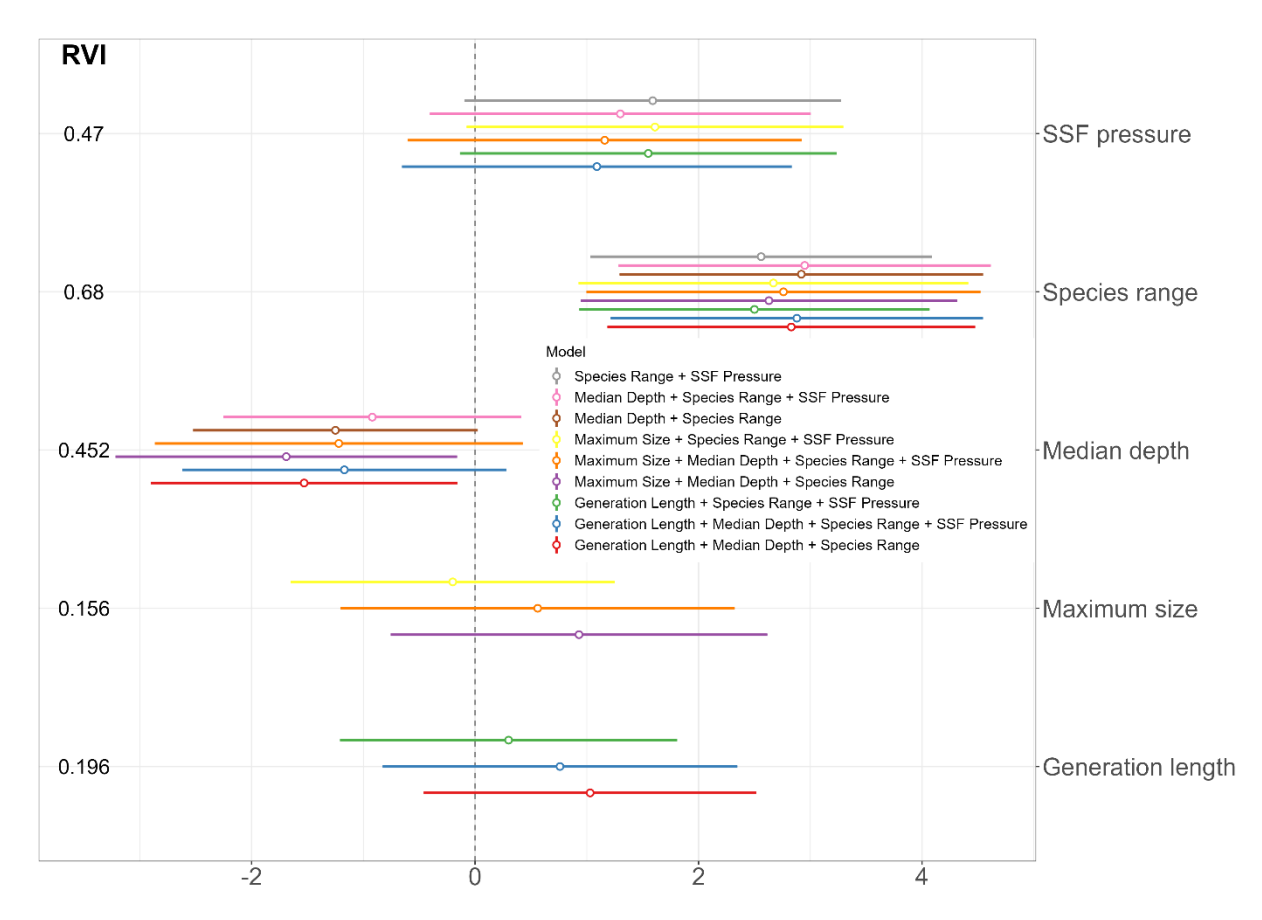


Figure 1.3 Mean effect (\pm 95% confidence intervals) of SSF pressure, species range (number of countries a species occurs in), median depth, maximum size, and generation length on threat status (IUCN Red List) for top 9 models with Δ AIC <2 (n=38). The Relative Variable Importance (RVI) is shown for each variable included in the top models. Effect sizes can be considered significant when confidence intervals do not overlap zero.

The performance of the top models may be limited by several exceptions to the general patterns discussed thus far. For example, the pelagic stingray (*Pteroplatytrygon violacea*), which has a global distribution occurring in 168 countries is classified as Least Concern, with the species facing relatively low SSF pressure despite its large geographic range (Figure 1.5). In contrast,

some species (*Myliobatis chilensis* and *M. peruvianus*) ranges only overlap with a couple of countries' Exclusive Economic Zones but face relatively high small-scale fishing pressure across large coastlines (Chile and Peru) (Figure 1.5). Devil rays (*Mobula* spp.) had the greatest median depths (except shallower-water species *M. thurstoni* and *M. munkiana*) but amongst the largest geographic ranges and are all classified as Endangered except *M. alfredi*, which is Vulnerable. Therefore, there are likely additional explanatory variables explaining variation in the threat of extinction for pelagic rays, such as fecundity and whether species aggregate.

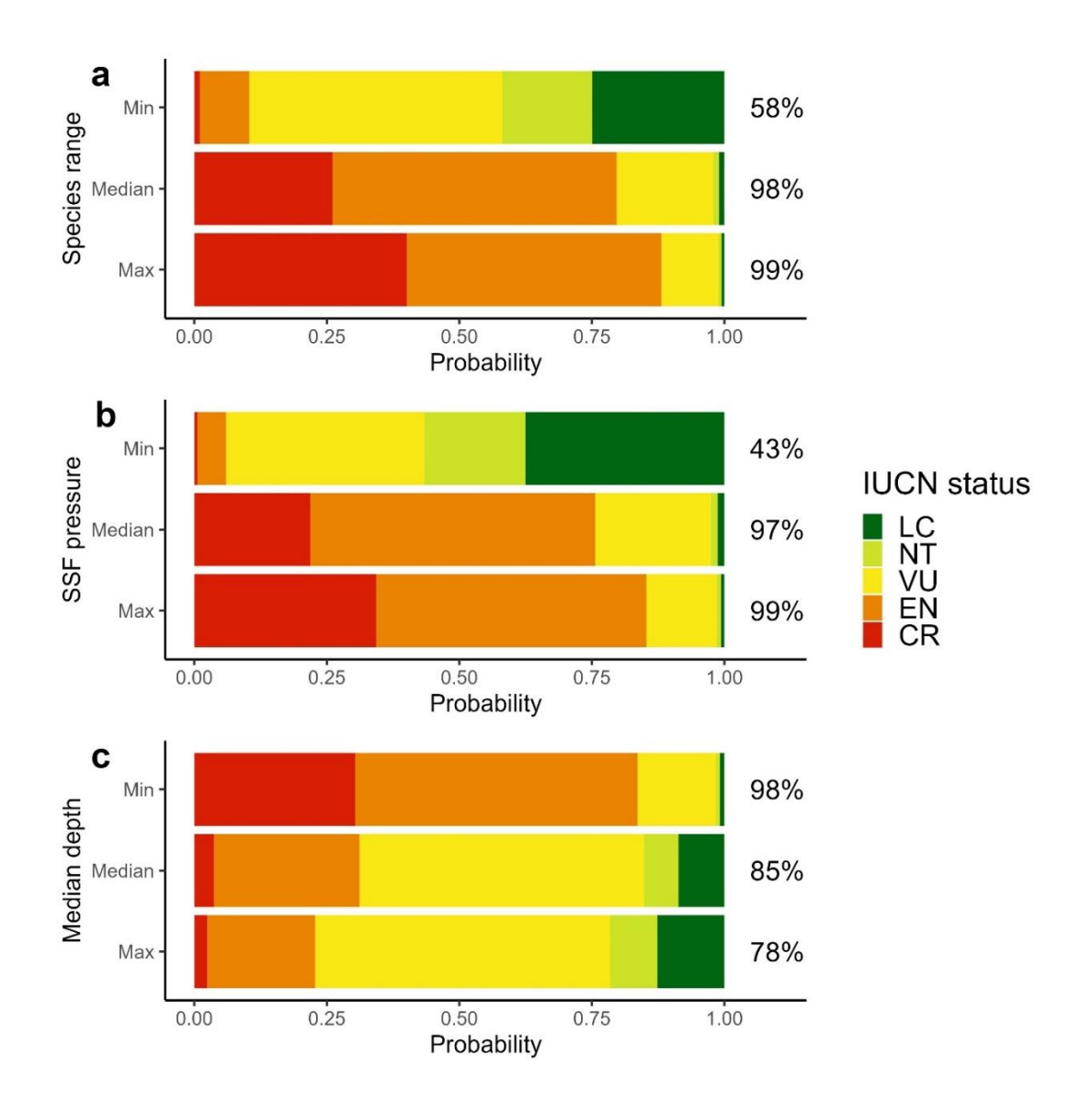


Figure 1.4. The effect of a) species range (number of countries a species occurs in), b) SSF pressure, and c) median depth (m) on the probability a pelagic ray species (n=38) is listed as Critically Endangered (CR, red) Endangered (EN, orange), Vulnerable (VU, yellow), Near Threatened (NT, light green), or Least Concern (LC, dark green) from the top (a and b) and third (c) ordinal regression models. The percentage of species threatened (CR, EN, and VU) is indicated at the end of each bar.

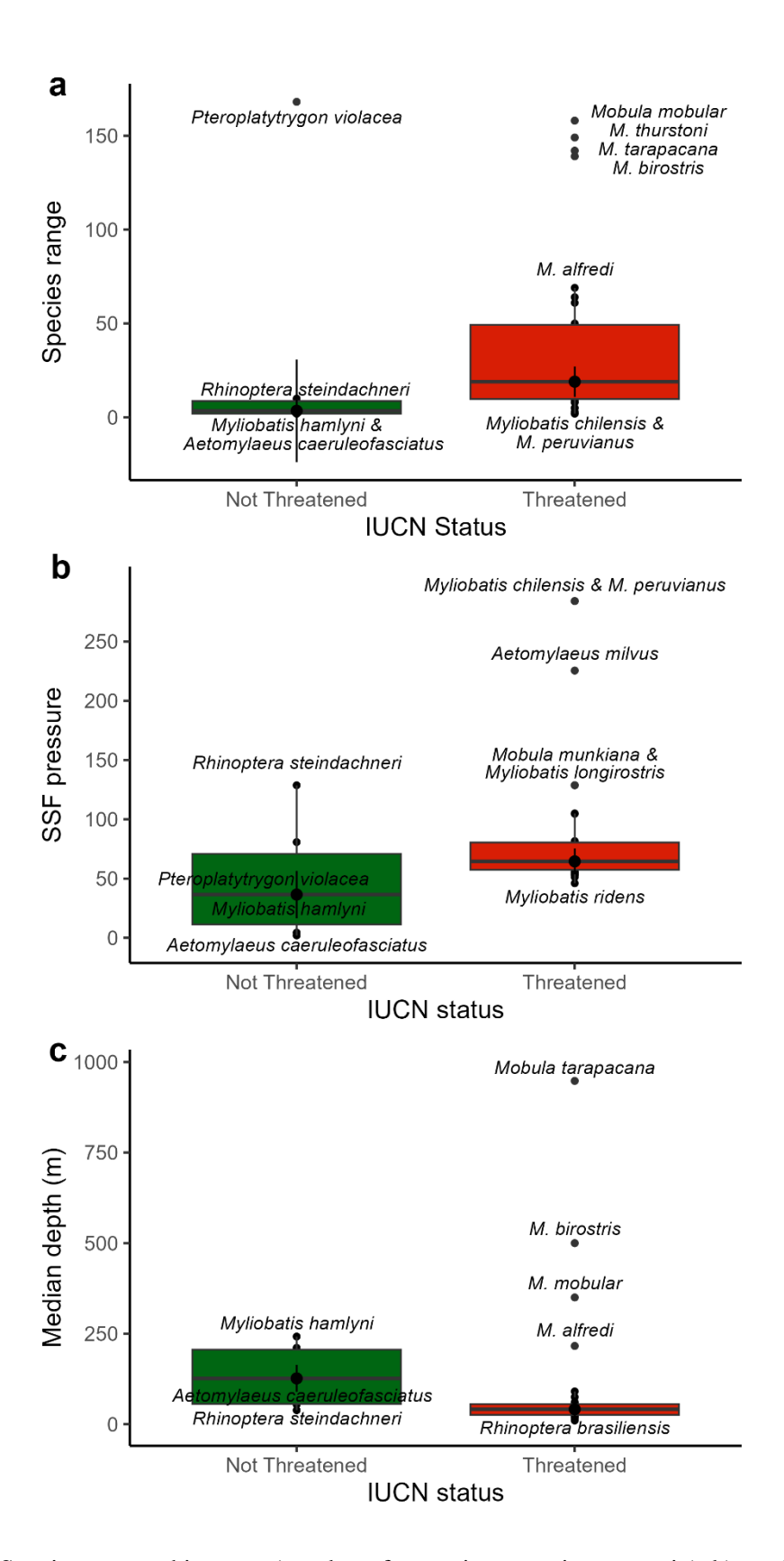


Figure 1.5. a) Species geographic range (number of countries a species occurs in), b) small-scale fishing (SSF) pressure, and c) median depth (m) for threatened (IUCN Red List statuses of Critically Endangered, Endangered, and Vulnerable) (n=32) and not threatened (Near Threatened and Least Concern) (n=6) pelagic ray species with black dots showing the median (\pm standard error and outliers).

1.5 Discussion

The extinction risk of pelagic rays was best predicted by species geographic range and SSF pressure, with higher probability of being threatened where a species occurs in a greater number of countries and is exposed to higher SSF pressure. Species with a greater depth range (greater median depth) also had a lower probability of being threatened, possibly because they have more refuge from fishing. The two Data Deficient pelagic ray species, *Aetomylaeus asperrimus* and *Rhinoptera neglecta*, were therefore predicted to have a low probability of being threatened because of their small geographic ranges and low exposure to small-scale fishing pressure. The majority of pelagic rays are threatened with extinction (32 out of 40 species) making them among the most threatened groups of sharks and rays. Science-based, transnational action is needed to conserve these species and ensure future sustainability of the fisheries catching them.

It was found that pelagic rays that occur in a greater number of countries had a higher probability of being threatened. This has also been found in a study assessing the extinction risk of coral reef sharks and rays (Sherman et al., 2023). Species with a larger geographic range, overlapping with more countries' national jurisdictions, will be subject to many different fisheries management regimes and more likely to encounter a lack of appropriate or enforced regulations (Dulvy et al., 2017). This is in contrast to marine mammals and terrestrial megafauna species where greater geographic range tends to predict lower extinction risk, likely due to more joined-up management regimes and increased availability of natural refuges from the threats (McClenachan et al., 2016; Davidson et al., 2012). For wide ranging marine species like some of the pelagic rays (Notarbartolo di Sciara, 1988; DeGroot et al., 2021; Ajemian & Powers, 2014), local protections may be ineffective, for example, they may not spend the majority of their time in any protected areas and be exposed to a lack of fishing management measures in other parts of their geographic range (Hilborn & Sinclair, 2021; Watson et al., 2019; Conners et al., 2022; Handley et al., 2020). For pelagic rays, this is also complicated by some species forming large aggregations that may overlap spatially and temporally with areas of high fishing pressure or poor management. Consideration of species range and distribution is therefore needed for more effective spatial protection, for example of key migration corridors, aggregation sites, or critical habitats (Boerder et al., 2019; Chin et al., 2023). This becomes increasingly complicated for species distributed across a higher number of countries, therefore requiring transnational coordinated action (Lascelles et al., 2014; McClenachan et al., 2016). It also means a thorough understanding of species biology and ecology is needed to design

effective management actions to protect species and populations across life history stages (e.g. mating areas and nursery sites) and behaviours (e.g. foraging grounds and movement patterns).

SSF pressure was more important than industrial fishing pressure in predicting the probability that a pelagic ray species was threatened. The role of SSF in driving the decline of sharks and rays, and marine megafauna more broadly, has typically been overlooked compared to industrial fisheries (Temple, Langner, et al., 2024). Yet, SSF contribution to global catch is significant, providing a livelihood and source of protein to millions of people, particularly in developing countries (Béné, 2006; Chuenpagdee et al., 2006; Zeller et al., 2006). There is a paucity of data in official statistics, with SSF and industrial catch reported together to FAO and often no information on fishing effort for many countries' SSF (Salas et al., 2007; Chuenpagdee et al., 2006; Alfaro-Shigueto et al., 2010). Rays are known to be an important component in many SSF (Catarci, 2004; Alfaro-Shigueto et al., 2010; Temple et al., 2019; Svarachorn et al., 2023) but catch composition from official statistics are typically reported at a lower taxonomic resolution, often aggregated with sharks (Catarci, 2004; FAO, 2021). Species-specific reporting and monitoring are needed but this is complicated by the morphological similarity of many pelagic ray species within the same family (Last et al., 2016) as well as the difficulty in species identification of traded products. Molecular approaches are increasingly used, particularly for trade, and will likely be more widely applicable in fisheries monitoring in the coming years (Prasetyo et al., 2023; Domingues et al., 2021; Cardeñosa et al., 2018). Ray species face a higher threat of extinction in tropical and sub-tropical, coastal waters where SSF are prevalent (Dulvy et al., 2021). The nature of SSF with remote and dispersed landing sites, poor enforcement capacity, and the complex socio-economic characteristics of the communities they support present a significant management challenge (Temple, Berggren, et al., 2024; Cinner et al., 2009; Booth et al., 2019). This is further complicated by their multi-gear, multi-species nature and utilisation (trade and subsistence) of non-target species.

It is important to consider the vertical as well as the horizontal movement and distribution of pelagic rays and how these affect exposure to fisheries. Depth was also found to be important in predicting the extinction risk of pelagic rays, with species occupying greater median depths less likely to be threatened, which has been found for sharks and rays more broadly (Walls & Dulvy, 2020; Sherman et al., 2023; Dulvy et al., 2021). This is likely due to the refuge from fisheries exposure provided by occupying greater depths outside high fishing pressure in shallower waters. Some species of pelagic rays, particularly devil rays, are capable of diving to depths of greater than 200 meters (outside of the epipelagic zone) and even to greater than 1000

meters (bathypelagic zone) (Andrzejaczek et al., 2022). These species likely still spend most of their time in shallower depths as seen for tagged reef manta rays (*Mobula alfredi*) (Andrzejaczek et al., 2020). Indeed, devil rays are still highly threatened due to overfishing (Lawson et al., 2017; Dulvy et al., 2021). Nevertheless, understanding of deep-diving behaviour and the implications for fisheries interactions may be important, particularly as deep-water sharks and rays are increasingly under threat with the growing fishing pressure in deep waters (Finucci et al., 2024; Braun et al., 2022).

Spatial overlap, both horizontal and vertical, of species distributions and fishing effort is only one component of susceptibility to being caught as part of ecological risk assessment (Hobday et al., 2011; Gallagher et al., 2012; Murua et al., 2021). Fishing gear selectivity and post-capture mortality (both at-vessel and post-release mortality) also need due consideration (Cortés et al., 2015; Cortés et al., 2010; Ellis et al., 2017). Both gear selectivity and post-capture mortality have implications for management and bycatch mitigation strategies, such as gear modifications and retention bans (Lemke & Simpfendorfer, 2023; Gilman, Chaloupka, et al., 2022). For example, J-shaped hooks were found to be responsible for significantly higher at-vessel mortality compared to circle hooks for the giant manta ray (M. birostris) and pelagic stingray (Pteroplatytrygon violacea) (Gilman, Chaloupka, et al., 2022). It is also important to consider incentives for changes to fisher behaviours towards more sustainable approaches (Pascoe et al., 2010; Gilman, Hall, et al., 2022). However, this is difficult where bycatch still has a value as with rays caught in many SSF. Whilst much of the fisheries catch of rays may be classed as unintentional (bycatch), the majority is utilised as food and other traded products (Dulvy et al., 2021), complicating fisheries management including by catch mitigation efforts, particularly for small-scale fisheries. Including social and economic factors in future trait-based analyses of extinction risk in rays could be an important avenue for future research and investigation of how it affects fisheries susceptibility and exposure. The socio-economic characteristics of a fishery will relate to species trait and threat indicators considered in this study, for example, larger-bodied individuals are often more economically valuable and therefore targeted (McClenachan et al., 2016).

Maximum size and generation length, which were used as indicators of a species intrinsic sensitivity to fishing, were relatively uninformative in predicting the probability of pelagic rays' extinction risk. This is surprising given body size and generation length are often key correlates of extinction risk for sharks and rays, with greater risk in larger species and those with longer generation lengths (Dulvy et al., 2021; Sherman et al., 2023; Hutchings et al., 2012). Larger

species tend to have lower intrinsic rates of population growth and therefore are less resilient to fishing mortality (Cortés, 2016; Denney et al., 2002). Similarly, species that mature later and live longer, leading to longer generation times, have lower population growth and rebound rates (Cortés, 2002; García et al., 2008; Juan-Jordá et al., 2015; Worm et al., 2013). Larger species also tend to have larger range sizes (Tamburello et al., 2015), which was found as an important predictor of extinction risk for pelagic rays. Maximum size ranged from 59cm (Aetomylaeus caeruleofasciatus) to seven meters (Mobula birostris) disc width and generation length from six (some eagle ray species and the pelagic stingray) to 29 years (manta rays). However, many of the pelagic rays are large-bodied, which may be why body size was not as important as a predictor of extinction risk for this group. Indeed, pelagic eagle rays and devil rays are amongst the most threatened chondrichthyan families (Dulvy et al., 2021). Interestingly, the pelagic stingray, which is a relatively smaller-bodied pelagic ray (maximum disc width of 96cm in captive individuals but 60-80cm in wild animals) (Mollet et al., 2002; Last et al., 2016) is classed as Least Concern despite having the largest geographic range of the pelagic rays, which was found to be a key predictor of extinction risk in this study. The pelagic stingray also has amongst the shortest generation lengths of pelagic rays, producing litters of 2-9 pups with a gestation period of 2-4 months (Last et al., 2016). At a lower taxonomic resolution, body size and generation length may be better predictors of extinction risk. However, when assessing extinction risk at a higher taxonomic resolution, a species' biology and ecology, and how this affects exposure to fisheries may be more important in predicting risk.

This study found that shallower water pelagic ray species with larger geographic ranges and greater exposure to small-scale fishing pressure were more likely to be threatened with extinction. *Aetomylaeus asperrimus* and *Rhinoptera neglecta*, currently classed as Data Deficient, had low probabilities of being threatened given their small geographic range and low exposure to small-scale fishing pressure. Body size and generation length were less important in explaining extinction risk for pelagic rays in contrast to previous studies for sharks and rays more broadly. It is therefore important to understand the intricacies of both the biological traits affecting a species resilience and indicators of fishing exposure. Trait-based modelling offers an opportunity to utilise available data, necessary for data-poor species and fisheries before they decline beyond recovery (Walls & Dulvy, 2020; Kindsvater et al., 2018; Horswill et al., 2019). Even for intrinsically sensitive species, well-enforced, science-based management can support fisheries and conserve species (Pacoureau et al., 2023; Simpfendorfer & Dulvy, 2017).

Chapter 2. Global patterns of intrinsic sensitivity to fishing in rays

2.1 Abstract

Overfishing, habitat loss, and climate change are driving population declines in many species. Understanding a species' capacity to recover from these and other threats is necessary for prioritising management. The maximum intrinsic rate of population increase (r_{max}) can be used to compare which species or groups are particularly sensitive to ongoing threats. To investigate global patterns of intrinsic sensitivity of rays (Superorder Batoidea), we calculated r_{max} of 85 species using a modified Euler-Lotka model that accounts for survival to maturity. We examined how r_{max} varies with body mass, temperature, and depth using an informationtheoretic approach through model selection, accounting for phylogenetic non-independence. Although we observed an overall positive relationship between r_{max} and temperature, we found (Orders warm-shallow-water rays Torpediniformes, Rhinopristiformes, Myliobatiformes) were more intrinsically sensitive to exploitation (lower r_{max}) than cold-deepwater skates (Order Rajiformes). We hypothesise that this pattern is likely driven by their different reproductive strategies as live-bearing rays have fewer offspring compared to egglaying skates, and caution that future research should focus on understanding differences in the mortality schedule of juveniles and sub-adults to understand if survival to maturity is comparable. Our findings highlight the high vulnerability of warm-shallow-water ray species to overexploitation and other threats due to their intrinsically low maximum population growth rates. These differences in r_{max} have conservation implications for our understanding of the geographic patterns in extinction risk, suggesting that tropical rays are more intrinsically sensitive.

2.2 Introduction

Understanding population growth rate is central to understanding species' responses to overfishing, habitat loss and degradation, and climate change (Yan et al., 2021; Webb et al., 2011). Species' vulnerability is a combination of intrinsic sensitivity and extrinsic exposure to fishing and other threats (Dulvy & Kindsvater, 2017; Juan-Jordá et al., 2015). Intrinsic sensitivity can be indexed by the maximum intrinsic rate of population increase (r_{max}), which in its simplest form, can be calculated from age at maturity, maximum age and annual reproductive output. r_{max} represents the theoretical maximum intrinsic population growth rate at low population sizes, i.e., in the absence of density-dependent processes (Pardo et al., 2018; Myers et al., 1999; Myers et al., 1997; Cortés et al., 2015) and is equal to the fishing mortality

that will cause a species or population to become extinct ($F_{extinct}$) (Gedamke et al., 2007; Dulvy et al., 2004). Understanding how r_{max} varies among species can therefore inform our understanding of sensitivity to exploitation, recovery potential, and can also be used as a Bayesian prior to help estimate catch limits in fisheries stock assessments (Martell & Froese, 2013; Patrick et al., 2010).

Chondrichthyans (shark, rays, and chimaeras; hereafter, referred to as 'sharks and rays') are a highly threatened taxon, with over one-third of species threatened with extinction (The International Union for the Conservation of Nature's (IUCN) Red List of Threatened Species categories of Vulnerable, Endangered, or Critically Endangered) due to overfishing (Dulvy et al., 2021). Sharks and rays are important sources of income and protein in the fisheries that are causing their decline, particularly small-scale fisheries in developing countries that comprise over 95% of the world's fishers (Pauly, 2006; Béné, 2006; Temple et al., 2019). Ensuring sustainability is crucial for both food security and healthy marine ecosystems (Simpfendorfer & Dulvy, 2017; Barrowclift et al., 2017). Sharks and rays typically have slow life histories including low somatic growth rates, late maturity, and low fecundity that result in relatively low r_{max} estimates (Cortés, 2000; García et al., 2008). Combined with limited density-dependent compensation in juvenile survival due to their narrow range of annual reproductive output, sharks and rays are extremely sensitive to elevated mortality from fisheries (Dulvy & Forrest, 2010; Quetglas et al., 2016; Cortés, 2002). There is, however, wide variation in life histories among sharks and rays, and even within rays there may be a range of r_{max} estimates that indicate their differing resilience to exploitation (Quetglas et al., 2016; Hutchings et al., 2012; Ward-Paige, 2017). Rays of the Superorder Batoidea are comprised of both live-bearing rays (Torpedo rays, Order Torpediniformes; Rhino rays, Rhinopristiformes; and stingrays, Myliobatiformes) and egg-laying skates (Rajiformes). Hereafter, we refer to these two lineages as 'rays' and 'skates', respectively. Live-bearing rays have much lower fecundities than egg-laying skates (Goodwin et al., 2002), probably limited by maternal body size (Wourms & Lombardi, 1992; Musick & Ellis, 2005; Wourms, 1977), whilst egg-laying skates face increased mortality from predation on eggs (Lucifora & García, 2004; Powter & Gladstone, 2008). Low fecundity likely limits r_{max} estimates (Pardo et al., 2018) and represents differences in reproductive allocation that influences population growth rates and generation lengths (Cortés, 2002; Juan-Jordá et al., 2013).

Maximum body size is a widely available predictor of extinction risk, with larger-bodied species typically at greater risk of decline and extinction due to slow life histories and low r_{max}

estimates (Jennings et al., 1998; Reynolds et al., 2005; Hutchings et al., 2012). However, where sufficient data allow, broader time-related life history traits including age at maturity, somatic growth rates, longevity, and mortality rates have been found to better explain life history variation and better correlate with extinction risk across different taxonomic groups (Chichorro et al., 2019; Anderson et al., 2011; Juan-Jordá et al., 2015). Theoretically and empirically, r_{max} has been shown to scale with body mass and temperature across taxa. This is likely due to r_{max} being closely tied to metabolic rate and trade-offs in energy allocated to survival, growth, and reproduction (Savage et al., 2004; Wong et al., 2021; White et al., 2022), such that r_{max} has been found to decrease with increasing body size in sharks and rays (Dulvy et al., 2014; Hutchings et al., 2012; Pardo & Dulvy, 2022). The expectation is that organisms with a higher metabolic rate in warmer waters (tropical, low latitudes) will tend towards 'faster' life histories, growing quickly to a smaller maximum body size (Healy et al., 2019; Reynolds, 2003), and consequently, have a higher r_{max} than those with slower metabolic rates and 'slower' life histories in cooler waters (temperate and polar, high latitudes) (Brown et al., 2004; Clarke & Johnston, 1999; Juan-Jordá et al., 2013). These temperature-related, latitudinal patterns may also be evident along depth gradients as temperatures generally decrease with increasing depth. Indeed, deep-water shark and ray species tend to have slower life histories and lower r_{max} estimates compared to continental shelf and pelagic species (Simpfendorfer & Kyne, 2009; García et al., 2008; Pardo & Dulvy, 2022).

Contrary to metabolic scaling expectations, there are some warm-shallow-water tropical rays, notably the filter-feeding devil rays (Mobula spp.), that have extremely low r_{max} (Dulvy et al., 2014; Pardo, Kindsvater, Cuevas-Zimbrón, et al., 2016). Pardo & Dulvy (2022) found that as body size increases, decreases in r_{max} were much steeper for warmer-water species, suggesting that a greater intrinsic sensitivity may also be playing a role in the higher extinction risk of tropical rays (Dulvy et al., 2021). Thus far, r_{max} estimates have been made for only a few ray and skate species (Dulvy et al., 2014; D'Alberto et al., 2019; Temple et al., 2020; Barbini et al., 2021; Lucifora et al., 2022; Barnett et al., 2013; Pardo, Kindsvater, Reynolds, et al., 2016).

Here, we calculate r_{max} for 85 ray and skate species where there were sufficient life history data available. We then use an information-theoretic approach, accounting for phylogenetic non-independence of species, to investigate how body mass, temperature, and depth may explain variation in r_{max} estimates for rays and skates.

2.3 Methods

First, we summarise data sources, including our literature search for life history data and methods used to estimate r_{max} . Second, we outline methods for obtaining body mass, depth, and temperature data. Third, we describe our analytical approach, including the metabolic scaling expectations and the statistical models associated with each hypothesis.

2.3.1 Collation of life history trait data and estimation of r_{max}

A database of published life history data for rays and skates was collated (Barrowclift & Dulvy, 2023). The database was developed from the generation lengths used in the recent IUCN Red List reassessments (Dulvy et al., 2021). To collate life history traits, searches were conducted in Web of Science and Google Scholar using the following search terms: age/growth/maturity/fecundity/litter size/life history/maximum intrinsic rate of population increase/productivity/reproductive biology AND ray* (wild character to return ray and rays) 'AND chondrichthy*' (wild character to return Chondrichthyes and chondrichthyan). The term 'ray*' has additional non-relevant usages so 'AND chondrichthy*' was added to the search term. The IUCN Red List (www.iucnredlist.org/) was also used to check species-specific life history parameters using information available in the 'Habitat and Ecology' tab, with references checked from the 'Bibliography' tab. Data were also taken from the life history database Sharkipedia (https://www.sharkipedia.org/) (Mull, Pacoureau, et al., 2022). Taxonomy was checked against Eschmeyer's Catalog of Fishes

(https://researcharchive.calacademy.org/research/ichthyology/catalog/fishcatmain.asp). We assigned life history data sourced from the literature to the most updated taxonomic nomenclature based on geographic distribution.

In its simplest form, r_{max} can be calculated from age at maturity (female age at 50% maturity, years; α_{mat}), maximum age (recorded for females where known, years; α_{max}), and annual reproductive output (number of female offspring assuming 1:1 sex ratio; b). These data were available for 85 ray (n=53) and skate (n=32) species.

To estimate r_{max} , we used a modified Euler-Lotka model that accounts for survival to maturity with the following equation (Pardo, Kindsvater, Reynolds, et al., 2016; Pardo et al., 2018; Cortés, 2016):

$$l_{\alpha_{mat}}b = e^{r_{max}\alpha_{mat}} - e^{-M}(e^{r_{max}})^{\alpha_{mat}^{-1}}, \tag{1}$$

where $l_{\alpha_{mat}}$ is the proportion of individuals surviving to maturity, which is calculated with:

$$l_{\alpha_{mat}} = (e^{-M})^{\alpha_{mat}}, \tag{2}$$

b is annual fecundity, M is the species-specific instantaneous natural mortality rate and α_{mat} is the age at maturity. We used a simple estimate of natural mortality (M) that is equivalent to the reciprocal of average lifespan, estimated with $M = 1/\omega$ (Pardo, Kindsvater, Reynolds, et al., 2016; Dulvy et al., 2004), where ω is an estimate of average lifespan in years. Average lifespan was assumed to be the midpoint between age at maturity (α_{mat}) and maximum age (α_{max}) (Pardo, Kindsvater, Reynolds, et al., 2016), estimated with:

$$\omega = \frac{(\alpha_{max} + \alpha_{mat})}{2} \tag{3}$$

Life history traits can vary within species and thus result in uncertainty in r_{max} ; therefore, we calculated 10,000 random deviates from a uniform distribution between minimum and maximum values of each life history parameter. We then estimated r_{max} with each of the life history values and took the median to generate a species-specific r_{max} value. Uncertainty in this r_{max} value was estimated as the 2.5% and 97.5% quantiles. If only point estimates were available, such as for α_{max} , then 10% was subtracted and added to get a minimum and maximum value, respectively. Where regional differences in life history trait data were described in the IUCN Red List assessments (n=7 species), r_{max} was calculated for each location and then a mean r_{max} for that species was used in further analyses.

2.3.2 Body mass, depth, and temperature-at-depth data

The maximum reported body mass (in grams) for each species was extracted from FishBase (Froese and Pauly, 2016) using the *rfishbase* package (Boettiger, Lang and Wainwright, 2012). Where maximum body mass data were unavailable, length-weight conversions available on FishBase were used to convert maximum length (cm) to weight (g). Data sourced from FishBase were manually checked from the original references and updated where necessary. Length-weight regression coefficient estimates were selected for females where possible and for the most appropriate length-measurement type (disc width or total length) depending on the species' body shape. If a length-weight conversion was unavailable for a species, then a length-weight conversion for a closely related species with a similar maximum size and body shape was used. Finally, there were two species where length-weight conversions were calculated from the Bayesian models available on FishBase (Froese et al., 2014).

Median depth estimates for each species were taken as the midpoint of the minimum and maximum depth ranges reported in the IUCN Red List Assessment of Threatened Species as

reported in Dulvy et al. (2021). Temperature-at-depth was then determined using species geographic range shape files available as part of a global reassessment of shark and ray species (see Dulvy et al. (2021) page e6 for details of distribution mapping and Data S3 for data sources available on the IUCN Red List of Threatened Species). Species distribution was overlaid with the International Pacific Research Center's interpolated dataset of gridded mean annual ocean temperatures across 27 depth levels (0-2000 m below sea level), which is based on measurements from the Argo Project (data available at http://apdrc.soest.hawaii.edu/projects/Argo/data/statistics/On_standard_levels/Ensemble_mea n/1x1/m00/index.html). The depth level that was closest to the species' median depth was selected from the grid and the temperature grid points were extracted across the species' distribution. Median temperature for each species was calculated from the distribution of temperature values.

2.3.3 How does r_{max} vary with body mass, temperature, and depth?

Across taxa, r_{max} has been shown to be related to body mass and temperature (Savage et al., 2004). These metabolic scaling expectations can be estimated with a linear model in natural logarithm (ln):

$$\ln(r_{max}) = \beta_0 + \beta_1 * \ln(M) + \beta_2 * 1/k_B T, \qquad (4)$$

where r_{max} is the maximum intrinsic rate of population increase (year⁻¹), β_0 is the intercept, β_1 is the mass-scaling coefficient, β_2 is the activation energy E, T is the temperature (in Kelvin) and k_B is the Boltzmann constant (8.617 × 10⁻⁵ eV).

Here, 24 models representing alternative hypotheses of how $r_{\rm max}$ may vary with body mass, temperature, and depth were compared using an information-theoretic approach (Burnham & Anderson, 2002) (Table 2.1). The above equation is the expectation from metabolic scaling theory and is one of the 24 hypotheses compared. $r_{\rm max}$ and adult body mass data were Intransformed. Temperature and depth data were standardised (scaled and centred) prior to analyses.

Table 2.1 The 24 models examined with associated hypotheses for how maximum intrinsic rate of population increase (r_{max}) varies with body mass M, inverse temperature ($1/k_BT$). depth and a composite temperature-depth index. The expected model from metabolic scaling theory is highlighted in grey. Note, Order was categorical for rays (Orders Myliobatiformes, Rhinopristiformes, and Torpediniformes) and skates (Order Rajiformes).

Model: $\ln(r_{\text{max}}) \sim$	Hypothesis: r_{max} varies with
1	$r_{\rm max}$ only
ln (<i>M</i>)	body mass only
depth	depth only
$1/k_BT$	temperature only
temperature-depth index	temperature-depth index only
ln(M) + depth	body mass and depth
$ln(M) + 1/k_BT$	body mass and temperature
ln(M) + temperature-depth index	body mass and temperature-depth index
ln(M) * depth	body mass and depth, and the effect of mass scaling coefficient varies with depth
$\ln(M) * 1/k_B T$	body mass and temperature, and the effect of mass scaling coefficient varies with temperature
ln(M) * temperature-depth index	body mass and temperature-depth index, and the effect of mass scaling coefficient varies with the temperature- depth index
1 + Order	Order
ln(M) + Order	body mass and Order
depth + Order	depth and Order
$1/k_BT$ + Order	temperature and Order
temperature-depth index + order	temperature-depth index and Order
lln(M) + depth + Order	body mass, depth, and Order
$ln(M) + 1/k_BT + Order$	body mass, temperature, and Order
ln(<i>M</i>) + temperature-depth index + Order	body mass, temperature-depth index, and Order
ln(M) * depth + Order	body mass, depth, and Order, and the effect of mass scaling coefficient varies with depth
$ln(M) * 1/k_BT + Order$	body mass, temperature, and Order, and the effect of mass scaling coefficient varies with temperature
ln(<i>M</i>) * temperature-depth index + Order	body mass, temperature-depth index, and Order, and the effect of mass scaling coefficient varies with the temperature-depth index
$ln(M) + 1/k_BT + depth$	body mass, temperature, and depth
$\ln(M) + 1/k_B T * \text{depth}$	body mass and the effect of temperature varies with depth

Twenty, random phylogenetic trees from the possible distribution of trees from Stein, Mull et al. (2018), and available at Vertlife.org, were used in analyses to include a random effect of phylogeny in all models. Note, the phylogeny was updated to reflect current taxonomic nomenclature, for example *Dasyatis americana* and *D. dipterura* in the phylogeny from Stein, Mull et al., (2018) were updated to *Hypanus americanus* and *H. diptererus*, respectively. There were two instances where the phylogenetic position of a species (*Aetobatus narutobiei* and *Maculabatis ambigua*) were not known, so the position (i.e., branch length or divergence time) of a closely related species (*A. flagellum* and *Maculabatis gerrardi*, respectively) was used instead. Taxonomic placement was also included as a categorical fixed term in the model to investigate how r_{max} scales with body mass, temperature, and depth in skates (Order Rajiformes) and rays (Orders Myliobatiformes, Rhinopristiformes, and Torpediniformes) given their different life history strategies (particularly high and low annual reproductive output, respectively) and distributions (encompassing different environmental temperatures and depths).

Phylogenetic generalised linear models were fitted to account for non-independence for closely related species using the pgls function in the caper package (Orme et al., 2018). In a pgls framework, the phylogeny is converted to a covariance matrix, which is included as a random effect and thus accounts for autocorrelation of the residuals due to species sharing various parts of evolutionary trajectories. The strength of the phylogenetic signal (i.e., how strong the residuals were correlated with the covariance matrix) is indicated by Pagel's λ , with a value of 1 meaning the residuals are perfectly correlated with the covariance matrix and a value of 0 meaning no correlation (Revell, 2010).

We assessed how sensitive our results were to the small variation in the random phylogenies used by re-fitting the models with a subset of 20 (randomly chosen) phylogenies available from Stein, Mull et al. (2018). The top model was always the same (Table 2.2) and we therefore only report results from using a single tree. We also assessed how sensitive our results were to the larger-bodied rays present in the dataset (body mass \geq 290 kg, n=8) by re-fitting models without these eight data points. The top model was the same (Table 2.3) and we therefore only report results using the full dataset.

Table 2.2 Corrected Akaike Information Criteria (Δ AICc) for the 24 models tested for how r_{max} varies with inverse temperature ($1/k_BT$), depth, adult body mass (M), the temperature-depth index, and Order, with 20 different phylogenetic trees obtained from Stein, Mull *et al.* (2018). The model with the lowest Δ AICc value in each iteration is highlighted in grey.

$\ln(r_{\text{max}}) \sim$	1	2	3	4	5	6	7	8	9	10	11	12	13	14	15	16	17	18	19	20
1	10.3	10.6	8.1	9.9	10.4	10.7	9.3	11.9	8.1	8.9	9.9	9.5	7.6	8.5	8.4	9.6	8.9	11.8	10.3	11.4
ln(M)	3	3.2	3.1	2.8	3.1	3.4	3.3	4.4	1.9	3.4	3.4	2	2.4	3.1	2.3	3.7	3.4	4.2	3.1	4
depth	7.6	7.9	5.4	7.8	7.2	7.5	5.4	8.1	6.7	5.4	7.1	8	5.7	5.9	6.1	6.3	5.4	7.5	7.6	8.4
$1/k_BT$	5.9	6.2	3.7	5.3	6.2	5.7	5.6	6.5	4.5	5.5	4.7	5	3.9	4.9	5	5.5	5.5	7.2	5.8	5.5
ln(M) + depth	1.4	1.4	1.4	1.6	1.1	1.4	0.9	1.6	1.3	0.9	1.7	1.6	1.2	1.2	1.1	1.3	0.9	1	1.3	2
$\ln(M) + 1/k_B T$	1.3	1.4	1.2	0.7	1.8	1.4	2.2	1.7	0.6	2.1	0.9	0.1	1.1	1.5	1.2	1.7	2.1	2.4	1.3	1
ln(M) * depth	3.6	3.3	3.6	3.6	3.3	3.6	3	3.6	3.2	2.9	3.9	3.7	3.4	3.1	3.2	3.4	2.9	2.9	3.5	3.7
$\ln(M) * 1/k_BT$	2.6	3.6	2.3	2.7	3.7	2.6	3.8	3.7	0.8	4.1	2.4	1.6	2.8	3.7	2.9	3.7	4.1	4.6	2.4	3.1
1 + Order	12.2	12.6	9.9	11.9	12.4	12.7	11.3	13.9	10.1	10.8	11.8	11.5	9.6	10.4	10.3	11.5	10.8	13.7	12.3	13.4
ln(M) + Order	5	5.2	5	4.8	5.2	5.4	5.4	6.4	3.9	5.3	5.4	4	4.4	5.1	4.3	5.7	5.3	6.2	5.1	6
depth + Order	9.2	9.4	6.8	9.4	8.9	9.1	7.1	9.8	8.4	6.7	8.7	9.7	7.4	7.5	7.9	7.9	6.7	8.9	9.2	9.9
$1/k_BT$ + Order	6.8	7	4.3	6.2	7.4	6.7	6.8	7.5	5.7	6	5.6	6	5.2	5.8	6.4	6.4	6	7.8	6.7	6.2
ln(M) + depth +	3	3	2.9	3.3	2.9	3.2	2.7	3.3	3	2.2	3.4	3.4	3	2.8	2.9	2.9	2.2	2.5	3	3.6
Order	3	3	2.)	3.3	2.)	3.2	2.1	3.3	5	2.2	J. T	J. T	3	2.0	2.)	2.7	2.2	2.3	3	3.0
$\ln(M) + 1/k_BT +$	2.5	2.5	2.1	1.9	3.3	2.7	3.6	3	2	2.9	2.2	1.5	2.5	2.6	2.6	2.9	2.9	3.4	2.5	2
Order									_											_
ln(M) * depth +	5.3	4.9	5.1	5.3	5.2	5.4	4.8	5.3	5.1	4.2	5.6	5.6	5.3	4.7	5.1	5.1	4.2	4.3	5.3	5.4
Order																				
$ln(M) * 1/k_BT + $ Order	3.8	4.7	3.1	3.9	5.2	3.9	5.3	4.9	2.3	4.9	3.5	2.9	4.3	4.8	4.3	4.9	4.9	5.7	3.7	4.2
$\ln(M) + 1/k_B T +$																				
depth	2.1	2.1	2.1	2	2.2	2.2	2.2	2.1	2	2.2	2	1.8	2.1	2.2	2.1	2.2	2.2	2.2	2.1	2
$\ln(M) + 1/k_B T *$																				
depth	1.7	2	1.7	1.8	1.9	1.9	1.9	2	1.9	2.1	1.5	0.8	1.8	2.7	2.6	2.7	2.1	2.5	1.1	1.6
temperature-depth	7 1	<i>5</i> 2	2	7 1	4.0	4.0	2.5	<i>r</i> 2	4.4	2.5	4.0	~ 1	2.4	2.0	4.1	4	2.5	<i>7</i> 1	7 1	7. 1
index	5.1	5.3	3	5.1	4.8	4.8	3.5	5.3	4.4	3.5	4.2	5.4	3.4	3.8	4.1	4	3.5	5.1	5.1	5.1

ln(<i>M</i>) +																				
temperature-depth	0	0	0	0	0	0	0	0	0	0	0	0	0	0	0	0	0	0	0	0
index																				
ln(M) *																				
temperature-depth	1.9	2.2	1.9	2.2	2	1.8	1.7	2.2	1.2	2.1	2.1	2.1	2	2.2	1.9	2.2	2.1	2.2	2	2.2
index																				
temperature-depth	6.1	6.2	3.7	6.1	6	5.9	4.8	6.4	5.7	4.1	5.4	6.7	4.7	4.8	5.5	5	4.1	5.8	6.2	6
index + Order	0.1	0.2	3.7	0.1	O	3.9	4.0	0.4	3.7	4.1	3.4	0.7	4.7	4.0	5.5	3	4.1	3.6	0.2	6
ln(M) +																				
temperature-depth	1.2	1.1	0.9	1.2	1.5	1.3	1.4	1.3	1.3	0.7	1.2	1.4	1.4	1.1	1.4	1.1	0.7	0.9	1.3	1.1
index + Order																				
ln(M) *																				
temperature-depth	3.2	3.3	2.9	3.4	3.5	3.2	3.2	3.6	2.8	2.9	3.4	3.6	3.5	3.3	3.4	3.4	2.9	3.1	3.4	3.3
index + Order																				

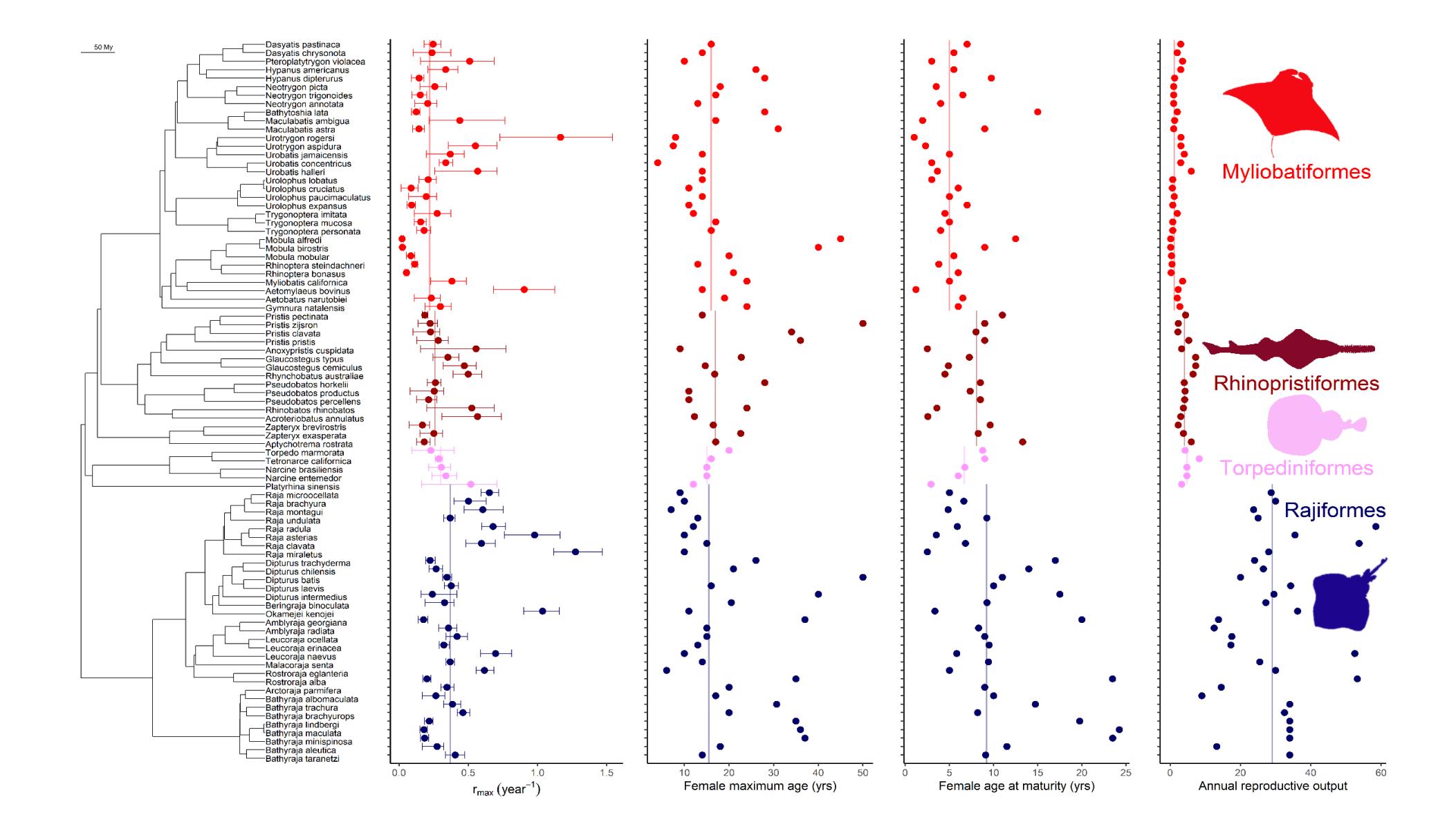


Figure 2.1 Phylogeny, maximum intrinsic rate of population increase (r_{max}), female maximum age in years, female age at maturity in years and annual reproductive output (number of female offspring) for 85 ray and skate species. Solid lines show median values for Myliobatiformes (n=32), Rhinopristiformes (n=16), Torpediniformes (n=5) and Rajiformes (n=32). Uncertainty in r_{max} estimate shown with 2.5% and 97.5% quantiles. A single phylogenetic tree from the possible distribution of trees from Stein, Mull, *et al.*, (2018) is displayed.

Depth and temperature were positively correlated (Pearson's r = 0.75), with a value higher than a threshold of 0.70 in which collinearity severely distorts model estimation (Dormann et al., 2013). We therefore used Principal Components Analysis (PCA) to collapse the temperature and depth variables into one Principal Component (PC), a composite temperature and depth index (PC1 axis; hereafter, temperature-depth index), that explained 87% of the variance. The temperature-depth index was included in place of temperature and depth in some models to examine whether a combined metric better explained r_{max} compared to these environmental variables alone (Table 2.1). We also estimated variance-inflation factors (VIF) to assess collinearity for all coefficients in the models using the car package (Fox & Weisberg, 2019). No VIF value was greater than two, except as expected when interactions were included, indicating that our models were robust to collinearity despite the strong correlation between temperature and depth. Models were compared using the corrected Akaike Information Criterion (AICc). If including a parameter improved the model's AICc by less than two units $(\Delta AICc \le 2)$, it was considered relatively uninformative (Arnold, 2010; Burnham & Anderson, 2002). All analyses were run in R version 4.1.2 (R Core Team, 2021) in RStudio (RStudio Team, 2021).

2.4 Results

Maximum population growth rate, r_{max} , was estimated using collated life history data (α_{max} , α_{mat} , and b) for 85 ray and skate species and r_{max} estimates varied between 0.0213 yr⁻¹ (in *Mobula alfredi*) and 1.28 yr⁻¹ (in *Raja miraletus*) (Figure 2.1). It was evident that there were two groupings of data: warm, shallow-water rays (n=53) with relatively low annual reproductive output and cold, deep-water skates (n=32) with higher annual reproductive output (Figure 2.1; Figure 2.2). Generally, compared to rays, the skates had a later age at maturity (α_{mat} : skates median = 9.20 ±1.09 SE; rays = 6.0 ±0.42 SE) and higher annual reproductive output (b: skates median = 29.10 ±2.17 SE; rays = 3.0 ±0.28 SE) but there was little difference in longevity (α_{max} :

skates median = 15.50 \pm 2.02 SE; rays = 16.0 \pm 1.28 SE). Consequently, skates had a higher median r_{max} (0.37 yr⁻¹ \pm 0.05 SE) compared to rays (0.25 yr⁻¹ \pm 0.03 SE).

Table 2.3 Comparison of $\ln(r_{\text{max}})$ models re-ran with data points for eight larger-bodied rays (body mass $M \ge 290 \text{ kg}$) removed, using corrected Akaike Information Criteria (AICc), number of parameters (n), negative log-likelihood (-LL), adjusted R^2 (Adj. R^2) and Akaike weights. The model with the lowest Δ AICc value is marked in bold and models with Δ AICc ≤ 2 are highlighted in grey. Models are ordered by ascending AICc, with the top model first.

$\ln(r_{\max}) \sim$	n	LL	AICc	Adj. R ²	ΔAICc	Weights
ln(M) + temperature-depth index	3	-57	120.3	0.06	0	0.126
temperature-depth index	2	-58.5	121.1	0.04	0.8	0.084
ln(M) + depth	3	-57.4	121.2	0.05	0.9	0.080
ln(M) + temperature-depth index + Order	4	-56.5	121.6	0.06	1.3	0.066
$\ln\left(M\right) + 1/k_BT$	3	-57.7	121.7	0.05	1.4	0.062
ln(M)	2	-59	122.1	0.03	1.8	0.051
depth	2	-59	122.2	0.02	1.9	0.049
$1/k_BT$	2	-59	122.2	0.03	1.9	0.049
temperature-depth index + Order	3	-58	122.3	0.04	2	0.046
ln(M) * temperature-depth index	4	-56.9	122.4	0.06	2.1	0.044
$ln(M) + 1/k_BT + depth$	4	-57	122.5	0.05	2.2	0.042
ln(M) + depth + Order	4	-57.2	122.9	0.05	2.6	0.034
1	1	-60.5	123	0	2.7	0.033
$ln(M) + 1/k_BT + Order$	4	-57.2	123	0.05	2.7	0.033
ln(M) * depth	4	-57.4	123.4	0.04	3.1	0.027
$1/k_BT$ + Order	3	-58.5	123.4	0.02	3.1	0.027
$ln(M) + 1/k_BT * depth$	5	-56.3	123.5	0.06	3.2	0.025
$\ln(M) * 1/k_BT$	4	-57.5	123.6	0.04	3.3	0.024
ln(M) * temperature-depth index + Order	5	-56.4	123.7	0.05	3.4	0.023
depth + Order	3	-58.7	123.8	0.02	3.5	0.022
ln(M) + Order	3	-58.9	124.1	0.02	3.8	0.019
1 + Order	2	-60.4	124.9	-0.01	4.6	0.013
$ln(M) * 1/k_BT + Order$	5	-57	124.9	0.04	4.6	0.013
ln(M) * depth + Order	5	-57.1	125.1	0.03	4.8	0.011

Table 2.4 Comparison of r_{max} models using corrected Akaike Information Criteria (AICc), number of parameters (n), negative log-likelihood (-LL), adjusted R^2 (Adj. R^2), and Akaike weights. Models are ordered by ascending AICc, with the top model highlighted in bold and models with Δ AICc < 2 highlighted in grey.

$\ln(r_{\text{max}}) \sim$	n	LL	AICc	Adj. R ²	ΔAICc	Weights
ln(M) + temperature-depth index	3	-65.4	137.2	0.14	0	0.177
ln(M) + temperature-depth index + Order	4	-65	138.4	0.14	1.2	0.097
$ln(M) + 1/k_BT$	3	-66.1	138.5	0.12	1.3	0.092
ln(M) + depth	3	-66.1	138.6	0.12	1.4	0.088
$ln(M) + 1/k_BT * depth$	5	-64.1	138.9	0.14	1.7	0.076
ln(M) * temperature-depth index	4	-65.3	139.1	0.13	1.9	0.068
$ln(M) + 1/k_BT + depth$	4	-65.4	139.3	0.13	2.1	0.062
$ln(M) + 1/k_BT + Order$	4	-65.6	139.7	0.12	2.5	0.051
$ln(M) * 1/k_BT$	4	-65.7	139.8	0.13	2.6	0.048
ln(M)	2	-68	140.2	0.09	3	0.039
ln(M) + depth + Order	4	-65.9	140.2	0.12	3	0.039
ln(M) * temperature-depth index + Order	5	-64.8	140.4	0.13	3.2	0.036
ln(M) * depth	4	-66.1	140.8	0.11	3.6	0.029
$ln(M) * 1/k_BT + Order$	5	-65.1	141	0.13	3.8	0.026
ln(M) + Order	3	-68	142.2	0.08	5	0.015
temperature-depth index	2	-69.1	142.3	0.07	5.1	0.014
ln(M) * depth + Order	5	-65.9	142.5	0.11	5.3	0.012
$1/k_BT$	2	-69.5	143.1	0.06	5.9	0.009
temperature-depth index + Order	3	-68.5	143.3	0.07	6.1	0.008
$1/k_BT$ + Order	3	-68.8	144	0.06	6.8	0.006
depth	2	-70.3	144.8	0.04	7.6	0.004
depth + Order	3	-70.1	146.4	0.04	9.2	0.002
1	1	-72.7	147.5	0	10.3	0.001
1 + Order	2	-72.6	149.4	-0.01	12.2	0

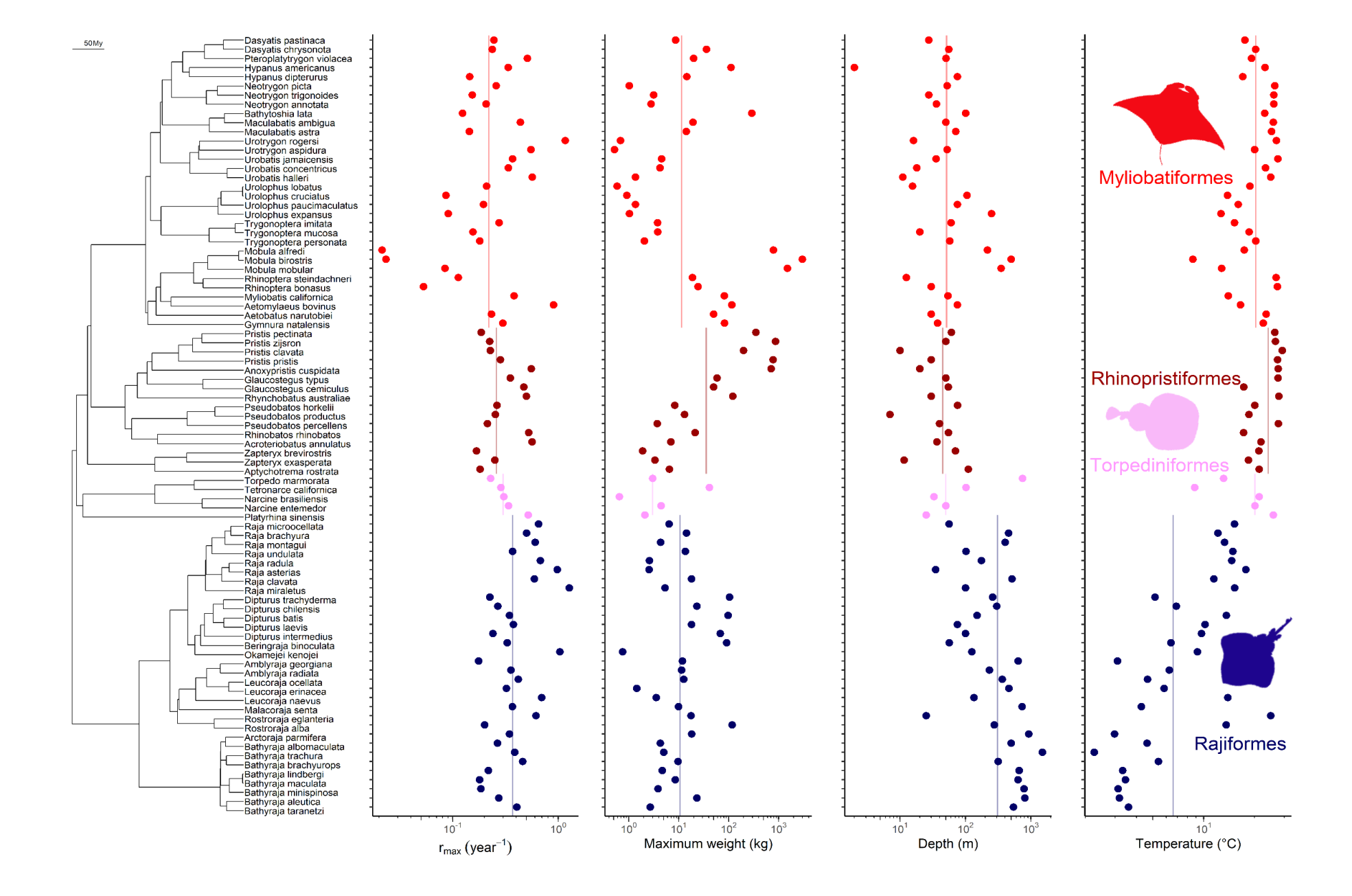


Figure 2.2 Phylogeny, maximum intrinsic rate of population increase (r_{max}) , maximum weight (kg), median depth (m) and median temperature (°C) in log10 space for 85 ray and skate species. Solid lines show median values for Myliobatiformes (n=32), Rhinopristiformes (n=16), Torpediniformes (n=5) and Rajiformes (n=32). A single phylogenetic tree from the possible distribution of trees from Stein, Mull et al., (2018) is displayed.

Six of the 24 models examined had $\triangle AICc < 2$, providing substantial support for describing variation in r_{max} across species (Burnham & Anderson, 2002) (Table 2.4). The top model with the greatest support (\triangle AICc=0) was for r_{max} varying with body mass and the temperature-depth index (adjusted R^2 =0.14). Including taxonomic Order in the relationship between r_{max} and body mass and the temperature-depth index, received approximately 55% of the support of the topranked model and resulted in no increase in adjusted R^2 (adjusted R^2 =0.14). The 95% confidence intervals for the coefficient estimate for Order in this model also overlapped zero suggesting that the effect size was not significant (Table 2.3). Including an interaction between body mass and the temperature-depth index received 38% of the support of the top-ranked model and explained less variation (adjusted $R^2=0.13$). Model results suggest that the temperature-depth index, temperature or depth can be used interchangeably. Models for r_{max} varying with body mass and temperature and body mass and depth received approximately 50% of the support of the top-ranked model and accounted for less variation (adjusted $R^2=0.12$). Finally, a model for r_{max} varying with body mass, temperature, and depth, with an interaction term between temperature and depth, received less than half of the support of the top-ranked model (approximately 43%) and accounted for the same variation (adjusted $R^2 = 0.14$). Eight other models had moderate support ($< 2 \Delta AICc \ge 4$), with marginal support for six other models $(\leq 5 \Delta AICc \geq 7)$ (Table 2.4).

The scaling of body mass in all models was shallower (-0.12 to -0.10) than expected from metabolic scaling theory (-0.33 to -0.25) (Table 2.5; Figure 2.3). Temperature had a positive effect on r_{max} as the coefficient of inverse temperature $1/k_BT$ (activation energy E) was consistently negative, suggesting r_{max} is higher in species found in warmer waters (Table 2.3). The effect of depth was negative across all models suggesting r_{max} is lower in species found at greater depths (Table 2.3). An overall positive relationship between r_{max} and temperature was evident in both rays and skates (Figure 2.4a) and was mirrored by a negative relationship between r_{max} and depth (Figure 2.4b), as would be expected from metabolic scaling theory. Although a shallower relationship, there was a negative relationship between r_{max} and body

mass when controlling for a constant temperature (Figure 2.5a), depth (Figure 2.5b), and temperature-depth index (Figure 2.6). Whilst r_{max} was found to be lower at greater depths (Figure 2.5b) in line with metabolic scaling theory, r_{max} was also found to be lower at warmer temperatures (Figure 2.5a), contrary to metabolic scaling expectations. Further, when controlling for a constant temperature-depth index, warm, shallow-water rays showed lower r_{max} compared to cold, deep-water skates (Figure 2.6). There was a strong phylogenetic signal from the residuals of r_{max} in all models examined, with Pagel's $\lambda \geq 0.87$ (Table 2.4).

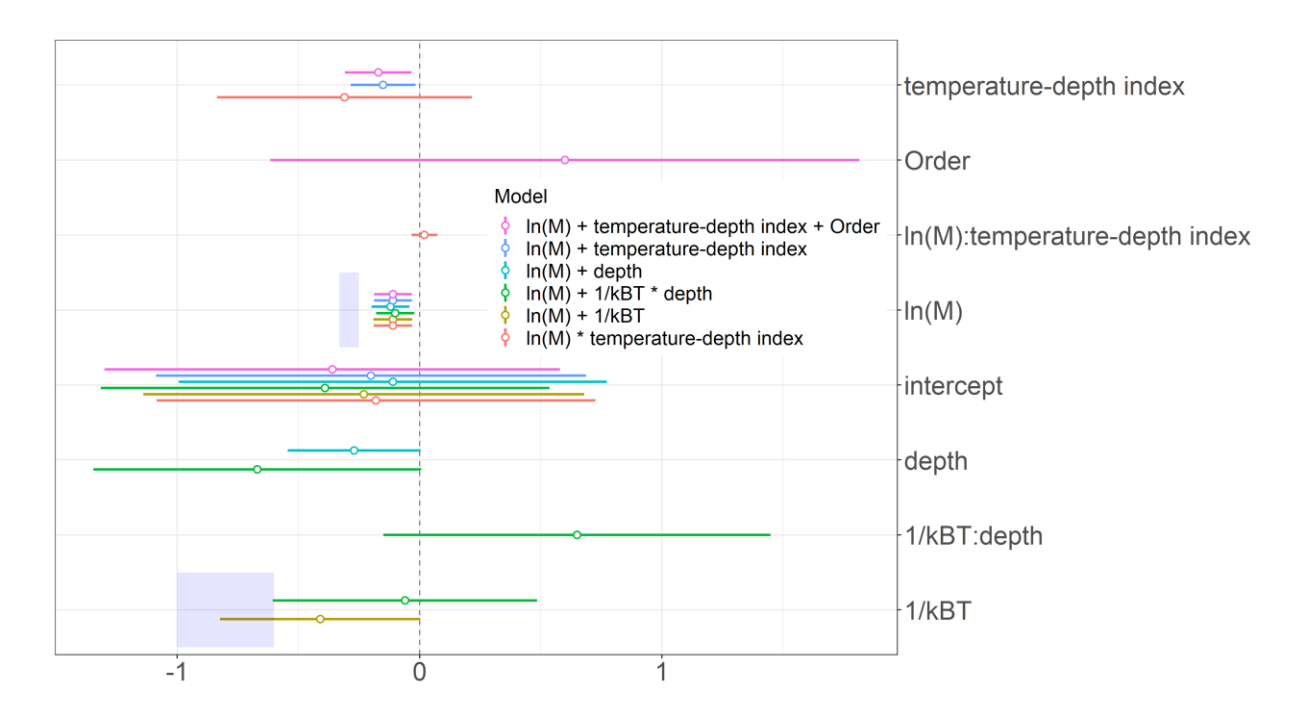


Figure 2.3 Coefficient estimates for the six models of $ln(r_{max})$ with AICc values < 2. Error bars show 95% confidence intervals. Effect sizes were considered significant when confidence intervals do not overlap zero. Shaded area shows the expected effect sizes for body mass (-0.33 to -0.25) and temperature (-1.0 to -0.6) based on metabolic theory.

Table 2.5 Coefficient estimates (95% confidence intervals estimated from standard errors shown in brackets) for all models of $\ln(r_{\text{max}})$. The model with the lowest Δ AICc value is marked in bold and the models with Δ AIC < 2 are highlighted in grey. Pagel's λ indicates the strength of the phylogenetic signal.

ln(r _{max}) ~	intercept	ln(M)	depth	$1/k_BT$	ln(M): depth	ln(M): 1/k _B T	Order	depth: $1/k_BT$	temperature -depth index	ln(M): temperature -depth index	Pagel's λ
1	-1.17		-	-	-	-		-	-	-	0.88
1	(-1.71, -0.62)	-					-				(0.69, 0.96)
1 + Order	-1.23	-	-	-	-	-	0.25	-	-	-	0.88
1 / 01461	(-1.85, -0.6)						(-1.05, 1.55)				(0.68, 0.96)
depth	-1.18	-	-0.32	-	-	-		-	-	-	0.88
	(-1.71, -0.65)		(-0.6, -0.03)				-				(0.68, 0.96)
depth + Order	-1.29	-	-0.33	-	-	-	0.47	-	-	-	0.87
•	(-1.9, -0.69)		(-0.62, -0.05)	0.55			(-0.8, 1.73)				(0.65, 0.96)
$1/k_BT$	-1.22	-	-	-0.55	-	-		-	-	-	0.89
, 5	(-1.76, -0.68)			(-0.96, -0.13)			0.74				(0.71, 0.97)
$1/k_BT$ + Order	-1.4	-	-	-0.61	-	-	(-0.57, 2.05)	-	-	-	0.89
	(-2.02 , -0.78) -0.01	-0.12		(-1.04, -0.18)			(-0.57, 2.05)				(0.68, 0.97) 0.88
ln(M)	(-0.91, 0.89)	-0.12 (-0.2, -0.05)	-		-	-	-	-	-	-	(0.69, 0.96)
	-0.91 , 0.89)	-0.12	-0.30	-	0						0.88
ln(M) * depth	(-1, 0.79)	(-0.2, -0.04)	(-1.75, 1.15)		(-0.15, 0.16)	-	-	-	-	-	(0.63, 0.96)
ln(M) * depth +	-0.21	-0.12	-0.29	-	0		0.43				0.87
Order	(-1.16, 0.73)	(-0.19, -0.04)	(-1.75, 1.17)	_	(-0.16, 0.16)	_	(-0.78, 1.65)	_	_	_	(0.59, 0.96)
	-0.2	-0.11	(-1.75 , 1.17)	-1.16	(-0.10, 0.10)	0.07	(-0.76, 1.03)	_	_	_	0.92
$ln(M) * 1/k_BT$	(-1.13, 0.73)	(-0.19, -0.03)		(-2.61, 0.29)	_	(-0.06, 0.21)	_				(0.72, 0.98)
$ln(M) * 1/k_BT +$	-0.39	-0.11	_	-1.26		0.08	0.69	_	_	_	0.91
Order	(-1.39, 0.61)	(-0.19, -0.03)		(-2.73, 0.21)	_	(-0.06, 0.22)	(-0.64, 2.01)				(0.69, 0.98)
ln(M) *	(1.05, 0.01)	(0.15 , 0.05)	_	-	-	-	(0.0 . , 2.01)	-			(0.05, 0.50)
temperature-depth	-0.18	-0.11							-0.31	0.02	0.90
index	(-1.08, 0.73)	(-0.19, -0.03)					_		(-0.84, 0.22)	(-0.04, 0.07)	(0.67, 0.97)
ln(M) *	, , ,	, ,	-	-	-	-		-	,	, , ,	,
temperature-depth	-0.34	-0.11					0.61		-0.32	0.02	0.89
index + Order	(-1.3, 0.62)	(-0.19, -0.03)					(-0.65, 1.86)		(-0.85, 0.21)	(-0.04, 0.07)	(0.63, 0.97)
In(M) + donth	-0.11	-0.12	-0.27	-	-	-		-	-	-	0.88
ln(M) + depth	(-0.99, 0.78)	(-0.19, -0.04)	(-0.55, 0)				-				(0.67, 0.96)
ln(M) + depth +	-0.21	-0.12	-0.29	-	-	-	0.43	-	-	-	0.87
Order	(-1.15, 0.72)	(-0.19, -0.04)	(-0.57, -0.01)				(-0.78, 1.65)				(0.64, 0.96)
$\ln{(\mathrm{M})} + 1/k_B T$	-0.23	-0.11		-0.41	-	-	-	-	-	-	0.89
	(-1.13, 0.68)	(-0.19, -0.03)	-	(-0.83, 0)							(0.68, 0.96)
$ln(M) + 1/k_BT *$	-0.39	-0.10	-0.67	-0.06	=	-	-	0.65	=	-	0.89
depth	(-1.31, 0.54)	(-0.18, -0.02)	(-1.35, 0.01)	(-0.6, 0.49)				(-0.15, 1.45)			(0.69, 0.97)

$\ln(\mathrm{M}) + 1/k_BT +$	-0.22	-0.11	-0.18	-0.28	-	-		-	-	-	0.88
depth	(-1.13, 0.68)	(-0.19, -0.03)	(-0.49, 0.13)	(-0.75, 0.19)			-				(0.67, 0.96)
$\ln(M) + 1/k_BT +$	-0.40	-0.10	-	-0.47	-	-	0.63	-	-	-	0.88
Order	(-1.37, 0.57)	(-0.18, -0.02)		(-0.9, -0.04)			(-0.63, 1.88)				(0.65, 0.96)
In (M) + Ondon	-0.07	-0.12	-		-	-	0.25	-	-	-	0.88
ln(M) + Order	(-1.02, 0.88)	(-0.2, -0.05)		-			(-0.99, 1.49)				(0.68, 0.96)
ln(M) +			-	-	-	-	-	-		-	
temperature-	-0.20	-0.11							-0.15		0.88
depth index	(-1.09, 0.69)	(-0.19, -0.03)							(-0.29, -0.02)		(0.67, 0.96)
ln(M) +			-	-	-	-		-		-	
temperature-depth	-0.36	-0.11					0.60		-0.17		0.87
index + Order	(-1.3, 0.58)	(-0.18, -0.03)					(-0.62, 1.81)		(-0.31, -0.03)		(0.63, 0.96)
temperature-depth	-1.21	-	-	-	-	-		-	-0.19	-	0.88
index	(-1.74, -0.68)						-		(-0.32, -0.05)		(0.69, 0.96)
temperature-depth	-1.37	-	-	-	-	-	0.67	-	-0.21	-	0.87
index + Order	(-1.97, -0.77)						(-0.59, 1.94)		(-0.35, -0.07)		(0.65, 0.96)

.

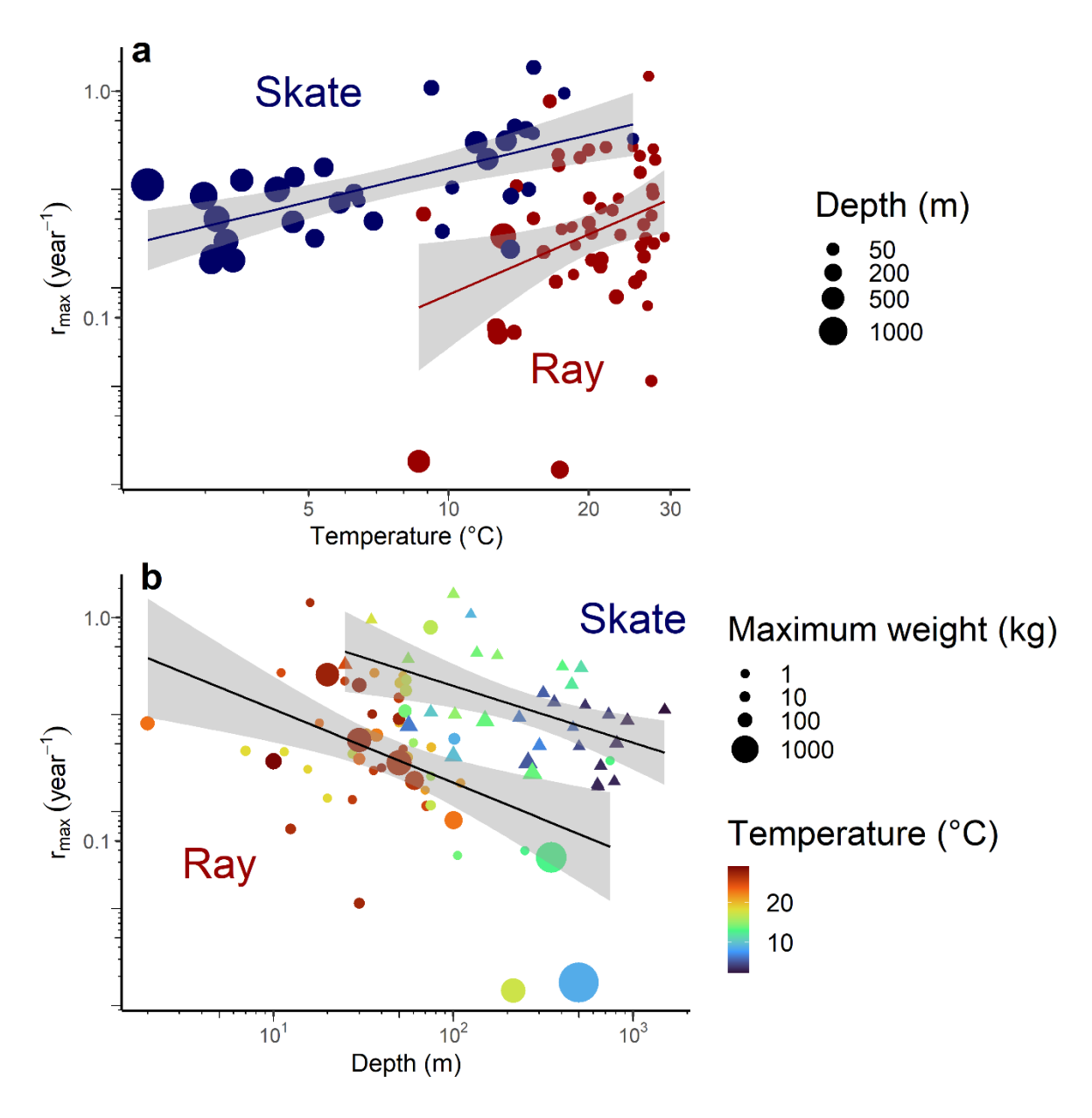


Figure 2.4 Relationship between maximum intrinsic rate of population increase (r_{max}) and a) temperature (°C) and b) depth (m) in log10 space for 53 ray (Orders Myliobatiformes, Rhinopristiformes, and Torpediniformes) and 32 skate (Order Rajiformes) species. a) Median depth (m) is shown by the point size, with a linear model fitted to ray (red) and skate (blue) points. b) Median temperature (°C) and maximum weight (kg) is shown by the point colours and size, respectively, with a linear model fitted to ray (circular) and skate (triangular) data points. The grey band around the fitted models show the confidence intervals.

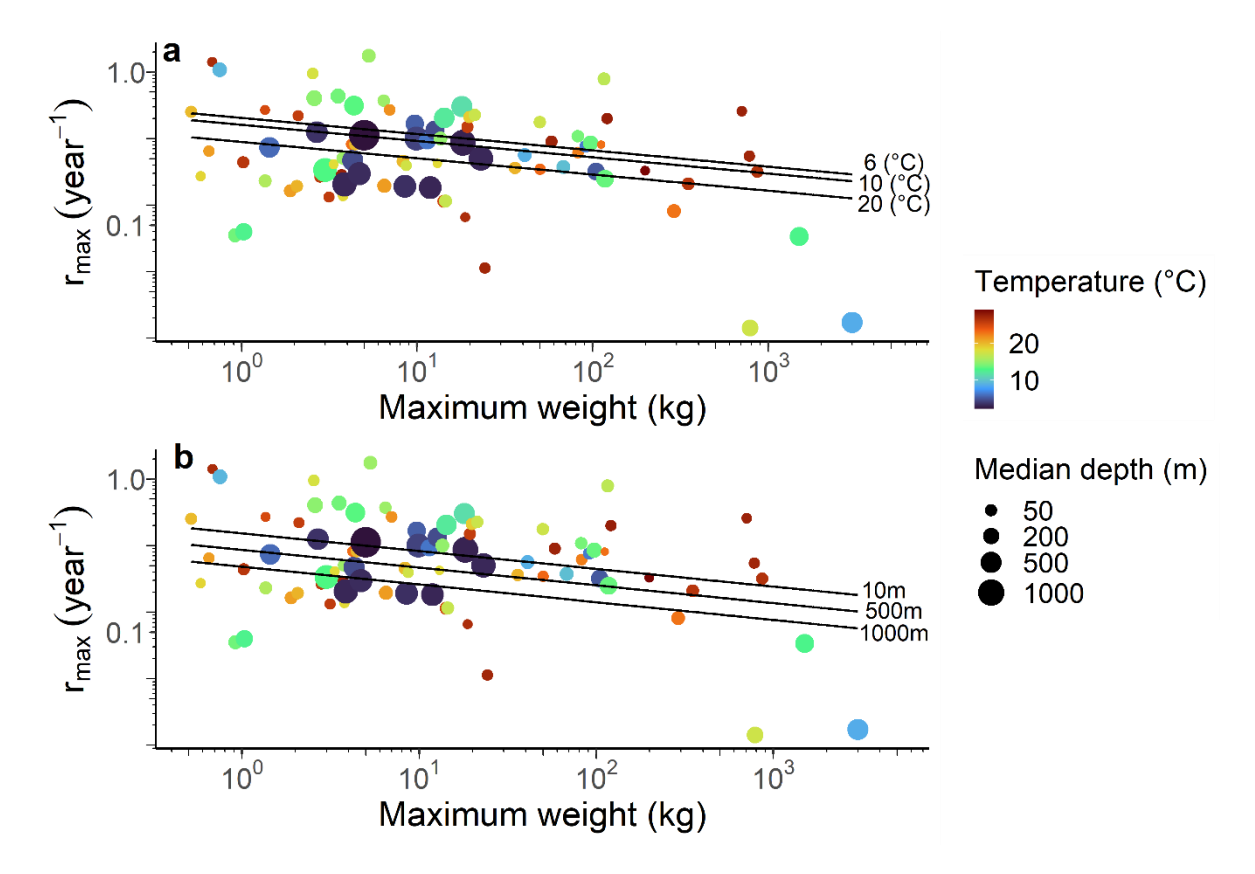


Figure 2.5 Relationship between maximum intrinsic rate of population increase (r_{max}) and body mass in $\log 10$ space for 85 ray species. Fitted lines show predicted relationships based on the top-ranked models: a) $\ln(r_{\text{max}}) \sim \ln(M) + (1/k_BT)$ and b) $\ln(r_{\text{max}}) \sim \ln(M) + \text{depth}$. Predicted allometric changes of r_{max} across a) median temperatures (6, 10, 20 °C) and b) median depths (10, 500, 1000 m). Median temperature and depth are shown by the point colour and size, respectively.

2.5 Discussion

We find empirical evidence for a positive relationship between the maximum intrinsic rate of population increase (r_{max}) and temperature. However, paradoxically, the live-bearing, tropical rays have a much lower r_{max} than egg-laying, temperate skates. Metabolic theory and empirical patterns suggest that, after controlling for body size, r_{max} should increase with temperature both among populations and across species (Bernhardt et al., 2018; Savage et al., 2004; Luhring & Delong, 2017). This positive relationship between temperature and r_{max} is consistent with the biogeographic pattern that deep-water species, including sharks, generally have lower r_{max} and are more prone to being overfished than their shallow-water relatives. We found good support for models that included temperature, depth, or a temperature-depth index in the relationship between r_{max} and body mass, such that depth may also be used as a proxy where temperature

data may not be available. Below we hypothesise that this paradoxical pattern arises because the cooler-deeper waters are dominated by skates, which are relatively fecund egg-layers, whereas the warmer-shallower waters are dominated by rays, which give birth to few, larger offspring. Next, we discuss (1) the temperature-related biogeography of r_{max} ; (2) intrinsic sensitivity to overexploitation and extinction risk; (3) life history correlates of population responses; (4) whether reproductive strategies can explain the r_{max} paradox (that warm-shallow-water tropical rays have lower r_{max} than cold-deep-water skates); (5) fisheries implications, and (6) future research directions.

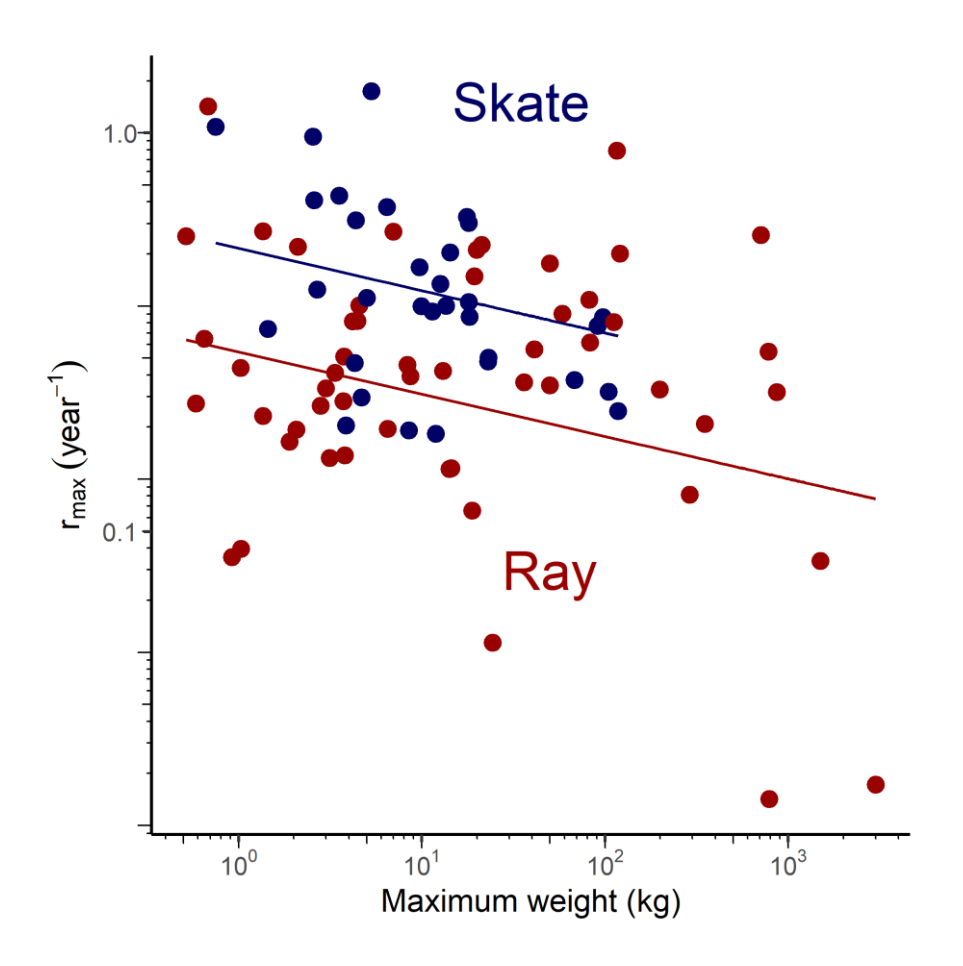


Figure 2.6 Relationship between maximum intrinsic rate of population increase (r_{max}) and body mass in log10 space for 53 ray species (Orders Myliobatiformes, Rhinopristiformes, and Torpediniformes) and 32 skate species (Order Rajiformes). Fitted lines show predicted relationships based on the top-ranked model: $ln(r_{max}) \sim ln(M)$ + temperature-depth index + Order. Predicted allometric changes of r_{max} across constant temperature-depth index (PC1 = 1) for ray (red) and skate (blue) data points.

There are a number of temperature-related, biogeographical patterns in r_{max} . Generally, biological processes are temperature-dependent, for example, metabolic rate increases exponentially with temperature above 15°C for ectotherms (Clarke & Johnston, 1999; Clarke, 2017; Dillon et al., 2010). Individual metabolic rate is fundamental to physiological performance and has effects at the population, community, and ecosystem levels (Brown et al., 2004; Pörtner, 2001). Consequently, experimental treatments of algal cultures exhibit increased population growth rates and lower carrying capacity at higher temperatures (Bernhardt et al., 2018; Luhring & Delong, 2017) and comparative analyses reveal that species found at warmer temperatures tend to have higher r_{max} compared to those found at cooler temperatures (Savage et al., 2004; Angilletta et al., 2010). It is therefore not surprising that r_{max} was found to increase with increasing environmental temperature for rays and skates in this study nor that r_{max} decreased with increasing depth. This is in line with theoretical and empirical temperaturerelated, latitudinal patterns that organisms with higher metabolic rates and 'fast' life histories in warmer waters (tropical, low latitudes) will have higher r_{max} , than those with slower metabolic rates and 'slow' life histories in cooler waters (temperate and polar, high latitudes) (Brown et al., 2004; Clarke & Johnston, 1999; Juan-Jordá et al., 2013). It follows that species with lower r_{max} at cooler, higher latitudes have been found to face greater population declines and therefore higher extinction risk than those with faster life histories at warmer, lower latitudes (Jennings et al., 1999; Juan-Jordá et al., 2015). Similarly, these temperature-related, latitudinal patterns may be evident over a depth gradient. This has been found in sharks, where cooler, deep-water species have a lower r_{max} (Pardo & Dulvy, 2022) and face higher extinction risk and lower population recovery rates (García et al., 2008; Simpfendorfer & Kyne, 2009).

Generally, deep-water sharks have lower somatic growth rates, later maturity, and greater longevity, with many live-bearing, deep-water sharks having a smaller body size and lower annual reproductive output (Rigby & Simpfendorfer, 2015). Consequently, r_{max} has been found to be lower in deep-water sharks compared to continental shelf and oceanic pelagic species (García et al., 2008). A similar pattern has been found using intrinsic rebound potentials, which is another measure of population growth rate (Simpfendorfer & Kyne, 2009; Smith et al., 1998). Expanding beyond these analyses that focussed on three categorical habitat types, Pardo & Dulvy (2022) investigated the effects of environmental temperature, depth, and mass scaling on r_{max} for sharks and rays. They found that deep-water species have a lower r_{max} due to the combined effects of cooler temperatures and an independent depth effect that could be due to multiple physiological and ecological factors, for example, lower secondary production at

greater depths (Jahnke, 1996). To date, this literature has focussed on sharks in which the phylogenetic divergence between deep-water species (Superorder Squalomorphii) and shallowwater species (Superorder Galeomorphii) is relatively distant, for example, deep-water Dogfishes (Order Squaliformes) compared to shallow-water Horn Sharks (Heterodontiformes) and Mackerel Sharks (Lamniformes). Indeed, the hypothesised sequence of evolution is that ancestral sharks were deep-water species with small brains and low reproductive investment that subsequently gave rise to shallow-water lineages with lower fecundity and larger more complex brains (Compagno, 1990; Mull et al., 2020). In our analysis of rays and skates, we also found that r_{max} decreased with increasing depth and that this was mirrored by the relationship with temperature but that shallow-water tropical rays still had a lower r_{max} relative to cold-deepwater temperate skates. Compared to sharks, the divergence between skates (Order Rajiformes) and other rays (Orders Myliobatiformes, Rhinopristiformes, and Torpediniformes) is more recent and clearly geographically defined, with the skates arising and radiating mainly in the Arctic polar and North Atlantic and North Pacific temperate latitudes and having a distinct pattern of egg-laying and much greater fecundity than the tropical rays (McEachran & Miyake, 1990; Frisk, 2010).

Instead of low temperature, we hypothesise the reason for slow life histories and low r_{max} estimates in deep-water sharks, such as Gulper Sharks (Family Centrophoridae), is their very low fecundity, typically less than five female offspring per year (Graham & Daley, 2011; Cotton et al., 2015; Paiva et al., 2011). Such low fecundity limits r_{max} and results in a low capacity for density-dependent compensation (Pardo et al., 2018). Similarly, many tropical rays have very low fecundity, notably the largest radiation of tropical rays: the Myliobatiformes. This Order has some species that produce only one to two very large offspring, no more frequently than once per year. For example, Devil rays (*Mobula* spp.) produce a single, large pup (rarely twins) born every 1-7 years (Rambahiniarison et al., 2018a; White et al., 2006; Marshall & Bennett, 2010). Consequently, they have amongst the lowest r_{max} found for sharks and rays, as found in this and previous studies (Pardo, Kindsvater, Cuevas-Zimbrón, et al., 2016; Dulvy, Pardo, et al., 2014; Rambahiniarison et al., 2018b). The fecundity of live-bearing shark and ray species more generally is lower when compared to egg-laying species of a similar body size, as they are limited by the size of the maternal body cavity given internal embryonic development (Wourms & Lombardi, 1992; Musick & Ellis, 2005). The study results suggest that skates may be different to deep-water sharks that live longer, mature later, and have a lower annual reproductive output, and consequently are more intrinsically sensitive (Rigby and Simpfendorfer, 2015). This variation around expectations from metabolic theory is likely due to their egg-laying reproductive strategy, resulting in higher fecundity and higher r_{max} (Pardo et al., 2018). This is in line with previous studies that have found higher extinction risk and slower population recovery rates in live-bearing, less fecund species (García et al., 2008; Simpfendorfer & Kyne, 2009).

Although our dataset includes species from all four Orders of rays and skates, including 18 of 26 families, there were only sufficient life history data to calculate r_{max} for 13% of assessed species on the IUCN Red List. There were no representatives from some families and therefore there may be exceptions to the observed global patterns in r_{max} discussed thus far. For example, there are some deep-water stingrays (Order Mylibatiformes) including Hexatrygon bickelli and Plesiobatis daviesi that were not in our dataset because their biology is poorly known. The former is live-bearing producing litter sizes of two to three pups, whilst the latter is likely viviparous with small litter sizes and a long gestation period (Finucci & García, 2024; Kyne & García, 2023; Ebert et al., 2002). Consequently both species likely have slow life histories, which would be more consistent with other deep-water chondrichthyans and suggest that fecundity may help explain variation in r_{max} observed amongst rays and skates. Equally, there are examples of shallow-water egg-laying skates such as Zearaja maugeana and Okamejei schmidti, which likely have relatively high fecundity based on congeners (e.g. of species used in our analyses O. kenojei lays 42-103 egg cases per year and D. batis and D. laevis lays 40-47 egg cases per year), although this remains unknown (Clark, 1922; Casey & Myers, 1998; Ishihara et al., 2002; Gedamke et al., 2005). Again, this would be more consistent with metabolic expectations for shallow-water chondrichthyans and suggest that differences in reproductive strategies are responsible for the deviation from metabolic theory for rays and skates in this study.

Skates in this study had a later median age at maturity, similar maximum age, but higher annual reproductive output compared to the rays. Whilst age at maturity has been found to be a major negative correlate of r_{max} (Hutchings et al., 2012), it is likely that the higher reproductive output is leading to higher r_{max} estimates, which may translate to lower intrinsic sensitivity. There will be a trade-off in energy investment in life history traits, such that offspring size is inversely related to fecundity, with less fecund species having larger offspring (Cortés, 2000). Recent work suggests that offspring size may be an important determinant of r_{max} (Denéchère et al., 2022). At the larger taxonomic scale, there are broadly two breeding strategies in marine organisms: well-provisioned offspring that are proportional in size compared to the maternal

body size, as seen generally in sharks and rays (Denéchère et al., 2022; Goodwin et al., 2002) and broadcast spawning in which offspring size (ovum diameter) is independent of maternal size and is typically 1-2 mm in diameter due to selection for pelagic dispersal in the plankton (as seen in teleosts; Duarte & Alcaraz, 1989). According to metabolic scaling theory, r_{max} scales with body mass with an exponent of -0.25 (Savage et al., 2004; Brown et al., 2004) but only when offspring size is proportional to adult size (Denéchère et al., 2022). Therefore, the paradox of lower r_{max} in warm-water rays could result from their larger offspring size (proportional to maternal body size) compared to the cooler-water skates, which lay pairs of eggs (mermaid's purses) that tend to be more consistently smaller in size despite a wide range in maternal sizes. Further, it would be interesting to explore differences in somatic growth rates between rays and skates as Denéchère *et al.* (2022) also found that there was variation around the -0.25 metabolic scaling expectation where somatic growth rates were proportional as opposed to independent of adult body mass (Denéchère et al., 2022).

Our finding that r_{max} is lower in the less fecund, tropical rays than the more fecund, coolerdwelling skates, has profound consequences for fisheries sustainability and extinction risk. First, our findings imply that warm-shallow-water rays are more intrinsically sensitive to exploitation than the skates. Yet, historically skates have been at greater risk of extinction, with the loss of the largest bodied skates from both sides of the North Atlantic (Brander, 1981; Dulvy & Reynolds, 2002; Walker & Heessen, 1996). However, these relatively fecund species disappeared due to the intense trawl fisheries and the lack of management for skates. Now with reduction in fishing mortality and skate quotas, we are seeing stabilisation and recovery of larger skates (McGeady et al., 2022; Bom et al., 2022; Moore, 2023). At that time, there was little comparative understanding of the state of tropical shark and ray fisheries. Over the past decade, it has become increasingly clear that tropical fisheries are particularly intense and relatively unregulated (Davidson et al., 2016; Booth et al., 2019; Sherman et al., 2023; Temple et al., 2019). The latest reassessment of all chondrichthyans has revealed greater threat in tropical coastal waters, with more than 75% of tropical and subtropical coastal species threatened. Our result suggests that while this is mainly due to intense, largely unregulated fisheries, the differential intrinsic sensitivity of rays may go a long way to explain why batoid species are particularly at risk in the tropics (Dulvy et al., 2021; Temple et al., 2019). These results underscore the need for effective fisheries management, through catch and effort control (Blaber et al., 2009; Yulianto et al., 2018). Our estimates are at the global species level, yet many species are widely distributed and there is considerable evidence for geographic trait variation due to local adaptation (Cope, 2006). There might be temptation to wait until the data are gathered from the locale of interest before using these r_{max} estimates in risk analyses and other forms of management guidance. Instead, we remind that we estimated r_{max} based on 10,000 random deviates from a uniform distribution between minimum and maximum values of each life history parameter (or $\pm 10\%$ for α_{max}), hence, local population specific values are likely encompassed within the posterior distributions of the global species r_{max} . Hence, we recommend using the current values, as well as gathering more locale-specific life history data.

Previous methods of estimating r_{max} for sharks and rays have assumed all juveniles survive to maturity at a similar rate of survivorship in the adult stage, independent of reproductive strategy (Pardo, Kindsvater, Reynolds, et al., 2016). However, juvenile survivorship likely varies with offspring size, in addition to lifespan, such that the survival to maturity may be greater in livebearing rays with few offspring compared to fecund, egg-laying skates with smaller offspring sizes. The proportion of offspring that survive to maturity is likely lower in highly fecund skates, for example, due to predation on egg cases (Lucifora & García, 2004; García et al., 2008), compared to fewer, larger offspring in live-bearing rays that have higher maternal investment and a higher chance of survival (Frisk et al., 2001). The survival of eggs relative to the annual reproductive output (in the absence of density-dependence) is something that needs more investigation to further explore whether survival to maturity is truly comparable between these different reproductive strategies.

In addition to offspring size and survival, and the influence of offspring size on r_{max} , future research could explore (1) somatic growth rates and the different dimensions of reproductive output, such as offspring size, and their relationship with r_{max} to better understand the reasons behind the higher intrinsic sensitivity (lower r_{max}) found for tropical rays; (2) consider alternate temperature data to improve the estimation of r_{max} ; and (3) access more data through imputation. First, this could include investigation of size-dependent mortality rates to account for offspring size and its effect on juvenile survival to maturity in estimations of r_{max} in order to investigate whether survival to maturity is truly comparable across reproductive strategies, such as between the live-bearing rays and egg-laying skates in this study. Further understanding of the relationship between offspring size and environmental temperature, given how the latter likely affects maternal investment, is also needed (Pettersen et al., 2020). Similarly, investigation of the relationship between r_{max} and somatic growth rate (von Bertalanffy k) or growth performance (Φ) relative to maternal size is required (Denéchère et al., 2022). A growth effect is likely correlated with temperature, with tropical species typically exhibiting faster growth

rates and lower longevity. Variation in somatic growth has been found to be important alongside juvenile survival in population fluctuations of marine fishes (Stawitz & Essington, 2019). Second, we used a widely available temperature dataset to ensure that our approach was consistent with other recent papers and ongoing work (Pardo & Dulvy, 2022), however, in the future, it would be useful to explore the opportunity to average bottom temperatures for demersal species, for example, using Bio-Oracle or even using global climate models (Assis et al., 2018). The ability to use simple traits to understand r_{max} and subsequently, relative sensitivity to exploitation, recovery potential, and fishing limits, is crucial for data-poor species. This study provides the foundations for using body mass, environmental temperature, and depth to predict r_{max} for rays and skates and potentially for predicting future r_{max} estimates using global climate model projections. Future calculations will likely be able to utilise more data such as known occupied depth ranges and temperature profiles from tagged individuals. Third, with the rate of species and population decline and extinction, it is crucial that we use available trait information to predict extinction risk and guide conservation (Green et al., 2022). New Bayesian approaches can use the trait covariation on strength and variation of intercorrelations to impute missing trait values (Kindsvater et al., 2018). This has great potential to expand the range of species that can be considered in these analyses and has recently been used to estimate 59 unobserved traits for 23 populations of tunas and billfishes (Horswill et al., 2019).

Overall, the findings indicate that warm-shallow-water rays tend to be more intrinsically sensitive to exploitation than cold-deep-water skates; this is concerning given the greater extrinsic exposure to overfishing in shallow, tropical coastal waters. This may help explain why we are now finding that tropical and subtropical species are facing such a high threat of extinction and highlights the need for effective fisheries management. The use of simple life history traits, including maximum body size, environmental temperature, and depth range, in concert with phylogenetic imputation, may be a useful approach for estimating r_{max} for use in ecological risk assessments.

Chapter 3. Does offspring size resolve a latitudinal population growth rate paradox in rays and skates?

3.1 Abstract

The maximum population growth rate, r_{max} , is a key determinant of the limits for sustainable fishing and is increasingly used in risk assessments. Macroecological theory suggests that warm-water species and populations will have higher r_{max} and therefore, will be less intrinsically sensitive to exploitation. However, warm-shallow-water tropical rays (orders Torpediniformes, Rhinopristiformes, and Myliobatiformes) paradoxically have lower r_{max} than cold-deep-water temperate skates (Rajiformes). Here, we seek to understand why these two related lineages deviate from macroecological theory. We build from recent advancements that suggest that offspring size, and not adult size, may be key to understanding population growth rates. Specifically, we examine how adult size, offspring size, temperature, and depth explain variation in r_{max} across 85 species of rays and skates. Our results show that the negative effect of offspring size upon r_{max} is greater and more important than adult size. Indeed, tropical rays had, on average, larger offspring and lower r_{max} compared to the temperate skates, despite living in warmer and shallower waters. Thus, despite the expectation from theory that tropical rays should have faster life histories and be more resilient to exploitation and other threats compared to temperate skates and other elasmobranch species, our work explains why these species are actually less resilient. It remains unclear as to why tropical rays have such large offspring but we hypothesise that this is due to the increasing body of evidence for greater predation risk in shallow tropical waters. Our work highlights the complex relationships among life histories and the environment and may help explain global biogeographic patterns of intrinsic sensitivity to overexploitation.

3.2 Introduction

A key challenge is understanding global patterns of life histories, which can help us predict species sensitivity to overfishing and other perturbations, particularly for data-poor species. Biogeographic patterns in life histories appear to be mediated by temperature, for example, Bergmann's rule states that terrestrial endotherms in cooler environments will be larger-bodied than their warmer relatives (Bergmann, 1847). Similarly, the Temperature-Size Rule (TSR) describes the observed pattern that ectothermic species and populations will generally grow faster to a smaller size at maturity (and presumably, smaller adult size) in warmer temperatures

(Atkinson, 1994; Atkinson & Sibly, 1997; Atkinson et al., 2006). Finally, metabolic theory suggests that species in warmer waters (e.g. in the tropics and shallow waters) with higher metabolic rates will tend to have 'faster' life histories than those in cooler waters (e.g. high latitude and deep waters) (Wong et al., 2021; Gravel et al., 2024; Juan-Jordá et al., 2013). Typically, species with faster life histories grow faster to a smaller maximum body size, mature earlier, and have shorter lifespans, resulting in higher maximum intrinsic rate of population increase, r_{max} (Denney et al., 2002; Hutchings et al., 2012). Collectively, Bergmann's rule, the TSR, and metabolic theory would predict that as temperatures rise, species' life histories would speed up, resulting in faster growth, smaller sizes at maturity, and ultimately, faster population growth rates.

The maximum intrinsic rate of population increase (r_{max}) is the average annual number of female spawners produced per female spawner at low population density (i.e. in the absence of density-dependence), which can vary with temperature biogeographically. It represents the maximum rate at which a population can grow and is an essential component of fisheries management to determine fishing limits and species' recovery potentials (Myers et al., 1997; Myers & Worm, 2005; Pardo, Kindsvater, Reynolds, et al., 2016). According to metabolic scaling expectations, r_{max} will scale with (adult) body mass (with an exponent of -0.25) and independently increases with temperature (Savage et al., 2004; Brown et al., 2004). This has been shown empirically both in experimentally manipulated populations as well as across species in the wild (Bernhardt et al., 2018; Luhring & Delong, 2017). For example, a positive relationship between r_{max} and temperature exists across Atlantic cod (Gadus morhua), which has greater r_{max} in warmer, more southerly populations (Myers et al., 1997; Savage et al., 2004). The biogeographic patterns of temperature (and food availability) were found to explain the life history patterns of tuna and mackerel (Scombridae) (Kindsvater et al., 2024). Further, cooler, temperate species with slower life histories experienced greater declines than tropical lower-latitude species with faster life histories, after controlling for fishing mortality (Juan-Jordá et al., 2015, 2011). More generally, the ratio of production to biomass (P:B) changes systematically with latitude across the world's fish communities. In the tropics, there is high production and low standing biomass compared to lower production and higher standing biomass in cooler temperate and polar latitudes (Jennings et al., 2008). Thus, understanding the metabolic basis for life histories such as somatic growth (Wong et al., 2021) and population

growth rate (Gravel et al., 2024) holds promise for understanding global change (Myers & Worm, 2005; Myers et al., 1997; Gravel et al., 2024).

As well as temperature and adult size, recent work suggests that offspring size may be important in explaining the scaling of r_{max} (Denéchère et al., 2022; Neuheimer et al., 2015). This leads us to wonder whether offspring size can also explain the diversity of r_{max} within, as well as across lineages. Rays (Orders Torpediniformes, Rhinopristiformes, and Myliobatiformes) and skates (Rajiformes) of the Superorder Batoidea are widely distributed across the world's oceans. Rays are generally found in shallow tropical and temperate waters (McEachran & Miyake, 1990; Frisk, 2010; Ebert & Compagno, 2007) but there are also deepwater species (e.g. *Plesiobatis daviesi* and *Hexatrygon bickelli*). Skates are typically distributed in the cooler waters of polar and temperate seas, as well as deeper, cool waters in the tropics, although there are also some shallow-water species (e.g. Zearaja maugeana and Okamejei schmidti). Metabolic theory would suggest that warm-shallow-water tropical rays should have higher r_{max} , yet paradoxically, they have lower r_{max} than cold-deep-water temperate skates (Barrowclift et al., 2023). Most tropical rays are live-bearers with very low fecundity and larger offspring compared to cooler-water skates that lay numerous eggs with smaller offspring size (Goodwin et al., 2002; Mull, Pennell, et al., 2022). This could mean that for two species with the same adult body mass, one with larger offspring (and fewer of them) may have a lower r_{max} and therefore, offspring size could affect the scaling of r_{max} (Denéchère et al., 2022; Burger et al., 2019). As such, we propose that batoids are an ideal taxon to test how offspring size influences the body mass-scaling of r_{max} and further, that offspring size may resolve the latitudinal paradox of r_{max} in rays and skates.

As well as being shaped by the intrinsic influence of temperature on metabolic rate (Gillooly et al., 2001), life histories are also shaped by extrinsic predation mortality (Sparholt, 1990; Gislason et al., 2010). The classic example is the experimental manipulation of predation on life history of the Guppy (*Poecilla reticulata*) (Reznick et al., 1990, 1996). Predation on larger individuals drove the evolution of greater metabolic rate and a fast-paced life history, including earlier maturation, reduced interbirth interval and greater reproductive allocation (Auer et al., 2018). More broadly, one hypothesis for the evolution of parental care (including viviparity) and large offspring size is to reduce the risk of mortality either of the offspring or of individuals later in life (Clutton-Brock, 1991; Goodwin et al., 2002; Pettersen et al., 2022). In elasmobranchs specifically, live-bearing and additional investment in offspring through

matrotrophy is more prevalent in the tropics, which may be a response to greater predation risk (Mull, Pennell, et al., 2022). Since Darwin, it has long been hypothesised that biotic interactions, such as predation, are more prevalent in shaping species biology and diversity towards the equator (Sunday et al., 2012; Schemske et al., 2009). This includes a greater selective pressure of predation in the tropics (Freestone et al., 2011, 2020). Recent experimental evidence from caged and uncaged epifaunal communities suggests predation rates are greater in shallow, tropical waters than at higher latitudes (Freestone et al., 2011, 2020; Ashton et al., 2022). Predation risk is emerging as a key determinant of tropical ray abundance; as sharks are fished down, ray abundance is increasing on coral reefs (Sherman et al., 2020; Simpfendorfer et al., 2023).

Here, we investigate whether larger offspring size of tropical rays explains their lower r_{max} compared to skates, while accounting for adult body size, temperature, and depth for 85 batoid species.

3.3 Methods

Firstly, we describe the calculation of r_{max} , including the source of the life history data used in the calculations. Second, we describe the calculation of environmental temperature-at-depth. Third, we summarise our analytical approach, including the statistical models used to assess different hypotheses of how r_{max} may vary with adult and offspring body mass, temperature, and depth.

3.3.1 Source of life history data and calculation of r_{max}

 r_{max} was calculated using a modified Euler-Lotka model, with a mortality estimator that accounts for survival to maturity (Pardo, Kindsvater, Reynolds, et al., 2016; Cortés, 2016) with the following equation:

$$l_{\alpha_{mat}}b = e^{r_{max}\alpha_{mat}} - e^{-M}(e^{r_{max}})^{\alpha_{mat}^{-1}},$$
 (1)

where $l_{\alpha_{mat}}$ is the proportion of individuals surviving to maturity, which is calculated with:

$$l_{\alpha_{mat}} = (e^{-M})^{\alpha_{mat}}, \tag{2}$$

b is annual fecundity, M is the species-specific instantaneous natural mortality rate, α_{mat} is the age at maturity, and α_{max} is the maximum age. Natural mortality (M) was estimated as $M = 1/\omega$ (Dulvy et al., 2004) where ω is an estimate of average lifespan in years and was assumed to be

the midpoint between age at maturity (α_{mat}) and maximum age (α_{max}) (Pardo, Kindsvater, Reynolds, et al., 2016) estimated with:

$$\omega = \frac{(\alpha_{max} + \alpha_{mat})}{2} \tag{3}.$$

The modified Euler-Lotka model aims to improve the estimation of r_{max} by accounting for different juvenile survival rates due to different reproductive strategies in sharks and rays (Pardo, Kindsvater, Reynolds, et al., 2016; Cortés, 2016). However, it is important to note that juvenile survival is likely to be lower in egg-laying skates that are more fecund and higher in live-bearing rays that produce fewer offspring (Frisk, Miller and Fogarty, 2001; García, Lucifora and Myers, 2008). The following life history traits were sourced from a published global life history database (compiled in Chapter 2): female age at 50% maturity (years; α_{mat}), maximum age (recorded for females where known, years; α_{max}), and annual reproductive output (number of female offspring assuming 1:1 sex ratio; *b*) for 85 ray (Torpedo rays, Torpediniformes; Rhino rays, Rhinopristiformes; and stingrays, Myliobatiformes) (n=53) and skate (Rajiformes) (n=32) species.

Estimates of adult body mass (maximum weight in grams) for the 85 batoid species were also sourced from the published life history database (Barrowclift & Dulvy, 2023). Offspring body mass (in grams) was estimated from offspring length (total length or disc width in cm) (note, this is hatching size for skates) reported in Rays of the World (Last et al., 2016), Sharkipedia (Mull, Pacoureau, et al., 2022), and IUCN Red List Assessments (Dulvy et al., 2021). Where offspring length data were unavailable for a species (n=14), offspring length was estimated from a similar species with similar maximum length and body shape (Barrowclift & Dulvy, 2023). The median offspring length was used where minimum and maximum offspring lengths were reported. The corresponding offspring body mass was then calculated using length-weight regression coefficients extracted from FishBase using the package rfishbase (Boettiger et al., 2012; Froese & Pauly, 2022; Barrowclift & Dulvy, 2023). Length-weight regression coefficients were selected for females where possible. If length-weight regressions were unavailable, estimates for a closely related species with similar body shape and maximum size were used (Barrowclift & Dulvy, 2023).

3.3.2 Calculation of environmental temperature-at-depth

Median depth and environmental temperature for the 85 ray and skate species were also used from Barrowclift *et al.*, 2023 (see Chapter 2) and their compilation is summarised next. Median

depth estimates for each species were taken from depth ranges of IUCN Red List assessments as compiled in Dulvy et al. (2021). Temperature-at-depth data were determined by overlaying a given species' distribution, using species range data shape files that were sourced from https://www.iucnredlist.org/, with the International Pacific Research Center's interpolated dataset of gridded mean annual ocean temperatures, which is based on measurements from the Argo Project (data available at:

http://apdrc.soest.hawaii.edu/projects/Argo/data/statistics/On_standard_levels/Ensemble_mea n/1x1/m00/index.html). Temperature grid points were extracted across the species' distribution from the depth level that was closest to the species' median depth and finally, the median temperature was calculated.

3.3.3 Statistical analyses

Metabolic scaling expectations for how r_{max} relates to body mass and temperature (Savage et al., 2004) can be estimated with the following linear model:

$$\ln(r_{max}) = \beta_0 + \beta_1 * \ln(M) + \beta_2 * 1/k_B T, \tag{4}$$

where r_{max} is the maximum intrinsic rate of population increase (year⁻¹), β_0 is the intercept, β_1 is the body mass-scaling coefficient, M is adult body mass in grams, β_2 is the activation energy E, T is the temperature (in Kelvin), and k_B is the Boltzmann constant (8.617 × 10⁻⁵ eV).

Following Denéchère et al., (2022), we also consider absolute and relative offspring size calculated as adult body mass divided by offspring body mass and include a term for adult-to-offspring size ratio ($M/M_{offspring}$) in some models. Hence, for the same adult body mass, larger offspring size would lead to a smaller adult-offspring size ratio. Using an information-theoretic approach, we include six additional models representing alternative hypotheses of how r_{max} may vary with (1) absolute offspring body mass $M_{offspring}$ (2) $M_{offspring}$ plus adult body mass M, and (3) adult-to-offspring size ratio ($M/M_{offspring}$), and compare these with 24 models representing hypotheses of how r_{max} may vary with adult body mass, temperature, and depth from Barrowclift $et\ al.$, 2023 (see Chapter 2) (Table 3.1) (Burnham & Anderson, 2002). The top models were the same and therefore we only present the 14 most relevant models in our results (Table 3.2). r_{max} , adult body mass, and offspring body mass data were natural log-transformed and temperature and depth data were standardised (scaled and centred) prior to analyses. A random phylogenetic tree from the distribution of trees in Stein, Mull et al., (2018). (available at Vertlife.org) was included as a random effect of phylogeny in all models, with

binomial nomenclature updated to reflect current taxonomic nomenclature. Models were fitted with an additional ten random trees to test the sensitivity of results to slight variations in the phylogenies; the results were nearly identical with the same top model, and therefore, results were reported for a single tree (Table 3.3). The phylogenetic position of two species was not known (*Aetobatus narutobiei* and *Maculabatis ambigua*), and therefore, two closely related species (*A. flagellum* and *M. gerrardi*, respectively) were used instead.

Phylogenetic generalised linear models were fitted using the pgls function in the caper package (Orme et al., 2018) to account for non-independence of closely related species. Models were also fitted without data (n=2) for two manta ray species (Mobula alfredi and M. birostris) with the largest offspring body masses to test sensitivity of results to their removal. The top models were the same and therefore results were presented for the full 85 species dataset (Table 3.4). Adult and offspring body mass were positively correlated (Pearson's r = 0.75) above a threshold of 0.7 in which collinearity severely distorts model estimation (Dormann et al., 2013). Inverse temperature and depth were also positively correlated (Pearson's r = 0.75). Variance-Inflation Factors (VIF) were estimated to assess collinearity for all coefficients in the models using the car package (Fox & Weisberg, 2019). VIF values were less than 2, except as expected when interactions were included, indicating that our models were robust to collinearity. The corrected Akaike Information Criterion (AICc) were used to compare models. If including a parameter improved the model's AICc by less than two units (Δ AICc \leq 2), it was considered relatively uninformative (Arnold, 2010; Burnham & Anderson, 2002). All analyses were run in R version 4.1.2 (R Core Team, 2021) in RStudio (RStudio Team, 2021).

3.4 Results

The maximum population growth rate r_{max} of batoids (n=85) was lower in species with larger offspring sizes (Figure 3.1; Figure 3.2a). This pattern was consistent across all models with or without the inclusion of adult body mass (Figure 3.1; Figure 3.2b). Although adult and offspring body mass were positively correlated (Figure 3.3a), offspring size was generally larger for warm-shallow-water tropical rays, with little difference in adult size relative to cold-deep-water temperate skates (Figure 3.4). Indeed, the effect of adult body mass on r_{max} was approximately half (-0.12) than expected from metabolic theory (-0.25; Figure 3.1; Table 3.5). Of the 14 models examined, the top model was for r_{max} varying with adult body mass, offspring body mass, and temperature (Δ AICc=0), describing the greatest amount of variation in r_{max}

across species (adjusted R^2 =0.18; Table 3.2). The second-ranked, more parsimonious model, which described r_{max} varying solely with offspring body mass was within 2 AICc units (Δ AICc = 0.6; Table 3.2) of the top model. This model had approximately 74% of the support of the top-ranked model (when compare the Akaike weights), accounted for slightly less variation (adjusted R^2 =0.16), and also had the lowest uncertainty (smallest confidence intervals) in how offspring body mass relates to r_{max} (Figure 3.1).

Including adult body mass in the relationship between $r_{\rm max}$ and offspring body mass received moderate support but did not increase $\Delta {\rm AICc}$ by more than two units ($\Delta {\rm AICc}$ =2.5), with only 29% of the support of the top-ranked model and accounting for slightly less variation (adjusted $R^2 = 0.15$). Including an interaction term between adult and offspring body mass received less support ($\Delta {\rm AICc}$ =3.8), with no increase in variation explained (adjusted R^2 =0.14) and only 15% of the support (Akaike weights) of the top model. Adult body mass explained more variation in $r_{\rm max}$ (larger effect size) when it was the sole mass predictor in the model (Table 3.5). However, once offspring body mass was included as a predictor, the variation in $r_{\rm max}$ explained by adult body mass shifts to offspring body mass, suggesting it is a better predictor of $r_{\rm max}$.

The effect of inverse temperature $1/k_BT$ and depth were negative across models indicating r_{max} is higher in warmer-shallower water species as would be expected from metabolic theory (Figure 3.2a; Table 3.5). When comparing the same models for adult body mass or offspring body mass with and without temperature, the effect of temperature did improve the support of the model, but only by roughly 2 AIC units. The scaling of temperature with r_{max} overlapped with the expectation of approximately -0.6 from metabolic theory (Figure 3.1; Figure 3.5). However, r_{max} was found to be lower at warmer temperatures based on the fitted top-model (Figure 2a). Yet, despite a weak negative relationship between offspring body mass and temperature for rays and skates (Figure 3.5a), less fecund species with larger offspring body mass (Figure 3.3b) tended to have lower r_{max} (Figure 3.2b; Figure 3.5a).

By comparison, the remaining models were not well supported ($\Delta AICc > 4$) (Table 3.2). Although larger offspring body mass, relative to adult body mass, resulted in a smaller adult-to-offspring size ratio (Figure 3.4; Figure 3.6), models including the adult-to-offspring size ratio were not well supported (Table 3.2). The effect sizes of offspring body mass and temperature were most strongly supported as the 95% confidence intervals did not overlap zero, compared to adult body mass (Figure 3.1). There was a strong phylogenetic signal from the residuals of r_{max} in all models (Pagel's $\lambda \ge 0.8$) (Table 3.5).

Table 3.1 All 30 models tested with associated hypotheses for how maximum intrinsic rate of population increase (r_{max}) varies with adult body mass M, offspring body mass $M_{offspring}$, inverse temperature $1/k_BT$, depth, and a temperature-depth index (PC1 axis from Principle Components Analysis of collapsed temperature and depth data in Barrowclift et al. (2023). Comparison of 30 ln(r_{max}) models using corrected Akaike Information Criteria (AICc), number of parameters (n), negative log-likelihood (-LL), R^2 , adjusted R^2 (Adj. R^2), difference in AICc from the top model (ΔAICc), and Akaike weights. Models are ordered by ascending AICc, with models with AICc < 2 shown in bold. Note, Order was categorical for rays (Orders Myliobatiformes, Rhinopristiformes, and Torpediniformes) and skates (Order Rajiformes).

Hypothesis: r _{max} varies with	Model: ln(r _{max}) ~	n	-LL	AICc	R^2	Adj. R ²	ΔAICc	Weights
adult and offspring body mass and temperature	$\ln(M) + \ln(M_{offspring}) + 1/k_BT$	4	-63	134.4	0.21	0.18	0	0.279
offspring body mass only	$\ln(M_{offspring})$	2	-65.4	135	0.17	0.16	0.6	0.207
adult and offspring body mass	$ln(M) + ln(M_{offspring})$	3	-65.3	136.9	0.17	0.15	2.5	0.08
adult body mass and temperature-depth index	ln(M) + temperature-depth index	3	-65.4	137.2	0.16	0.14	2.8	0.069
adult and offspring body mass, and the effect of mass scaling coefficient varies with offspring size	$ln(M) * ln(M_{offspring})$	4	-64.9	138.2	0.17	0.14	3.8	0.042
adult body mass, temperature-depth index, and Order	ln(M) + temperature-depth index + Order	4	-65	138.4	0.17	0.14	4	0.038
adult body mass and temperature	$\ln(M) + 1/k_B T$	3	-66.1	138.5	0.14	0.12	4.1	0.036
adult body mass and depth	ln(M) + depth	3	-66.1	138.6	0.14	0.12	4.2	0.034
adult body mass and the effect of temperature varies with depth	$ln(M) + 1/k_BT * depth$	5	-64.1	138.9	0.18	0.14	4.5	0.029
adult body mass and temperature-depth index, and the effect of mass scaling coefficient varies with the temperature-depth index	ln(M) * temperature-depth index	4	-65.3	139.1	0.16	0.13	4.7	0.027
adult body mass, temperature, and depth	$\ln(M) + 1/k_BT + \text{depth}$	4	-65.4	139.3	0.16	0.13	4.9	0.027
adult body mass, temperature, and Order	$\ln(M) + 1/k_BT + \text{depin}$ $\ln(M) + 1/k_BT + \text{Order}$	4	-65.6	139.7	0.16	0.13	5.3	0.024
adult body mass and temperature, and the effect of mass scaling coefficient varies with temperature	$\ln(M) * 1/k_B T$	4	-65.7	139.8	0.16	0.13	5.4	0.019
adult body mass only	ln(M)	2	-68	140.2	0.1	0.09	5.8	0.015

adult body mass, depth, and Order	ln(M) + depth + Order	4	-65.9	140.2	0.15	0.12	5.8	0.015
adult body mass, temperature-depth index, and Order, and the effect of mass scaling coefficient varies with the temperature-depth index	ln(M) * temperature-depth index + Order		-64.8	140.4	0.17	0.13	6	0.014
adult body mass and depth, and the effect of mass scaling coefficient varies with depth	ln(M) * depth	4	-66.1	140.8	0.14	0.11	6.4	0.011
adult body mass, temperature, and Order, and the effect of mass scaling coefficient varies with temperature	$ln(M) * 1/k_BT + Order$	5	-65.1	141	0.17	0.13	6.6	0.01
adult body mass and Order	ln(M) + Order	3	-68	142.2	0.11	0.08	7.8	0.006
temperature-depth index only	temperature-depth index	2	-69.1	142.3	0.08	0.07	7.9	0.005
adult body mass, depth, and Order, and the effect of mass scaling coefficient varies with depth	ln(M) * depth + Order	5	-65.9	142.5	0.15	0.11	8.1	0.005
temperature only	$1/k_BT$	2	-69.5	143.1	0.07	0.06	8.7	0.004
temperature-depth index and Order	temperature-depth index + Order	3	-68.5	143.3	0.09	0.07	8.9	0.003
temperature and Order	$1/k_BT$ + Order	3	-68.8	144	0.09	0.06	9.6	0.002
depth only	depth	2	-70.3	144.8	0.05	0.04	10.4	0.002
adult:offspring size ratio and temperature	$ln(M/M_{offspring}) + 1/k_BT$	3	-69.2	144.8	0.08	0.06	10.4	0.002
depth and Order	depth + Order	3	-70.1	146.4	0.06	0.04	12	0.001
average r_{max} (i.e. intercept-only model)	1	1	-72.7	147.5	0	0	13.1	0
Order	1 + Order	2	-72.6	149.4	0	-0.01	15	0
adult:offspring size ratio only	$\ln(M/M_{offspring})$	2	-72.7	149.5	0	-0.01	15.1	0

Table 3.2 The 14 models examined with associated hypotheses for how maximum intrinsic rate of population increase (r_{max}) varies with adult body mass M, inverse temperature $1/k_BT$, depth. Comparison of models using corrected Akaike Information Criteria (AICc), number of parameters (n), negative log-likelihood (-LL), adjusted R^2 , difference in AICc from the top model (Δ AICc), and Akaike weights. Models are ordered by ascending AICc, with models with AICc < 2 shown in bold.

Hypothesis: r_{max} varies with	Model: ln(r _{max}) ~	n	-LL	AICc	R^2	Adj. R^2	ΔAICc	Weights
adult and offspring body mass and temperature	$\ln(M) + \ln(M_{offspring}) + 1/k_BT$	4	-63	134.4	0.21	0.18	0	0.357
offspring body mass only	$\ln(M_{offspring})$	2	-65.4	135	0.17	0.16	0.6	0.264
adult and offspring body mass	$ln(M) + ln(M_{offspring})$	3	-65.3	136.9	0.17	0.15	2.5	0.102
adult and offspring body mass, and the effect of mass scaling coefficient varies with offspring size	$\ln(M) * \ln(M_{offspring})$	4	-64.9	138.2	0.17	0.14	3.8	0.053
adult body mass and temperature	$\ln(M) + 1/k_B T$	3	-66.1	138.5	0.14	0.12	4.1	0.046
adult body mass and depth	ln(M) + depth	3	-66.1	138.6	0.14	0.12	4.2	0.044
adult body mass and the effect of temperature varies with depth	$ln(M) + 1/k_BT * depth$	5	-64.1	138.9	0.18	0.14	4.5	0.038
adult body mass, temperature, and depth	$ln(M) + 1/k_BT + depth$	4	-65.4	139.3	0.16	0.13	4.9	0.031
adult body mass and temperature, and the effect of mass scaling coefficient varies with temperature	$\ln(M) * 1/k_B T$	4	-65.7	139.8	0.16	0.13	5.4	0.024
adult body mass only	ln(M)	2	-68	140.2	0.1	0.09	5.8	0.02
adult body mass and depth, and the effect of mass scaling coefficient varies with depth	ln(M) * depth	4	-66.1	140.8	0.14	0.11	6.4	0.015
(inverse) temperature only	$1/k_BT$	2	-69.5	143.1	0.07	0.06	8.7	0.005
depth only	depth	2	-70.3	144.8	0.05	0.04	10.4	0.002
average r_{max} (i.e. intercept-only model)	1	1	-72.7	147.5	0	0	13.1	0.001

Table 3.3 Comparison of $14 \ln(r_{\text{max}})$ models fitted with 10 different phylogenetic trees obtained from Stein, Mull et al., (2018) (available on Vertlife.org) using corrected Akaike Information Criteria (AICc). The model with lowest AICc for each iteration is shown in bold.

$\ln(r_{\rm max}) \sim$	1	2	3	4	5	6	7	8	9	10
1	13.1	15.4	13.7	12.9	12.5	13	12.8	11.5	12.5	13.6
ln(M)	5.8	10.1	6	6.1	6.5	6.4	5.5	5.6	6.5	6.8
depth	10.4	13.6	10.8	9.9	9.2	10.9	9.6	10.1	9.2	12.8
$1/k_BT$	8.7	12	9.7	7.8	7.3	9	8.6	7.8	7.3	8.8
ln(M) + depth	4.2	9	4.6	4.6	4.8	4.9	3.5	5.1	4.8	6.6
$\ln(M) + 1/k_B T$	4.1	8.5	4.8	3.9	4.1	4.8	4.2	4.2	4.1	4.4
ln(M) * depth	6.4	10.6	6.6	6.6	6.9	7.1	5.7	6.9	6.9	8
$\ln(M) * 1/k_B T$	5.4	10.7	5.8	4.6	5.3	6.6	6.1	4.6	5.3	6.5
$ln(M) + 1/k_BT + depth$	4.9	9.7	5.7	5	5.1	5.7	4.6	5.6	5.1	6.2
$ln(M) + 1/k_BT * depth$	4.5	9.8	5.5	4.9	5.4	6	4.3	5.6	5.4	4.1
$\ln(M_{offspring})$	0.6	0.4	0.3	0.8	1.2	0.6	0.5	0.5	1.2	1
$ln(M) + ln(M_{offspring})$	2.5	2.6	2	2.7	3	2.3	2.1	2.3	3	2.9
$ln(M) * ln(M_{offspring})$	3.8	3.4	3.6	4.1	4.4	4	3.5	3.7	4.4	3.6
$\ln(M) + \ln(M_{offspring}) + 1/k_BT$	0	0	0	0	0	0	0	0	0	0

Table 3.4 Comparison of 14 $\ln(r_{\text{max}})$ models fitted without data for two manta ray species (*Mobula alfredi* and *M. birostris*) with largest offspring sizes using corrected Akaike Information Criteria (AICc), number of parameters (n), negative log-likelihood (-LL), R^2 , adjusted R^2 (Adj. R^2), difference in AICc from the top model (Δ AICc), and Akaike weights. Models are ordered by ascending AICc, with models with AICc < 2 shown in bold.

$\ln(r_{\text{max}}) \sim$	n	-LL	AICc	R^2	Adj. R ²	ΔAICc	Weights
$\ln(M_{offspring})$	2	-61.2	126.5	0.1	0.09	0	0.231
$\ln(M) + \ln(M_{offspring}) + 1/k_BT$	4	-59.3	127	0.14	0.11	0.5	0.18
ln(M) + depth	3	-61	128.2	0.1	0.08	1.7	0.099
$\ln(M) + 1/k_BT$	3	-61.1	128.5	0.1	0.08	2	0.085
$ln(M) + ln(M_{offspring})$	3	-61.1	128.5	0.1	0.08	2	0.085
$ln(M) + 1/k_BT + depth$	4	-60.4	129.3	0.12	0.09	2.8	0.057
$\ln(M) * \ln(M_{offspring})$	4	-60.4	129.4	0.12	0.08	2.9	0.054
ln(M)	2	-62.7	129.6	0.07	0.05	3.1	0.049
$ln(M) + 1/k_BT * depth$	5	-59.6	129.9	0.14	0.09	3.4	0.042
ln(M) * depth	4	-61	130.4	0.11	0.07	3.9	0.033
$\ln(M) * 1/k_BT$	4	-60.9	130.4	0.11	0.08	3.9	0.033
$1/k_BT$	2	-63.4	131	0.05	0.04	4.5	0.024
depth	2	-63.6	131.4	0.04	0.03	4.9	0.02
1	1	-65.5	133	0	0	6.5	0.009

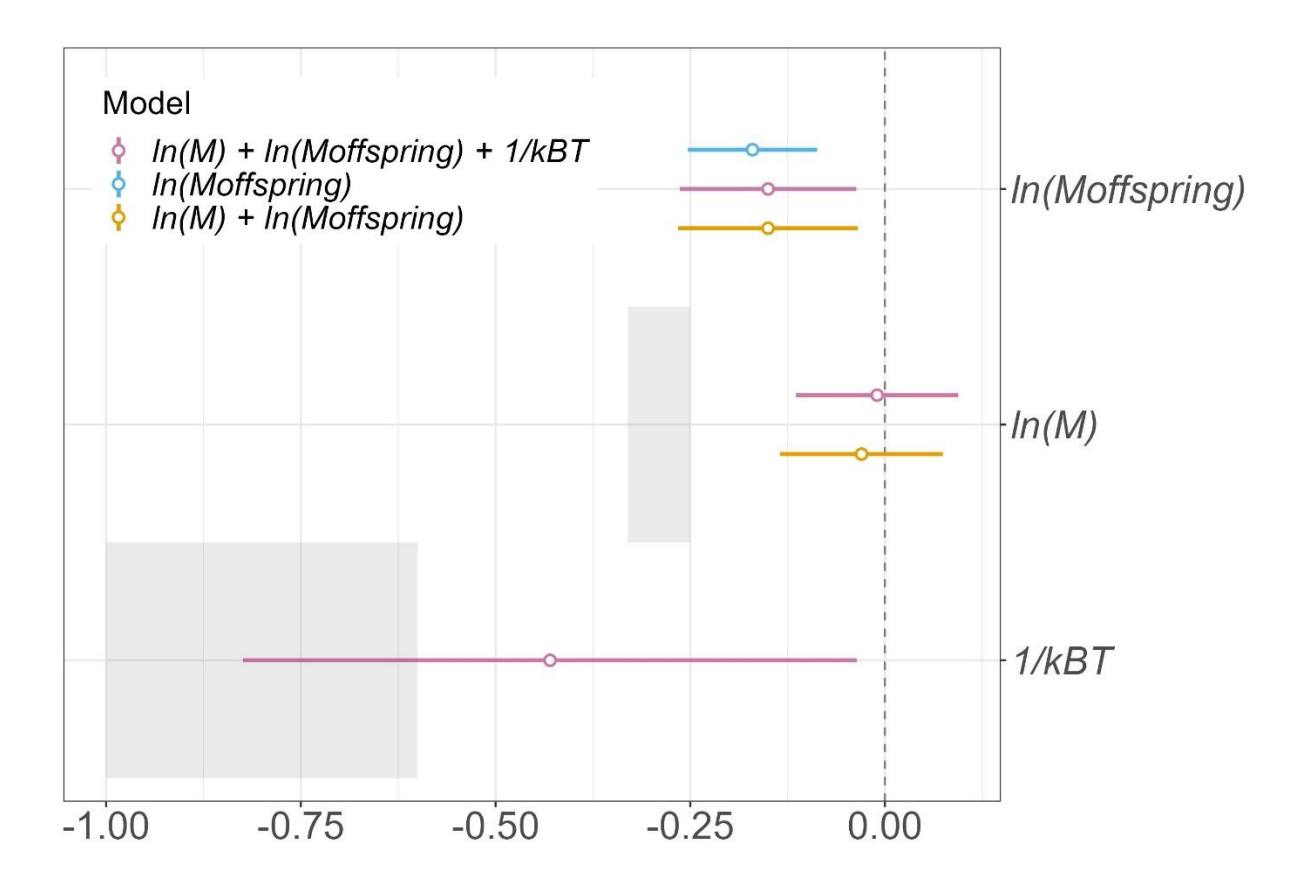


Figure 3.1 Coefficient plot showing the effect sizes for offspring body mass ($M_{offspring}$), adult body mass (M), and inverse temperature ($1/k_BT$) on r_{max} in the top three models. Error bars show the 95% confidence intervals and effect sizes are considered significant when confidence intervals do not overlap zero. The grey boxes show the expected effect size for adult body mass (-0.33 to -0.25) and temperature (-1.0 to -0.6) based on metabolic theory.

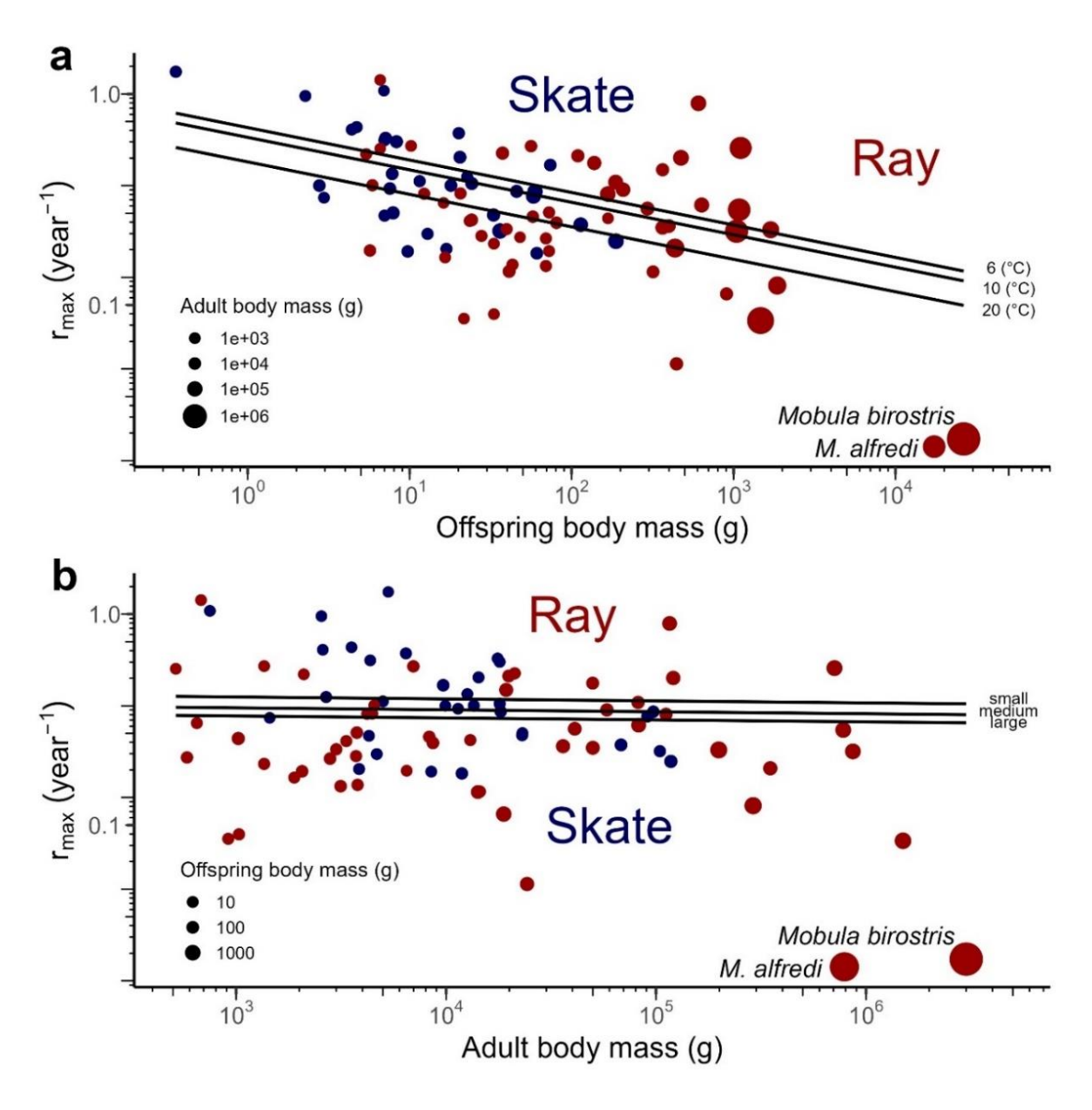


Figure 3.2 Relationship between maximum intrinsic rate of population increase (r_{max}) and a) offspring body mass (g) and b) adult body mass (g) in log10 space for 85 ray (n=53, red points) and skate (n=32, blue points) species. Fitted lines show the predicted relationships for the top model: $\ln(r_{max}) \sim \ln(M) + \ln(M_{offspring}) + 1/k_BT$, where M is adult body mass, $M_{offspring}$ is offspring body mass, and $1/k_BT$ is inverse temperature, across (a) three temperatures (6, 10, 20°C) with fixed median adult body mass and (b) three median offspring body masses (small, skates; medium, all species; large; rays) with fixed temperature (10°C). (a) Adult body mass (g) and (b) offspring body mass (g) are shown by the point size. Fitting the top model across different median adult weights (e.g. small, skates; medium, all species; large; rays) does not change the fitted relationship.

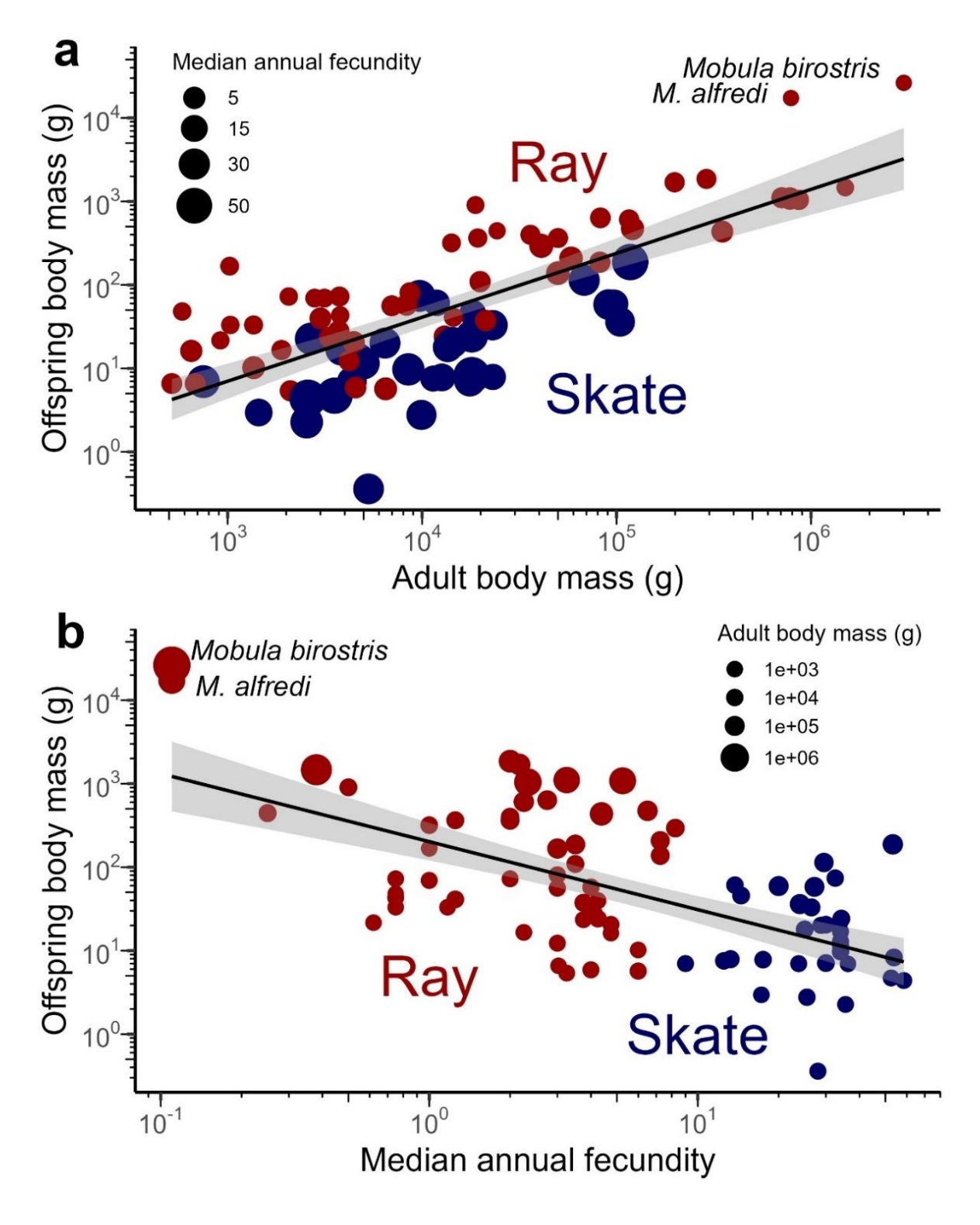


Figure 3.3 Relationship between offspring body mass (g) and a) adult body mass (g) and b) median annual fecundity in $\log 10$ space for 85 species of ray (n=53, red points) and skate (n=32, blue points). (a) Median annual fecundity and (b) adult body mass (g) are shown by the point size.

Table 3.5 Coefficient estimates (95% confidence intervals estimated from standard errors shown in brackets) for all models of $ln(r_{max})$. The model with the lowest $\Delta AICc$ value is marked in bold and models with $\Delta AICc < 2$ are highlighted in grey. Pagel's λ indicates the strength of the phylogenetic signal.

In(<i>r</i> _{max}) ~	intercept	In(M)	depth	$1/k_BT$	In(<i>M</i>): depth	In(<i>M</i>): 1/ <i>k_BT</i>	$1/k_BT$: depth	In(M _{offspring})	In(M): In(M _{offspring})	Pagel's λ
1	-1.17									0.88
1	(-1.71, -0.62)	-	-	-	-	-	-	-	-	(0.69, 0.96)
depth	-1.18		-0.32							0.88
иерип	(-1.71, -0.65)	-	(-0.6, -0.03)	-	-	-	-	-	-	(0.68, 0.96)
1 /l T	-1.22			-0.55						0.89
$1/k_BT$	(-1.76, -0.68)	-	-	(-0.96, -0.13)	-	-	-	-	-	(0.71, 0.97)
In(M)	-0.01	-0.12								0.88
111(171)	(-0.91, 0.89)	(-0.2, -0.05)	-	-	-	-	-	-	-	(0.69, 0.96)
In(M) * depth	-0.1	-0.12	-0.3		0					0.88
iii(<i>ivi</i>) * deptii	(-1, 0.79)	(-0.2, -0.04)	(-1.75, 1.15)	-	(-0.15, 0.16)	-	-	-	-	(0.63, 0.96)
$ln(M) * 1/k_BT$	-0.2	-0.11		-1.16		0.07				0.92
III(IVI) 1/KBI	(-1.13, 0.73)	(-0.19, -0.03)	-	(-2.61, 0.29)	-	(-0.06, 0.21)	-	-	-	(0.72, 0.98)
In(M) *	-0.89	0.03						-0.02	-0.01	0.82 (0.51,
$ln(M_{offspring})$	(-2.39, 0.61)	(-0.14, 0.2)	-	-	-	-	-	(-0.32, 0.28)	(-0.04, 0.02)	0.94)
ln/1/1) i donth	-0.11	-0.12	-0.27							0.88
In(M) + depth	(-0.99, 0.78)	(-0.19, -0.04)	(-0.55, 0)	-	-	-	-	-	-	(0.67, 0.96)
$ln(M) + 1/k_BT$	-0.23	-0.11		-0.41						0.89
$\Pi(W) + 1/\kappa_B I$	(-1.13, 0.68)	(-0.19, -0.03)	-	(-0.83, 0)	-	-	-	-	-	(0.68, 0.96)
$ln(M) + 1/k_BT *$	-0.39	-0.1	-0.67	-0.06			0.65			0.89
depth	(-1.31, 0.54)	(-0.18, -0.02)	(-1.35, 0.01)	(-0.6, 0.49)	-	-	(-0.15, 1.45)	-	-	(0.69, 0.97)
$\ln(M) + 1/k_BT +$	-0.22	-0.11	-0.18	-0.28						0.88
depth	(-1.13, 0.68)	(-0.19, -0.03)	(-0.49, 0.13)	(-0.75, 0.19)	-	-	-	-	-	(0.67, 0.96)
In(M) +	-0.34	-0.03						-0.15		0.82
$ln(M_{offspring})$	(-1.21, 0.54)	(-0.14, 0.07)	-	-	-	-	-	(-0.26, -0.03)	-	(0.53, 0.94)
In(M) +										
$ln(M_{offspring}) +$	-0.56	-0.01		-0.43				-0.15		0.81
$1/k_BT$	(-1.44, 0.32)	(-0.11, 0.09)	-	(-0.82, -0.04)	-	-	-	(-0.27 , -0.04)	-	(0.46, 0.94)
In(Moffspring)	-0.54 (-1.09, 0.01)	_	_	_	_	_	-	-0.17 (-0.26, -0.09)	-	0.80 (0.52, 0.93)

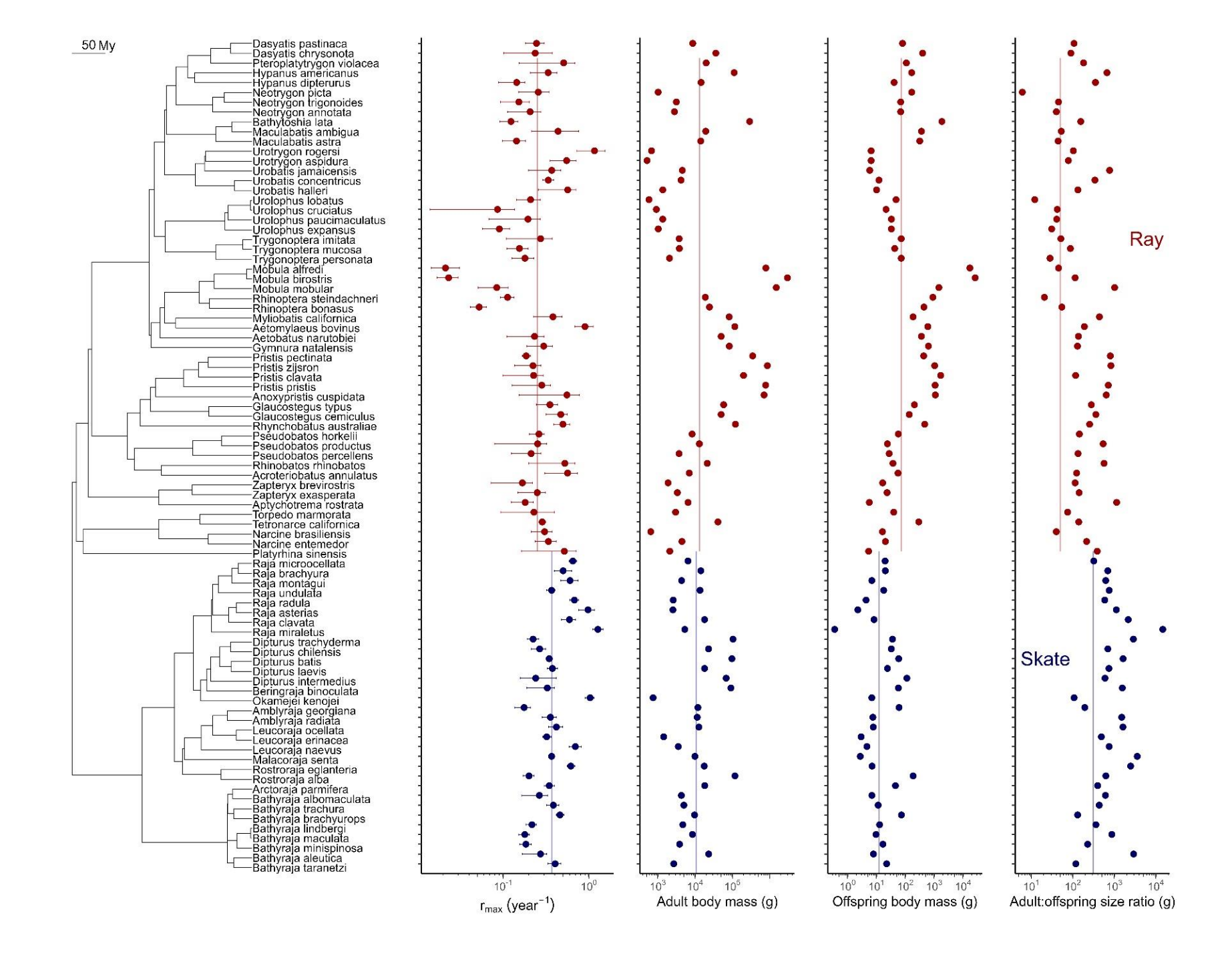


Figure 3.4 Phylogeny, maximum intrinsic rate of population increase (r_{max}), adult and offspring body mass (g), and adult:offspring size ratio in log10 space for 85 ray (n=53, red points) and skate (n=32, blue points) species. Solid lines show median values. Uncertainty in r_{max} estimate shown with 2.5% and 97.5% quantiles. Phylogenetic tree from Stein, Mull et al., (2018) (available on Vertlife.org) with binomial nomenclature updated to reflect current taxonomic nomenclature.

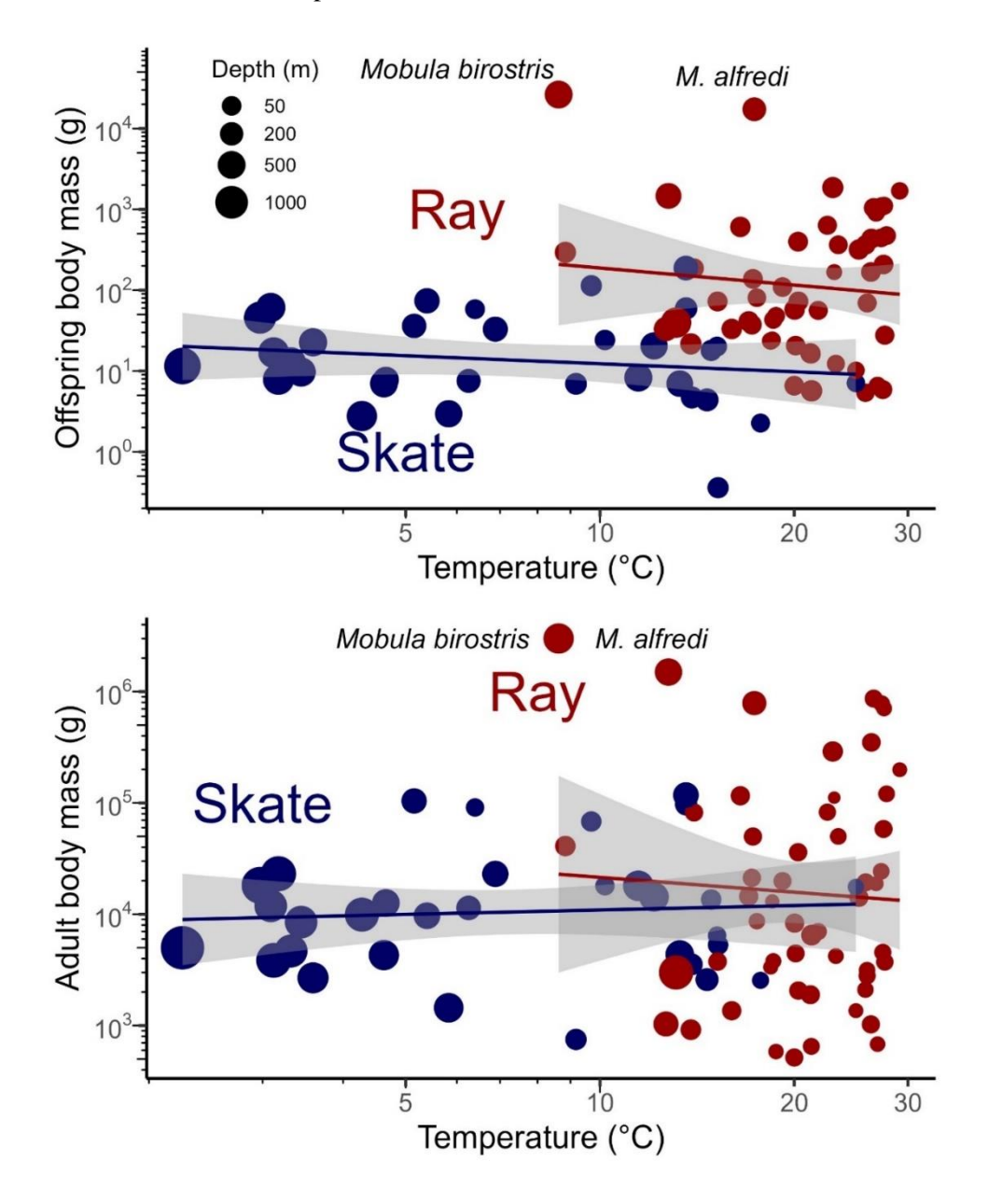


Figure 3.5 Relationship between temperature (°C) and a) offspring body mass (g) and b) adult body mass (g) in log space for 85 ray (n=53, indicated by red points) and skate (n=32, indicated by blue points) species. Median depth of occurrence (m) is shown by the point size, with a linear model fitted to ray and skate data points. The grey bands around the fitted models show the confidence intervals.

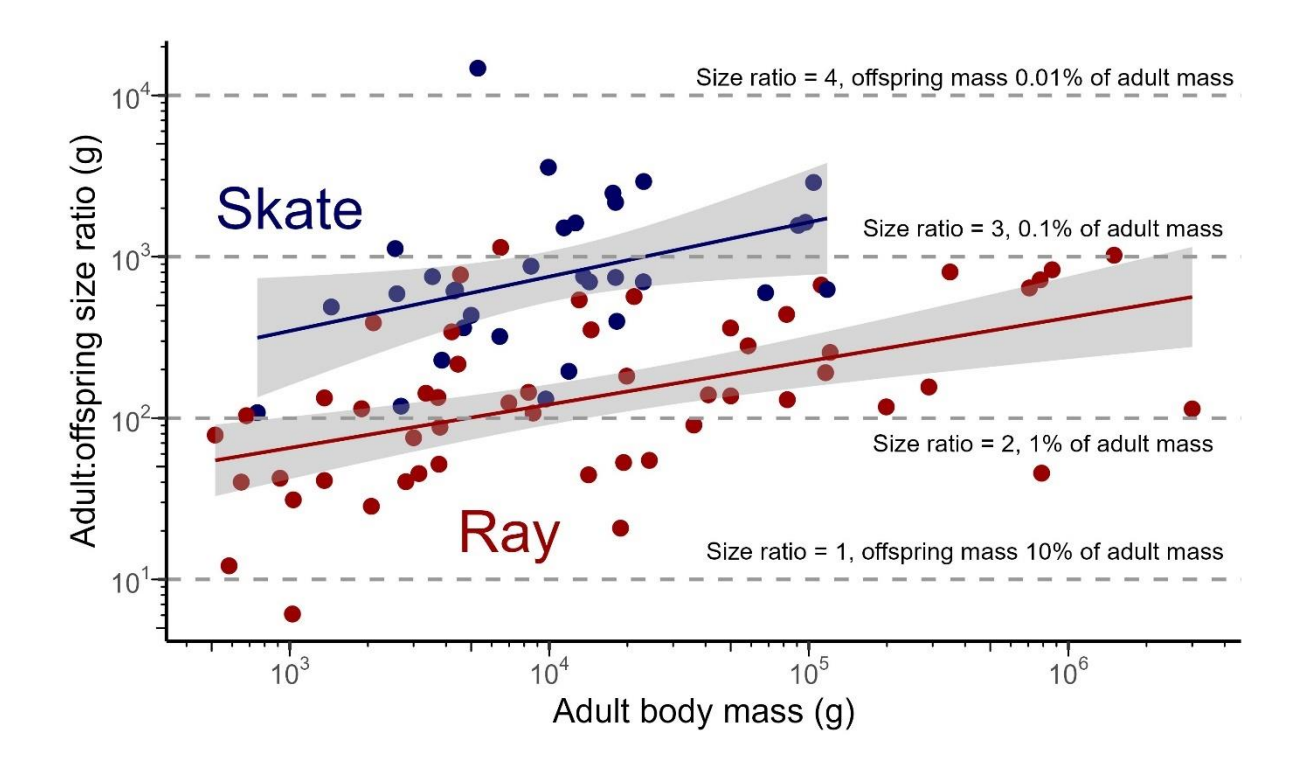


Figure 3.6 Relationship between adult:offspring size ratio (g) and adult body mass (g) in $\log 10$ space for 85 ray (n=53, indicated by red points) and skate (n=32, indicated by blue points) species. The grey bands around the fitted models show the confidence intervals and grey dashed lines show adult:offspring size ratios of 1 to 4 where offspring size is 10 to 0.01% of adult body mass, respectively.

3.5 Discussion

We show evidence that offspring size modulated the well-studied relationship between $r_{\rm max}$ and temperature (and depth). Specifically, species with larger absolute offspring size have lower population growth rates. This finding helps to explain the paradox of why shallow-water tropical rays have lower population growth rates, compared to cold, deep-water temperate skates with smaller offspring size. This hypothesis has greater support than the metabolic expectation that faster life histories occur in warmer habitats. Instead, this is more consistent with recent work that suggests the metabolic scaling expectation of $r_{\rm max}$ with body mass is only found when offspring size is considered (Denéchère et al., 2022). Denéchère et al. (2022) found that the scaling of $r_{\rm max}$ varied across taxa and only matched metabolic expectations (-0.25) when offspring body mass is proportional to adult body mass (equal adult-to-offspring size ratio). For elasmobranchs specifically, the scaling of $r_{\rm max}$ with adult body mass matched metabolic expectations (Denéchère et al., 2022). However, we found that although the scaling of $r_{\rm max}$ for the group of elasmobranchs we examined - batoids - was around -0.25, this slope was for

offspring body mass and not adult body mass, which did not have a large effect size. Indeed, on average, the effect size of offspring body mass on r_{max} was twice as large as adult body mass. We also posit that the high predation risk in the tropics drives selection of larger adult and offspring body sizes of tropical rays. Next, we consider: (1) how our results differ from the typical temperature and latitudinal patterns in life histories; (2) the evolution of live-bearing and how selection in response to predation risk results in large offspring for tropical rays; and (3) future directions and caveats.

We found that absolute offspring size disrupted the typical life-history patterns in batoids. Compared to the cold-habitat skates, warm-shallow-water tropical rays have recently been found to have lower r_{max} and therefore greater intrinsic sensitivity to anthropogenic threats such as overfishing (Barrowclift et al., 2023). This contrasts with typical metabolic scaling patterns of life histories in relation to temperature and depth. In warmer temperatures, organisms generally grow faster, mature earlier, and attain smaller maximum body sizes resulting in faster generation times and higher production to biomass ratios (Munch & Salinas, 2009; Beukhof et al., 2019; Jennings et al., 2008). This also leads to latitudinal and depth-related patterns of temperature and size whereby organisms in shallower, warmer, and/or lower latitude waters have higher metabolic rates and therefore 'faster' life histories compared to organisms in deeper, cooler, and/or higher latitude waters (Wong et al., 2021; Pardo & Dulvy, 2022; Juan-Jordá et al., 2013). In sharp contrast however, we found that larger absolute offspring size in tropical rays disrupted these typical life-history patterns. Indeed, including offspring size in models had greater support and explained greater variation in r_{max} compared to adult body mass alone, or when including temperature and depth. When offspring size is proportional to adult size, excluding bet-hedging broadcast spawners, offspring size plays a larger role in determining r_{max} than temperature. While this has previously been shown across large taxonomic groups of mammals and sharks (Denéchère et al., 2022), the novelty here is that we have shown this effect within a lineage of contrasting offspring sizes. Specifically, the differences in r_{max} between warm, shallow-water rays and cold-habitat skates are likely due to their different reproductive strategies - as live-bearing rays have fewer, larger offspring compared to egg-laying skates with large numbers of smaller offspring - as hypothesised in Barrowclift et al. (2023). This pattern differs from the typical pattern in vertebrates and invertebrates. Generally, offspring size tends to have a negative relationship with temperature due to differences in maternal investment, with females producing larger, better-provisioned offspring in colder environments (Marshall, 2021; Pettersen et al., 2020). This large-offspringin-the-cold pattern is supported by both a cross cohort experiment of bryozoans (Marshall, 2021) and a metanalysis spanning 72 species from five ectotherm phyla (Pettersen et al., 2020). Similarly, we found a weak negative relationship between offspring size and temperature for rays and a near flat relationship for skates. However, tropical rays generally have larger offspring sizes than cooler-water-temperate skates. It may be that offspring size is largely independent of temperature for batoids, with both employing very different reproductive strategies, raising the question as to why large offspring sizes have evolved in shallow-water, tropical rays.

Live-bearing has been hypothesised to have evolved from egg-laying in order to increase the survival of offspring through a controlled maternal environment and greater protection from predators (Wourms, 1994; Goodwin et al., 2002). In live-bearing species, offspring size is constrained by the size of the maternal body cavity but results in offspring with greater survival (Musick & Ellis, 2005; Wourms & Lombardi, 1992). Whereas in egg-laying species, size is limited by nutrients stored in the yolk sac (Conrath & Musick, 2012). The egg-laying reproductive strategy of skates is thought to be advantageous because it requires less energy and shorter reproductive cycles but there will be survival consequences for the offspring due to smaller size, and, thus, greater risk of predation (Goodwin et al., 2002). We found that offspring size had a negative relationship with annual fecundity, reflecting the trade-off between th(Cortés, 2000; Duarte & Alcaraz, 1989)s, 2000; Duarte & Alcaraz, 1989). We also confirmed the expectation that larger ray species tend to have larger and more offspring (Cortés, 2000). Offspring size will affect juvenile survival to maturity, which is important to consider, given the maternal trade-off between lifetime reproductive output, which likely varies between egglaying and live-bearing reproductive modes (Pardo, Kindsvater, Reynolds, et al., 2016). In the calculation of r_{max} for elasmobranchs, there is the pragmatic assumption that juvenile survival to maturity is the same as the survival rate of adult ages (a consistent mortality estimator). However, our key finding suggests the average mortality depends on offspring size, presumably with larger absolute offspring sizes (typical of tropical rays) having lower predation risk than smaller offspring (typical of colder-water skates). This then leads to the question as to why it might be advantageous for tropical, warm-water rays to have larger offspring than temperate, cold-habitat skates?

The ancestral reproductive mode of sharks and rays is egg-laying with the subsequent evolution of live-bearing and a particularly high degree of maternal investment found in the shallow-tropical elasmobranch species (Mull, Pennell, et al., 2022; Dulvy & Reynolds, 1997). The

diversification and radiation of elasmobranchs throughout shallow tropical shelf seas and the pelagic zone appears to be associated with the evolution of live-bearing and multiple mechanisms for providing additional maternal investment in offspring (Mull, Pennell, et al., 2022). The question that remains is why live-bearing with additional maternal investment has evolved. Predation tends to be size-based in the marine realm (Barnes et al., 2010; Verity & Smetacek, 1996). We speculate that shallow-water, tropical rays have evolved larger offspring in response to selection pressure from greater predation risk in the tropics. Increased offspring size reduces the threat of predation i.e. has been selected for to reduce juvenile mortality (Sibly et al., 2018; Olsson et al., 2016; Cortés, 2000). We further speculate that this predation risk drove the evolution of live-bearing, and in particular the convergent evolution of multiple forms of matrotrophy (maternal supply of nutrients during gestation). Generally, offspring size is larger in chondrichthyans compared to teleost fishes in which live-bearing appears to have evolved in particularly small-bodied taxa, suggesting the drivers of viviparity are fundamentally different in chondrichthyans (Goodwin et al., 2002). Predation risk has generally been hypothesised to increase towards the tropics, with recent empirical work finding greater predation rates on epifaunal communities in shallow, tropical waters compared to high latitude waters (Ashton et al., 2022). This is relevant to potential greater predation on eggs and juveniles in tropical waters. Fisheries-driven decline in sharks, which predate on batoids, has led to increases in ray abundance, which would be consistent with predation driving community structure on tropical coral reefs (Sherman et al., 2020; Simpfendorfer et al., 2023).

Given Bergmann's rule and the Temperature-Size-Rule (TSR), adult body size of temperate skates in cooler waters would be expected to be larger than tropical rays in warmer waters. However, our results suggest there is wide variation in adult body size across batoids and, generally, the tropical rays are larger than cooler-water skates. We speculate above that the larger offspring sizes and live-bearing are a result of elevated predation in the tropics; given the body cavity constraint on offspring size of live-bearers we further speculate that large offspring size would require the evolution of larger adult body sizes in tropical rays that would allow greater maternal investment. This is consistent with the adult body size differences being the opposite of what might be expected under a TSR hypothesis, i.e. larger in tropical rays and smaller in cool-water skates, and may explain this exception to the TSR where tropical rays attain larger sizes at higher temperatures (Atkinson, 1995). Instead, our findings are more consistent with a mortality theory of life histories, and specifically the mortality arising from predation risk and offspring size (Auer et al., 2018; Glazier, 2023).

We found that offspring size explained good variation in r_{max} for rays and skates and is another simple life history trait alongside adult maximum body mass that could be used to estimate r_{max} . Simple variables that are widely available such as these life history traits, environmental temperature, and depth range have the potential to predict population growth rates and therefore extinction risk, fishing limits, and recovery potential, which is especially necessary for datapoor species (Pardo & Dulvy, 2022; Barrowclift et al., 2023). Given the strong phylogenetic signal in the r_{max} residuals, it is likely maximum population growth rate is shaped by biological traits that are evolutionary conserved, which would allow for predictive modelling of r_{max} based on phylogenetic relationships (Pardo & Dulvy, 2022). Additional variation in r_{max} that was not explained by our models may be explained by further environmental and physiological variables such as dissolved oxygen or metabolic rate (Gravel et al., 2024; Pardo & Dulvy, 2022). Empirical estimates of juvenile mortality for sharks and rays are still needed to better understand juvenile survival across species with different life history strategies (incorporating how growth and mortality varies with body size). Whilst the mortality estimator used in the modified Euler-Lotka model to calculate r_{max} accounts for juvenile survival to maturity, sizedependent mortality rates could be explored to investigate differences across reproductive and offspring size strategies. Our results suggest that these differences may be key to understanding biogeographic patterns in extinction risk. We hypothesise that greater predation risk in the tropics has driven the evolution of larger offspring size to increase offspring survival in tropical rays, potentially through live-bearing reproductive mode, increased matrotrophy, and larger adult body sizes. Consequently, shallow-water tropical rays have lower population growth rates and are more intrinsically sensitive to overfishing than may be expected from metabolic ecology.

Chapter 4. Age, growth, and intrinsic sensitivity of Endangered Spinetail (Mobula mobular) and Bentfin devil rays (M. thurstoni) in the Indian Ocean

4.1 Abstract

Devil rays (Mobula spp.) are caught in fisheries across the Indian Ocean, where there have been reports of significant recent declines. Globally, the few populations studied have extremely low population growth rates due to low fecundity and long reproductive cycles, making them highly vulnerable to overfishing. To allow for assessment of the current sustainability of devil ray catch in the Indian Ocean, we provide best first estimates of age using the caudal vertebrae; somatic growth rate using a Bayesian, multi-model approach; maximum intrinsic rate of population increase (r_{max}) ; and fishing mortality for Endangered Spinetail Devil Ray (Mobula mobular) and Bentfin Devil Ray (M. thurstoni) sampled from small-scale fisheries catch in Indonesia, Kenya, and Pakistan. The oldest individuals of M. mobular (n=79) and M. thurstoni (n=59) were 17.5 and six years, respectively. Both species had relatively low growth rates (k=0.05 and 0.19 year⁻¹, respectively) and low r_{max} (0.094 and 0.092 year⁻¹, respectively) indicating that they are highly sensitive to overexploitation. Fishing mortality F estimates (0.15) and 0.17 year⁻¹, respectively) were higher than r_{max} and exploitation ratio E (0.70 and 0.74, respectively) were higher than an optimum value of 0.5 for biological sustainability for both species, suggesting that the fisheries catches of the species are unsustainable. We demonstrate an approach to assess data-poor species and apply this to two Indian Ocean devil ray species. We caution that age estimates were based on the assumption of annual growth band pair deposition, which was unable to be validated. Nevertheless, the results present best first estimates of key life history parameters for these Endangered species in the Indian Ocean and highlight the urgent need for management actions to reduce catch of all devil rays to prevent species extirpation and aid in population recovery.

4.2 Introduction

Sharks and rays (Class Chondrichthyes, Subclass Elasmobranchii) generally exhibit slower growth, later sexual maturity, and lower fecundity than their teleost counterparts (Gravel et al., 2024; Compagno, 1990; Cortés, 2000). These life history traits result in lower population growth rates that restrict recovery potential (Dulvy & Forrest, 2010; Cortés, 2002) and make many species intrinsically sensitive to fisheries exploitation (Quetglas et al., 2016; García et al., 2008). Approximately 37% of chondrichthyans are threatened with extinction due to overfishing (Dulvy et al., 2021). Variations in life history among and within species, coupled

with differing exploitation rates, results in differences in fisheries resilience and localised extinction risk (Trinnie et al., 2014; Jacobsen & Bennett, 2010; Lombardi-Carlson et al., 2003). Data on species and population-specific life history traits are therefore critical in predicting extinction risk and rebound potential, demographic modelling, fisheries stock assessments, and achieving sustainable fisheries management and global conservation goals (Frisk et al., 2001; Cortés, 2002; Barnett et al., 2019).

Devil rays (Mobula spp., Family Mobulidae) are one of the most threatened chondrichthyan families (Dulvy et al., 2021). All devil ray species are listed on CITES (Convention on International Trade in Endangered Species of wild fauna and flora) Appendix II and CMS (Convention on the conservation of Migratory Species of wild animals) Appendices I and II, which regulate international trade and coordinate inter-governmental conservation efforts, respectively. Devil rays face high fisheries exploitation as target species and bycatch in both industrial and small-scale fisheries (Croll et al., 2016), exacerbated by an international market for their gill plates, which are used for food and traditional medicine in East Asia (O'Malley et al., 2017; Lawson et al., 2017). The Food and Agriculture Organisation of the United Nations (FAO) statistics indicate an annual global catch of over 4000 tonnes, a likely underestimate (FAO, 2023; Clarke, McAllister, et al., 2006; Pauly & Zeller, 2016). Devil rays have amongst the lowest maximum intrinsic rate of population increase (r_{max}) and therefore highest intrinsic sensitivity to overfishing (Dulvy, Pardo, et al., 2014; Pardo, Kindsvater, Cuevas-Zimbrón, et al., 2016; Rambahiniarison et al., 2018b). This sensitivity is in part due to their extremely low fecundity (Pardo et al., 2018), with species in this genus known to produce only a single pup per litter (rarely twins) every 1-7 years, following a 12-month gestation period (Last et al., 2016; Stevens et al., 2018). These life history traits have been observed in only a handful of studies and locations for these circumglobal, tropical and warm-temperate species (Marshall & Bennett, 2010; Stevens, 2016; Kashiwagi, 2014; Doumbouya, 2011; Notarbartolo di Sciara, 1988; Broadhurst et al., 2019, 2018; Villavicencio-Garayzar, 1991; Ehemann et al., 2017).

Despite there being several studies on devil ray life histories, there has only been a single aging study to date (Cuevas-Zimbrón et al., 2013). Given the importance of demographic data in assessing fisheries sustainability (Musick & Bonfil, 2005) and considering the broad distributions of some devil ray species (Couturier et al., 2012), further understanding of species and population-specific life history parameters is needed for effective evidence-based management (Barnett et al., 2019). Available evidence suggests that coastal and continental shelf devil ray species may exhibit genetic population structuring, including *M. kuhlii* and *M*.

alfredi between the eastern and western Indian Ocean as well as *M. mobular* and *M. alfredi* between the Indian Ocean and the Pacific (Humble et al., 2023; Hosegood et al., 2020; Venables et al., 2020; Lassauce et al., 2022). However, highly migratory and more offshore species including *M. thurstoni* and *M. birostris* show no evidence of population structuring, potentially due to more opportunity for gene flow (Humble et al., 2023; Hosegood et al., 2020). The extent of genetic population structuring and connectivity will have implications for the status of devil ray species and populations and to inform the most effective conservation actions.

Countries in the Indian Ocean region are among those reporting the highest devil ray catches (Ward-Paige et al., 2013; Couturier et al., 2012; Croll et al., 2016; Lawson et al., 2017). Six of the seven devil ray species in the Indian Ocean are listed as Endangered by the IUCN Red List; the Vulnerable reef manta ray (M. alfredi) being the only exception (IUCN, 2024). Devil rays are commonly caught in small-scale fisheries, primarily in gillnets, that provide important sources of protein and income for coastal communities, particularly in low-income countries (Temple et al., 2019; Flounders, 2020; Temple, Berggren, et al., 2024). Even where devil rays are not targeted in small-scale fisheries, they will often be retained for their meat and gill plates due to their high value (White et al., 2006; Moazzam, 2018). Devil rays are also caught in industrial tuna fisheries, mainly utilising purse-seine but also in longline and drift gillnet fishing gears (Shahid et al., 2018; Flounders, 2020). There is evidence of significant declines in sightings and fisheries catch (over 90%) in some loc(Moazzam, 2018; Rohner et al., 2017; Lewis et al., 2015; Fernando & Stewart, 2021; Carpenter et al., 2023)t, 2021; Carpenter et al., 2023). These declines led the Indian Ocean Tuna Commission (IOTC) to adopt a resolution (19/03) for the conservation of devil rays, including recommending collection of speciesspecific data for fisheries catches (IOTC, 2019). The IOTC resolution prohibits retention of devil rays and encourages live release, although this does not apply to subsistence fisheries where rays are consumed locally by the fishers. Life history parameters need to be defined to inform devil ray species assessments within the Indian Ocean region.

The aim of this study is to improve the knowledge of devil ray life histories by producing disc width-weight relationships, estimating age, growth, and maximum intrinsic rate of population increase (r_{max}) for M. mobular and M. thurstoni caught in small-scale fisheries in Indonesia, Kenya, and Pakistan. We further use the disc width-at-age dataset to estimate total mortality, fishing mortality, and the exploitation ratio for the two species.

4.3 Methods

4.3.1 Sample collection and species identification

Spinetail devil ray ($Mobula\ mobular$) (n=103) and Bentfin devil ray ($M.\ thurstoni$) (n=89) were opportunistically sampled from small-scale fisheries landing sites in Cilacap Fishing Port, Central Java (n=15) and Palabuhanratu, West Java, Indonesia (n=100) between July 2020 and December 2022; Kilifi Central, Kilifi, Kenya (n=43) between February and March 2021; and Karachi Fish Harbour, Sindh, Pakistan (n=37) between June 2021 and October 2022 with the consent of fishers and/or traders (Figure 4.1). A further three individuals of Sicklefin devil ray ($M.\ tarapacana$) were sampled in Indonesia.

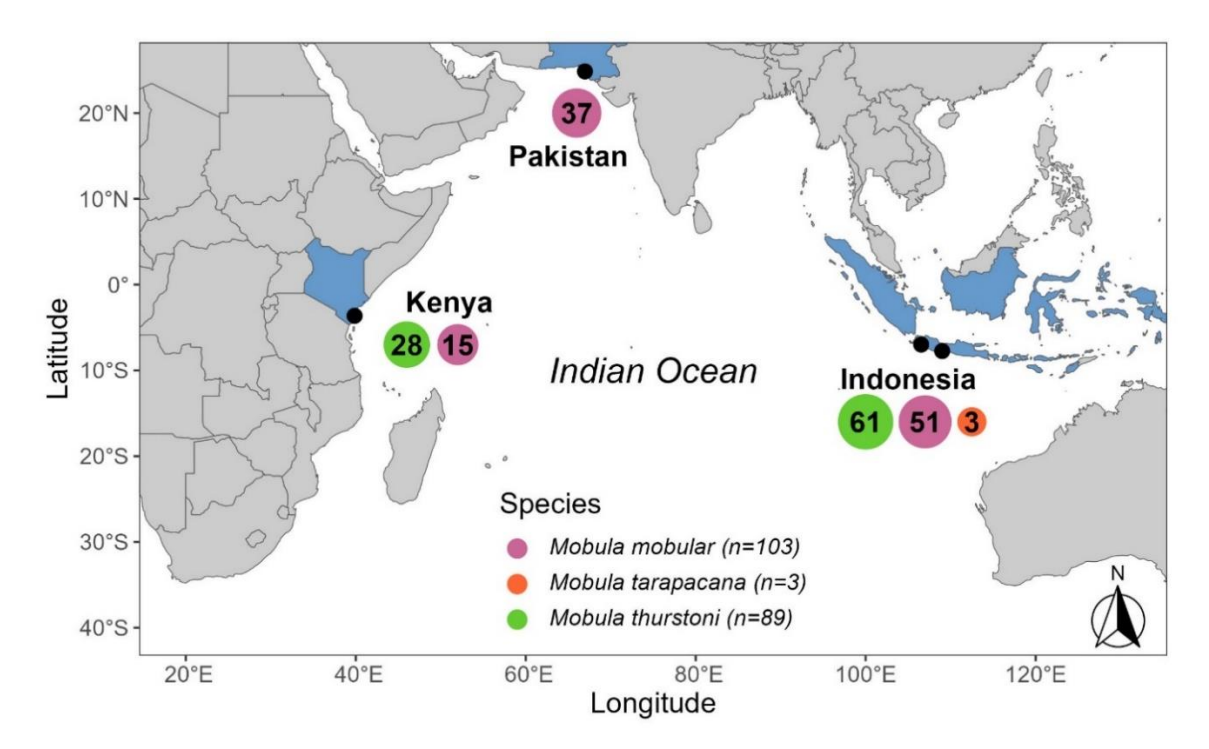


Figure 4.1 Sampling locations for *Mobula mobular*, *M. thurstoni*, and *M. tarapacana* across the Indian Ocean (n=195).

A minimum of two photos were taken showing the entire dorsal and ventral surface of each individual to aid species identification based on morphological characteristics (Figure 4.2). Devil rays are easily identifiable to genus level by the presence of cephalic lobes (extending from each side of their head). Of the seven devil ray species present in the Indian Ocean, *M. mobular* was identifiable by the distinct white tip on the dorsal fin and a caudal spine behind the dorsal fin, whilst *M. thurstoni* also has a distinct white tip on the dorsal fin (becoming faint in adults) but no caudal spine and is easily identifiable by the front of the wingtips curving in

distinctly (Figure 4.2) (Last et al., 2016; Stevens et al., 2018). *M. tarapacana* is easily identified by its long and strongly falcate (curved like a sickle) pectoral fins and a distinct bony ridge along the middle of the dorsal surface. There was therefore strong certainty in morphological species identification.

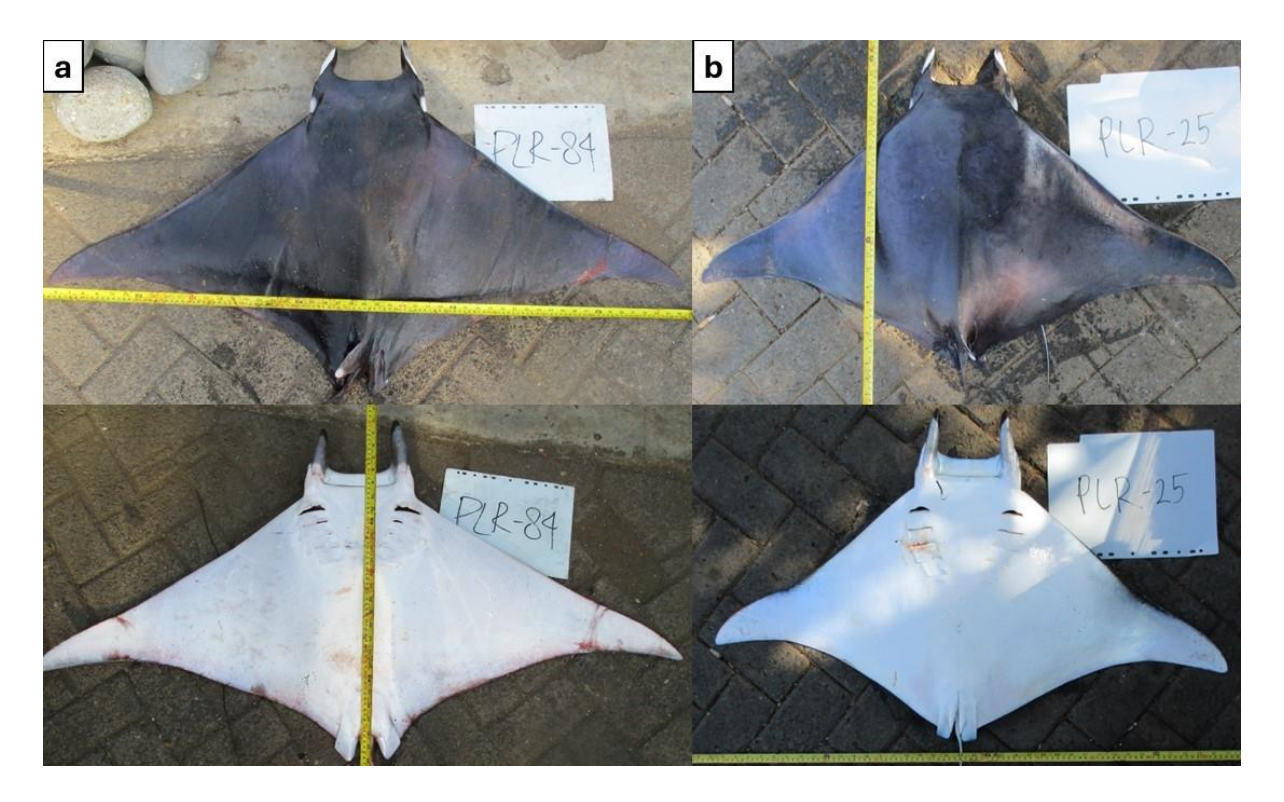


Figure 4.2 The two main species sampled in this study: a) Spinetail devil ray (*Mobula mobular*) and b) Bentfin devil ray (*M. thurstoni*).

The sex, disc width (DW, straight line length measurement between the wing tips) in cm, and weight in kg of every individual was recorded. Where possible, vertebrae samples (n=141) were taken from the caudal portion of the vertebral column for aging and were stored at -20°C (Figure 4.2a) (Cuevas-Zimbrón et al., 2013). Male maturity (immature or mature) was recorded based on the calcification of claspers, whereby only male specimens with fully calcified claspers were considered mature (Walker, 2005). Where fishers and traders consented (M. mobular, n=27; M. thurstoni, n=6), female reproductive tracts were dissected to determine maturity, with females considered mature by the presence (mature) or absence (immature) of well-developed eggs in the ovaries (Walker, 2005). Species were mainly caught in gillnet (bottom-set and drift, n=184) fishing gear but also longline (n=2), handline (n=2), and purse

seine (n=4) in Indonesia. Samples were collected under research permits where necessary, including from The National Research and Innovation Agency (BRIN) in Indonesia (no. 28/TU.B5.4/SIP/VI/2021 and 12/SIP.EXT/IV/FR/8/2022). Due diligence was undertaken to ensure compliance with the Nagoya Protocol on Access to Genetic Resources. Samples were exported to the United Kingdom under the following **CITES** export (00098/SAJI/LN/PRL/IX/2021; 00525/SAJI/LN/PRL/VIII/2022; and P-121/2022) and import permits (610843/01;/02;/03;/04;/05;/06; 621633/01;02; and 625390/01;/02) as well as an authorisation for importation of animal by-products (ITIMP21.1211).

4.3.2 Disc width-weight relationship

Species- and location-specific DW frequency distributions were fit using 5cm size bins for M. mobular and M. thurstoni. Bayesian linear models were fit to natural log (ln) transformed DW and weight data for M. mobular (n=101) and M. thurstoni (n=76) (Froese et al., 2014). Due to small sample sizes, all models were fit for each species across locations and for combined sex. Informative priors were constrained for a and b constants based on estimates available on FishBase (Froese & Pauly, 2022), which was approximately 0.005 (-5 for log(a)) and 3 for a and b, respectively (Table 4.1). We also compared the effect on posteriors with parameter estimates using weaker priors with the same mean of the distributions but higher variance (Table 4.1). A weakly informative prior is used for the variance σ^2 in all models (Table 4.1).

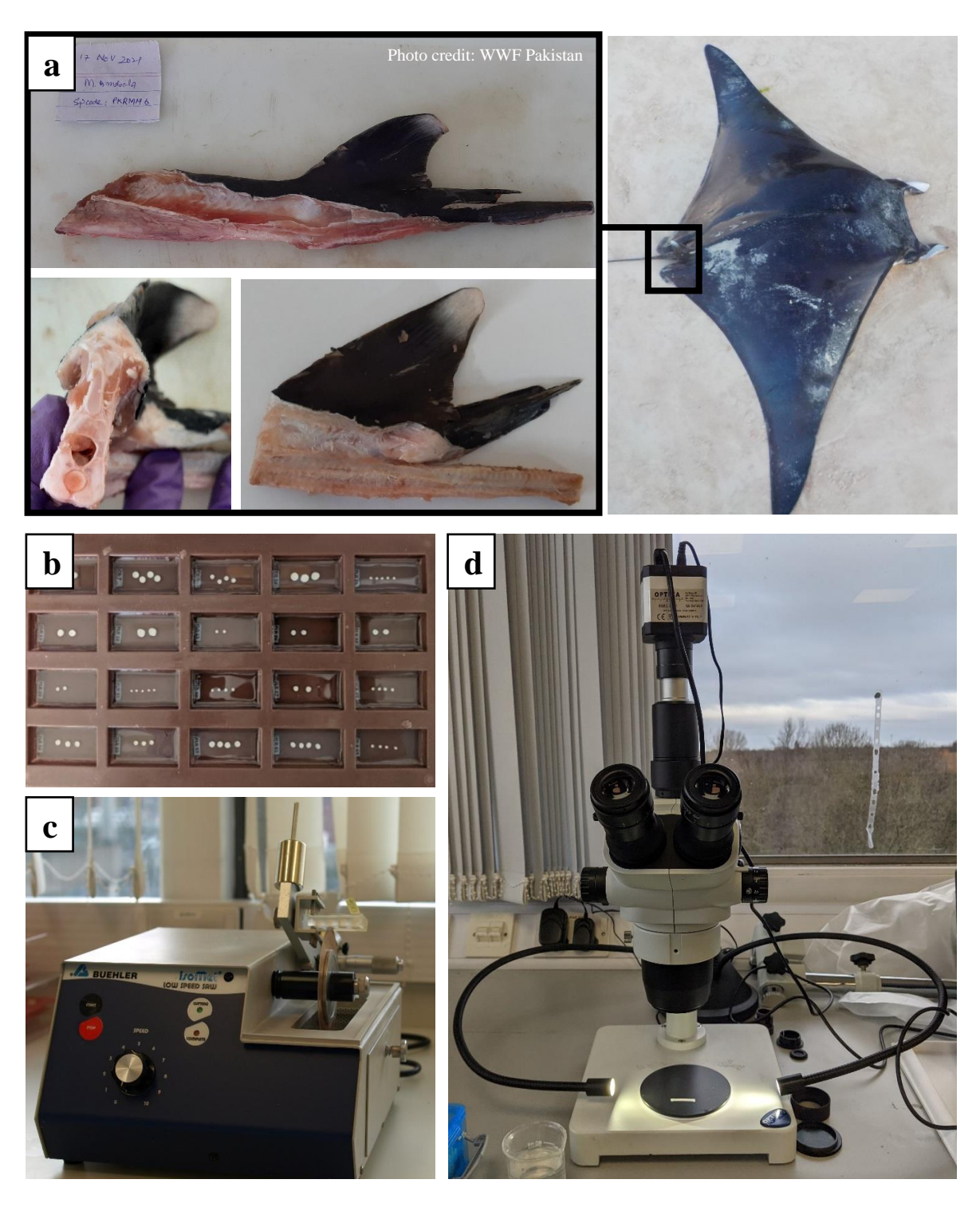


Figure 4.3 Preparation of *Mobula* spp. vertebrae sections for age determination including: a) portion of the vertebral column where caudal vertebrae samples were taken; b) embedded vertebrae centra in an epoxy resin in silicon moulds; c) longitudinal sectioning of set vertebrae centra using a Buehler IsoMet Low-Speed Diamond Blade Saw fit with two 4 inch blades and a 3.5 inch 0.5mm plastic separator; and d) imaging of vertebrae sections for age determination using an Optika dissecting microscope with a fitted camera, illuminated from above using reflected light and from either side using a double-armed fibre optic light source.

Table 4.1 Strong and weaker priors used for each parameter in Bayesian length-weight regression, growth models, and length-maturity regression models for *Mobula mobular* (n=79) and *M. thurstoni* (n=59).

Species	Model	Parameter	Strong priors	Weaker priors
	DW-weight	b	normal(3, 0.5)	normal(3, 1)
	linear	log(a)	<i>normal</i> (-5, 1)	<i>normal</i> (-5, 3)
	regression	σ^2	halfCauchy(0, 30000)	halfCauchy(0, 30000)
M. mobular	Age-maturity	β	normal(0,10)	normal(0,10)
and <i>M</i> .	logistic	а	normal(logit(0.5) +	normal(0,10)
thurstoni	regression	и	beta * α_{mat} , 10)	
	DW-maturity	β	normal(0,10)	normal(0,10)
	logistic	a	normal(logit(0.5) +	normal(0,10)
	regression		beta * DW _{mat} , 10)	
	Growth models	k	uniform(0, 2)	uniform(0, 2)
	(von	DW_0	normal(900, 200)	normal(900, 300)
	Bertalanffy,	DW_{∞}	normal(3500*kappa,	normal(3500*kappa,
	Gompertz,	DW_{∞}	100)	400)
M. mobular	Logistic,	kappa	gamma(1000, 990)	gamma(200, 198)
M. moduai	Lester)	σ^2	halfCauchy(0, 30000)	halfCauchy(0, 30000)
	Lester	T	normal(4, 1)	normal(4, 4)
	(biphasic)	h	normal(500, 1000)	normal(500, 1000)
	growth model	t_1	normal(0, 20)	normal(0, 10)
	growth moder	σ^2	halfCauchy(0, 30000)	halfCauchy(0, 30000)
	Growth models	k	uniform(0, 2)	uniform(0, 2)
	(von	DW_0	normal(700, 200)	normal(700, 300)
	Bertalanffy,	DW_{∞}	normal(1970*kappa,	normal (1970*kappa,
	Gompertz,	DW_{∞}	100)	400)
M. thurstoni	Logistic,	kappa	gamma(1000, 980)	gamma(200, 196)
M. marsiom	Lester)	σ^2	halfCauchy(0, 30000)	halfCauchy(0, 30000)
	Lester	T	normal(4, 1)	normal(4, 4)
	(biphasic)	h	normal(500, 1000)	normal(500, 1000)
	growth model	t_1	normal(0, 5)	normal(0, 10)
	growth model	σ^2	halfCauchy(0, 30000)	halfCauchy(0, 30000)

4.3.3 Age estimation using caudal vertebrae

In line with Cuevas-Zimbrón et al. (2013), we found no vertebral centra in the thoracic portion of the vertebral column and vertebrae size increased in the caudal portion of the vertebral column below the origin of the dorsal fin. We therefore sampled caudal vertebrae for age estimation (Figure 4.2a). Neural and haemal arches along with excess tissue were removed from vertebrae samples using a scalpel. Vertebrae were subsequently placed into 5% diluted bleach for a maximum of five minutes depending on vertebrae size to remove any remaining connective tissue and then rinsed with distilled water. Cleaned vertebrae centra samples were left to air dry overnight. Vertebrae centra were submerged in a mixture of EpoxiCure 2 Resin

20-3430128 (4 parts) and EpoxiCure 2 Hardener 20-3432128 (1 part) in silicon moulds and left to set for three days (Figure 4.3b). After trialling several vertebral section widths (600, 450, 300, and 150μm), a Buehler IsoMet Low-Speed Diamond Blade Saw fitted with two 4-inch blades and a 3.5 inch 0.5mm plastic separator was used to cut one longitudinal section through the centre of each vertebral centra at a thickness of approximately 300-400μm (Figure 4.2c). Staining the vertebral sections with 0.01% Crystal Violet solution (Schwartz, 1983) as in Cuevas-Zimbrón et al. (2013), was trialed but did not substantially enhance banding clarity.

A drop of water was added to the vertebral section, which was placed on black card prior to imaging. Each vertebral section was imaged using an Optika dissecting microscope with a fitted camera (Optika WF Series 4083.WiFi), illuminated from above using reflected light and from either side using a double-armed fibre optic light source (Figure 4.3d). A 1.2X magnification was used for consistency. Optika Vision Lite 2.1 software was used to capture the image and export as a jpeg file. Each vertebral section was imaged on both sides and the image with the clearest view of the growth bands was used for age determination. Images of vertebral sections were enhanced in Adobe Photoshop Elements 2021 Photo Editor (Version: 19.0) following guidance in Campana (2014) to adjust the greyscale and sharpness to enhance the readability of banding patterns (Figure 4.4).

Age was estimated based on the assumption of annual growth band pair deposition, with one translucent and one opaque band equating to one band pair (annulus) indicating one year of age (Cailliet et al., 2006, 1983). The birth mark was identified as the first band with a distinct change in the angle of the *corpus calcareum* and was not counted when estimating age (REF_(Neer & Thompson, 2005; Campana, 2014; Cuevas-Zimbrón et al., 2013)14; Cuevas-Zimbrón et al., 2013). Banding was read along the *corpus calcareum* near the lateral edge (Campana, 2014). Adobe Photoshop Elements (2021 Photo Editor) was used to annotate enhanced images to indicate annual growth bands (Figure 4.4). The annuli were counted for each imaged section to age individuals to the nearest 0.5 year. A mean was then calculated from the counts of the two sections to give an estimated age per individual. Aging was conducted independently by two readers without access to contextual information such as animal size. If the mean estimates of the two readers differed by less than one year, the mean of these two values was taken as the best estimate for that individual (Goldman, 2005). This is a more conservative approach than in many other studies due to the limited sample size (Temple et al., 2020; Smith et al., 2012). If mean estimates differed by more than one year, then ages were re-estimated with both readers

together. If agreement was not reached (n=0), samples would have been removed from further analyses (Goldman, 2005).

The Bland-Altman approach for method comparison was used to quantify agreement, precision, and bias in age reads within each reader (comparing the age estimate between two sections per specimen) and between the two readers (comparing the mean age estimate for each specimen) (Temple et al., 2020; Bland & Altman, 2003, 1999). Linear models of the mean age read for each specimen against the difference between reads for each specimen were used to check for bias in the relationship between reads (within and between readers). Limits of Agreement using the 95% mean confidence interval of the difference between reads was also used to define precision in age reads (within and between readers). Standard metrics of agreement used in aging studies were also presented for comparison: the average percent error, coefficient of variation, percent agreement and percent agreement ±1 year (Beamish & Fournier, 1981; Chang, 1982) but note these latter measures are known to be flawed (Cailliet et al., 2006; Goldman, 2005). Validation of band pair periodicity (i.e. the assumption of annual growth band pair deposition) was not possible using marginal increment analysis or edge analysis due to insufficient sample numbers across all months of the year (Table 4.2) and other validation methods such as mark-recapture of chemically tagged fish were not possible in this study (Campana, 2001; Cailliet et al., 2006).

Table 4.2 Age frequency for sampled *Mobula mobular* (n=79) and *M. thurstoni* (n=59) by location, sex, and month.

Species	Date	Indonesia	Pakistan
	January	2	-
	March	-	10
	May	1	-
M 1 1 1 1	June	-	1
Mobula mobular	July	1	-
	September	10	15
	October	31	3
	November	3	2
	January	11	-
M 1 1 11 1 1 1 1 1 1 1 1 1 1 1 1 1 1 1	September	6	-
Mobula thurstoni	October	40	-
	November	2	-

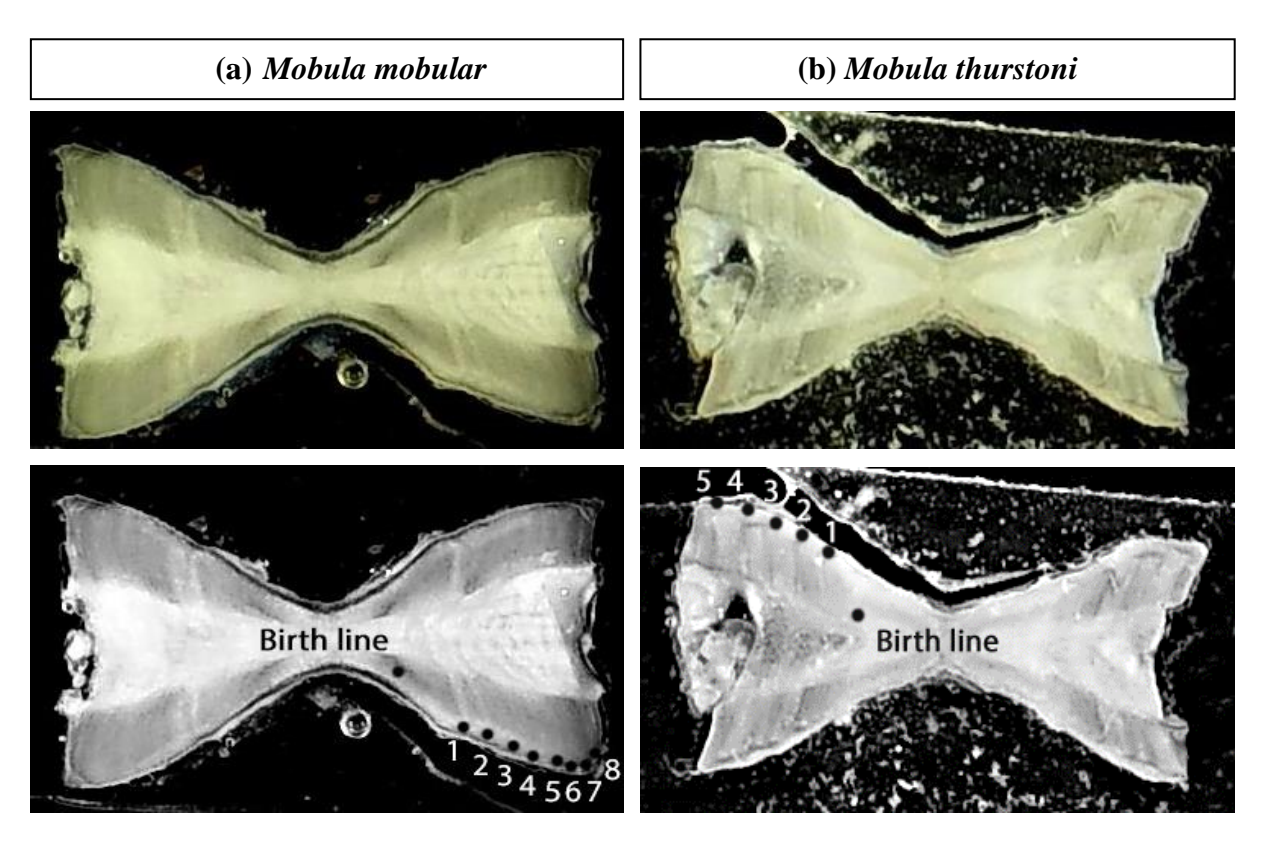


Figure 4.4 Images of a) *Mobula mobular* and b) *M. thurstoni* vertebrae sections for age determination using an Optika dissecting microscope with a fitted camera, illuminated from above using reflected light and from either side using a double-armed fibre optic light source, and enhanced in Adobe Photoshop Elements 2021 Photo Editor (Version: 19.0), annotated with birth line and annual growth bands. The imaged sections are from a) a male *M. mobular* aged as 8 years and b) a male *M. thurstoni* aged as 5 years caught in a small-scale gillnet fishery in Cilacap, Central Java, Indonesia between September-October 2020.

4.3.4 Estimating growth

A Bayesian, multi-model approach was used to estimate growth using the DW-at-age dataset for *M. mobular* and *M. thurstoni*, incorporating prior knowledge of maximum size and size-at-birth to set informative priors (Pardo, Kindsvater, Cuevas-Zimbrón, et al., 2016). The DW-at-age datasets were missing samples for the largest individuals based on known maximum sizes and classical growth models using a frequentist approach are sensitive to missing data points (Siegfried & Sansó, 2006). Therefore, a Bayesian approach likely provides growth estimates that are more biologically relevant than a classical, frequentist approach (Pardo, Kindsvater, Cuevas-Zimbrón, et al., 2016; Smart & Grammer, 2021). Whilst the von Bertalanffy growth model is the most commonly used and generally best-fitting growth model for elasmobranchs, a multi-model approach is required to ensure the most appropriate model is fitted (Smart et al., 2016). An information-theoretic approach was used to choose the best fitting model by

comparing leave-one-out information criterion (LOOIC) (Vehtari et al., 2017). To account for multiplicative error, equations were log-transformed with an error term added. The following models were fit and compared:

the three-parameter von Bertalanffy equation (von Bertalanffy, 1938):

$$log(DW_t) = log(DW_{\infty} - (DW_{\infty} - DW_0)e^{-kt}) + \epsilon_t$$
 (1)

the Lester biphasic growth function (Lester et al., 2004):

$$log(DW_t) = log(h(t - t_1)) + \epsilon_t \text{ when } t \le T$$
(2a)

$$log(DW_t) = log\left(DW_{\infty}\left(1 - e^{-k(t - DW_0)}\right)\right) + \epsilon_t \text{ when } t > T$$
 (2b)

the three-parameter Gompertz growth function (Ricker, 1975),

$$log(DW_t) = log\left(DW_0 e^{\left(log\left(\frac{DW_\infty}{DW_0}\right)(1 - e^{-kt})\right)}\right) + \epsilon_t$$
(3)

and the logistic growth function (Ricker, 1979),

$$log(DW_t) = log\left(\frac{DW_{\infty}DW_0e^{kt}}{DW_{\infty} + DW_0(e^{kt} - 1)}\right) + \in_t$$
(4)

where DW_t is the disc width at age t, DW_{∞} is the asymptotic disc width, DW_0 is disc width at age zero, k is a growth constant, h is the juvenile growth rate (disc width per unit time), t_1 is the asymptotic hypothetical age at length 0, and T is the last immature age. The Lester biphasic growth model did not converge for either species and was therefore not reported in the results.

Reported maximum sizes are 350cm DW (individual from the Mediterranean) and 197cm DW (individual from the Phillipines) for *M. mobular* and *M. thurstoni*, respectively, with size-at-birth reportedly 90-160cm and 70-90cm, respectively (Rambahiniarison et al., 2018b; Notarbartolo di Sciara, 1988; Notarbartolo di Sciara et al., 2020). Asymptotic size in fishes can be estimated from maximum size using the following equation (Froese & Binohlan, 2000):

$$DW_{\infty} = 10^{0.044 + 0.9841 * (\log_{10}(DW_{max}))}$$
 (5)

where DW_{max} is the maximum size in centimetres. For a DW_{max} of 350cm for M. mobular and 197cm for M. thurstoni, this resulted in $DW_{\infty}=1.01 * DW_{max}$ and $DW_{\infty}=1.02 * DW_{max}$, respectively. Hyperpriors were set for this parameter, defined as kappa, and based on a gamma distribution with a mean of 1.01 and 1.02, respectively. The probability distribution of kappa was set between 0.7 and 1.3 (Froese & Binohlan, 2000; Pardo, Kindsvater, Cuevas-Zimbrón, et al., 2016). Priors were also constrained for DW_0 around size-at-birth. The same priors were used across models for DW_0 , DW_{∞} , and σ for each species as these parameters can be interpreted in the same way (Smart & Grammer, 2021; Smart et al., 2016) (Table 4.1). There is prior information on k for the von Bertalanffy growth model for M. mobular (Pardo, Kindsvater, Cuevas-Zimbrón, et al., 2016) but since k is unique to each growth model tested and therefore not comparable across models (Smart et al., 2016), an uninformative prior was used for all models (Table 4.1). For the Lester biphasic growth model, T was constrained around the minimum age at maturity for M. mobular, which was estimated between five to six years in a previous study (Pardo, Kindsvater, Cuevas-Zimbrón, et al., 2016; Cuevas-Zimbrón et al., 2013). A prior with a normal distribution and a mean of four years was therefore used to account for a lag between the start of reproductive investment and maturity (Wilson et al., 2018). Age-atmaturity is unknown for *M. thurstoni* but is inferred from *M. mobular*. Uninformative priors were used for h and t_1 parameters.

As well as setting informative priors, we compare the effect on posteriors with parameter estimates using weaker priors with the same mean of the distributions but higher variance (Table 4.1). A weakly informative prior is used for the variance σ^2 in all growth models. We trialled fitting uninformative priors with uniform distributions but the model did not converge well because there were insufficient data to fit an asymptotic curve due to the low number of larger and older individuals; this means the chosen priors were not truly uninformative (Van Dongen, 2006).

Finally, we used the top model to test for potential regional differences in growth between Indian Ocean *M. mobular* (Indonesia and Pakistan) and *M. mobular* caught off Mexico (Cuevas-Zimbrón et al., 2013). Bayesian models were written in Stan and conducted in RStan version 2.21.0 (Stan Development Team, 2023). To allow comparison of length-at-age estimates, the top growth function for *M. mobular* was also fit using a frequentist approach. The top growth function for *M. thurstoni* did not converge when fit using a frequentist approach, likely due to the lack of older individuals in the dataset. Self-starter functions from the package *FSA* (Ogle et al., 2022) were first used to generate reasonable starting values for growth model

parameters and nonlinear regression models were fit using the package *nlstools* (Baty et al., 2015). The 95% confidence intervals for growth curves and coefficients were calculated using bootstrapping with replacement for 10,000 iterations.

4.3.5 Estimation of maximum intrinsic rate of population increase

The maximum intrinsic rate of population increase (r_{max}) was estimated for M. mobular and M. thurstoni using a modified Euler-Lotka model that accounts for survival to maturity (Pardo, Kindsvater, Reynolds, et al., 2016; Cortés, 2016):

$$l_{\alpha_{mat}}b = e^{r_{max}\alpha_{mat}} - e^{-M}(e^{r_{max}})^{\alpha_{mat-1}}$$
(6)

where $l_{\alpha_{mat}}$ is survival to maturity, b is the annual reproductive output of female offspring, α_{mat} is female age-at-maturity, and M is the instantaneous rate of natural mortality. $l_{\alpha_{mat}}$ is calculated as:

$$l_{\alpha_{mat}} = (e^{-M})^{\alpha_{mat}} \tag{7}$$

M is estimated as:

$$M = \left(\frac{\alpha_{max} + \alpha_{mat}}{2}\right)^{-1} \tag{8}$$

where α_{max} is female maximum age.

The limited sample size and temporal period of sampling in this study meant the annual reproductive output b of M. mobular and M. thurstoni could not be determined. Both species are known to produce a single pup, occasionally two pups per litter, over a 12-month gestation period and have a reproductive cycle of one to three years with resting periods (Rambahiniarison et al., 2018; Doumbouya, 2011). Assuming a 1:1 sex ratio, we estimate a plausible range of b using the following equation:

$$b = 0.5 \left(\frac{l}{i}\right) \tag{9}$$

where l is litter size and i is breeding interval. b was therefore bound between 0.17 (based on a single pup and triennial reproductive cycle) and 1 (two pups and annual reproductive cycle).

 α_{mat} and DW at 50% maturity DW_{mat} were estimated using Bayesian logistic regressions for both species for combined sex using strong and weaker priors. However, M. thurstoni logistic regression models did not fit the DW- and age-maturity data well due to limited observations of mature individuals (n=2) and therefore parameter estimates are not presented. Parameter

estimates for M. mobular were similar and therefore only presented for stronger priors in the results. There are no direct estimates of age at maturity available for M. thurstoni but there is an estimate of DW_{mat} of 150cm (Rambahiniarison et al., 2018; Notarbartolo di Sciara, 1988). Using age and growth data from this study, α_{mat} for M. thurstoni was therefore assumed to mature between 5 and 6 years. Size at maturity for females and males of both species have been found to be similar (Rambahiniarison et al., 2018; Stevens et al., 2018). We used the range of α_{mat} estimated to set the lower and upper bounds of α_{mat} for each species.

To estimate M, we need to estimate α_{max} . We used the theoretical age that each species reached 95% and 99% DW_{∞} to bound our α_{max} estimate, which is calculated as $5\ln(2)k^{-1}$ and $7\ln(2)k^{-1}$, respectively (Fabens, 1965; Ricker, 1979). The maximum observed age in this study was less than the 95% DW_{∞} and was therefore used as the lower bound. r_{max} was estimated using the nlminb function in R from the package stats (R Core Team, 2021). A Monte Carlo approach was used whereby 10,000 random deviates were drawn from a uniform distribution between minimum and maximum values of b, α_{mat} , α_{max} , and M to account for uncertainty within these parameters (Dulvy et al., 2014; Temple et al., 2020).

4.3.6 Estimation of total mortality, fishing mortality, and the exploitation ratio

The top growth model was used to estimate age to the nearest year for M. mobular (n=103) and M. thurstoni (n=89) given DW. Total instantaneous mortality rate Z (± 95 % CI), which is a combination of fishing mortality F and natural mortality M, was calculated using the Chapman-Robson catch curve with the package FSA (Smith et al., 2012; Ogle et al., 2022). This assumes the individuals in this study are one population with minimal migration and that sampling from the fishery is random and non-selective across age and size classes. The ages of M. mobular and M. thurstoni fully recruited to the fishery (three and two years, respectively) were assumed to be the peak abundance, with Z estimated from four and three years of age, respectively. 10,000 draws were made from the estimated ranges of natural mortality M and Z, with uniform and normal probability distributions assumed, respectively. F was then estimated by subtracting the ranges of M from the ranges of Z. Exploitation ratio E was calculated by dividing the ranges of fishing mortality F by the ranges of Z. Median F, r_{max} , and exploitation ratio E estimates were compared whereby r_{max} is equivalent to the fishing mortality that will drive a species to extinction ($F_{extinct}$) and E is the ratio of F to M where if F = M then E is 0.5, representing an optimum value for biological sustainability (Pauly, 1983; Gulland, 1971). Total annual mortality rate A was also estimated from Z, where $1 - e^{(-Z)}$, as an estimate of the proportion of individuals in a closed population (assuming no immigration, recruitment, or emigration) that die in one year.

All data analyses and visualisations were conducted in R version 4.1.2 (R Core Team, 2021).

4.4 Results

4.4.1 Disc width-weight relationship

Mobula mobular sampled in this study ranged between 62 and 260cm DW, whilst *M. thurstoni* ranged between 75 and 190cm DW (Figure 4.5). Juveniles and mature individuals of both sexes were sampled for each species as indicated by maturity status assessments as well as known offspring size and size at maturity (IUCN, 2022) (Figure 4.5). However, only two mature *M. thurstoni* individuals were recorded (both male). Two individuals of *M. mobular* were smaller (62cm and 87cm DW) than the minimum known offspring size for this species (90cm DW) (Figure 4.5). A few individuals close to the known maximum size of *M. thurstoni* were sampled; however, this species possibly reaches 220cm DW (Jabado & Ebert, 2015) and the largest possible individuals of *M. mobular* were likely not sampled as indicated by known maximum sizes (IUCN, 2022) (Figure 4.5).

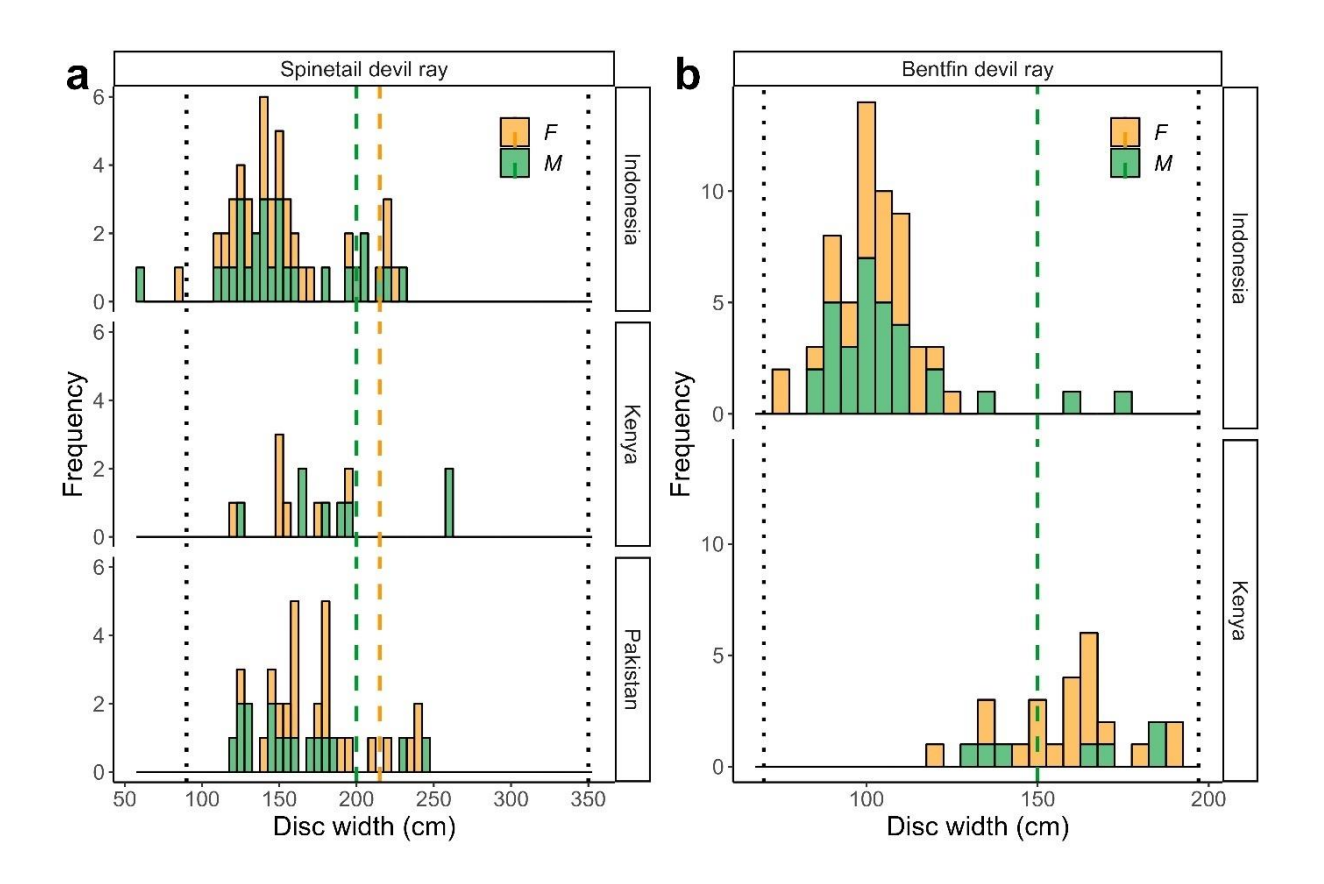


Figure 4.5 Disc width (cm) frequency distribution for a) Spinetail devil ray (M. mobular) (n=103) and b) Bentfin devil ray (M. thurstoni) (n=89) sampled from Indonesia (n=112), Kenya (n=43), and Pakistan (n=37) with known female (orange dashed) and male (green dashed) minimum size at maturity; minimum offspring size and maximum size (black dotted lines) for each species indicated (IUCN, 2023).

Table 4.3 Mean estimates (95% Credible Intervals) of Bayesian length-weight regression, growth models, and length-maturity regression models using strong and weaker priors for *Mobula mobular* (n=79) and *M. thurstoni* (n=59).

Species	Model	01		Weaker priors
	DW-weight linear	β	2.51 (2.30, 2.71)	2.51 (2.31, 2.70)
	regression	log(a)	-9.26 (-10.28 , -8.19)	-9.27 (-10.25 , -8.24)
	regression	σ^2	0.27 (0.24, 0.32)	0.27 (0.24, 0.32)
		k	0.05 (0.04, 0.06)	0.06 (0.03, 0.11)
	von Bertalanffy	DW_0	1166.53 (1085.5, 1246.79)	1162.64 (1070.34 , 1249.08)
	growth model	DW_{∞}	3502.95 (3214.2 , 3795.37)	3311.95 (2545.35 , 4184.92)
		σ^2	0.12 (0.1, 0.14)	0.12 (0.1, 0.14)
		k	0.08 (0.06, 0.09)	0.09 (0.06, 0.16)
Mobula	Gompertz growth	DW_0	1197.67 (1125.27 , 1270.53)	1186.47 (1096.77, 1269)
mobular	model	DW_{∞}	3490.26 (3195.5, 3789.21)	3146.85 (2439.22 , 4073.06)
тобиш		σ^2	0.12 (0.1, 0.14)	0.12 (0.1, 0.14)
		k	0.11 (0.08, 0.13)	0.14 (0.09, 0.22)
	Logistic growth	DW_0	1222.28 (1158.27 , 1287.63)	1200.65 (1111.93 , 1284.85)
	model	DW_{∞}	3474.85 (3187, 3773.44)	2994.05 (2340.35 , 3938.02)
		σ^2	0.12 (0.1, 0.14)	0.12 (0.1, 0.14)
	Age-maturity	β	0.66 (0.35, 1.04)	0.70 (0.37, 1.09)
	logistic regression	а	-5.46 (-8.49 , -3.24)	-5.70 (-8.74 , -3.32)
	DW-maturity	β	0.07 (0.04, 0.09)	0.10 (0.06, 0.16)
	logistic regression	а	-13.72 (-19.0 , -8.90)	-20.79 (-31.62, -12.71)
	DW-weight linear	β	2.84 (2.60, 3.06)	2.84 (2.61 , 3.06)
	regression	log(a)	-10.74 (-11.77, -9.61)	-10.74 (-11.79 , -9.63)
	regression		0.23 (0.19, 0.28)	0.23 (0.19, 0.28)
		k	0.1 (0.07, 0.15)	0.11 (0.05, 0.24)
	von Bertalanffy	DW_0	849.86 (789.17, 906.01)	851.93 (788.04 , 907.96)
	growth model	DW_{∞}	2014.78 (1777.36 , 2245.42)	2113.41 (1481.71 , 2845.3)
Mobula		σ^2	0.1 (0.08, 0.12)	0.1 (0.08, 0.12)
thurstoni		k	0.14 (0.09, 0.22)	0.14 (0.08, 0.26)
inursioni	Gompertz growth	DW_0	862.72 (811.98, 911.67)	864.77 (809.56, 915.81)
	model	DW_{∞}	2047.37 (1664.56 , 2438.92)	2155.38 (1524.94 , 2909.55)
		σ^2	0.1 (0.08, 0.12)	0.1 (0.08, 0.12)
		k	0.19 (0.14, 0.25)	0.18 (0.12, 0.31)
	Logistic growth	DW_0	870.21 (823.47 , 916.42)	873 (821.75 , 920.05)
	model	DW_{∞}	2022.11 (1796.58 , 2252.17)	2178.12 (1549.54 , 2929.75)
		σ^2	0.1 (0.08, 0.12)	0.09 (0.08, 0.11)

There was little difference in *a* and *b* estimates with strong and weaker priors and therefore the Bayesian linear disc width-weight relationship was presented for strong priors only for each species (Table 4.3; Figure 4.6).

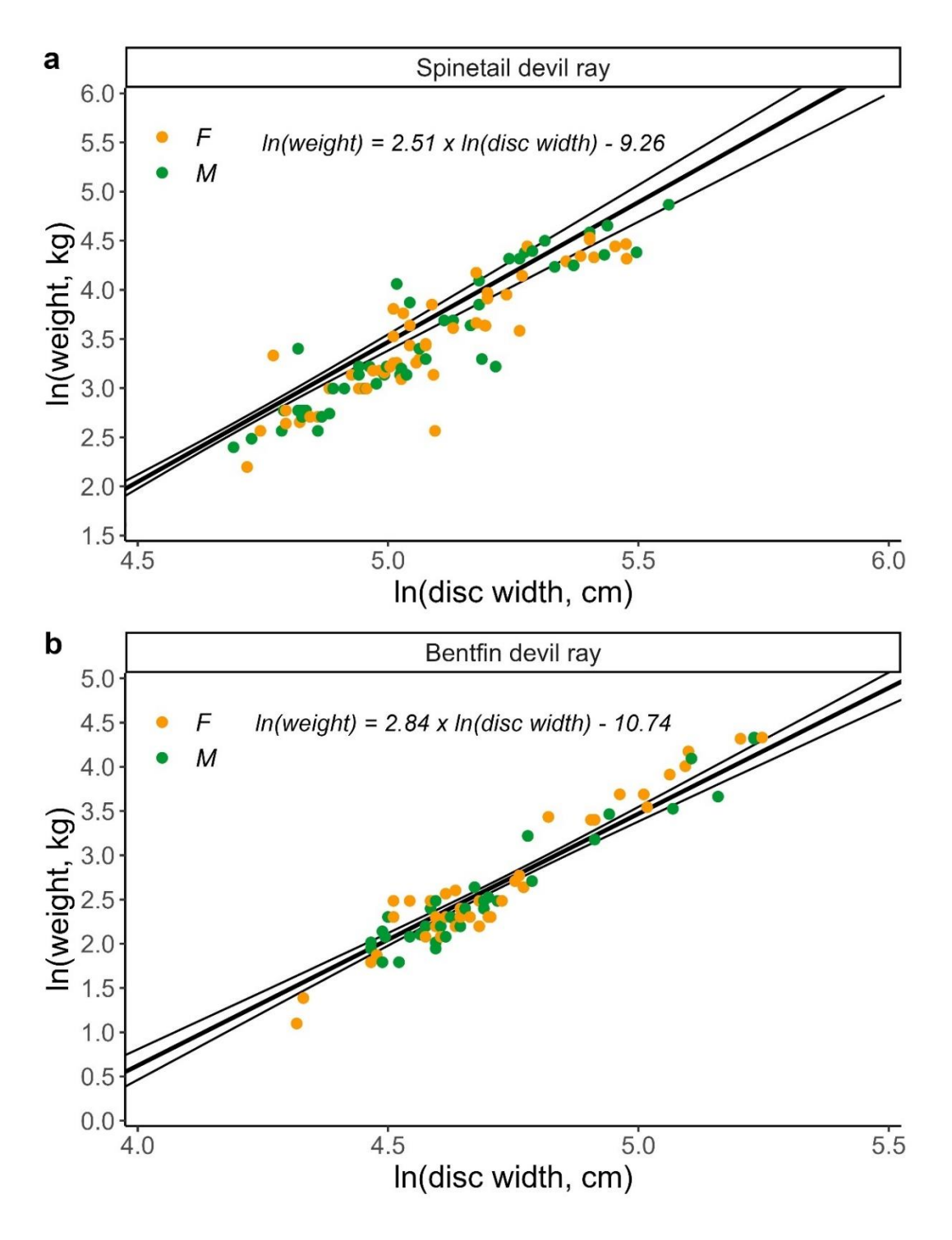


Figure 4.6 Natural log-transformed disc width (cm) and weight (kg) Bayesian linear relationship (with 95% credible intervals) for female (orange) and male (green) a) Spinetail devil ray (M. mobular) (n=101) and b) Bentfin devil ray (M. thurstoni) (n=76).

4.4.2 Age estimation using caudal vertebrae

Vertebral samples for age estimation in M. mobular (n=79) came from Indonesia (n=48) and Pakistan (n=31), with individuals younger than one years old sampled for both sex and maximum ages of 17.5 and 12.5 years for females (n=41) and males (n=38), respectively. Vertebral samples for age estimation in M. thurstoni (n=59) came from Indonesia, with all females (n=29) aged under two years old and males (n=30) ranging from less than one years old to six years old. The caudal vertebrae of M. tarapacana (n=3) showed clear banding, suggesting this method would be viable for future aging studies with a greater sample size. The three individuals sampled were aged at 1.5, 6, and 8 years for specimens with 152 (female), 237 (male), and 210cm (female) DW, respectively.

Bland-Altman analyses of M. mobular reads showed no evidence of bias within reader 1 (M. mobular, R^2 =0.0259, F=3.08, p=0.0834; M. thurstoni, R^2 =0.0170, F=2.00, p=0.163) or reader 2 (M. mobular, R^2 =0.00761, F=1.60, p=0.210; M. thurstoni, R^2 =0.00504, F=1.29, p=0.260) (Figure 4.7). There was evidence of significant bias between readers for M. mobular (R^2 =0.0742, F=7.26, p<0.001) but not for M. thurstoni (R^2 =0.0126, F=1.74, p=0.192) (Figure 4.7). For all individuals that initially differed by more than one year, consensus was reached between readers, likely overcoming this bias. Average percent error, coefficient of variation, percent agreement, percent agreement ± 1 year are also presented alongside Bland-Altman limits of agreement (Table 4.4; Figure 4.7). The variability in age band counts was consistent with other shark and ray aging studies (Temple et al., 2020; Jacobsen & Bennett, 2010; Baje et al., 2018; Gutteridge et al., 2013). Higher variability in M. thurstoni reads is likely due to younger age estimates meaning smaller differences in age band counts can cause inflated error estimates (Baje et al., 2018).

Table 4.4 Estimates of ageing agreement, precision, and bias in age reads for *Mobula mobular* (n=79) and M. thurstoni (n=59) within and between two readers: Average Percent Error (APE), Coefficient of Variation (CV), Percent Agreement (PA), PA ± 1 year, and Bland-Altman Limits of Agreement (LOA).

Species	Estimate	PA (%)	PA ± 1 year (%)	CV (%)	APE (%)	LOA (± years)
Mobula	Within reader 1	64.6	23.3	5.94	4.20	1.63
	Within reader 2	36.7	50.7	15.8	11.2	2.03
mobular	Between readers 1 and 2	41.8	22.7	10.1	7.17	1.44
14 1 1	Within reader 1	81.4	5.88	3.86	2.73	0.57
Mobula	Within reader 2	89.8	7.02	2.52	1.78	0.54
thurstoni	Between readers 1 and 2	78.0	0.00	2.44	1.73	0.33

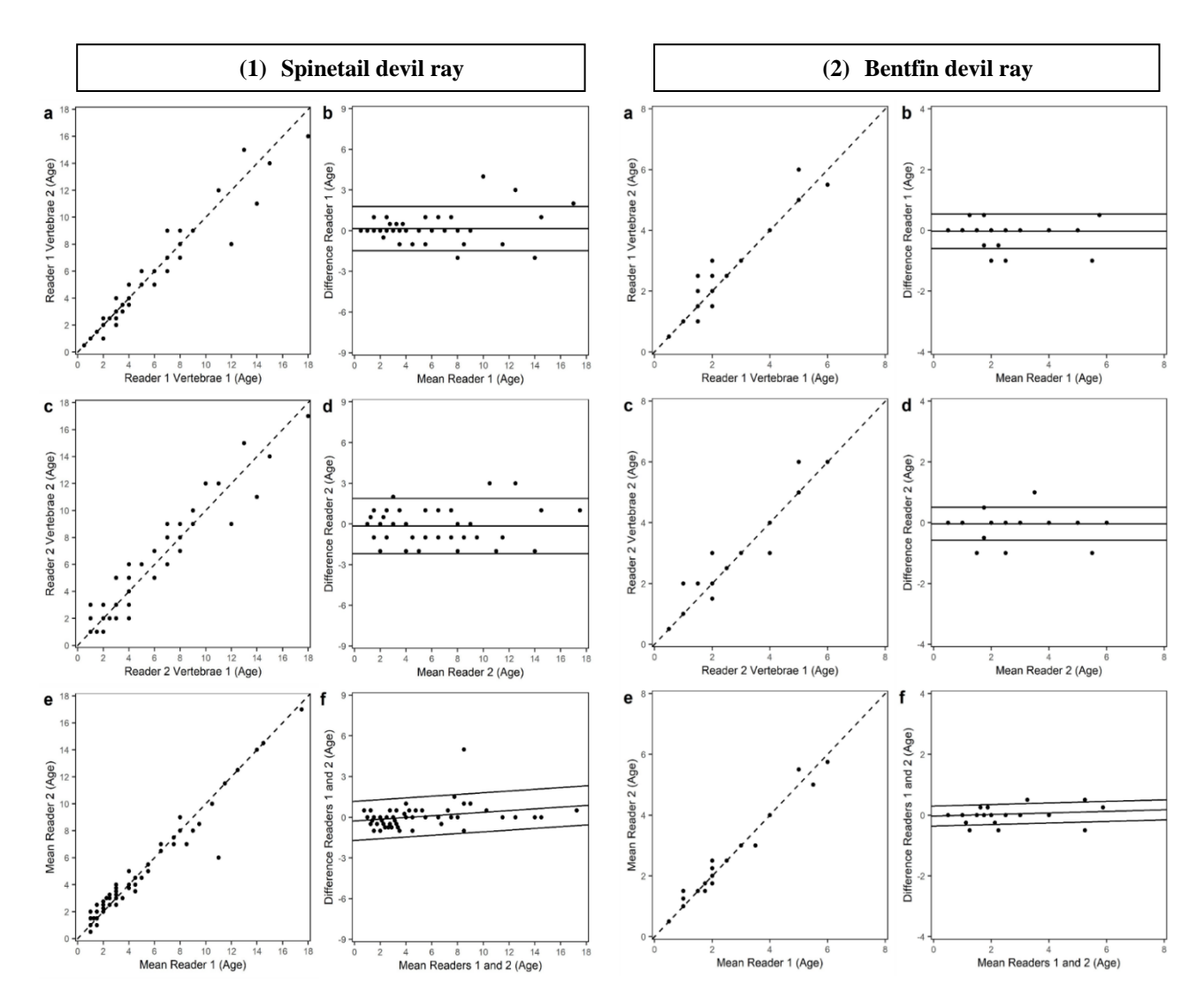


Figure 4.7 Bland-Altman analyses of agreement, precision, and bias in age estimates (year \pm 0.5) within and between readers for 1) Spinetail devil ray (M. mobular) (n=79) and 2) Bentfin devil ray (M. thurstoni) (n=59). Plots show the relationship between: vertebrae age band counts for a) reader 1 and c) reader 2 and between e) mean vertebrae age band counts from readers 1 and 2. b) Bland-Altman plots display bias and precision between vertebrae age band counts for b) reader 1 and d) reader 2 and between f) mean vertebrae age band counts from readers 1 and 2.

4.4.3 Estimating growth

Of the four growth models tested, the three-parameter von Bertalanffy and logistic growth models with stronger priors fit best for M. mobular and M. thurstoni DW-at-age data, respectively, based on LOOIC (Table 4.5; Figure 4.7). These top models resulted in k and DW_{∞} estimates of 0.05 year⁻¹ and 350cm for M. mobular and 0.19 year⁻¹ and 202cm for M. thurstoni, respectively. The mean DW_{∞} estimates from the top models were in line with maximum

observed sizes for M. mobular (350cm) and M. thurstoni (197cm), suggesting the Bayesian models produced plausible estimates of growth rates. Bayesian models with strong priors resulted in lower mean k estimates and higher mean DW_{∞} estimates for M. mobular compared to models with weaker priors (Table 4.3; Figure 4.8). Whereas, models with weaker priors resulted in higher or the same mean k and DW_{∞} estimates for M. thurstoni (Table 4.3; Figure 4.8). The M. thurstoni (Table 4.3; Figure 4.8). The thurstoni (Table 4.3; Figure 4.8) also fitted a von Bertalanffy growth model (0.12 year-1) (Pardo, Kindsvater, Cuevas-Zimbrón, et al., 2016) to the only other published length-at-age dataset for this species sampled in Mexico (Cuevas-Zimbrón et al., 2013) (Figure 4.11). We used a different offspring and maximum size as informative priors (based on currently available literature) to re-estimate thurstoni (0.086 year-1) dataset as well as for thurstoni mobular sampled in Indonesia (0.056 year-1) and Pakistan (0.048 year-1) in this study; this also showed Indian Ocean devil rays had lower growth rates (Figure 4.11). Parameter estimates from all growth models are presented (Table 4.3).

The von Bertalanffy growth parameter estimates from the frequentist model were k=0.10 year⁻¹ (95% CI 0.03 year⁻¹, 0.19 year⁻¹), DW_{∞} =262.65cm (95% CI 222.98cm, 453.38cm), and DW_0 = 112.27cm (95% CI 96.46cm, 124.71cm). The frequentist approach resulted in a higher k and lower DW_{∞} estimate, with higher uncertainty (95% confidence intervals), than the top von Bertalanffy Bayesian model (Figure 4.9). The DW_{∞} estimate was much lower than the known maximum size of M. mobular (350cm) suggesting the frequentist approach may have underestimated the asymptotic size and therefore overestimated k (due to a more bent curve).

Table 4.5 'Leave One Out' cross validation Information Criterion (LOOIC) and LOOIC standard error (se) for growth model analyses for *Mobula mobular* and *M. thurstoni*. The best model with the lowest LOOIC and largest weight for each species is shown in bold.

Species	Model	Parameter	LOOIC	LOOIC se	Weight
	von Bertalanffy	Strong	-109.11	10.04	1
	von Bertalanffy	Weaker	-108.89	10.11	3.62E-06
Mobula	Gompertz	Strong	-108.31	10.01	6.39E-07
mobular	Gompertz	Weaker	-108.96	10.04	3.24E-05
	Logistic	Strong	-106.97	10.03	7.95E-07
	Logistic	Weaker	-108.74	10.02	2.42E-05
	von Bertalanffy	Strong	-106.06	11.98	2.49E-09
	von Bertalanffy	Weaker	-105.97	12.11	4.54E-07
Mobula	Gompertz	Strong	-107.28	11.87	1.80E-06
thurstoni	Gompertz	Weaker	-107	11.98	3.23E-08
	Logistic	Strong	-108.19	11.59	1
	Logistic	Weaker	-108.01	11.83	0.000406

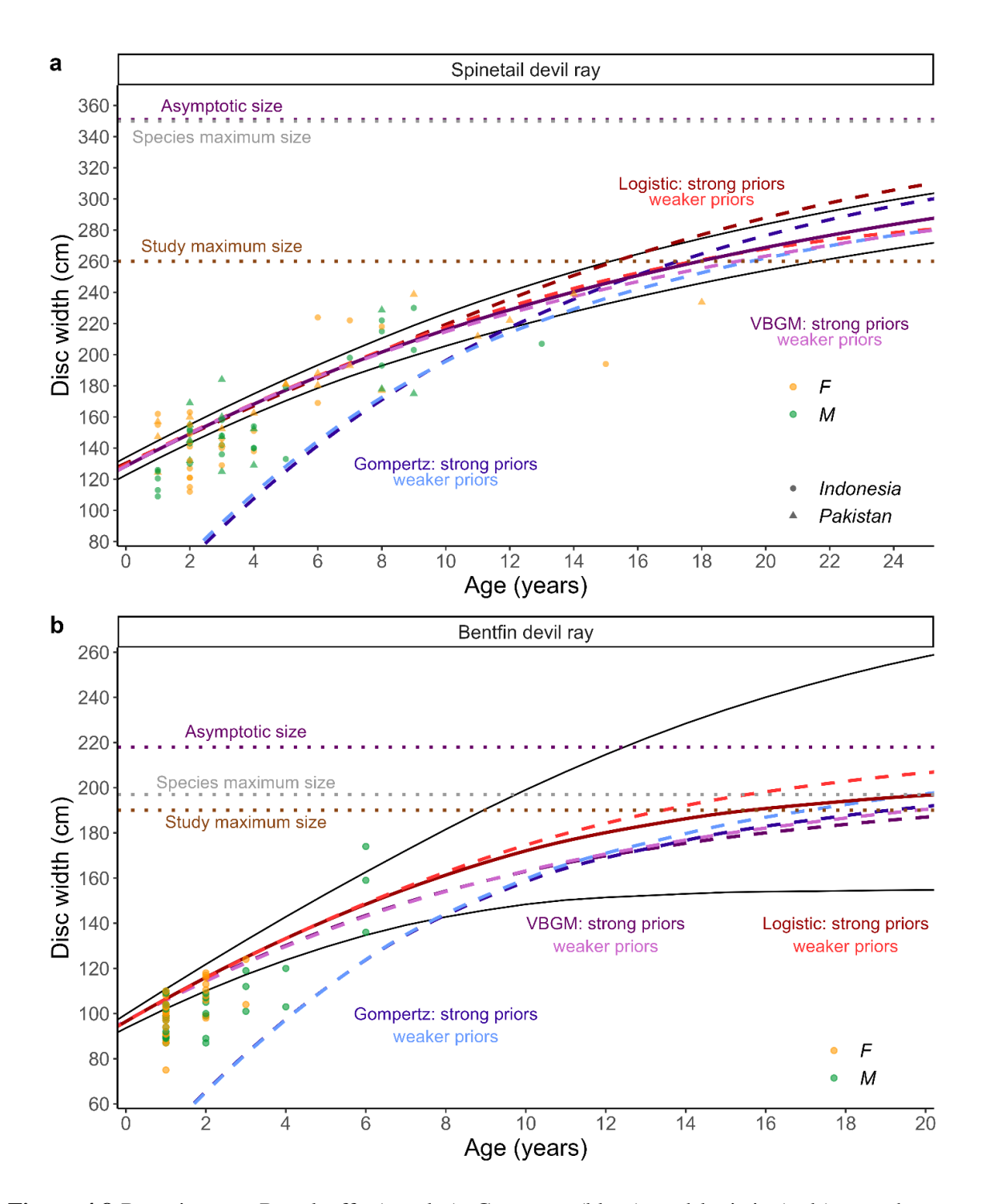


Figure 4.8 Bayesian von Bertalanffy (purples), Gompertz (blues), and logistic (reds) growth curves describing the disc width and age (nearest year) relationship for a) combined female (n=41) and male (n=38) Spinetail devil ray (M. mobular) (n=79) and b) combined female (n=29) and male (n=30) Bentfin devil ray (M. thurstoni) (n=59) length-at-age data from individuals sampled in Indonesia (circles) and Pakistan (triangles). The top model for each species is shown with a solid line with 95% credible intervals shown with solid black lines. Remaining models are shown with dashed lines. Dotted lines show the asymptotic size (DW_{∞}) estimate for the top model, the maximum observed size for the species (black) and the maximum observed size in this study (brown).

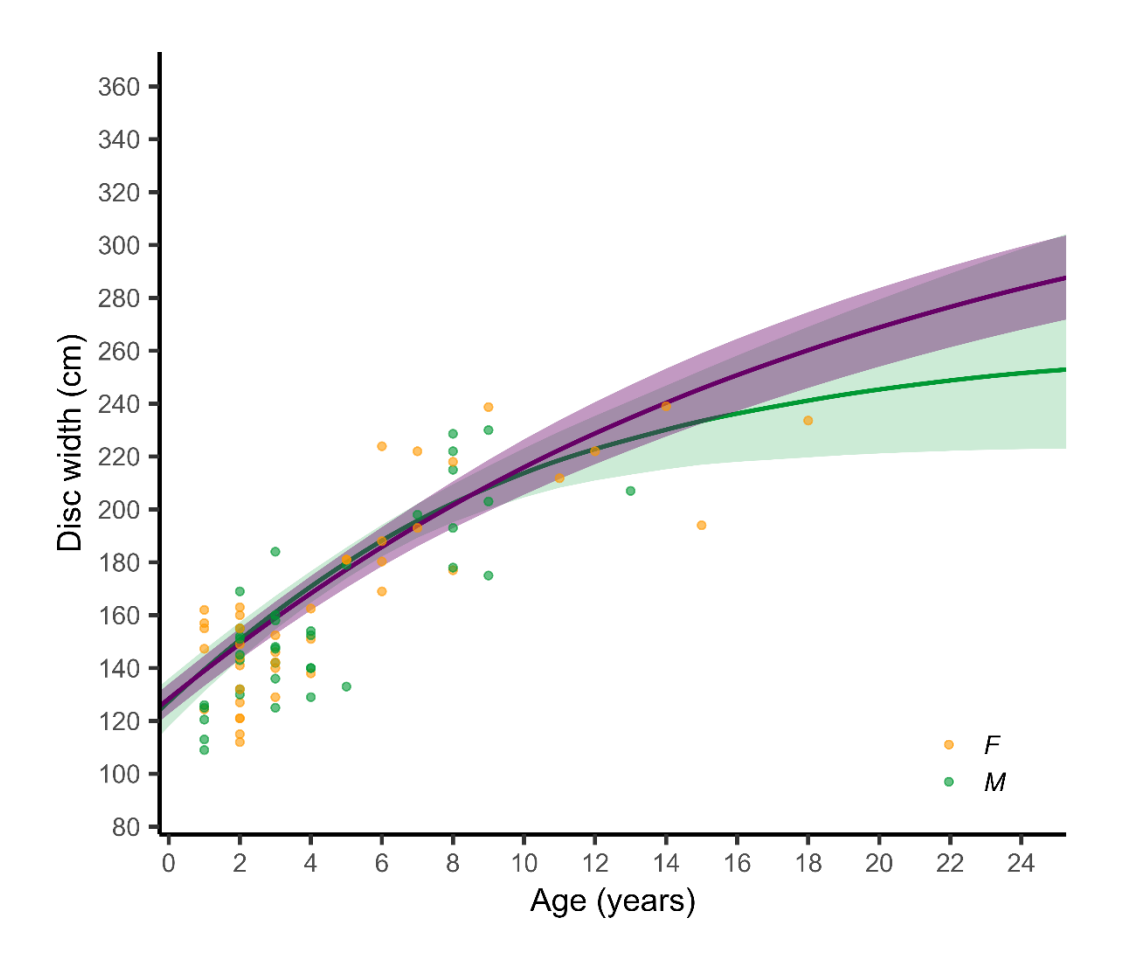


Figure 4.9 Comparison between length-at-age estimates determined from Bayesian (purple) and frequentist (green) von Bertalanffy growth models, with 95% credible intervals and 95% confidence intervals, respectively, for combined female (n=41) and male (n=38) Spinetail devil ray (M. mobular) (n=79).

4.4.4 Estimation of maximum intrinsic rate of population increase

M. mobular had an estimated mean α_{mat} of 8.2 years (95% CI 6.8 years, 10.3 years) and mean DW_{mat} of 204cm (95% CI 191cm, 219cm) (Figure 4.12). The smallest observed mature M. mobular and M. thurstoni individuals were 193 and 171cm, which equates to 7.9 and 10.4 years, respectively (predicted using the top fitting growth model for each species). The former is within the calculated range of age at maturity for M. mobular and we therefore assume female α_{mat} ranges uniformly between 6.8 and 10.3 years. For M. thurstoni, a DW_{mat} of 150cm from a previous study (Rambahiniarison et al., 2018; Notarbartolo di Sciara, 1988) equates to 7 years and we therefore assume α_{mat} ranges uniformly between 7 and 10.4 years.

Female α_{max} was calculated based on age at 95% DW_{∞} (Ricker, 1979) and 99% DW_{∞} (Fabens, 1965) giving 69.3 and 97.0 years, respectively, for M. mobular and 18.2 and 25.5 years for M. thurstoni. The α_{max} estimates for M. mobular are likely unrealistically high due to the growth curve not reaching an asymptote and therefore an upper bound of 26 years was used for both species. The maximum observed age of M. thurstoni was 6 years but this is unlikely to represent true maximum age. The observed maximum age of M. thurstoni in this study was 17.5 years and so this was used as the lower bound for α_{max} for both species. Therefore α_{max} was assumed to uniformly range between 17.5 and 26 years for both species. Using the 10,000 drawn estimates of $that{b}$, $that{c}$, and $that{c}$, $that{c}$ median instantaneous natural mortality $that{d}$ was calculated as 0.066 (95th percentiles 0.057, 0.078) for $that{d}$. thurstoni. Resultant median $that{c}$ was calculated as 0.094 year-1 (95th percentiles 0.024, 0.147) for $that{d}$. thurstoni and 0.092 year-1 (95th percentiles 0.024, 0.145) for $that{d}$ for thurstoni, respectively (Figure 4.13).

4.4.5 Estimation of total mortality, fishing mortality, and the exploitation ratio

Full recruitment to the fishery for M. mobular and M. thurstoni was estimated at three and two years, respectively, based on the peak abundance from catch curve analysis (Figure 4.14). Total instantaneous mortality Z was similar for both species (M. mobular: 0.215 year⁻¹, 95% CI 0.157, 0.272; M. thurstoni: 0.232 year⁻¹, 95% CI 0.136, 0.328), which translated to an annual mortality rate A of approximately 20% (M. mobular: 19.3%, 95% CI 0.146, 0.238; M. thurstoni: 20.7%, 95% CI 0.128, 0.280). Median fishing mortality F was estimated as 0.15 year⁻¹ (95th percentiles -0.046, 0.340) and 0.17 year⁻¹ (95th percentiles -0.125, 0.462) for *M. mobular* and *M. thurstoni*, respectively. Estimates of F for both species, although highly uncertain, are higher than our r_{max} estimates (0.094 and 0.092 year⁻¹), suggesting that current fishing mortality will drive the species towards extinction and is therefore unsustainable (Myers & Mertz, 1998; Dulvy et al., 2004; Gedamke et al., 2007), within the assumptions made. Estimated median exploitation ratio E (ratio of F to M) was estimated as 0.70 (95th percentiles -0.67, 0.86) for M. mobular and 0.74 (95th percentiles -1.66, 2.85) for M. thurstoni (Figure 4.13). Approximately 80% of the proportion of the estimated distribution of E is greater than the optimal value for biological sustainability of E=0.5 for both species, reinforcing that there is a high likelihood that M. mobular and M. thurstoni are overfished (Figure 4.11) (Gulland, 1971; Pauly, 1983).

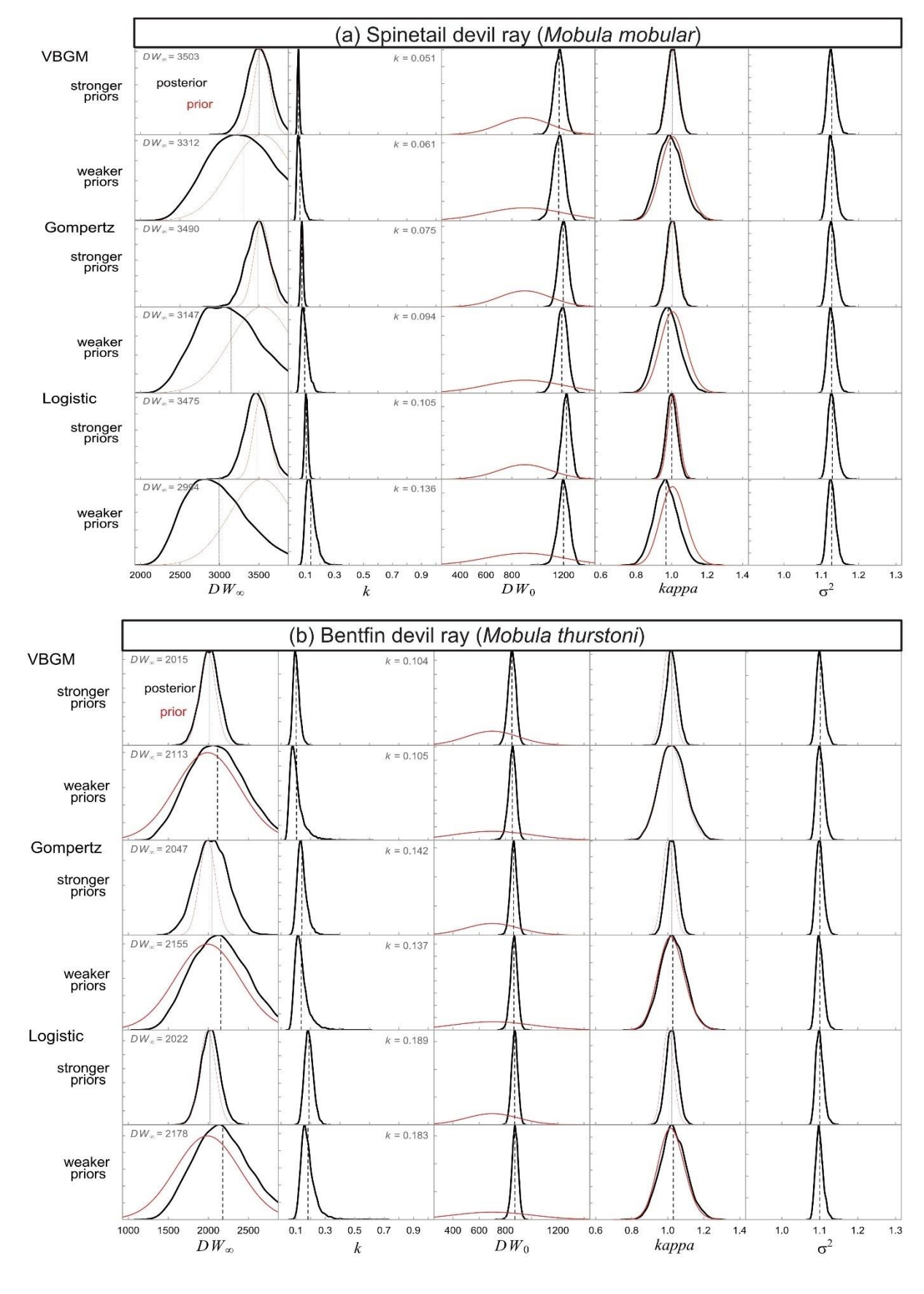


Figure 4.10 Posterior (black lines) and prior (red lines) distributions for von Bertalanffy growth parameters $(k, DW_{\infty}, \text{ and } DW_0)$, the hyperprior kappa, and the error term (σ^2) for three Bayesian models

(von Bertalanffy, Gompertz, and Logistic) with strong and weaker priors fitted to a) Spinetail devil ray (*Mobula mobular*) and b) Bentfin devil ray (*M. thurstoni*) disc width-at-age data. Dashed lines show mean values and mean k and DW_{∞} , indicated on each plot.

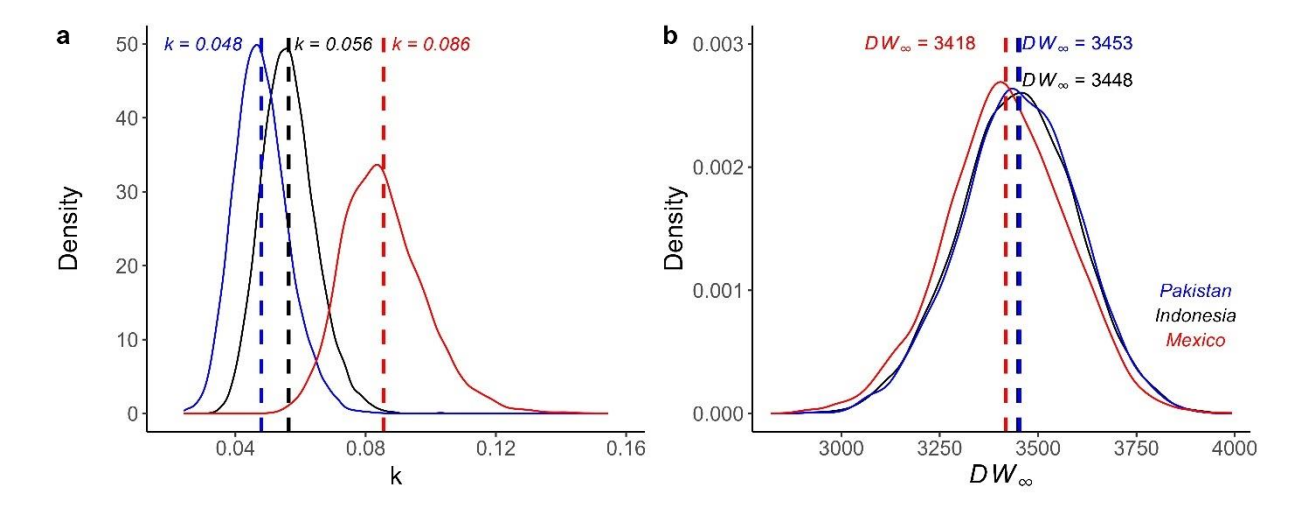


Figure 4.11 Posterior distribution for von Bertalanffy growth parameters a) k and b) DW_{∞} for Bayesian models with strong priors fitted to Indian Ocean M. mobular disc width-at-age data from this study using samples from Indonesia (blue) and Pakistan (black) and previous studies using samples from Mexico (red) (Cuevas-Zimbrón et al. 2013; Pardo, Kindsvater, Cuevas-Zimbrón, et al., 2016).

4.5 Discussion

Our results indicate that current fisheries exploitation of devil rays in Indian Ocean small-scale fisheries is unsustainable, with fishing mortality higher than r_{max} estimates and exploitation ratio exceeding a threshold for biological sustainability. We found that both M. mobular and M. thurstoni had low somatic and population growth rates (low r_{max}), relative to most other chondrichthyans. Indian Ocean M. mobular also had a lower growth rate than found for this species in another region. We present the first published age and growth estimates for M. thurstoni, the first direct age-at-maturity estimate for any Mobula species, and only the second published aging study for M. mobular, including a record of the oldest individual published. We caution that neither of these aging studies have been able to validate the assumption of annual band deposition used. However, given the data paucity in devil ray life history and conservation urgency for these Endangered species, our results provide best first life history estimates for these species in the Indian Ocean. We discuss (1) unsustainable fisheries catches of Indian Ocean devil rays; (2) how life history estimates compare to these species in other

regions; (3) regional and global management implications; and (4) future research directions and caveats of the estimated life history estimates.

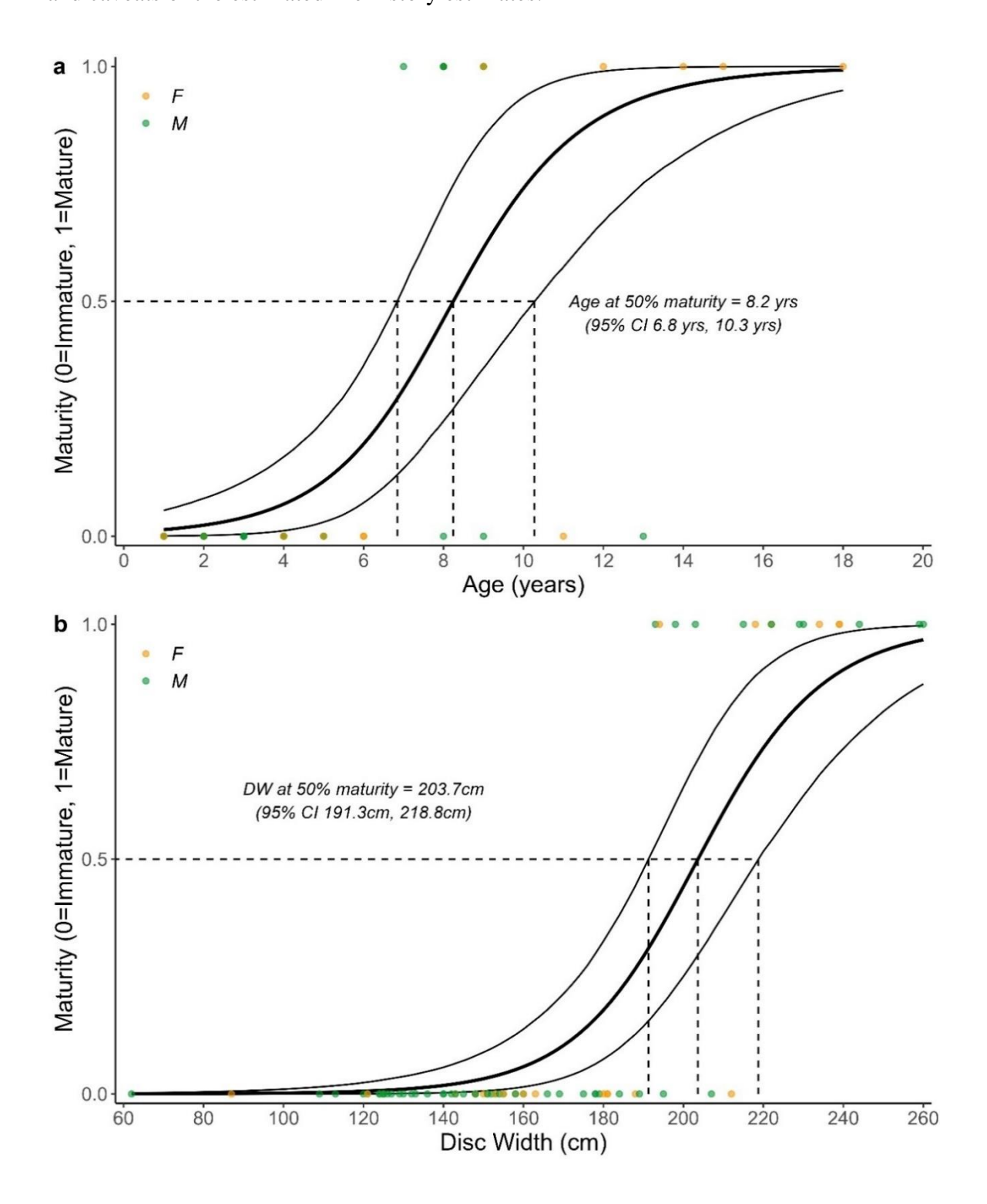


Figure 4.12 Bayesian logistic regression with strong priors describing the relationship between a) age (n=56) and b) disc width (n=73) and maturity status for M. mobular with 95% Credible Intervals. Age and disc width at 50% maturity (with 95% Credible Intervals) are shown with dashed lines.

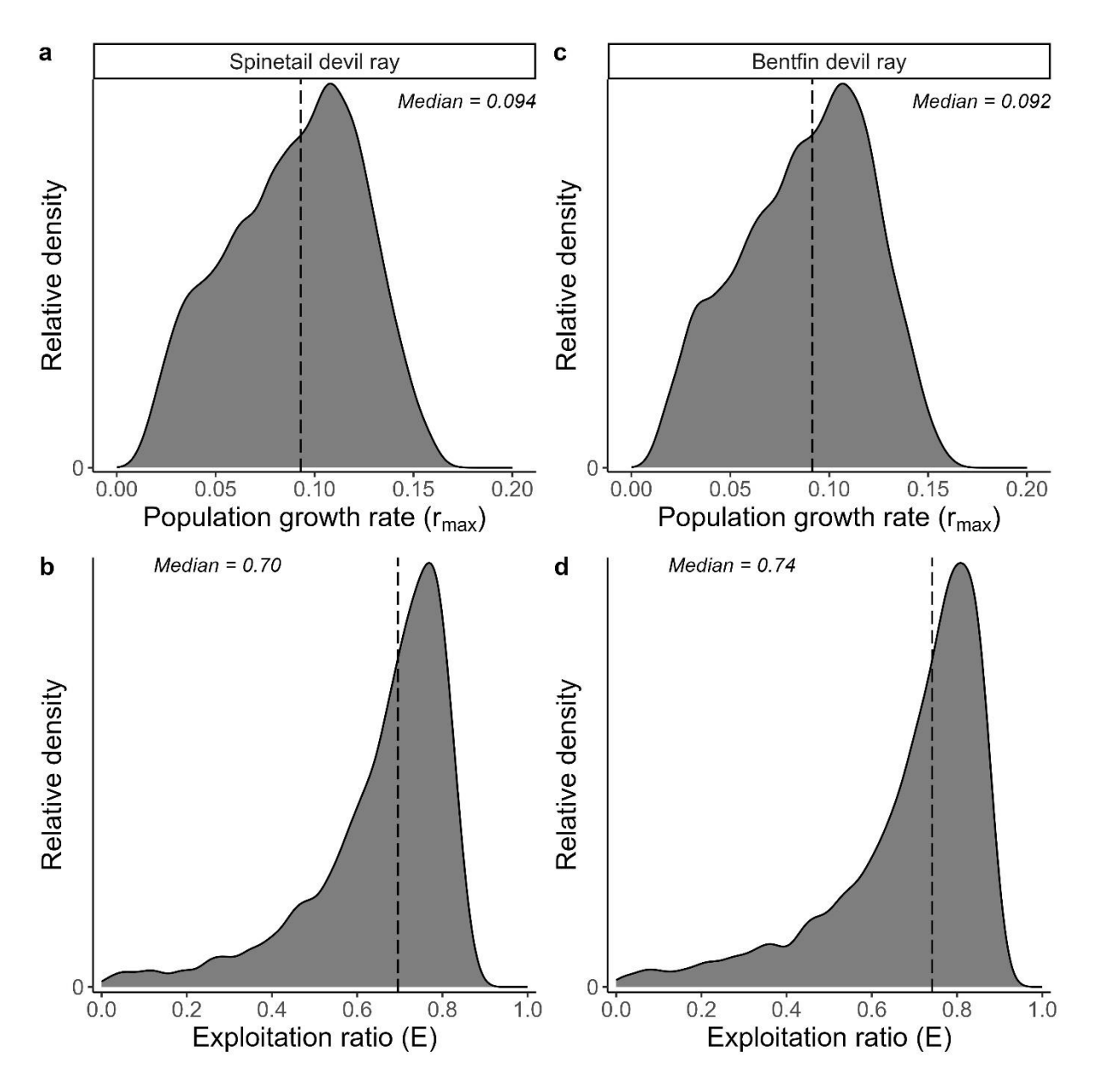


Figure 4.13 Distribution of estimated maximum intrinsic population growth rate (r_{max}) and exploitation ratio (E) for M. mobular (a and b, respectively) and M. thurstoni (c and d, respectively). Dashed lines show median values.

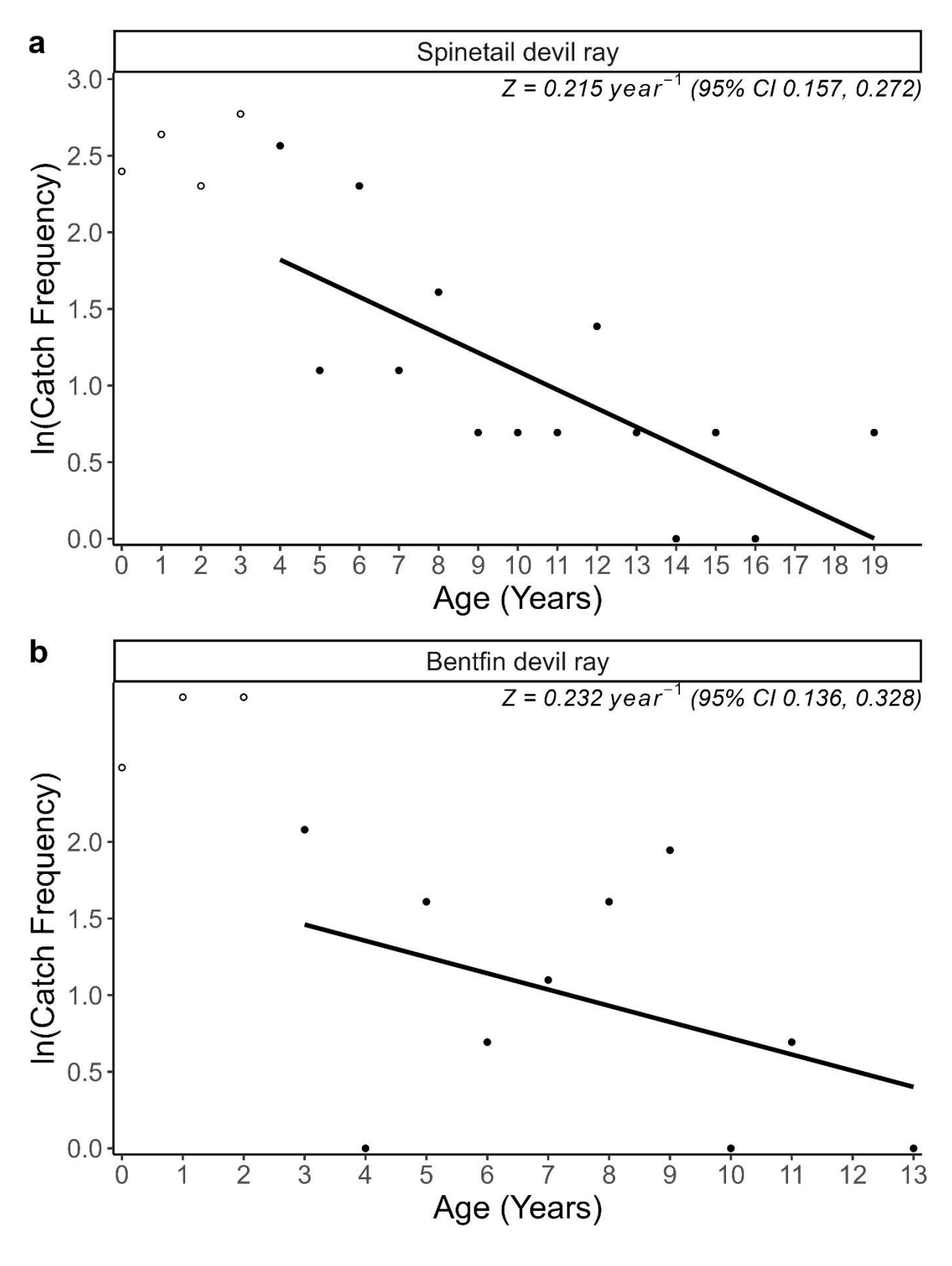


Figure 4.14 Chapman-Robson catch curve for a) Spinetail devil ray ($Mobula\ mobular$) (n=103) and b) Bentfin devil ray ($M.\ thurstoni$) (n=89) from Indian Ocean small-scale fisheries. Age class for full recruitment to the fishery was 3 and 2 years, respectively, and catch curve regression lines between ages 4 to 18 and 3 to 13, respectively. Total mortality Z indicated.

The distribution of the exploitation ratio E for both M. mobular and M. thurstoni, alongside the disparity between fishing mortality F and r_{max} , suggests a high likelihood of overfishing. We found that M. mobular $(r_{max}=0.094 \text{ year}^{-1})$ and M. thurstoni $(r_{max}=0.092 \text{ year}^{-1})$ had low r_{max} , which aligns with other studies that found devil rays have amongst the lowest r_{max} of all chondrichthyans, alongside deep sea species (Dulvy et al., 2014; Pardo, Kindsvater, Cuevas-Zimbrón, et al., 2016; Simpfendorfer & Kyne, 2009). This is likely due to very low reproductive outputs (Pardo et al., 2018). Although we did not observe any pregnant females in our study, a litter size of one, rarely two pups, has been observed in several studies for M. mobular and other devil ray species (Rambahiniarison et al., 2018; Broadhurst et al., 2018; Notarbartolo di Sciara, 1988). Given the low fecundity and large offspring sizes of devil rays, they likely have weaker density-dependent regulation and therefore lower potential to withstand and recover from fishing exploitation (Kindsvater et al., 2016; Forrest & Walters, 2009). That is not to say that high fecundity alone is indicative of greater resilience (Reynolds et al., 2005; Kindsvater et al., 2016). All M. thurstoni aged from Indonesian small-scale fisheries were less than six years old (n=59), with the majority ≤ 2 years (n=49), primarily caught between September and January. Gillnets are generally selective for a narrower size range where the smallest individuals can swim through the net and the largest avoid become meshed and therefore captured (Harry et al., 2022); this may be why the largest individuals were not sampled in this study, as well as the difficulty landing larger catch. Further, the larger offspring size of many rays and sharks often means they are vulnerable to capture, which would be the case for large devil ray offspring (Harry et al., 2022; Simpfendorfer, 1999). Understanding gear selectivity is important for fisheries management to target specific species or size classes and to implement effective bycatch mitigation (Lemke & Simpfendorfer, 2023; Harry et al., 2011; Thorpe & Frierson, 2009; Braccini et al., 2022). Selection for young M. thurstoni may also be due to temporal size segregation, which has been found for M. thurstoni in the Gulf of California (Notarbartolo di Sciara, 1988). Limiting catch to sub-adults in a fishery whilst allowing adults to breed can be an effective management strategy (Prince, 2002), yet protecting these age classes is also needed for future reproductive output of the stock (Kindsvater et al., 2016; Hixon et al., 2013). Our findings indicate that full recruitment to the fishery mainly occurs in sub-adults for both species before they have reached maturity.

Growth rate estimates in this study are in line with larger-bodied chondrichthyans typically having low somatic growth rates, later maturity, and higher extinction risk (Hutchings et al., 2012; Jennings et al., 1998). Yet, the study also provides initial evidence for geographic

variation in devil ray life history. Our growth estimate for M. mobular was lower than published growth estimates for this species sampled off Mexico (Cuevas-Zimbrón et al., 2013; Pardo, Kindsvater, Cuevas-Zimbrón, et al., 2016). The Mexico length-at-age dataset had a similar length range to ours, with both lacking the largest size classes based on known maximum size for this species. M. mobular are reported to exhibit variation in size across their range (Marshall et al., 2022), which could result in growth differences. Estimates from both studies are still indicative of relatively slow growth for the species, which alongside the large body size of M. mobular, is associated with greater intrinsic sensitivity and higher extinction risk (Reynolds et al., 2005; Jennings et al., 1998). We present the first direct age-at-maturity estimate of 8 years in Indian Ocean M. mobular, which was later than previous estimates, taking 2-3 years longer to mature compared to the same species off Mexico (5-6 years) (Pardo, Kindsvater, Cuevas-Zimbrón, et al., 2016; Cuevas-Zimbrón et al., 2013). This equates to a 15-20% reduction in lifetime reproductive output based on a maximum age of 20-26 years. Further, a delay in pregnancy from the onset of maturity has also been reported for this species, likely due to the large offspring size and long gestation period, where high maternal investment is needed (Rambahiniarison et al., 2018). Our estimates match closely with age-at-maturity estimates (7.4-9.1 years) reported from a study in the Philippines (Rambahiniarison et al., 2018) that used size-at-maturity estimates and the Von Bertalanffy growth model from Cuevas-Zimbrón et al. (2013), with alternative model parameters (Cuevas-Zimbrón et al., 2013; Pardo, Kindsvater, Cuevas-Zimbrón, et al., 2016). We found a higher, yet still relatively low, k estimate for M. thurstoni which is the first published estimate. We also present the first age-at-maturity estimate of seven years for M. thurstoni. Overall, this resulted in r_{max} estimates for both species that were comparable with previous estimates for *M. mobular* (median of 0.077 year⁻¹, 95th percentiles 0.042, 0.108) (Pardo et al., 2016) and manta rays (single estimate for M. alfredi and M. birostris) (median of 0.116 year⁻¹, 95th percentiles 0.089, 0.139) (Dulvy et al., 2014), suggesting that Indian Ocean devil rays are at high risk of local depletion from overfishing.

Understanding the life history of a species can be key in informing the most effective actions to manage threats but there is uncertainty in the best sustainable management options for preventing species extinction (Kindsvater et al., 2016; Denney et al., 2002; Sadovy, 2005). The conservative life history of devil rays makes it unlikely that they can withstand the fishing mortality rate found in this study (Dulvy et al., 2008; Dulvy et al., 2014; Stevens et al., 2000). Although there is substantial variation in the maximum size of devil rays between species, ranging from 110cm for *M. munkiana* to 700cm DW for *M. birostris* (Last et al., 2016), their

low reproductive output limits their population growth rates. This is likely why consistently low r_{max} estimates have been found for devil rays with different maximum body sizes including for M. mobular and M. thurstoni in this study. Estimates of r_{max} are sensitive to the duration of the reproductive cycle (Dulvy et al., 2014), which is something that has only been reported in a handful of studies (Marshall & Bennett, 2010; Broadhurst et al., 2019; Rambahiniarison et al., 2018). We tried to account for this uncertainty by using a Monte Carlo approach but variation in annual reproductive output may lead to substantial variations in population growth rate that needs to be accounted for (Dulvy et al., 2014). Therefore, species- and region-specific life history estimates are key in informing accurate and localised demographic and sustainability assessments for devil rays (Dulvy et al., 2014).

Whilst devil rays are listed on CITES Appendix II and CMS Appendices I and II, national protections within the Indian Ocean are limited and the small-scale fisheries they are caught in typically have poor fisheries monitoring, regulation, and enforcement. This includes countries reporting some of the largest catch, such as Indonesia where we sampled in this study (Dulvy et al., 2014; Croll et al., 2016). Blanket bans on devil ray species as a sole management approach in small-scale fisheries would likely prove insufficient as effective management and enforcement needs to be tailored to the local context (Temple, Berggren, et al., 2024; Booth et al., 2019). Devil ray catches are often high value per individual and can contribute to a high proportion of the economic value of small-scale fisheries providing a financial incentive to exploit them (Temple, Berggren, et al., 2024). Small-scale fisheries are typically multi-gear and multi-species, making a management approach targeted towards a single species challenging (Herrón et al., 2019). Most devil ray catches occurred in gillnets and so management should prioritise interventions in these fisheries. One management approach could be to encourage safe release of live-caught devil rays entangled in gillnets, with many Regional Fisheries Management Organisations, including the Indian Ocean Tuna Commission, requiring live release and recommending safe handling practices (IOTC, 2019). Although gillnet discard mortality can be high (Dapp et al., 2016), there is some indication that mobulid rays be more capable of post-release survival due to their spiracle depending on soak time (Broadhurst & Cullis, 2020). However, this can be challenging in small-scale fisheries where devil rays and other elasmobranchs caught incidentally are often utilised for subsistence and trade. Wider understanding of social and economic drivers of catch and fisher behavior is therefore also needed for effective implementation of management actions (Booth et al., 2023; Barrowclift et al., 2017; Temple, Berggren, et al., 2024).

There is still insufficient life history data across the ranges of M. mobular and M. thurstoni to fully understand geographic differences as well as a lack of understanding of population structure. Gear selectivity may also mean that samples are not representative of the population and may truncate the population age structure, which could lead to biased growth estimates given the effects of fishing on the population (Thorson & Simpfendorfer, 2009; Walker et al., 1998). The observed difference in growth for M. mobular between our study and the previous study of the same species off Mexico, could be partly due to a more limited number of individuals sampled in larger size classes in our dataset (DW>2 m), whereby informative priors are still not "bending" the growth curve (a more bent curve results in faster doubling rates towards the asymptote and therefore a higher k estimate and concomitantly a lower DW_{∞} estimate). The lack of "bending" of the growth curve can also explain the unreasonably large estimates of α_{max} for M. mobular based on asymptotic size. Whilst we aimed to quantify any uncertainty and bias in age reads through human error, with commonly used techniques and the Bland-Altman approach, this error could have been carried through to our growth modelling (Harry et al., 2022). We also assumed annual deposition of growth bands on vertebral centra but this could not be validated here and is not yet validated for any mobulid species, as with many elasmobranchs. Indeed, this may not be a valid assumption, with band pair deposition potentially being more variable and age likely underestimated, particularly for larger and older individuals (Harry, 2018; Natanson et al., 2018; James & Natanson, 2020). This can lead to additional uncertainty in age estimates as well as that of reader error that can be carried forward to subsequent analyses utilising length-at-age datasets (Harry et al., 2022).

If the age of larger individuals in this study were underestimated, this could lead to an underestimated growth coefficient (less bent curve) given the seemingly missing older individuals resulting in a higher asymptotic length estimate (Harry, 2018). However, the DW_{∞} estimates were in line with known maximum lengths for both species suggesting the Bayesian growth models had produced plausible estimates of growth rates. A greater maximum age would also mean these species live for longer and may have lower natural mortality than estimated and consequently lower productivity and resilience to fishing. However, greater longevity would also mean a higher lifetime reproductive output implying greater productivity, presenting a complex picture. Growth band pairs may also vary along the vertebral column as found in five batoid species, potentially due to body growth and shape, more reflective of structural needs than an annual cycle, suggesting they do not accurately represent a single age estimate (James & Natanson, 2020). For devil rays in this study, banding was only visible in

the caudal portion of the vertebrae, which were used to provide best first length-at-age estimates of devil rays in the Indian Ocean. However, we acknowledge these limitations and add to recommendations that more accurate aging methods are needed to ensure appropriate and effective fisheries and population assessments of these species.

Similar assumptions in catch curve analysis can also lead to potential biases in our total mortality estimate where they may not be met. These include an unselective fishery, constant recruitment and natural mortality across age classes, a closed population, and sufficient sample size to represent the age structure of the population (Smith et al., 2012). Understanding the assumptions made and the limitations are important in appropriate use of life history estimates. Continued exploration of novel aging techniques are still needed given it is not possible to age all elasmobranch species due to vertebral morphology and lack of growth band pair formation (Burke et al., 2020) as well as the limitations with current aging methods as discussed above. Indeed, with devil rays, we found caudal vertebrae were the most calcified part of the vertebral column with clear banding, as was found previously for M. mobular (Cuevas-Zimbrón et al., 2013). Difficulty in assessing female maturity and reproductive cycle as in this study is a common issue given low sample sizes across the year with the seasonality of many fisheries. A potential method that has been tested is the use of ultrasound (Froman et al., 2023), which would be useful for live and larger individuals as well as being a less destructive sampling method. It could also be a potential way to avoid dissection of landed rays, which fishers and traders do not always agree to, making it difficult to determine female maturity and reproductive cycle.

Given data deficiencies for devil rays and many other elasmobranchs, and the difficulty in addressing these gaps, data-poor methods need to be utilised with available information to ensure sustainable fisheries. Low sample size is a common issue in elasmobranch age and growth studies. Bayesian growth modelling can provide a useful alternative to fixing model parameters, which has been shown to bias growth estimates (Pardo et al., 2013), particularly when the smallest and largest age classes are lacking (Pardo, Kindsvater, Cuevas-Zimbrón, et al., 2016; Mukherji et al., 2021; Smart & Grammer, 2021). We found both species had relatively slow growth, late age-at-maturity, low r_{max} , and therefore high intrinsic sensitivity to fisheries exploitation (Reynolds et al., 2005; Cortés, 2000, 2002). However, there is inter- and intraspecific variation in devil ray growth rates that warrants species- and population- estimates to inform more accurate species/population/stock assessment models. We demonstrate a suitable data-poor approach to generate age, growth, and r_{max} estimates for Endangered M. mobular and M. thurstoni to inform these assessments. Our findings reinforce previous works showing that

devil rays can only withstand relatively low catch rates, and we show that these rates are almost certainly being outstripped by current targeted and incidental catch rates in small-scale and industrial fisheries in the Indian Ocean. Implementation of evidence-based fisheries management is critically needed for these species in Indian Ocean small-scale fisheries given their conservative life history and socio-economic value.

Chapter 5. Thesis conclusions

5.1 Overview

Over one-third of the 644 ray species (Class Chondrichthyes, Superorder Batoidea) assessed on the IUCN Red List are threatened with extinction due to overfishing (Dulvy et al., 2021). An additional 10% are Data Deficient and there are still new species being discovered (Moore et al., 2020; Weigmann et al., 2020; Last et al., 2023) that need to be described and assessed (Last et al., 2016). Fishing has led to the collapse of several ray species populations (Brander, 1981; Dulvy & Reynolds, 2002; Dulvy et al., 2016; Sherman, Simpfendorfer, Haque, et al., 2023; Kyne et al., 2020; Yan et al., 2021) and the first extinction of a marine fish due to overfishing - the Java Stingaree (*Urolophus javanicus*) (Constance et al., 2023). A number of fisheries management and trade tools have been established in response to growing concern over shark and ray fisheries' sustainability. These include the implementation of National Plans of Action for sharks (NPOA shark) recommended by the United Nations Food and Agriculture Organisation (FAO) in 1999, the Convention on International Trade in Endangered Species (CITES) with the first shark species listed in 2002 (Vincent et al., 2014), bans on finning and carcass discards in many countries (Davidson et al., 2016; Lack & Sant, 2009), non-retention bans by Regional Fisheries Management Organisations (RFMOs) (Shiffman et al., 2016; Tolotti et al., 2015), and the Convention of Migratory Species Memorandum of Understanding for Sharks (CMS MoU sharks) (Fowler, 2012). Yet, rays and sharks still face increasing threat of extinction from overfishing and populations continue to decline (Davidson et al., 2016; Worm et al., 2024; Dulvy et al., 2021). However, it is possible for populations to recover (Moore, 2023) and for future sustainable fishing if well-enforced, science-based management is implemented (Simpfendorfer & Dulvy, 2017; Pacoureau et al., 2023).

In Chapter 1, it was evident that pelagic ray species (Order Myliobatiformes) with a larger geographic range and greater exposure to Small-Scale Fisheries (SSF) pressure were at higher risk of extinction. This highlights the need for trans-national and -regional management efforts where species ranges overlap multiple national jurisdictions to ensure appropriate protection. This needs to be throughout a species' lifetimes where understanding and protection of migration routes and critical habitats, such as nursery areas, feeding and mating areas are needed (Martins et al., 2018; Boerder et al., 2019; Chin et al., 2023; Pendoley et al., 2014). There is now limited species refuge from intense fishing pressure with the increasing expansion

of industrial fisheries into the "high seas" since the 1950s (Queiroz et al., 2019; Tickler et al., 2018) and deeper waters (Finucci et al., 2024). Well-enforced, science-based fisheries management measures are therefore crucial to ensure that fishing mortality is sustainable. For example, marine protected areas need to be appropriately located (Davidson & Dulvy, 2017) and appropriately enforced (Vianna et al., 2016; Di Lorenzo et al., 2022). SSF pressure was found to be a better predictor of extinction risk for pelagic rays than industrial fishing pressure (Chapter 1). However, SSF have typically been understudied and further research focus is needed to move beyond the well-studied fisheries for high-valued commercial stocks, typically in high-income countries (Moore & Grubbs, 2019; Hilborn et al., 2020). This will require improved resources, increased local capacity, and political will (Sala et al., 2018; Jacquet et al., 2010; Pauly, 2006; Moore & Grubbs, 2019). This is essential given the important role of SSF for current and future sustainability of ocean resources and food security (Pauly, 2006; Béné et al., 2007), with a significant contribution to global employment (Teh & Sumaila, 2013; Béné et al., 2010) and the nutritional value provided from marine fisheries (Hicks et al., 2019; Béné et al., 2015).

Given that a lack of data often limits population and fisheries stock assessments for rays and that the rate of decline is outpacing the ability to address empirical data gaps, data-poor assessment approaches are needed (Cortés & Brooks, 2018; Cortés et al., 2012). Better utilisation of available data to inform status assessments and draw inference through phylogenetic, environmental, and life history trait relationships can help guide conservation and management actions (Kindsvater et al., 2018; Horswill et al., 2019; Thorson et al., 2017). In Chapter 2, an assessment was conducted to investigate if more widely available data on body mass, temperature, and depth could explain variation in calculated r_{max} for 85 ray species, providing the foundations to predict r_{max} for data-poor species. This revealed a paradox whereby tropical rays (Orders Torpediniformes, Rhinopristiformes, and Myliobatiformes) were found to be more intrinsically sensitive to fishing and other anthropogenic threats (e.g. climate change) compared to temperate skates (Rajiformes). This was in contrast to metabolic expectations and raised further concern for tropical rays that already face a disproportionate threat of extinction (Dulvy et al., 2021). The reason for the paradox is further explored in Chapter 3 where it was found that offspring size explained high variation in r_{max} of rays and that a larger offspring size relative to adult size in tropical rays resulted in lower population

growth rates. Understanding of intrinsic sensitivity and drivers of extinction risk is therefore important in prioritising management and conservation efforts.

It is crucially important to collect life history data to best inform population and species assessments where possible. In Chapter 4, key life history parameters (growth, age at maturity, and r_{max}) for Endangered devil rays ($Mobula\ mobula\ models. It was found that both devil ray species had low somatic and population growth rates relative to other chondrichthyans and that current levels of fishing mortality were likely unsustainable in the Indian Ocean. The inter- and intra-specific variation in devil ray life history found in the research highlights the need for species- and population-specific estimates to inform more accurate assessments. Well-enforced, evidence-based fisheries management actions for devil rays in the Indian Ocean is critically needed to prevent further species decline and aid population recovery.$

5.2 Administrative challenges faced and recommendations for biological sampling

This PhD project aimed to work with up to ten project collaborators in countries across the Indian Ocean to facilitate data and biological sample collection from devil rays (*Mobula* spp.) caught in small-scale fisheries. This required significant administration during the four-year PhD to formalise collaborations and to comply with the Nagoya Protocol and CITES (Figure 5.1). This required navigating collaborating countries' and the UK's relevant legislation in order to export and import samples for laboratory work to take place at Newcastle University, United Kingdom. This included age determination from vertebrae samples and DNA extraction from muscle tissue samples for future use in determining the genetic population structure of devil rays across the Indian Ocean. This presented a number of challenges (Figure 5.1) and below is an overview of recommendations based on the experiences from implementing sample collection for devil rays that may be helpful when coordinating international biological sampling research.

• *Consider storage and shipment of samples*. Ethanol (>95%) is a favoured and effective medium for tissue preservation for molecular genetic analyses (Nagy, 2010). However, ethanol is not readily available in some countries and can also present issues as it may be regarded as "dangerous goods" for shipment. Whilst small quantities can be shipped

in individual sample tubes, it is important to consider that ethanol evaporates easily (recommend using microcentrifuge tubes with screw caps with o-rings) and will erase permanent marker if there is leakage (recommend additional labelling e.g. put waterproof paper with sample number written in pencil inside sample tubes). As an alternative, 20% salt-saturated Dimethylsulfoxide (DMSO) is a cheap storage medium that is effective at room temperature (Oosting et al., 2020; Nagy, 2010), which is important to consider given limited freezer storage at remote landing sites. Vertebrae samples are best stored frozen in labelled sample bags until ready for preparation (Cailliet & Goldman, 2004). Where not possible, tissue can be removed and samples dried for shipment (however, samples will need to be rehydrated to cut vertebrae centra). Finally, it is important to take duplicate samples of tissue and vertebrae samples and store these in-country as back-up and for future shipments for sequencing and age determination where necessary. For tissue samples, it is crucial to consider the ratio of medium to sample (ideally 5:1 for ethanol and DMSO) in order to preserve good quality DNA (i.e. do not put too much tissue in one sample tube as the tissue will continue to degrade without enough preservative solution). When sampling from fisheries catch, it is important to preserve the DNA as soon as possible, especially in situations where there may have been a significant amount of time since capture.

- Identify in-country permit agencies and contact details for any required paperwork.

 Contact the relevant office at the earliest opportunity as administrative tasks required in international biological sampling projects can be a time consuming and bureaucratic process (Watanabe, 2017), particularly within the constraints of funding periods. Always follow up with reminders of enquires as project priorities may not align with those of permitting agencies. Where possible, discuss in-person or via a video / phone rather than relying on email correspondence. In-country project collaborators are crucial to facilitating all these steps.
- *Contingency planning*. Although there are some key steps that can be taken, there will always be external factors that may implement project implementation (e.g. COVID pandemic / natural disasters) (Figure 5.1). This is especially true when working with samples from fisheries catch that can fluctuate due to a range of environmental, social, economic, and political factors.

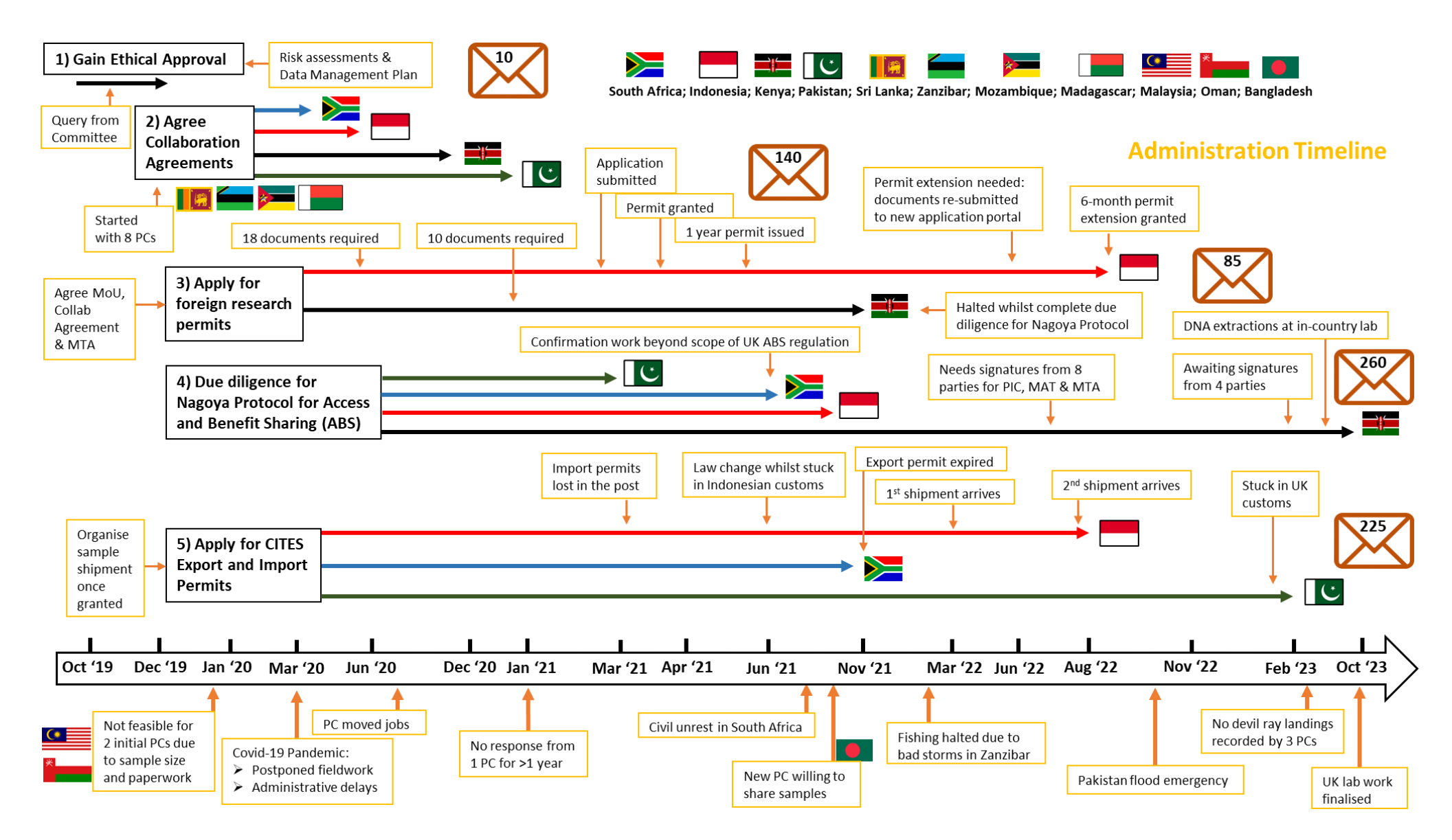


Figure 5.1 Timeline (October 2019 – 2023) of administrative tasks and challenges encountered during biological sampling (vertebrae and muscle tissue - genetic resources) of Indian Ocean *Mobula* spp. (listed on CITES Appendix II) from fisheries catch through a network of international Project Collaborators (PCs) in order to investigate life history and population structure. A conservative estimate of 720 emails were sent over the four-year duration, with the estimated number of emails sent for each step of the process indicated by envelope icons. From eight initial PCs, biological samples were eventually received from four PCs and countries (Indonesia, Kenya, Pakistan, and South Africa). Acronyms include MoU (Memorandum of Understanding), MTA (Material Transfer Agreement), PIC (Prior Informed Consent), and MAT (Mutually Agreed Terms).

5.3 Future research directions to inform conservation and management

Unassessed global fish stocks account for approximately half of marine fisheries landings and ultimately, more accurate data are needed to understand the status of unassessed fisheries (Ovando et al., 2021; Hilborn et al., 2020; Costello et al., 2012). Catch is currently underestimated in official FAO fisheries statistics, which is widely used as the only global database, particularly for small-scale fisheries catch in developing countries (Pauly & Zeller, 2016; Garibaldi, 2012; Zeller et al., 2015; Temple et al., 2019, 2018). Underestimated ray and shark catches (Clarke, McAllister, et al., 2006; Worm et al., 2013, 2024) are exacerbated by misidentification due to morphological similarity and ongoing taxonomic uncertainty (Tillett et al., 2012; Last et al., 2023). Further catch statistics are collected by Regional Fisheries Management Organisations (RFMOs), with some reporting catch of rays and sharks, however, there are also gaps in the taxonomic resolution, reporting by fishing sector (e.g. industrial versus small-scale), and of discards (Heidrich et al., 2022). The quality of reported data has implications for interpretation of catch trends, ability to conduct accurate stock assessments, and may ultimately cause mismanagement of fisheries resources that threatens the future sustainability of global fisheries (Watson & Pauly, 2001; Jacquet et al., 2010). Separate reporting of SSF and industrial catches as well as discards and retained catches by FAO members would be a key step to improve the database (Pauly & Charles, 2015; Mucientes et al., 2022). This will likely require on-board monitoring of all catches (target, non-target, and discard) by observers or camera deployments, the latter of which have been shown to be more cost-effective and representative of catch (van Helmond et al., 2020; Bartholomew et al., 2018). Vessel Monitoring Systems (VMS) have allowed better monitoring of fishing effort and catches but are currently more widely used for industrial fisheries (Lee et al., 2010; Kindt-Larsen et al.,

2011; Kroodsma et al., 2018). Although there is an indication that the shark and ray fin and gill plate trade is decreasing, better resolution of trade data is needed along with combatting illegal trade (Eriksson & Clarke, 2015; Wu, 2016; Prasetyo et al., 2021) in the same way as for fisheries catch data (Agnew et al., 2009).

Whilst many rays and sharks are caught as bycatch (Oliver et al., 2015; Lewison et al., 2004; Stevens et al., 2000), mitigation and fisheries management efforts are complicated by their commercial and subsistence value. There has been a reduction in discards but this does not necessarily mean a reduction is fishing mortality; where sharks and rays may have historically been classed as relatively low value, they are now more often retained with the depletion or management restrictions of high valued target catch (Kelleher, 2005; Dent & Clarke, 2015; Dulvy et al., 2021). Gillnets are the most widely used gear type in SSF as they are relatively low cost and effective at capturing many different species (Fernando & Stewart, 2021; Berninsone et al., 2020; Anderson et al., 2020). Unfortunately, their lack of selectivity also makes them the primary problem for fishing mortality of sharks, rays, and other marine megafauna (Lewison et al., 2004; Jabado, 2018; Reeves et al., 2013; Pechham et al., 2007; Moore, 2015). The need to move away from gillnets is recognised but often challenging given their effectiveness and where other methods might result in lower catch and income (Fernando & Stewart, 2021; Rojas-Bracho & Reeves, 2013). Therefore, holistic approaches understanding the drivers of fishers' behaviours as well as accounting for trade-offs between socio-economic factors and conservation objectives are needed to aid fisheries management decisions (Booth et al., 2020, 2023; Iwane et al., 2021). 'One size fits all' is generally not effective at dealing with the complexities of ray and shark fisheries; management therefore needs to be adaptable in order to be effective to the local context (Dulvy et al., 2017; Booth et al., 2019).

Whilst there is still a need for the collection of life history data from dead specimens in order to inform effective status assessments, future research will likely move towards less destructive sampling methods (Heupel & Simpfendorfer, 2010; Salvador et al., 2022). Currently, it is difficult to age and determine maturity, fecundity, and reproductive cycles of rays without dissection. Although, novel methods such as ultrasound are starting to be used, (Froman et al., 2023), which could potentially help when sampling catches that fishers do not want to cut before selling as well as sampling live individuals. Given uncertainty in age band counts, particularly for older individuals (Harry, 2018; Natanson et al., 2018), new technologies are also needed for ageing, for example near-infrared spectroscopy that has the potential to be non-lethal (Rigby et al., 2018).

Fisheries landings provide a good sampling opportunity to collect life history data where individuals have already been caught and landed but there will be inherent biases in these data. For example, where gears are selective for a particular size class or where species segregate by age or sex classes that overlap with fishing grounds. Often ray and shark data come from catch records and other fishery-dependent sources but there is a need for fisheries-independent data (Oliver et al., 2015; Lyons et al., 2013). Particularly where the knowledge base often comes from more well-studied species and regions. Satellite tags, aerial surveys, and Baited Remote Underwater Video systems (BRUVs) are becoming increasingly used to independently determine species occurrence, relative abundance, and to track ray distributions (Queiroz et al., 2019; Waldo et al., 2024; Shea et al., 2020; Oleksyn et al., 2021), information necessary for conservation and management (Hays et al., 2019). Independent fisheries monitoring approaches will be needed as part of a sampling strategy to address current species and geographic data gaps (Salvador et al., 2022; Shiffman et al., 2020).

Genetic approaches will likely be a key component of moving towards non-lethal sampling, fisheries-independent data, and addressing issues surrounding monitoring of fisheries catches (e.g. morphological similarity, illegal fishing and trade). This includes the use of environmental DNA to determine species presence, diversity, relative abundance, and even population structure, particularly for elusive and threatened species (Dunn et al., 2023; Dugal et al., 2022; Mariani et al., 2021; Leurs et al., 2023). Genetic approaches to identify species composition of fisheries catch and trade monitoring to help with the issue of traceability for management and enforcement controls will become more widely applicable as cost decreases and rapid assessment of multiple species becomes increasingly available (Cardeñosa et al., 2018). DNA barcoding is already being used to identify trade of CITES-listed and endangered species, particularly where difficult to determine species identity from traded products such as meat, shark fin, and gill plates (Shen et al., 2024; Wainwright et al., 2018; Clarke, Magnussen, et al., 2006). There is also the possibility of molecular aging and determining maximum lifespan (Mayne et al., 2019; Budd et al., 2023; Prasetyo et al., 2023), which may help with uncertainties from aging using vertebrae. Although currently lacking for rays and sharks (Pearce et al., 2021), the increase of genomic resources including reference genomes and species-specific data (Naylor et al., 2012; Hara et al., 2018) can also help prioritise conservation efforts for taxa that are evolutionary distinctive (Stein, Mull et al., 2018). Conserving taxonomic and genetic diversity as part of ray conservation and management of fisheries, and biodiversity conservation more broadly, are important to consider (Hoban et al., 2021; Domingues et al., 2018). Whilst this thesis addressed life history gaps for devil ray species, the next research priority should be to investigate the genetic population structure, which is lacking for many ray species, yet important for effective conservation and fisheries management (Dudgeon et al., 2012). Necessary tissue samples to facilitate genetic analyses have been collected during this PhD research (Figure 5.1) and will be used during planned post-doctoral research. Molecular approaches offer an exciting avenue for future fisheries and species assessments that alongside improved fisheries catch data and wider application of novel fisheries-independent monitoring can help work towards recovery and prevention of further decline of rays.

5.4 Conclusion

The research presented in this thesis has collected new and utilised available life history data of rays to infer global patterns in intrinsic sensitivity to fishing and contributed to addressing data paucity in the life history parameters for two Endangered devil ray species (*Mobula* spp.). It has further provided methods for data-poor approaches that can be used to inform fisheries sustainability assessments, setting fishing limits, and predicting rebound potentials for species where data are lacking and are likely to decline before there is time to fully address data paucity. The vulnerability of tropical rays is highlighted, many of which are already threatened with extinction, facing high exposure to fisheries, and have slow population growth rates. Improved fisheries monitoring, implementation and enforcement of science-based fisheries management, and wider incorporation of socio-economic factors in research and management are needed to conserve rays and ensure sustainable fisheries. The research outputs provide evidence necessary for policy and management to prevent ray species extirpation and extinction.

References

- Agnew, D.J., Pearce, J., Pramod, G., Peatman, T., Watson, R., Beddington, J.R. & Pitcher, T.J. (2009) 'Estimating the worldwide extent of illegal fishing', PLOS ONE, 4(2), p. e4570.
- Ajemian, M.J. & Powers, S.P. (2014) 'Towed-float satellite telemetry tracks large-scale movement and habitat connectivity of myliobatid stingrays', Environmental Biology of Fishes, 97(9), pp. 1067–1081.
- Alfaro-Shigueto, J., Mangel, J.C., Pajuelo, M., Dutton, P.H., Seminoff, J.A. & Godley, B.J. (2010) 'Where small can have a large impact: Structure and characterization of small-scale fisheries in Peru', Fisheries Research, 106(1), pp. 8–17.
- Allison, E.H., Perry, A.L., Badjeck, M.C., Neil Adger, W., Brown, K., Conway, D., Halls, A.S., Pilling, G.M., Reynolds, J.D., Andrew, N.L. & Dulvy, N.K. (2009) 'Vulnerability of national economies to the impacts of climate change on fisheries', Fish and Fisheries, 10(2), pp. 173–196.
- Anderson, R.C., Herrera, M., Ilangakoon, A.D., Koya, K.M., Moazzam, M., Mustika, P.L. & Sutaria, D.N. (2020) 'Cetacean bycatch in Indian Ocean tuna gillnet fisheries', Endangered Species Research, 41pp. 39–53.
- Anderson, S.C., Farmer, R.G., Ferretti, F., Houde, A.L.S. & Hutchings, J.A. (2011) 'Correlates of vertebrate extinction risk in Canada', BioScience, 61(7), pp. 538–549.
- Andrzejaczek, S., Chapple, T., Curnick, D., Carlisle, A., Castleton, M., Jacoby, D., Peel, L., Schallert, R., Tickler, D. & Block, B. (2020) 'Individual variation in residency and regional movements of reef manta rays Mobula alfredi in a large marine protected area', Marine Ecology Progress Series, 639pp. 137–153.
- Andrzejaczek, S., Lucas, T.C.D., Goodman, M.C., Hussey, N.E., Armstrong, A.J., Carlisle, A., Coffey, D.M., Gleiss, A.C., Huveneers, C., Jacoby, D.M.P., Meekan, M.G., Mourier, J., Peel, L.R., Abrantes, K., Afonso, A.S., Ajemian, M.J., Anderson, B.N., Anderson, S.D., Araujo, G., et al. (2022) 'Diving into the vertical dimension of elasmobranch movement ecology', Science Advances, 8(33), p. 1754.
- Angilletta, M.J., Huey, R.B. & Frazier, M.R. (2010) 'Thermodynamic effects on organismal performance: Is hotter better?', Physiological and Biochemical Zoology, 83(2), pp. 197–206.
- Arnold, T.W. (2010) 'Uninformative parameters and model selection using Akaike's Information Criterion', The Journal of Wildlife Management, 74(6), pp. 1175–1178.
- Aschliman, N.C. (2014) 'Interrelationships of the durophagous stingrays (Batoidea: Myliobatidae)', Environmental Biology of Fishes, 97(9), pp. 967–979.
- Aschliman, N.C., Nishida, M., Miya, M., Inoue, J.G., Rosana, K.M. & Naylor, G.J.P. (2012) 'Body plan convergence in the evolution of skates and rays (Chondrichthyes: Batoidea)', Molecular Phylogenetics and Evolution, 63(1), pp. 28–42.

- Ashton, G. V., Freestone, A.L., Duffy, J.E., Torchin, M.E., Sewall, B.J., Tracy, B., Albano, M., Altieri, A.H., Altvater, L., Bastida-Zavala, R., Bortolus, A., Brante, A., Bravo, V., Brown, N., Buschmann, A.H., Buskey, E., Barrera, R.C., Cheng, B., Collin, R., et al. (2022) 'Predator control of marine communities increases with temperature across 115 degrees of latitude', Science, 376(6598), pp. 1215–1219.
- Assis, J., Tyberghein, L., Bosch, S., Verbruggen, H., Serrão, E.A. & De Clerck, O. (2018) 'Bio-ORACLE v2.0: Extending marine data layers for bioclimatic modelling', Global Ecology and Biogeography, 27(3), pp. 277–284.
- Atkinson, D. (1995) 'Effects of temperature on the size of aquatic ectotherms: Exceptions to the general rule', Journal of Thermal Biology, 20(1–2), pp. 61–74.
- Atkinson, D. (1994) 'Temperature and organism size-A biological law for ectotherms?', Advances in Ecological Research, 25(C), pp. 1–58.
- Atkinson, D., Morley, S.A. & Hughes, R.N. (2006) 'From cells to colonies: At what levels of body organization does the "temperature-size rule" apply?', Evolution & development, 8(2), pp. 202–214.
- Atkinson, D. & Sibly, R.M. (1997) 'Why are organisms usually bigger in colder environments? Making sense of a life history puzzle', Trends in ecology & evolution, 12(6), pp. 235–239.
- Auer, S.K., Dick, C.A., Metcalfe, N.B. & Reznick, D.N. (2018) 'Metabolic rate evolves rapidly and in parallel with the pace of life history', Nature Communications, 9(14), p. 6.
- Baje, L., Smart, J.J., Chin, A., White, W.T. & Simpfendorfer, C.A. (2018) 'Age, growth and maturity of the Australian sharpnose shark Rhizoprionodon taylori from the Gulf of Papua', PLoS ONE, 13(10), p. e0206581.
- Barbini, S.A., Sabadin, D.E., Román, J.M., Scarabotti, P.A. & Lucifora, L.O. (2021) 'Age, growth, maturity and extinction risk of an exploited and endangered skate, Atlantoraja castelnaui, from off Uruguay and northern Argentina', Journal of Fish Biology, 99(4), pp. 1328–1340.
- Barnes, C., Maxwell, D., Reuman, D.C. & Jennings, S. (2010) 'Global patterns in predator-prey size relationships reveal size dependency of trophic transfer efficiency', Ecology, 91(1), pp. 222–232.
- Barnett, L.A.K., Jacobsen, N.S., Thorson, J.T. & Cope, J.M. (2019) 'Realizing the potential of trait-based approaches to advance fisheries science', Fish and Fisheries, 20(5), pp. 1034–1050.
- Barnett, L.A.K., Winton, M. v., Ainsley, S.M., Cailliet, G.M. & Ebert, D.A. (2013) 'Comparative demography of skates: life-history correlates of productivity and implications for management', PLOS ONE, 8(5), p. e65000.
- Barrowclift, E. & Dulvy, N.K. (2023) Life history and maximum weight database for rays (Class Chondrichthyes, Superorder Batoidea) up to June 2022. [Online] [online].

Available from: https://figshare.com/articles/dataset/Life_history_database_for_rays_Class_Chondrichth yes_Superorder_Batoidea_up_to_June_2022/20182109.

- Barrowclift, E., Gravel, S.M., Pardo, S., Bigman, J., Berggren, P. & Dulvy, N.K. (2023) 'Tropical rays are intrinsically more sensitive to overfishing than the temperate skates', Biological Conservation, 281p. 110003.
- Barrowclift, E., Temple, A.J., Stead, S., Jiddawi, N.S. & Berggren, P. (2017) 'Social, economic and trade characteristics of the elasmobranch fishery on Unguja Island, Zanzibar, East Africa', Marine Policy, 83pp. 128–136.
- Bartholomew, D.C., Mangel, J.C., Alfaro-Shigueto, J., Pingo, S., Jimenez, A. & Godley, B.J. (2018) 'Remote electronic monitoring as a potential alternative to on-board observers in small-scale fisheries', Biological Conservation, 219pp. 35–45.
- Bassos-Hull, K., Wilkinson, K.A., Hull, P.T., Dougherty, D.A., Omori, K.L., Ailloud, L.E., Morris, J.J. & Hueter, R.E. (2014) 'Life history and seasonal occurrence of the spotted eagle ray, Aetobatus narinari, in the eastern Gulf of Mexico', Environmental Biology of Fishes, 97(9), pp. 1039–1056.
- Baty, F., Ritz, C., Charles, S., Brutsche, M. & Flandrois, Jean-Pierre Delignette-Muller, M.-L. (2015) 'A toolbox for nonlinear regression in R: The package nlstools', Journal of Statistical Software, 66(5), pp. 1–21.
- Beamish, R.J. & Fournier, D.D.A. (1981) 'A method for comparing the precision of a set of age determinations', Canadian Journal of Fisheries and Aquatic Sciences, 38(8), pp. 982–983.
- Belhabib, D., Greer, K. & Pauly, D. (2018) 'Trends in industrial and artisanal catch per effort in West African fisheries', Conservation Letters, 11(1), p. e12360.
- Béné, C. (2009) 'Are Fishers Poor or Vulnerable? Assessing Economic Vulnerability in Small-Scale Fishing Communities', The Journal of Development Studies, 45(6), pp. 911–933.
- Béné, C. (2006) 'Small-scale fisheries: assessing their contribution to rural livelihoods in developing countries'. FAO Fisheries Circular No. 1008 (FAO Rome).
- Béné, C., Barange, M., Subasinghe, R., Pinstrup-Andersen, P., Merino, G., Hemre, G.I. & Williams, M. (2015) 'Feeding 9 billion by 2050 Putting fish back on the menu', Food Security, 7(2), pp. 261–274.
- Béné, C., Chijere, A.D.G., Allison, E.H., Snyder, K. & Crissman, C. (2012) 'Design and implementation of fishery modules in integrated household surveys in developing countries'. Document prepared for the Living Standards Measurement Study Integrated Surveys on Agriculture project
- Béné, C., Hersoug, B. & Allison, E.H. (2010) 'Not by rent alone: Analysing the pro-poor functions of small-scale fisheries in developing countries', Development Policy Review, 28(3), pp. 325–358.

- Béné, C., Macfadyen, G. & Allison, E. (2007) 'Increasing the contribution of small-scale fisheries to poverty alleviation and food security'. Food and Agriculture Organisation of the United Nations
- Bergmann, C. (1847) 'Ueber die Verhältnisse der Wärmeökonomie der Thiere zu ihrer Grösse', Göttinger Studien, 1pp. 595–708.
- Berkes, F., Mahon, R., McConney, P., Pollnac, R. & Pomeroy, R. (2001) Managing Small-Scale Fisheries. Alternative Directions and Methods International Development Research Centre, Ottawa, Canada (2001).
- Bernhardt, J.R., Sunday, J.M. & O'Connor, M.I. (2018) 'Metabolic theory and the temperature-size rule explain the temperature dependence of population carrying capacity', The American Naturalist, 192(6), pp. 687–697.
- Berninsone, L.G., Bordino, P., Gnecco, M., Foutel, M., Mackay, A.I. & Werner, T.B. (2020) 'Switching gillnets to longlines: An alternative to mitigate the bycatch of Franciscana dolphins (Pontoporia blainvillei) in Argentina', Frontiers in Marine Science, 7p. 533709.
- Beukhof, E., Frelat, R., Pecuchet, L., Maureaud, A., Dencker, T.S., Sólmundsson, J., Punzón, A., Primicerio, R., Hidalgo, M., Möllmann, C. & Lindegren, M. (2019) 'Marine fish traits follow fast-slow continuum across oceans', Scientific reports, 9(1), p. 17878.
- Blaber, S.J.M., Dichmont, C.M., White, W., Buckworth, R., Sadiyah, L., Iskandar, B., Nurhakim, S., Pillans, R., Andamari, R., Dharmadi & Fahmi (2009) 'Elasmobranchs in southern Indonesian fisheries: The fisheries, the status of the stocks and management options', Reviews in Fish Biology and Fisheries, 19(3), pp. 367–391.
- Bland, J.M. & Altman, D.G. (2003) 'Applying the right statistics: Analyses of measurement studies', Ultrasound in obstetrics & gynecology, 22(1), pp. 85–93.
- Bland, J.M. & Altman, D.G. (1999) 'Measuring agreement in method comparison studies', Statistical methods in medical research, 8(2), pp. 135–160.
- Boerder, K., Schiller, L. & Worm, B. (2019) 'Not all who wander are lost: Improving spatial protection for large pelagic fishes', Marine Policy, 105pp. 80–90.
- Boettiger, C., Lang, D.T. & Wainwright, P.C. (2012) 'rfishbase: Exploring, manipulating and visualizing FishBase data from R', Journal of Fish Biology, 81(6), pp. 2030–2039.
- Bom, R.A., Brader, A., Batsleer, J., Poos, J.J., van der Veer, H.W. & van Leeuwen, A. (2022) 'A long-term view on recent changes in abundance of common skate complex in the North Sea', Marine Biology, 169(11), pp. 1–14.
- Booth, H., Ichsan, M., Hermansyah, R.F., Rohmah, L.N., Naira, K.B., Adrianto, L. & Milner-Gulland, E.J. (2023) 'A socio-psychological approach for understanding and managing bycatch in small-scale fisheries', People and Nature, 5(3), pp. 968–980.

- Booth, H., Squires, D. & Milner-Gulland, E.J. (2020) 'The mitigation hierarchy for sharks: A risk-based framework for reconciling trade-offs between shark conservation and fisheries objectives', Fish and Fisheries, 21(2), pp. 269–289.
- Booth, H., Squires, D. & Milner-Gulland, E.J. (2019) 'The neglected complexities of shark fisheries, and priorities for holistic risk-based management', Ocean & Coastal Management, 182p. 104994.
- Braccini, M., Hesp, A. & Walker, T.I. (2022) 'Gillnet selectivity for non-targeted shark species in temperate Australia', Fisheries Management and Ecology, 29(5), pp. 724–733.
- Brander, K. (1981) 'Disappearance of common skate Raia batis from Irish Sea', Nature, 290(5801), pp. 48–49.
- Braun, C.D., Arostegui, M.C., Thorrold, S.R., Papastamatiou, Y.P., Gaube, P., Fontes, J. & Afonso, P. (2022) 'The functional and ecological significance of deep diving by large marine predators', Annual Review of Marine Science, 14(Volume 14, 2022), pp. 129–159.
- Broadhurst, M.K. & Cullis, B.R. (2020) 'Mitigating the discard mortality of non-target, threatened elasmobranchs in bather-protection gillnets', Fisheries Research, 222p. 105435.
- Broadhurst, M.K., Laglbauer, B.J.L. & Bennett, M.B. (2019) 'Gestation and size at parturition for Mobula kuhlii cf. eregoodootenkee', Environmental Biology of Fishes, 102pp. 1009–1014.
- Broadhurst, M.K., Laglbauer, B.J.L., Burgess, K.B. & Coleman, M.A. (2018) 'Reproductive biology and range extension for Mobula kuhlii cf. eregoodootenkee', Endangered Species Research, 35pp. 71–80.
- Brown, J.H., Gillooly, J.F., Allen, A.P., Savage, V.M. & West, G.B. (2004) 'Toward a metabolic theory of ecology', Ecology, 85(7), pp. 1771–1789.
- Budd, A.M., Mayne, B., Berry, O. & Jarman, S. (2023) 'Fish species lifespan prediction from promoter cytosine-phosphate-guanine density', Molecular Ecology Resources,
- Burger, J.R., Hou, C. & Brown, J.H. (2019) 'Toward a metabolic theory of life history', Proceedings of the National Academy of Sciences of the United States of America, 116(52), pp. 26653–26661.
- Burke, P.J., Raoult, V., Natanson, L.J., Murphy, T.D., Peddemors, V. & Williamson, J.E. (2020) 'Struggling with age: Common sawsharks (Pristiophorus cirratus) defy age determination using a range of traditional methods', Fisheries Research, 231p. 105706.
- Burnham, K.P. & Anderson, D.R. (2002) Model Selection and Multimodel Inference: A Practical Information-Theoretic Approach. 2nd edition. Springer New York.
- Cailliet, G.M. & Goldman, K.J. (2004) 'Age Determination and Validation in Chondrichthyan Fishes', in Jeffrey C Carrier, John A Musick, & Michael R Heithaus (eds.) Biology of Sharks and Their Relatives. [Online]. Boca Raton, Florida: CRC Press. pp. 399–447.

- Cailliet, G.M., Martin, L.K., Kusher, D., Wolf, P. & Weldon, B.A. (1983) Techniques for enhancing vertebral bands in age estimation of California elasmobranchs IN: Proceedings of the International Workshop on Age Determination of Oceanic Pelagic Fishes: Tunas, Billfishes, and Sharks.
- Cailliet, G.M., Smith, W.D., Mollet, H.F. & Goldman, K.J. (2006) 'Age and growth studies of chondrichthyan fishes: the need for consistency in terminology, verification, validation, and growth function fitting', Environmental Biology of Fishes 2006 77:3, 77(3), pp. 211–228.
- Campana, S.E. (2001) 'Accuracy, precision and quality control in age determination, including a review of the use and abuse of age validation methods', Journal of Fish Biology, 59(2), pp. 197–242.
- Campana, S.E. (2014) Age determination of elasmobranchs, with special reference to Mediterranean species: a technical manual: Studies and Reviews. General Fisheries Commission for the Mediterranean. No. 94. Rome, FAO 2014.
- Cardeñosa, D., Quinlan, J., Shea, K.H. & Chapman, D.D. (2018) 'Multiplex real-time PCR assay to detect illegal trade of CITES-listed shark species', Scientific Reports 2018 8:1, 8(1), pp. 1–10.
- Carpenter, M., Parker, D., Dicken, M.L. & Griffiths, C.L. (2023) 'Multi-decade catches of manta rays (Mobula alfredi, M. birostris) from South Africa reveal significant decline', Frontiers in Marine Science, 10p. 1128819.
- Casey, J.M. & Myers, R.A. (1998) 'Near extinction of a large, widely distributed fish', Science, 281(5377), pp. 690–692.
- Catarci, C. (2004) 'World markets and industry of selected commercially-exploited aquatic species with an international conservation profile'. FAO Fisheries Circular No. 990
- Chang, W.Y.B. (1982) 'A statistical method for evaluating the reproducibility of age determination', Canadian Journal of Fisheries and Aquatic Sciences, 39(8), pp. 1208–1210.
- Chichorro, F., Juslén, A. & Cardoso, P. (2019) 'A review of the relation between species traits and extinction risk', Biological Conservation, 237pp. 220–229.
- Chin, A., Molloy, F.J., Cameron, D., Day, J.C., Cramp, J., Gerhardt, K.L., Heupel, M.R., Read, M. & Simpfendorfer, C.A. (2023) 'Conceptual frameworks and key questions for assessing the contribution of marine protected areas to shark and ray conservation', Conservation Biology, 37(1), p. e13917.
- Chin, A., Molloy, F.J., Cameron, D., Day, J.C., Cramp, J., Gerhardt, K.L., Heupel, M.R., Read, M., Simpfendorfer, C.A., John Molloy, F., Cameron, D., Day, J.C., Cramp, J., Leeann Gerhardt, K., Heupel, M.R. & Simpfendorfer, C.A. (2023) 'Conceptual frameworks and key questions for assessing the contribution of marine protected areas to shark and ray conservation', Conservation Biology, 37(1), pp. 1–13.

- Christensen, R. (2023) ordinal—Regression Models for Ordinal Data. p.p. R package version 2023.12-4.
- Chuenpagdee, R., Liguori, L., Palomares, M.L.D.D. & Pauly, D. (Daniel) (2006) 'Bottom-up, global estimates of small-scale marine fisheries catches', Fisheries Centre Research Reports, 14(8), .
- Cinner, J.E., Daw, T. & McClanahan, T.R. (2009) 'Socioeconomic factors that affect artisanal fishers' readiness to exit a declining fishery', Conservation Biology, 23(1), pp. 124–130.
- Clark, R.S. (1922) 'Rays and skates (Raiœ) no. 1.—Egg-capsules and young', Journal of the Marine Biological Association of the United Kingdom, 12(4), pp. 578–643.
- Clarke, A. (2017) Principles of thermal ecology; temperature, energy and life. Cambridge University Press.
- Clarke, A. & Johnston, N.M. (1999) 'Scaling of metabolic rate with body mass and temperature in teleost fish', Journal of Animal Ecology, 68(5), pp. 893–905.
- Clarke, S.C., Magnussen, J.E., Abercrombie, D.L., McAllister, M.K. & Shivji, M.S. (2006) 'Identification of shark species composition and proportion in the Hong Kong shark fin market based on molecular genetics and trade records', Conservation Biology, 20(1), pp. 201–211.
- Clarke, S.C., McAllister, M.K., Milner-Gulland, E.J., Kirkwood, G.P., Michielsens, C.G.J., Agnew, D.J., Pikitch, E.K., Nakano, H. & Shivji, M.S. (2006) 'Global estimates of shark catches using trade records from commercial markets', Ecology Letters, 9(10), pp. 1115–1126.
- Clutton-Brock, T.H. (1991) The Evolution of Parental Care. Princeton. Princeton, New Jersey:
- Compagno, L.J.V.V. (1990) 'Alternative life-history styles of cartilaginous fishes in time and space', Environmental Biology of Fishes, 28(1), pp. 33–75.
- Conners, M.G., Sisson, N.B., Agamboue, P.D., Atkinson, P.W., Baylis, A.M.M., Benson, S.R., Block, B.A., Bograd, S.J., Bordino, P., Bowen, W.D., Brickle, P., Bruno, I.M., González Carman, V., Champagne, C.D., Crocker, D.E., Costa, D.P., Dawson, T.M., Deguchi, T., Dewar, H., et al. (2022) 'Mismatches in scale between highly mobile marine megafauna and marine protected areas', Frontiers in Marine Science, 9p. 897104.
- Conrath, C. & Musick, J. (2012) 'Reproductive Biology of Elasmobranchs', in J Jeffrey C. Carrier, John A. Musick, & Michael R. Heithaus (eds.) Biology of Sharks and Their Relatives. 2nd edition [Online]. Boca Raton, London, New York, Washington, D.C.: CRC Press. pp. 291–312.
- Constance, J., Ebert, D.A., Fahmi, Finucci, B., Simeon, B. & Kyne, P.M. (2023) Urolophus javanicus. [Online] [online]. Available from: https://www.iucnredlist.org/species/60095/229337053 (Accessed 3 April 2024).

- Cope, J.M. (2006) 'Exploring intraspecific life history patterns in sharks', Fishery Bulletin National Oceanic and Atmospheric Administration, 104(2), pp. 311–320.
- Cortés, E. (2002) 'Incorporating uncertainty into demographic modeling: Application to shark populations and their conservation', Conservation Biology, 16(4), pp. 1048–1062.
- Cortés, E. (2000) 'Life History Patterns and Correlations in Sharks', Reviews in Fisheries Science, 8(4), pp. 299–344.
- Cortés, E. (2016) 'Perspectives on the intrinsic rate of population growth' Justin Travis (ed.), Methods in Ecology and Evolution, 7(10), pp. 1136–1145.
- Cortés, E., Arocha, F., Beerkircher, L., Carvalho, F., Domingo, A., Heupel, M., Holtzhausen, H., Santos, M.N., Ribera, M. & Simpfendorfer, C. (2010) 'Ecological risk assessment of pelagic sharks caught in Atlantic pelagic longline fisheries', Aquatic Living Resources, 23(1), pp. 25–34.
- Cortés, E. & Brooks, E.N. (2018) 'Stock status and reference points for sharks using data-limited methods and life history', Fish and Fisheries, 19(6), pp. 1110–1129.
- Cortés, Enric, Brooks, E.N. & Gedamke, T. (2012) 'Population Dynamics, Demography, and Stock Assessment', in Jeffrey C. Carrier, John A. Musick, & Michael R. Heithaus (eds.) Biology of Sharks and Their Relatives: Second Edition. 2nd edition [Online]. Boca Raton: CRC Press. pp. 453–485.
- Cortés, E., Brooks, E.N. & Gedamke, T. (2012) 'Population dynamics, demography, and stock assessment', in J. C. Carrier, J. A. Musick, & M. R. Heithaus (eds.) Biology of sharks and their relatives,. 2nd edition [Online]. Boca Raton, Florida: CRC Press. pp. 449–481.
- Cortés, E., Brooks, E.N. & Shertzer, K.W. (2015) 'Risk assessment of cartilaginous fish populations', ICES Journal of Marine Science, 72(3), pp. 1057–1068.
- Cortés, E., Domingo, A., Miller, P., Forselledo, R., Mas, F., Arocha, F., Campana, S., Coelho, R., Da Silva, C., Hazin, F.H. V, Holtzhausen, H., Keene, K., Lucena, F., Ramirez, K., Santos, M.N., Semba-Murakami, Y., Yokawa, K., Medeiros, M. & Irmaos, /N -Dois (2015) 'Expanded ecological risk assessment of pelagic sharks caught in Atlantic pelagic longline fisheries', Collective Volume of Scientific Papers ICCAT, 71(6), pp. 2637–2688.
- Costello, C., Ovando, D., Hilborn, R., Gaines, S.D., Deschenes, O. & Lester, S.E. (2012) 'Status and solutions for the world's unassessed fisheries', Science, 338(6106), pp. 517–520.
- Cotton, C.F., Dean Grubbs, R., Dyb, J.E., Fossen, I. & Musick, J.A. (2015) 'Reproduction and embryonic development in two species of squaliform sharks, Centrophorus granulosus and Etmopterus princeps: evidence of matrotrophy?', Deep Sea Research Part II: Topical Studies in Oceanography, 115(1), pp. 41–54.
- Couturier, L.I.E., Marshall, A.D., Jaine, F.R.A., Kashiwagi, T., Pierce, S.J., Townsend, K.A., Weeks, S.J., Bennett, M.B. & Richardson, A.J. (2012) 'Biology, ecology and conservation of the Mobulidae', Journal of Fish Biology, 80(5), pp. 1075–1119.

- Couturier, L.I.E., Newman, P., Jaine, F.R.A., Bennett, M.B., Venables, W.N., Cagua, E.F., Townsend, K.A., Weeks, S.J. & Richardson, A.J. (2018) 'Variation in occupancy and habitat use of Mobula alfredi at a major aggregation site', Marine Ecology Progress Series, 599pp. 125–145.
- Croll, D.A., Dewar, H., Dulvy, N.K., Fernando, D., Francis, M.P., Galván-Magaña, F., Hall, M., Heinrichs, S., Marshall, A., Mccauley, D., Newton, K.M., Notarbartolo-Di-Sciara, G., O'Malley, M., O'Sullivan, J., Poortvliet, M., Roman, M., Stevens, G., Tershy, B.R. & White, W.T. (2016) 'Vulnerabilities and fisheries impacts: The uncertain future of manta and devil rays', Aquatic Conservation: Marine and Freshwater Ecosystems, 26(3), pp. 562–575.
- Cuevas-Zimbrón, E., Sosa-Nishizaki, O., Pérez-Jiménez, J.C. & O'Sullivan, J.B. (2013) 'An analysis of the feasibility of using caudal vertebrae for ageing the spinetail devilray, Mobula japanica (Müller and Henle, 1841)', Environmental Biology of Fishes, 96(8), pp. 907–914.
- D'Alberto, B.M., Carlson, J.K., Pardo, S.A. & Simpfendorfer, C.A. (2019) 'Population productivity of shovelnose rays: Inferring the potential for recovery', PLoS ONE, 14(11), .
- Dapp, D.R., Walker, T.I., Huveneers, C. & Reina, R.D. (2016) 'Respiratory mode and gear type are important determinants of elasmobranch immediate and post-release mortality', Fish and Fisheries, 17(2), pp. 507–524.
- Davidson, A.D., Boyer, A.G., Kim, H., Pompa-Mansilla, S., Hamilton, M.J., Costa, D.P., Ceballos, G. & Brown, J.H. (2012) 'Drivers and hotspots of extinction risk in marine mammals', Proceedings of the National Academy of Sciences of the United States of America, 109(9), pp. 3395–3400.
- Davidson, L.N.K. & Dulvy, N.K. (2017) 'Global marine protected areas to prevent extinctions', Nature Ecology & Evolution 2017 1:2, 1(2), pp. 1–6.
- Davidson, L.N.K., Krawchuk, M.A. & Dulvy, N.K. (2016) 'Why have global shark and ray landings declined: improved management or overfishing?', Fish and Fisheries, 17(2), pp. 438–458.
- Dean, M.N., Bizzarro, J.J., Clark, B., Underwood, C.J. & Johanson, Z. (2017) 'Large batoid fishes frequently consume stingrays despite skeletal damage', Royal Society Open Science, 4p. 170674.
- DeGroot, B.C., Bassos-Hull, K., Wilkinson, K.A., Lowerre-Barbieri, S., Poulakis, G.R. & Ajemian, M.J. (2021) 'Variable migration patterns of whitespotted eagle rays Aetobatus narinari along Florida's coastlines', Marine Biology, 168(2), pp. 1–21.
- Denéchère, R., van Denderen, P.D. & Andersen, K.H. (2022) 'Deriving population scaling rules from individual-level metabolism and life history traits', The American Naturalist, 199(4), pp. 564–575.

- Denney, N.H., Jennings, S. & Reynolds, J.D. (2002) 'Life-history correlates of maximum population growth rates in marine fishes', Proceedings of the Royal Society of London. Series B: Biological Sciences, 269(1506), pp. 2229–2237.
- Dent, F. & Clarke, S. (2015) State of the global market for shark products.
- Dillon, M.E., Wang, G. & Huey, R.B. (2010) 'Global metabolic impacts of recent climate warming', Nature, 467(7316), pp. 704–706.
- Domingues, R.R., Hilsdorf, A.W.S., Gadig, O.B.F., Wagner, A., Hilsdorf, S., Bismarck, O. & Gadig, F. (2018) 'The importance of considering genetic diversity in shark and ray conservation policies', Conservation Genetics, 19(3), pp. 501–525.
- Domingues, R.R., Vasconcellos Bunholi, I., Pinhal, D., Antunes, A. & Fernandes Mendonça, F. (2021) 'From molecule to conservation: DNA-based methods to overcome frontiers in the shark and ray fin trade', Conservation Genetics Resources, 13pp. 231–247.
- Van Dongen, S. (2006) 'Prior specification in Bayesian statistics: Three cautionary tales', Journal of Theoretical Biology, 242(1), pp. 90–100.
- Dormann, C.F., Elith, J., Bacher, S., Buchmann, C., Carl, G., Carré, G., Marquéz, J.R.G., Gruber, B., Lafourcade, B., Leitão, P.J., Münkemüller, T., Mcclean, C., Osborne, P.E., Reineking, B., Schröder, B., Skidmore, A.K., Zurell, D. & Lautenbach, S. (2013) 'Collinearity: A review of methods to deal with it and a simulation study evaluating their performance', Ecography, 36(1), pp. 27–46.
- Doumbouya, F. (2011) 'Biologie et écologie des Mobulidae en République de Guinée: Cas de Mobula thurstoni', in Colloque international sur les Requins. [Online]. 2011 Dakar, Senegal: .
- Duarte, C.M. & Alcaraz, M. (1989) 'To produce many small or few large eggs: A size-independent reproductive tactic of fish', Oecologia 1989 80:3, 80(3), pp. 401–404.
- Dudgeon, C.L., Blower, D.C., Broderick, D., Giles, J.L., Holmes, B.J., Kashiwagi, T., Krück, N.C., Morgan, J.A.T., Tillett, B.J. & Ovenden, J.R. (2012) 'A review of the application of molecular genetics for fisheries management and conservation of sharks and rays', Journal of Fish Biology, 80(5), pp. 1789–1843.
- Dugal, L., Thomas, L., Jensen, M.R., Sigsgaard, E.E., Simpson, T., Jarman, S., Thomsen, P.F. & Meekan, M. (2022) 'Individual haplotyping of whale sharks from seawater environmental DNA', Molecular Ecology Resources, 22(1), pp. 56–65.
- Dulvy, N. & Forrest, R. (2010) Life Histories, Population Dynamics, and Extinction Risks in Chondrichthyans. In book: Sharks and Their Relatives II: Biodiversity, Adaptive Physiology, and Conservation. J. C. Carrier, J. A. Musick, & M. R. Heithaus (eds.). CRC Press.
- Dulvy, N.K., Baum, J.K., Clarke, S., Compagno, L.J.V., Cortés, E., Domingo, A., Fordham, S., Fowler, S., Francis, M.P., Gibson, C., Martínez, J., Musick, J.A., Soldo, A., Stevens, J.D. & Valenti, S. (2008) 'You can swim but you can't hide: The global status and conservation

- of oceanic pelagic sharks and rays', Aquatic Conservation: Marine and Freshwater Ecosystems, 18(5), pp. 459–482.
- Dulvy, N.K., Davidson, L.N.K., Kyne, P.M., Simpfendorfer, C.A., Harrison, L.R., Carlson, J.K. & Fordham, S. V. (2016) 'Ghosts of the coast: global extinction risk and conservation of sawfishes', Aquatic Conservation: Marine and Freshwater Ecosystems, 26(1), pp. 134–153.
- Dulvy, N.K., Ellis, J.R., Goodwin, N.B., Grant, A., Reynolds, J.D. & Jennings, S. (2004) 'Methods of assessing extinction risk in marine fishes', Fish and Fisheries, 5(3), pp. 255–276.
- Dulvy, Nicholas K., Fowler, S.L., Musick, J.A., Cavanagh, R.D., Kyne, P.M., Harrison, L.R., Carlson, J.K., Davidson, L.N., Fordham, S. V, Francis, M.P., Pollock, C.M., Simpfendorfer, C.A., Burgess, G.H., Carpenter, K.E., Compagno, L.J., Ebert, D.A., Gibson, C., Heupel, M.R., Livingstone, S.R., et al. (2014) 'Extinction risk and conservation of the world's sharks and rays', eLife, 3p. 590.
- Dulvy, N.K. & Kindsvater, H.K. (2017) 'The Future Species of Anthropocene Seas', in Phillip S. Levin & Melissa R. Poe (eds.) Conservation for the Anthropocene Ocean: Interdisciplinary Science in Support of Nature and People. [Online]. Academic Press. pp. 39–64.
- Dulvy, N.K., Pacoureau, N., Rigby, C.L., Pollom, R.A., Jabado, R.W., Ebert, D.A., Finucci, B., Pollock, C.M., Cheok, J., Derrick, D.H., Herman, K.B., Sherman, C.S., VanderWright, W.J., Lawson, J.M., Walls, R.H.L., Carlson, J.K., Charvet, P., Bineesh, K.K., Fernando, D., et al. (2021) 'Overfishing drives over one-third of all sharks and rays toward a global extinction crisis', Current Biology, 31(21), pp. 4773-4787.e8.
- Dulvy, N K, Pardo, S.A., Simpfendorfer, C.A. & Carlson, J.K. (2014) 'Diagnosing the dangerous demography of manta rays using life history theory', PeerJ, 2014(1), p. e400.
- Dulvy, N.K. & Reynolds, J. (1997) 'Evolutionary transitions among egg-laying, live-bearing and maternal inputs in sharks and rays', Proceedings of the Royal Society of London, B, 264pp. 1309–1315.
- Dulvy, N.K. & Reynolds, J.D. (2002) 'Predicting extinction vulnerability in skates', Conservation Biology, 16(2), pp. 440–450.
- Dulvy, N.K., Simpfendorfer, C.A., Davidson, L.N.K., Fordham, S. V., Bräutigam, A., Sant, G. & Welch, D.J. (2017) 'Challenges and priorities in shark and ray conservation', Current Biology, 27(11), pp. R565–R572.
- Dunn, N., Curnick, D.J., Carbone, C., Carlisle, A.B., Chapple, T.K., Dowell, R., Ferretti, F., Jacoby, D.M.P., Schallert, R.J., Steyaert, M., Tickler, D.M., Williamson, M.J., Block, B.A. & Savolainen, V. (2023) 'Environmental DNA helps reveal reef shark distribution across a remote archipelago', Ecological Indicators, 154p. 110718.

- Ebert, D.A. & Compagno, L.J.V. (2007) 'Biodiversity and systematics of skates (Chondrichthyes: Rajiformes: Rajoidei)', Environmental Biology of Fishes, 80(2–3), pp. 111–124.
- Ebert, D.A., Cowley, P.D. & Compagno, L.J. V (2002) 'First records of the longnose spiny dogfish Squalus blainvillei (Squalidae) and the deep-water stingray Plesiobatis davies (Urolophidae) from South African waters', South African Journal of Marine Science, 24(1), pp. 355–357.
- Ehemann, N.R., González-González, L. V. & Trites, A.W. (2017) 'Lesser devil rays Mobula cf. hypostoma from Venezuela are almost twice their previously reported maximum size and may be a new sub-species', Journal of Fish Biology, 90(3), pp. 1142–1148.
- Ellis, J.R., McCully Phillips, S.R., Poisson, F., Phillips, S.R.M. & Poisson, F. (2017) 'A review of capture and post-release mortality of elasmobranchs', Journal of Fish Biology, 90(3), pp. 653–722.
- Eriksson, H. & Clarke, S. (2015) 'Chinese market responses to overexploitation of sharks and sea cucumbers', Biological Conservation, 184pp. 163–173.
- Fabens, A.J. (1965) 'Properties and fitting of the von Bertalanffy growth curve', Growth, 29pp. 265–289.
- FAO (2023) Fishery and Aquaculture Statistics. Global Fish Processed Products Production 1976-2021 (FishStatJ). In: FAO Fisheries and Aquaculture Division [online]. Rome. Updated 2023. www.fao.org/fishery/statistics/software/fishstatj/en.
- FAO (2021) Global capture production.
- Fernando, D. & Stewart, J.D. (2021) 'High bycatch rates of manta and devil rays in the "small-scale" artisanal fisheries of Sri Lanka', PeerJ, 9p. e11994.
- Finucci, B. & García, E. (2024) Hexatrygon bickellii. [Online] [online]. Available from: https://www.iucnredlist.org/species/161674/124526129 (Accessed 29 July 2024).
- Finucci, B., Pacoureau, N., Rigby, C.L., Matsushiba, J.H., Faure-Beaulieu, N., Sherman, C.S., VanderWright, W.J., Jabado, R.W., Charvet, P., Mejía-Falla, P.A., Navia, A.F., Derrick, D.H., Kyne, P.M., Pollom, R.A., Walls, R.H.L., Herman, K.B., Kinattumkara, B., Cotton, C.F., Cuevas, J.-M., et al. (2024) 'Fishing for oil and meat drives irreversible defaunation of deepwater sharks and rays', Science, 383(6687), pp. 1135–1141.
- Flounders, F. (2020) The impact of the IOTC fisheries on mobulid rays: status and interactions, data availability, and recommendations for management.
- Forrest, R.E. & Walters, C.J. (2009) 'Estimating thresholds to optimal harvest rate for long-lived, low-fecundity sharks accounting for selectivity and density dependence in recruitment', Canadian Journal of Fisheries and Aquatic Sciences, 66(12), pp. 2062–2080.

- Fowler, S.L. (2012) 'First meeting of the signatories to the Memorandum of Understanding on the conservation of migratory sharks', in Background Paper on the Conservation Status of Migratory Sharks. [Online]. 2012 Bonn, Germany: . p. 26.
- Fox, J. & Weisberg, S. (2019) An {R} Companion to Applied Regression, Third Edition. Thousand Oaks CA: Sage.
- Freestone, A.L., Carroll, E.W., Papacostas, K.J., Ruiz, G.M., Torchin, M.E. & Sewall, B.J. (2020) 'Predation shapes invertebrate diversity in tropical but not temperate seagrass communities', Journal of Animal Ecology, 89(2), pp. 323–333.
- Freestone, A.L., Osman, R.W., Ruiz, G.M. & Torchin, M.E. (2011) 'Stronger predation in the tropics shapes species richness patterns in marine communities', Ecology, 92(4), pp. 983–993.
- Frisk, M. (2010) 'Life History Strategies of Batoids', in C. Carrier, J.A. Musick, & M.R. Heithaus (eds.) Sharks and their Relatives II: Biodiversity, Adaptive Physiology, and Conservation. [Online]. Boca Raton: CRC Press. pp. 283–316.
- Frisk, M.G., Miller, T.J. & Fogarty, M.J. (2001a) 'Estimation and analysis of biological parameters in elasmobranch fishes: a comparative life history study', Canadian Journal of Fisheries and Aquatic Sciences, 58(5), pp. 969–981.
- Frisk, M.G., Miller, T.J. & Fogarty, M.J. (2001b) 'Estimation and analysis of biological parameters in elasmobranch fishes: A comparative life history study', Canadian Journal of Fisheries and Aquatic Sciences, 58(5), pp. 969–981.
- Froese, R. & Binohlan, C. (2000) 'Empirical relationships to estimate asymptotic length, length at first maturity and length at maximum yield per recruit in fishes, with a simple method to evaluate length frequency data', Journal of Fish Biology, 56(4), pp. 758–773.
- Froese, R. & Pauly, D. (2022) FishBase. World Wide Web electronic publication. www.fishbase.org, (08/2022). [Online]
- Froese, R., Thorson, J.T. & Reyes, R.B. (2014) 'A Bayesian approach for estimating length-weight relationships in fishes', Journal of Applied Ichthyology, 30(1), pp. 78–85.
- Froman, N., Genain, M.A., Stevens, G.M.W. & Pearce, G.P. (2023) 'Use of underwater contactless ultrasonography to elucidate the internal anatomy and reproductive activity of manta and devil rays (family: Mobulidae)', Journal of Fish Biology, 103(2), pp. 305–323.
- Gallagher, A.J., Kyne, P.M. & Hammerschlag, N. (2012) 'Ecological risk assessment and its application to elasmobranch conservation and management', Journal of fish biology, 80(5), pp. 1727–1748.
- García, V.B., Lucifora, L.O. & Myers, R.A. (2008) 'The importance of habitat and life history to extinction risk in sharks, skates, rays and chimaeras', Proceedings of the Royal Society B: Biological Sciences, 275(1630), pp. 83–89.

- Garibaldi, L. (2012) 'The FAO global capture production database: A six-decade effort to catch the trend', Marine Policy, 36(3), pp. 760–768.
- Gedamke, T., DuPaul, W.D. & Musick, J.A. (2005) 'Observations on the life history of the barndoor skate, Dipturus laevis, on Georges Bank (western North Atlantic)', Journal of Northwest Atlantic Fishery Science, 35pp. 67–78.
- Gedamke, T., Hoenig, J.M., Musick, J.A., DuPaul, W.D. & Gruber, S.H. (2007) 'Using demographic models to determine intrinsic rate of increase and sustainable fishing for elasmobranchs: Pitfalls, advances, and applications', North American Journal of Fisheries Management, 27(2), pp. 605–618.
- Gillooly, J.F., Brown, J.H., West, G.B., Savage, V.M. & Charnov, E.L. (2001) 'Effects of size and temperature on metabolic rate', Science, 293(5538), pp. 2248–2251.
- Gilman, E., Chaloupka, M., Benaka, L.R., Bowlby, H., Fitchett, M., Kaiser, M. & Musyl, M. (2022) 'Phylogeny explains capture mortality of sharks and rays in pelagic longline fisheries: A global meta-analytic synthesis', Scientific Reports, 12(1), pp. 1–14.
- Gilman, E., Hall, M., Booth, H., Gupta, T., Chaloupka, M., Fennell, H., Kaiser, M.J., Karnad, D. & Milner-Gulland, E.J. (2022) 'A decision support tool for integrated fisheries bycatch management', Reviews in Fish Biology and Fisheries 2022 32:2, 32(2), pp. 441–472.
- Gislason, H., Daan, N., Rice, J.C. & Pope, J.G. (2010) 'Size, growth, temperature and the natural mortality of marine fish', Fish and Fisheries, 11(2), pp. 149–158.
- Glazier, D.S. (2023) 'The relevance of time in biological scaling', Biology, 12p. 1084.
- Goldman, K.J. (2005) Age and growth of elasmobranch fishes. FAO Fisheries Technical Paper, 474.
- Goodwin, N.B., Dulvy, N.K. & Reynolds, J.D. (2002) 'Life-history correlates of the evolution of live bearing in fishes', Philosophical Transactions of the Royal Society of Biological Sciences, 357pp. 259–267.
- Graham, K.J. & Daley, R.K. (2011) 'Distribution, reproduction and population structure of three gulper sharks (Centrophorus, Centrophoridae) in south-east Australian waters', Marine and Freshwater Research, 62(6), pp. 583–595.
- Gravel, S., Bigman, J., Pardo, S., Wong, S. & Dulvy, N. (2024) 'Metabolism, population growth, and the fast-slow life history continuum of marine fishes', Fish and Fisheries, 25pp. 349–361.
- Green, S.J., Brookson, C.B., Hardy, N.A. & Crowder, L.B. (2022) 'Trait-based approaches to global change ecology: moving from description to prediction', Proceedings of the Royal Society B: Biological Sciences, 289(1971), p. 20220071.
- Gulland, J.J.A. (1971) The fish resources of the ocean. J.J.A Gulland (ed.). Surrey, United Kingdom: Fishing News (Books) Ltd.

- Gupta, T., Booth, H., Arlidge, W., Rao, C., Manoharakrishnan, M., Namboothri, N., Shanker, K. & Milner-Gulland, E.J. (2020) 'Mitigation of elasmobranch bycatch in trawlers: A case study in Indian fisheries', Frontiers in Marine Science, 7p. 553356.
- Gutteridge, A.N., Huveneers, C., Marshall, L.J., Tibbetts, I.R., Bennett, M.B., Gutteridge, A.N., Huveneers, C., Marshall, L.J., Tibbetts, I.R. & Bennett, M.B. (2013) 'Life-history traits of a small-bodied coastal shark', Marine and Freshwater Research, 64(1), pp. 54–65.
- Handley, J.M., Pearmain, E.J., Oppel, S., Carneiro, A.P.B., Hazin, C., Phillips, R.A., Ratcliffe, N., Staniland, I.J., Clay, T.A., Hall, J., Scheffer, A., Fedak, M., Boehme, L., Pütz, K., Belchier, M., Boyd, I.L., Trathan, P.N. & Dias, M.P. (2020) 'Evaluating the effectiveness of a large multi-use MPA in protecting Key Biodiversity Areas for marine predators', Diversity and Distributions, 26(6), pp. 715–729.
- Haque, A.B., D'Costa, N.G., Washim, M., Baroi, A.R., Hossain, N., Hafiz, M., Rahman, S. & Biswas, K.F. (2021) 'Fishing and trade of devil rays (Mobula spp.) in the Bay of Bengal, Bangladesh: Insights from fishers' knowledge', Aquatic Conservation: Marine and Freshwater Ecosystems, 31(6), pp. 1392–1409.
- Hara, Y., Yamaguchi, K., Onimaru, K., Kadota, M., Koyanagi, M., Keeley, S.D., Tatsumi, K., Tanaka, K., Motone, F., Kageyama, Y., Nozu, R., Adachi, N., Nishimura, O., Nakagawa, R., Tanegashima, C., Kiyatake, I., Matsumoto, R., Murakumo, K., Nishida, K., et al. (2018) 'Shark genomes provide insights into elasmobranch evolution and the origin of vertebrates', Nature Ecology & Evolution 2018 2:11, 2(11), pp. 1761–1771.
- Harry, A. V., Smart, J.J. & Pardo, S.A. (2022) 'Understanding the Age and Growth of Chondrichthyan Fishes', in Jeffrey C. Carrier, Colin A. Simpfendorfer, Michael R. Heithaus, & Kara E. Yopak (eds.) Biology of Sharks and Their Relatives. Third [Online]. Boca Raton: CRC Press, Taylor & Francis Group. pp. 177–202.
- Harry, A. V., Tobin, A.J., Simpfendorfer, C.A., Welch, D.J., Mapleston, A., White, J., Williams, A.J. & Stapley, J. (2011) 'Evaluating catch and mitigating risk in a multispecies, tropical, inshore shark fishery within the Great Barrier Reef World Heritage Area', Marine and Freshwater Research, 62(6), pp. 710–721.
- Harry, A.V. (2018) 'Evidence for systemic age underestimation in shark and ray ageing studies', Fish and Fisheries, 19(2), pp. 185–200.
- Hays, G.C., Bailey, H., Bograd, S.J., Bowen, W.D., Campagna, C., Carmichael, R.H., Casale, P., Chiaradia, A., Costa, D.P., Cuevas, E., Nico de Bruyn, P.J., Dias, M.P., Duarte, C.M., Dunn, D.C., Dutton, P.H., Esteban, N., Friedlaender, A., Goetz, K.T., Godley, B.J., et al. (2019) 'Translating marine animal tracking data into conservation policy and management', Trends in ecology & evolution, 34(5), pp. 459–473.
- Healy, K., Ezard, T.H.G., Jones, O.R., Salguero-Gómez, R. & Buckley, Y.M. (2019) 'Animal life history is shaped by the pace of life and the distribution of age-specific mortality and reproduction', Nature Ecology & Evolution 2019 3:8, 3(8), pp. 1217–1224.

- Heidrich, K.N., Juan-Jordá, M.J., Murua, H., Thompson, C.D.H., Meeuwig, J.J. & Zeller, D. (2022) 'Assessing progress in data reporting by tuna Regional Fisheries Management Organizations', Fish and Fisheries, 23pp. 1264–1281.
- van Helmond, A.T., Mortensen, L.O., Plet-Hansen, K.S., Ulrich, C., Needle, C.L., Oesterwind, D., Kindt-Larsen, L., Catchpole, T., Mangi, S., Zimmermann, C., Jakob Olesen, H., Bailey, N., Bergsson, H., Dalskov, J., Elson, J., Hosken, M., Peterson, L., McElderry, H., Ruiz, J., et al. (2020) 'Electronic monitoring in fisheries: Lessons from global experiences and future opportunities', Fish and Fisheries, 21pp. 162–189.
- Herrón, P., Castellanos-Galindo, G.A., Stäbler, M., Díaz, J.M. & Wolff, M. (2019) 'Toward ecosystem-based assessment and management of small-scale and multi-gear fisheries: Insights from the tropical eastern Pacific', Frontiers in Marine Science, 6(MAR), p. 435376.
- Heupel, M.R. & Simpfendorfer, C.A. (2010) 'Science or slaughter: Need for lethal sampling of sharks', Conservation Biology, 24(5), pp. 1212–1218.
- Hicks, C.C., Cohen, P.J., Graham, N.A.J., Nash, K.L., Allison, E.H., D'Lima, C., Mills, D.J., Roscher, M., Thilsted, S.H., Thorne-Lyman, A.L. & MacNeil, M.A. (2019) 'Harnessing global fisheries to tackle micronutrient deficiencies', Nature 2019 574:7776, 574(7776), pp. 95–98.
- Hilborn, R., Amoroso, R.O., Anderson, C.M., Baum, J.K., Branch, T.A., Costello, C., De Moor, C.L., Faraj, A., Hively, D., Jensen, O.P., Kurota, H., Little, L.R., Mace, P., McClanahan, T., Melnychuk, M.C., Minto, C., Osio, G.C., Parma, A.M., Pons, M., et al. (2020) 'Effective fisheries management instrumental in improving fish stock status', Proceedings of the National Academy of Sciences of the United States of America, 117(4), pp. 2218–2224.
- Hilborn, R. & Sinclair, A.R.E. (2021) 'Biodiversity protection in the 21st century needs intact habitat and protection from overexploitation whether inside or outside parks', Conservation Letters, 14(4), .
- Hixon, M.A., Johnson, D.W., Sogard, S.M. & BOFFFFs, S.M. (2013) 'Food for thought BOFFFFs: On the importance of conserving old-growth age structure in fishery populations', ICES Journal of Marine Science, 71(8), pp. 2171–2185.
- Hoban, S., Bruford, M.W., Funk, W.C., Galbusera, P., Griffith, M.P., Grueber, C.E., Heuertz, M., Hunter, M.E., Hvilsom, C., Stroil, B.K., Kershaw, F., Khoury, C.K., Laikre, L., Lopes-Fernandes, M., MacDonald, A.J., Mergeay, J., Meek, M., Mittan, C., Mukassabi, T.A., et al. (2021) 'Global commitments to conserving and monitoring genetic diversity are now necessary and feasible', Bioscience, 71(9), p. 964.
- Hobday, A.J., Smith, A.D.M., Stobutzki, I.C., Bulman, C., Daley, R., Dambacher, J.M., Deng, R.A., Dowdney, J., Fuller, M., Furlani, D., Griffiths, S.P., Johnson, D., Kenyon, R., Knuckey, I.A., Ling, S.D., Pitcher, R., Sainsbury, K.J., Sporcic, M., Smith, T., et al. (2011) 'Ecological risk assessment for the effects of fishing', Fisheries Research, 108(2–3), pp. 372–384.

- Horswill, C., Kindsvater, H.K., Juan-Jordá, M.J., Dulvy, N.K., Mangel, M. & Matthiopoulos, J. (2019) 'Global reconstruction of life-history strategies: A case study using tunas', Journal of Applied Ecology, 56(4), pp. 855–865.
 - Hosegood, J., Humble, E., Ogden, R., de Bruyn, M., Creer, S., Stevens, G.M.W., Abudaya, M., Bassos-Hull, K., Bonfil, R., Fernando, D., Foote, A.D., Hipperson, H., Jabado, R.W., Kaden, J., Moazzam, M., Peel, L.R., Pollett, S., Ponzo, A., Poortvliet, M., et al. (2020) 'Phylogenomics and species delimitation for effective conservation of manta and devil rays', Molecular Ecology, 29(24), pp. 4783–4796.
 - Humble, E., Hosegood, J., Carvalho, G., Mark De Bruyn, |, Creer, S., Guy, |, Stevens, M.W., Armstrong, A., Deakos, M., Fernando, D., Froman, N., Peel, L.R., Pollett, | Stephen, Ponzo, A., Stewart, J.D., Wintner, S., Ogden, | Rob & Alexander, A. (2023) 'Comparative population genomics of manta rays has global implications for management', Molecular Ecology, 00pp. 1–14.
 - Hutchings, J.A., Myers, R.A., García, V.B., Lucifora, L.O. & Kuparinen, A. (2012) 'Life-history correlates of extinction risk and recovery potential', Ecological Applications, 22(4), pp. 1061–1067.
 - IOTC (2019) IOTC CIRCULAR 2019-27.
 - Ishihara, H., Mochizuki, T., Homma, K. & Taniuchi, T. (2002) 'Reproductive strategy of the Japanese common skate (spiny rasp skate) Okamejei kenojei'. Elasmobranch Biodiversity, Conservation and Management, Occasional Paper of the IUCN Species Survival Commission
 - IUCN (2024) The IUCN Red List of Threatened Species. [Online]
 - Iwane, M.A., Leong, K.M., Vaughan, M. & Oleson, K.L.L. (2021) 'When a shark is more than a shark: A sociopolitical problem-solving approach to fisher-shark interactions', Frontiers in Conservation Science, 2p. 669105.
 - Jabado, R.W. (2018) 'The fate of the most threatened order of elasmobranchs: Shark-like batoids (Rhinopristiformes) in the Arabian Sea and adjacent waters', Fisheries Research, 204pp. 448–457.
 - Jabado, R.W. & Ebert, D.A. (2015) Sharks of the Arabian Seas: An Identification Guide. Dubai, United Arab Emirates: The International Fund for Animal Welfare (IFAW).
 - Jacobsen, I.P. & Bennett, M.B. (2010) 'Age and growth of Neotrygon picta, Neotrygon annotata and Neotrygon kuhlii from north-east Australia, with notes on their reproductive biology', Journal of Fish Biology, 77(10), pp. 2405–2422.
 - Jacquet, J., Zeller, D. & Pauly, D. (2010) 'Counting fish: A typology for fisheries catch data', Journal of Integrative Environmental Sciences, 7(2), pp. 135–144.
 - Jahnke, R.A. (1996) 'The global ocean flux of particulate organic carbon: Areal distribution and magnitude', Global Biogeochemical Cycles, 10(1), pp. 71–88.

- James, K.C. & Natanson, L.J. (2020) 'Positional and ontogenetic variation in vertebral centra morphology in five batoid species', Marine and Freshwater Research, 72(6), pp. 887–898.
- Jennings, S., Greenstreet, S.P.R. & Reynolds, J.D. (1999) 'Structural change in an exploited fish community: A consequence of differential fishing effects on species with contrasting life histories', Journal of Animal Ecology, 68(3), pp. 617–627.
- Jennings, S., Mélin, F., Blanchard, J.L., Forster, R.M., Dulvy, N.K. & Wilson, R.W. (2008) 'Global-scale predictions of community and ecosystem properties from simple ecological theory', Proceedings of the Royal Society B: Biological Sciences, 275(1641), pp. 1375–1383.
- Jennings, S., Reynolds, J.D. & Mills, S.C. (1998) 'Life history correlates of responses to fisheries exploitation', Proceedings of the Royal Society B: Biological Sciences, 265(1393), p. 333.
- Juan-Jordá, M.J., Mosqueira, I., Cooper, A.B., Freire, J. & Dulvy, N.K. (2011) 'Global population trajectories of tunas and their relatives', Proceedings of the National Academy of Sciences of the United States of America, 108(51), pp. 20650–20655.
- Juan-Jordá, M.J., Mosqueira, I., Freire, J. & Dulvy, N.K. (2013) 'Life in 3-D: Life history strategies in tunas, mackerels and bonitos', Reviews in Fish Biology and Fisheries, 23(2), pp. 135–155.
- Juan-Jordá, M.J., Mosqueira, I., Freire, J. & Dulvy, N.K. (2015) 'Population declines of tuna and relatives depend on their speed of life', Proceedings of the Royal Society B: Biological Sciences, 282(1811), .
- Kashiwagi, T. (2014) Conservation biology and genetics of the largest living rays: manta rays. PhD thesis. [Online]. University of Queensland.
- Kelaher, B.P., Monteforte, K.I., Morris, S.G., Schlacher, T.A., March, D.T., Tucker, J.P. & Butcher, P.A. (2023) 'Drone-based assessment of marine megafauna off wave-exposed sandy beaches', Remote Sensing, 15(16), p. 4018.
- Kelleher, Kieran. (2005) Discards in the world's marine fisheries: an update.
- Kindsvater, H.K., Dulvy, N.K., Horswill, C., Juan-Jordá, M.J., Mangel, M. & Matthiopoulos, J. (2018) 'Overcoming the data crisis in biodiversity conservation'. Trends in Ecology and Evolution 33 (9) p.pp. 676–688.
- Kindsvater, H.K., Juan-Jordá, M.-J., Dulvy, N.K., Horswill, C., Matthiopoulos, J., Mangel, M. & Holly Kindsvater, C.K. (2024) 'Size-dependence of food intake and mortality interact with temperature and seasonality to drive diversity in fish life histories', Evolutionary Applications, 17(2), p. e13646.
- Kindsvater, H.K., Mangel, M., Reynolds, J.D. & Dulvy, N.K. (2016) 'Ten principles from evolutionary ecology essential for effective marine conservation', Ecology and Evolution, 6(7), pp. 2125–2138.

- Kindt-Larsen, L., Kirkegaard, E. & Dalskov, J. (2011) 'Fully documented fishery: A tool to support a catch quota management system', ICES Journal of Marine Science, 68(8), pp. 1606–1610.
- Kiszka, J.J., Heithaus, M.R. & Quod, J.P. (2015) 'Stingrays as possible facilitators for foraging trevallies in a nearshore sandflat', Marine Biodiversity, 45(4), pp. 625–626.
- Kroodsma, D.A., Mayorga, J., Hochberg, T., Miller, N.A., Boerder, K., Ferretti, F., Wilson, A., Bergman, B., White, T.D., Block, B.A., Woods, P., Sullivan, B., Costello, C. & Worm, B. (2018) 'Tracking the global footprint of fisheries', Science, 359(6378), pp. 904–908.
- Kyne, P. & García, E. (2023) Plesiobatis daviesi. [Online] [online]. Available from: https://www.iucnredlist.org/en (Accessed 29 July 2024).
- Kyne, P.M., Jabado, R.W., Rigby, C.L., Dharmadi, Gore, M.A., Pollock, C.M., Herman, K.B., Cheok, J., Ebert, D.A., Simpfendorfer, C.A. & Dulvy, N.K. (2020) 'The thin edge of the wedge: Extremely high extinction risk in wedgefishes and giant guitarfishes', Aquatic Conservation: Marine and Freshwater Ecosystems, 30(7), pp. 1337–1361.
- Lack, M. & Sant, G. (2009) Trends in Global Shark Catch and Recent Developments in Management.
- Lascelles, B., Notarbartolo Di Sciara, G., Agardy, T., Cuttelod, A., Eckert, S., Glowka, L., Hoyt, E., Llewellyn, F., Louzao, M., Ridoux, V. & Tetley, M.J. (2014) 'Migratory marine species: Their status, threats and conservation management needs', Aquatic Conservation: Marine and Freshwater Ecosystems, 24(S2), pp. 111–127.
- Lassauce, H., Dudgeon, C.L., Armstrong, A.J., Wantiez, L. & Carroll, E.L. (2022) 'Evidence of fine-scale genetic structure for reef manta rays Mobula alfredi in New Caledonia', Endangered Species Research, 47pp. 249–264.
- Last, P.R., Weigmann, S. & Naylor, G.J.P. (2023) 'The Indo-Pacific stingray Genus Brevitrygon (Myliobatiformes: Dasyatidae): Clarification of historical names and description of a new species, B. manjajiae sp. nov., from the Western Indian Ocean', Ocean Diversity, 15(1213), .
- Last, P.R., White, W.T., de Carvalho, M.R., Seret, B., Naylor, G.J.P. & Stehmann, M. (2016) Rays of the world. CSIRO Publishing.
- Lawson, J.M., Fordham, S. V., O'Malley, M.P., Davidson, L.N.K., Walls, R.H.L., Heupel, M.R., Stevens, G., Fernando, D., Budziak, A., Simpfendorfer, C.A., Ender, I., Francis, M.P., di Sciara, G.N. & Dulvy, N.K. (2017) 'Sympathy for the devil: A conservation strategy for devil and manta rays', PeerJ, 2017(3), p. e3027.
- Lee, Janette, South, Andy B, Jennings Lee, S., Lee, J, South, A B & Jennings, S. (2010) 'Developing reliable, repeatable, and accessible methods to provide high-resolution estimates of fishing-effort distributions from vessel monitoring system (VMS) data', ICES Journal of Marine Science, 67(6), pp. 1260–1271.

- Lemke, L.R. & Simpfendorfer, C.A. (2023) 'Gillnet size selectivity of shark and ray species from Queensland, Australia', Fisheries Management and Ecology, 30(3), pp. 300–309.
- Lester, N.P., Shuter, B.J. & Abrams, P.A. (2004) 'Interpreting the von Bertalanffy model of somatic growth in fishes: The cost of reproduction', Proceedings of the Royal Society of London. Series B: Biological Sciences, 271(1548), pp. 1625–1631.
- Leurs, G., Verkuil, Y.I., Hijner, N., Saalmann, F., Dos Santos, L., Regalla, A., Ledo Pontes, S., Yang, L., Naylor, G.J.P., Olff, H. & Govers, L.L. (2023) 'Addressing data-deficiency of threatened sharks and rays in a highly dynamic coastal ecosystem using environmental DNA', Ecological Indicators, 154p. 110795.
- Lewis, S.A., Setiasih, N., Dharmadi, F., O'Malley, M.P., Campbell, S.J., Yusuf, M. & Sianipar, A. (2015) 'Assessing Indonesian manta and devil ray populations through historical landings and fishing community interviews', PeerJ PrePrints,
- Lewison, R.L., Crowder, L.B., Read, A.J. & Freeman, S.A. (2004) 'Understanding impacts of fisheries bycatch on marine megafauna', Trends in Ecology & Evolution, 19(11), pp. 598–604.
- Lombardi-Carlson, L.A., Cortés, E., Parsons, G.R. & Manire, C.A. (2003) 'Latitudinal variation in life-history traits of bonnethead sharks, Sphyrna tiburo, (Carcharhiniformes:Sphyrnidae) from the eastern Gulf of Mexico', Marine and Freshwater Research, 54(7), pp. 875–883.
- Di Lorenzo, M., Calò, A., Di Franco, A., Milisenda, G., Aglieri, G., Cattano, C., Milazzo, M. & Guidetti, P. (2022) 'Small-scale fisheries catch more threatened elasmobranchs inside partially protected areas than in unprotected areas', Nature Communications, 13(1), pp. 1–11.
- Lucifora, L.O. & García, V.B. (2004) 'Gastropod predation on egg cases of skates (Chondrichthyes, Rajidae) in the southwestern Atlantic: Quantification and life history implications', Marine Biology, 145(5), pp. 917–922.
- Lucifora, L.O., Scarabotti, P.A. & Barbini, S.A. (2022) 'Predicting and contextualizing sensitivity to overfishing in Neotropical freshwater stingrays (Chondrichthyes: Potamotrygonidae)', Reviews in Fish Biology and Fisheries, 32pp. 669–686.
- Luhring, T.M. & Delong, J.P. (2017) 'Scaling from metabolism to population growth rate to understand how acclimation temperature alters thermal performance', Integrative and Comparative Biology, 57(1), pp. 103–111.
- Lyons, K., Jarvis, E.T., Jorgensen, S.J., Weng, K., O'Sullivan, J., Winkler, C. & Lowe, C.G. (2013) 'The degree and result of gillnet fishery interactions with juvenile white sharks in southern California assessed by fishery-independent and -dependent methods', Fisheries Research, 147pp. 370–380.
- Mariani, S., Fernandez, C., Baillie, C., Magalon, H. & Jaquemet, S. (2021) 'Shark and ray diversity, abundance and temporal variation around an Indian Ocean Island, inferred by eDNA metabarcoding', Conservation Science and Practice, 3(6), p. e407.

- Marshall, A., Barreto, R., Carlson, J., Fernando, D., Fordham, S., Francis, M.P., Herman, K., Jabado, R.W., Liu, K.M., Rigby, C.L. & Romanov, E. (2022) Mobula mobular (amended version of 2020 assessment). [Online] [online]. Available from: https://dx.doi.org/10.2305/IUCN.UK.2022-1.RLTS.T110847130A214381504.en (Accessed 29 November 2023).
- Marshall, A.D. & Bennett, M.B. (2010) 'Reproductive ecology of the reef manta ray Manta alfredi in southern Mozambique', Journal of fish biology, 77(1), pp. 169–190.
- Marshall, D.J. (2021) 'Temperature-mediated variation in selection on offspring size: A multi-cohort field study', Functional Ecology, 35(10), pp. 2219–2228.
- Martell, S. & Froese, R. (2013) 'A simple method for estimating MSY from catch and resilience', Fish and Fisheries, 14(4), pp. 504–514.
- Martins, A.P.B., Heupel, M.R., Chin, A. & Simpfendorfer, C.A. (2018) 'Batoid nurseries: Definition, use and importance'. Marine Ecology Progress Series 595 p.pp. 253–267.
- Mayne, B., Berry, O., Davies, C., Farley, J. & Jarman, S. (2019) 'A genomic predictor of lifespan in vertebrates', Scientific Reports, 9(1), p. 17866.
- McClenachan, L., Cooper, A.B. & Dulvy, N.K. (2016) 'Rethinking trade-driven extinction risk in marine and terrestrial megafauna', Current Biology, 26(12), pp. 1640–1646.
- McEachran, J. & Miyake, T. (1990) Zoogeography and Bathymetry of skates (Chondrichthyes, Rajoidei). H.L. Pratt, S.H. Gruber, & T. Taniuchi (eds.). NOAA Technical Report National Marine Fisheries Service 90.
- McGeady, R., Loca, S.L. & McGonigle, C. (2022) 'Spatio-temporal dynamics of the common skate species complex: Evidence of increasing abundance', Diversity and Distributions, 28(11), pp. 2403–2415.
- McGoodwin, J.R. (2001) 'Understanding the cultures of fishing communities: A key to fisheries management and food security'. Food and Agriculture Organization of the United Nations
- Moazzam, M. (2018) 'Unprecedented decline in the catches of mobulids: an important component of tuna gillnet fisheries of the Northern Arabian Sea'. IOTC-2018-WPEB14-30
- Mollet, H.F., Ezcurra B, J.M., O'sullivan, J.B., Ezcurra, J.M., O'sullivan, J.B., Ezcurra B, J.M. & O'sullivan, J.B. (2002) 'Captive biology of the pelagic stingray, Dasyatis violacea (Bonaparte, 1832)', Marine and Freshwater Research, 53(2), pp. 531–541.
- Moore, A.B. (2023) 'A ray of hope? The re-appearance of Irish Sea skate decades after local extinction', Journal of Fish Biology, 102(6), pp. 1503–1505.
- Moore, A.B.M. (2015) 'A review of sawfishes (Pristidae) in the Arabian region: Diversity, distribution, and functional extinction of large and historically abundant marine

- vertebrates', Aquatic Conservation: Marine and Freshwater Ecosystems, 25(5), pp. 656–677.
- Moore, A.B.M. & Grubbs, R.D. (2019) 'Shark and ray conservation research: Absent where the need is greatest', Aquatic Conservation: Marine and Freshwater Ecosystems, 29(11), pp. 2017–2017.
- Moore, A.B.M., Last, P.R. & Naylor, G.J.P. (2020) 'Hemitrygon yemenensis sp. nov., a new species of stingray (Myliobatoidea: Dasyatidae) from the northwestern Indian Ocean', Zootaxa, 4819(2), pp. 364-374-364-374.
- Moore, A.B.M., Séret, B. & Armstrong, R. (2019) 'Risks to biodiversity and coastal livelihoods from artisanal elasmobranch fisheries in a Least Developed Country: The Gambia (West Africa)', Biodiversity and Conservation, 28(6), pp. 1431–1450.
- Mucientes, G., Vedor, M., Sims, D.W. & Queiroz, N. (2022) 'Unreported discards of internationally protected pelagic sharks in a global fishing hotspot are potentially large', Biological Conservation, 269p. 109534.
- Mukherji, Sushmita, Smart, Jonathan, Baje, Leontine, Chin, Andrew, White, W., Simpfendorfer, Colin A, Mukherji, S, Smart, J, Baje, L, Chin, A & Simpfendorfer, C A (2021) 'Preliminary age and growth estimates of the blue shark (Prionace glauca) from Papua New Guinea', Environmental Biology of Fishes, 104pp. 1163–1176.
- Mull, C., Pacoureau, N., Pardo, S., Saldaña Ruiz, L., Rodriguez, E., Finucci, B., Haack, M., Harry, A., Judah, A., VanderWright, W., Yin, J., Kindsvater, H. & Dulvy, N. (2022) 'Sharkipedia: A curated open-access database of shark and ray life history traits and abundance time-series', Scientific Data., 9(559), .
- Mull, C., Pennell, M., Yopak, K. & Dulvy, N. (2022) 'Maternal investment evolves with larger body size and higher diversification rate in sharks and rays', bioRxiv,
- Mull, C.G., Yopak, K.E. & Dulvy, N.K. (2020) 'Maternal investment, ecological lifestyle, and brain evolution in sharks and rays', The American Naturalist, 195(6), pp. 1056–1069.
- Munch, S.B. & Salinas, S. (2009) 'Latitudinal variation in lifespan within species is explained by the metabolic theory of ecology', PNAS August, 18(33), pp. 13860–13864.
- Murua, H., Griffiths, S.P., Hobday, A.J., Clarke, S.C., Cortés, E., Gilman, E.L., Santiago, J., Arrizabalaga, H., de Bruyn, P., Lopez, J., Aires-da-Silva, A.M. & Restrepo, V. (2021) 'Shark mortality cannot be assessed by fishery overlap alone', Nature, 595pp. E4–E7.
- Musick, J.A. & Bonfil, R. (2005) 'Elasmobranch Fisheries Management Techniques'. FAO Fisheries Technical Paper 474
- Musick, J.A. & Ellis, J.K. (2005) 'Reproductive Evolution of Chondrichthyans', in William C. Hamlett (ed.) Reproductive Biology and Phylogeny of Chondrichthyes. 1st edition [Online]. Boca Raton: CRC press. pp. 45–78.

- Myers, R.A., Bowen, K.G. & Barrowman, N.J. (1999) 'Maximum reproductive rate of fish at low population sizes', Canadian Journal of Fisheries and Aquatic Sciences, 56(12), pp. 2404–2419.
- Myers, Ransom A., Hutchings, J.A. & Barrowman, N.J. (1997) 'Why do fish stocks collapse? The example of cod in Atlantic Canada', Ecological Applications, 7(1), pp. 91–106.
- Myers, R.A. & Mertz, G. (1998) 'The limits of exploitation: A precautionary approach', Ecological Applications, 8(1), pp. S165–S169.
- Myers, Ransom A, Mertz, G. & Fowlow, P.S. (1997) 'Maximum population growth rates and recovery times for Atlantic cod, Gadus morhua', Fishery Bulletin, 95pp. 762–772.
- Myers, R.A. & Worm, B. (2005) 'Extinction, survival or recovery of large predatory fishes', Philosophical transactions of the Royal Society of London. Series B, Biological sciences, 360(1453), pp. 13–20.
- Nagy, Z.T. (2010) 'A hands-on overview of tissue preservation methods for molecular genetic analyses', Organisms Diversity and Evolution, 10(1), pp. 91–105.
- Natanson, L.J., Skomal, G.B., Hoffmann, S.L., Porter, M.E., Goldman, K.J. & Serra, D. (2018) 'Age and growth of sharks: Do vertebral band pairs record age?', Marine and Freshwater Research, 69(9), pp. 1440–1452.
- Navia, A.F., Mejía-Falla, P.A., López-García, J., Giraldo, A. & Cruz-Escalona, V.H. (2017) 'How many trophic roles can elasmobranchs play in a marine tropical network?', Marine and Freshwater Research, 68(7), pp. 1342–1353.
- Naylor, G.J.P., Caira, J.N., Jensen, K., Rosana, K.A.M., White, W.T. & Last, P.R. (2012) 'A DNA sequence—based approach to the identification of shark and ray species and its implications for global elasmobranch diversity and parasitology', Bulletin of the American Museum of Natural History, 367pp. 1–262.
- Neer, J.A. & Thompson, B.A. (2005) 'Life history of the cownose ray, Rhinoptera bonasus, in the northern Gulf of Mexico, with comments on geographic variability in life history traits', Environmental Biology of Fishes, 73(3), pp. 321–331.
- Neuheimer, A.B., Hartvig, M., Heuschele, J., Hylander, S., Kiørboe, T., Olsson, K.H., Sainmont, J. & Andersen, K.H. (2015) 'Adult and offspring size in the ocean over 17 orders of magnitude follows two life history strategies', Ecology, 96(12), pp. 3303–3311.
- Notarbartolo di Sciara, G. (1988) 'Natural history of the rays of the genus Mobula in the Gulf of California', Fishery Bulletin, 86pp. 45–66.
- Notarbartolo di Sciara, G., Stevens, G. & Fernando, D. (2020) 'The giant devil ray Mobula mobular (Bonnaterre, 1788) is not giant, but it is the only spinetail devil ray', Marine Biodiversity Records, 13(1), p. 4.
- Ogle, D.H., Doll, J.C., Wheeler, P. & Dinno, A. (2022) FSA: Fisheries Stock Analysis.

- Oleksyn, S., Tosetto, L., Raoult, V., Joyce, K.E. & Williamson, J.E. (2021) 'Going batty: The challenges and opportunities of using drones to monitor the behaviour and habitat use of rays', Drones 2021, Vol. 5, Page 12, 5(1), p. 12.
- Oliver, S., Braccini, M., Newman, S.J. & Harvey, E.S. (2015) 'Global patterns in the bycatch of sharks and rays', Marine Policy, 54pp. 86–97.
- Olsson, K.H., Gislason, H. & Andersen, K.H. (2016) 'Differences in density-dependence drive dual offspring size strategies in fish', Journal of Theoretical Biology, 407pp. 118–127.
- O'Malley, M. p., Townsend, K.A., Hilton, P., Heinrichs, S. & Stewart, J.D. (2017) 'Characterization of the trade in manta and devil ray gill plates in China and South-east Asia through trader surveys', Aquatic Conservation: Marine and Freshwater Ecosystems, 27(2), pp. 394–413.
- Oosting, T., Hilario, E., Wellenreuther, M. & Ritchie, P.A. (2020) 'DNA degradation in fish: Practical solutions and guidelines to improve DNA preservation for genomic research', Ecology and Evolution, 10(16), pp. 8643–8651.
- Orme, D., Freckleton, R., Thomas, G., Petzoldt, T., Fritz, S., Isaac, N. & Pearse, W. (2018) caper: Comparative analyses of phylogenetics and evolution in R.
- O'Shea, O.R., Thums, M., Van Keulen, M. & Meekan, M. (2011) 'Bioturbation by stingrays at Ningaloo Reef, Western Australia', Marine and Freshwater Research, 63(3), pp. 189–197.
- Ovando, D., Hilborn, R., Monnahan, C., Rudd, M., Sharma, R., Thorson, J.T., Rousseau, Y. & Ye, Y. (2021) 'Improving estimates of the state of global fisheries depends on better data', Fish and Fisheries, 22(6), pp. 1377–1391.
- Pacoureau, N., Carlson, J.K., Kindsvater, H.K., Rigby, C.L., Winker, H., Simpfendorfer, C.A., Charvet, P., Pollom, R.A., Barreto, R., Samantha Sherman, C., Talwar, B.S., Skerritt, D.J., Rashid Sumaila, U., Matsushiba, J.H., VanderWright, W.J., Yan, H.F. & Dulvy, N.K. (2023) 'Conservation successes and challenges for wide-ranging sharks and rays', Proceedings of the National Academy of Sciences of the United States of America, 120(5), p. e2216891120.
- Pacoureau, N., Rigby, C.L., Kyne, P.M., Sherley, R.B., Winker, H., Carlson, J.K., Fordham, S. V., Barreto, R., Fernando, D., Francis, M.P., Jabado, R.W., Herman, K.B., Liu, K.M., Marshall, A.D., Pollom, R.A., Romanov, E. V., Simpfendorfer, C.A., Yin, J.S., Kindsvater, H.K., et al. (2021) 'Half a century of global decline in oceanic sharks and rays', Nature 2021 589:7843, 589(7843), pp. 567–571.
- Paiva, R.B., Neves, A., Sequeira, V. & Gordo, L. (2011) 'Reproductive parameters of the commercially exploited deep-water shark, Deania calcea (Centrophoridae)', Cybium: International Journal of Ichthyology, 2(35), pp. 131–140.
- Pardo, S.A., Cooper, A.B. & Dulvy, N.K. (2013) 'Avoiding fishy growth curves', Methods in Ecology and Evolution, 4(4), pp. 353–360.

- Pardo, S.A., Cooper, A.B., Reynolds, J.D. & Dulvy, N.K. (2018) 'Quantifying the known unknowns: Estimating maximum intrinsic rate of population increase in the face of uncertainty', ICES Journal of Marine Science, 75(3), pp. 953–963.
- Pardo, S.A. & Dulvy, N.K. (2022) 'Body mass, temperature, and depth shape the maximum intrinsic rate of population increase in sharks and rays', Ecology and Evolution, 12p. e9441.
- Pardo, S.A., Kindsvater, H.K., Cuevas-Zimbrón, E., Sosa-Nishizaki, O., Carlos Pérez-Jiménez, J. & Dulvy, N.K. (2016) 'Growth, productivity, and relative extinction risk of a data-sparse devil ray', Scientific Reports, 6p. 33745.
- Pardo, S.A., Kindsvater, H.K., Reynolds, J.D. & Dulvy, N.K. (2016) 'Maximum intrinsic rate of population increase in sharks, rays, and chimaeras: The importance of survival to maturity', Canadian Journal of Fisheries and Aquatic Sciences, 73(8), pp. 1159–1163.
- Pascoe, S., Innes, J., Holland, D., Fina, M., Thebaud, O., Townsend, R., Sanchirico, J., Arnason, R., Wilcox, C. & Hutton, T. (2010) 'Use of incentive-based management systems to limit bycatch and discarding', International Review of Environmental and Resource Economics, 4(2), pp. 123–161.
- Patrick, W.S., Spencer, P., Link, J., Cope, J., Field, J., Kobayashi, D., Lawson, P., Gedamke, T., Cortés, E., Ormseth, O., Bigelow, K. & Overholtz, W. (2010) 'Using productivity and susceptibility indices to assess the vulnerability of United States fish stocks to overfishing', Fishery Bulletin, 108(3), pp. 305–322.
- Pauly, D. (2006) 'Major trends in small-scale marine fisheries, with emphasis on developing countries, and some implications for the social sciences', Maritime Studies, 4(2), pp. 7–22.
- Pauly, D. (1983) 'Some simple methods for the assessment of tropical fish stocks'. Food and Agriculture Organization of the United Nations
- Pauly, D. & Charles, A. (2015) 'Counting on small-scale fisheries', Science, 347(6219), pp. 242–243.
- Pauly, D. & Zeller, D. (2016) 'Catch reconstructions reveal that global marine fisheries catches are higher than reported and declining', Nature Communications 2016 7:1, 7(1), pp. 1–9.
- Pauly, D. & Zeller, D. (2015) Sea Around Us Concepts, Design and Data. [Online]
- Pearce, J., Fraser, M.W., Sequeira, A.M.M. & Kaur, P. (2021) 'State of shark and ray genomics in an era of extinction', Frontiers in Marine Science, 8p. 744986.
- Pechham, S.H., Maldonado Diaz, D., Walli, A., Ruiz, G., Crowder, L.B. & Nichols, W.J. (2007) 'Small-Scale Fisheries Bycatch Jeopardizes Endangered Pacific Loggerhead Turtles', PLOS ONE, 2(10), p. e1041.

- Pendoley, K.L., Schofield, G., Whittock, P.A., Ierodiaconou, D. & Hays, G.C. (2014) 'Protected species use of a coastal marine migratory corridor connecting marine protected areas', Marine Biology, 161(6), pp. 1455–1466.
- Pettersen, A.K., Schuster, L. & Metcalfe, N.B. (2022) 'The evolution of offspring size: A metabolic scaling perspective', Integrative and Comparative Biology, 62(5), pp. 1492–1502.
- Pettersen, A.K., White, C.R., Bryson-Richardson, R.J. & Marshall, D.J. (2020) 'Linking life-history theory and metabolic theory explains the offspring size-temperature relationship', Ecology Letters, 22(3), pp. 518–526.
- Pörtner, H. (2001) 'Climate change and temperature-dependent biogeography: Oxygen limitation of thermal tolerance in animals', Naturwissenschaften, 88(4), pp. 137–146.
- Powter, D.M. & Gladstone, W. (2008) 'Embryonic mortality and predation on egg capsules of the Port Jackson shark Heterodontus portusjacksoni (Meyer)', Journal of Fish Biology, 72(3), pp. 573–584.
- Prasetyo, A.P., McDevitt, A.D., Murray, J.M., Barry, J., Agung, F., Muttaqin, E. & Mariani, S. (2021) 'Shark and ray trade in and out of Indonesia: Addressing knowledge gaps on the path to sustainability', Marine Policy, 133p. 104714.
- Prasetyo, A.P., Murray, J.M., Kurniawan, M.F.A.K., Sales, N.G., McDevitt, A.D. & Mariani, S. (2023) 'Shark-dust: Application of high-throughput DNA sequencing of processing residues for trade monitoring of threatened sharks and rays', Conservation Letters, 16(5), p. e12971.
- Prince, J. (2002) 'Gauntlet fisheries for elasmobranchs—the secret of sustainable shark fisheries', Journal of Northwest Atlantic Fishery Science, 35pp. 407–416.
- Queiroz, N., Humphries, N.E., Couto, A., Vedor, M., da Costa, I., Sequeira, A.M.M., Mucientes, G., Santos, A.M., Abascal, F.J., Abercrombie, D.L., Abrantes, K., Acuña-Marrero, D., Afonso, A.S., Afonso, P., Anders, D., Araujo, G., Arauz, R., Bach, P., Barnett, A., et al. (2019) 'Global spatial risk assessment of sharks under the footprint of fisheries', Nature, 572(7770), pp. 461–466.
- Quetglas, A., Rueda, L., Alvarez-Berastegui, D., Guijarro, B. & Massutí, E. (2016) 'Contrasting Responses to Harvesting and Environmental Drivers of Fast and Slow Life History Species', PLOS ONE, 11(2), p. e0148770.
- R Core Team (2021) R. Vienna, Austria: R Foundation for Statistical Computing.
- Rambahiniarison, J.M., Lamoste, M.J., Rohner, C.A., Murray, R., Snow, S., Labaja, J., Araujo, G. & Ponzo, A. (2018b) 'Life history, growth, and reproductive biology of four mobulid species in the Bohol Sea, Philippines', Frontiers in Marine Science, 5(AUG), p. 269.
- Reeves, R.R., McClellan, K. & Werner, T.B. (2013) 'Marine mammal bycatch in gillnet and other entangling net fisheries, 1990 to 2011', Endangered Species Research, 20(1), pp. 71–97.

- Revell, L.J. (2010) 'Phylogenetic signal and linear regression on species data', Methods in Ecology and Evolution, 1(4), pp. 319–329.
- Reynolds, J.D. (2003) 'Life Histories and Extinction Risk', in T. M Blackburn & K.J. Gaston (eds.) Macroecology. [Online]. Oxford: Blackwell Publishing.
- Reynolds, J.D., Dulvy, N.K., Goodwin, N.B. & Hutchings, J.A. (2005) 'Biology of extinction risk in marine fishes', Proceedings of the Royal Society B: Biological Sciences, 272(1579), pp. 2337–2344.
- Reznick, D.A., Bryga, H. & Endler, J.A. (1990) 'Experimentally induced life-history evolution in a natural population', Nature 1990 346:6282, 346(6282), pp. 357–359.
- Reznick, D.N., Butler IV, M.J., Rodd, F.H. & Ross, P. (1996) 'Life-history evolution in guppies (Poecilia reticulata) 6. Differential mortality as a mechanism for natural selection', Evolution, 50(4), pp. 1651–1660.
- Ricker, W.E. (1975) 'Computation and interpretation of biological statistics of fish populations', Fisheries Research Board of Canada Bulletin, 191pp. 1–382.
- Ricker, W.E. (1979) 'Growth rates and models', Fish Physiology, New York,pp. 673–743.
- Rigby, C., Foley, W. & Simpfendorfer, C. (2018) 'Near-infrared spectroscopy for shark ageing and biology', in JC Carrier, MR Heithaus, & CA Simpendorfer (eds.) Shark research: emerging technologies and applications for the field and laboratory. [Online]. Boca Raton, FL: CRC Press. pp. 201–127.
- Rigby, C. & Simpfendorfer, C.A. (2015) 'Patterns in life history traits of deep-water chondrichthyans', Deep Sea Research Part II: Topical Studies in Oceanography, 115pp. 30–40.
- Rohner, C.A., Flam, A.L., Pierce, S.J. & Marshall, A.D. (2017) 'Steep declines in sightings of manta rays and devilrays (Mobulidae) in southern Mozambique', PeerJ PrePrints,
- Rojas-Bracho, L. & Reeves, R.R. (2013) 'Vaquitas and gillnets: Mexico's ultimate cetacean conservation challenge', Endangered Species Research, 21(1), pp. 77–87.
- RStudio Team (2021) 'RStudio'. RStudio: Integrated Development Environment for R.
- Sadovy, Y. (2005) 'Trouble on the reef: the imperative for managing vulnerable and valuable fisheries', Fish and Fisheries, 6(3), pp. 167–185.
- Sala, E., Mayorga, J., Costello, C., Kroodsma, D., Palomares, M.L.D., Pauly, D., Rashid Sumaila, U. & Zeller, D. (2018) 'The economics of fishing the high seas', Science Advances, 4(6), .
- Salas, S., Chuenpagdee, R., Seijo, J.C. & Charles, A. (2007) 'Challenges in the assessment and management of small-scale fisheries in Latin America and the Caribbean', Fisheries Research, 87(1), pp. 5–16.

- Salvador, J.J., Kyle, S.V.H., Salvador, J.J., Micheli, F., White, T.D., Andrzejaczek, S., Arnoldi, N.S., Block, B., Butner, C., Micheli, F., White, T.D., Kyle, S.V.H., Alfaro-Shigueto, J., Mangel, J.C., Alfaro-Shigueto, J., Baum, J.K., Britten, G.L., Caballero, S., Cardeñosa, D., et al. (2022) 'Emergent research and priorities for shark and ray conservation', Endangered Species Research, 47pp. 171–203.
- Savage, V.M., Gillooly, J.F., Brown, J.H., West, G.B. & Charnov, E.L. (2004) 'Effects of body size and temperature on population growth', The American Naturalist, 163(3), pp. 429–441.
- Schemske, D.W., Mittelbach, G.G., Cornell, H. V., Sobel, J.M. & Roy, K. (2009) 'Is there a latitudinal gradient in the importance of biotic interactions?', Annual Review of Ecology, Evolution, and Systematics, 40(Volume 40, 2009), pp. 245–269.
- Schwartz, F.J. (1983) 'Shark ageing methods and age estimation of Scalloped Hammerhead, Sphyrna lewini, and Dusky, Carcharhinus obscurus, Sharks based on vertebral ring counts'. Proceedings of the International Workshop on Age Determination of Oceanic Pelagic Fisheries. NOAA Technical Report NMFS 8.
- Shahid, U., Moazzam, M., Kiszka, J.J., Fernando, D., Rambahiniarison, J., Harvey, A., Rosady, V. & Cornish, A.S. (2018) 'A regional perspective on the mobulid ray interactions with surface fisheries in the Indian Ocean'. IOTC-2018-WPEB14-29_Rev1
- Shea, B.D., Benson, C.W., de Silva, C., Donovan, D., Romeiro, J., Bond, M.E., Creel, S. & Gallagher, A.J. (2020) 'Effects of exposure to large sharks on the abundance and behavior of mobile prey fishes along a temperate coastal gradient', PLOS ONE, 15(3), p. e0230308.
- Sheaves, M. (2009) 'Consequences of ecological connectivity: The coastal ecosystem mosaic', Marine Ecology Progress Series, 391pp. 107–115.
- Shen, K.L.S., Cheow, J.J., Cheung, A.B., Koh, R.J.R., Mun, A.K.X., Lee, Y.N., Lim, Y.Z., Namatame, M., Peng, E., Vintenbakh, V., Lim, E.X.Y. & Wainwright, B.J. (2024) 'DNA barcoding continues to identify endangered species of shark sold as food in a globally significant shark fin trade hub', PeerJ, 12p. e16647.
- Sherman, C., Digel, E., Zubick, P., Eged, J., Haque, A., Matsushiba, J., Simpfendorfer, C., Sant, G. & Dulvy, N. (2023) 'High overexploitation risk due to management shortfall in highly traded requiem sharks', Conservation Letters, 16p. e12940.
- Sherman, S.C., Heupel, M., Moore, S., Chin, A. & Simpfendorfer, C. (2020) 'When sharks are away, rays will play: Effects of top predator removal in coral reef ecosystems', Marine Ecology Progress Series, 641pp. 145–157.
- Sherman, S.C., Simpfendorfer, C.A., Haque, A.B., Digel, E.D., Zubick, P., Eged, J., Matsushiba, J.H., Sant, G. & Dulvy, N.K. (2023) 'Guitarfishes are plucked: Undermanaged in global fisheries despite declining populations and high volume of unreported international trade', Marine Policy, 155p. 105753.

- Sherman, S.C., Simpfendorfer, C.A., Pacoureau, N., Matsushiba, J.H., Yan, H.F., Walls, R.H.L., Rigby, C.L., VanderWright, W.J., Jabado, R.W., Pollom, R.A., Carlson, J.K., Charvet, P., Bin Ali, A., Fahmi, Cheok, J., Derrick, D.H., Herman, K.B., Finucci, B., Eddy, T.D., et al. (2023) 'Half a century of rising extinction risk of coral reef sharks and rays', Nature Communications, 14(1), pp. 1–11.
- Shiffman, D.S., Ajemian, M.J., Carrier, J.C., Daly-Engel, T.S., Davis, M.M., Dulvy, N.K., Grubbs, R.D., Hinojosa, N.A., Imhoff, J., Kolmann, M.A., Nash, C.S., Paig-Tran, E.W.M., Peele, E.E., Skubel, R.A., Wetherbee, B.M., Whitenack, L.B. & Wyffels, J.T. (2020) 'Trends in chondrichthyan research: An analysis of three decades of conference abstracts', Copeia, 108(1), pp. 122–131.
- Shiffman, D.S., Hammerschlag, N., Shiffman, D. & Abess, J. (2016) 'Shark conservation and management policy: a review and primer for non-specialists', Animal Conservation, 19(5), pp. 401–412.
- Short, R.E., Gelcich, S., Little, D.C., Micheli, F., Allison, E.H., Basurto, X., Belton, B., Brugere, C., Bush, S.R., Cao, L., Crona, B., Cohen, P.J., Defeo, O., Edwards, P., Ferguson, C.E., Franz, N., Golden, C.D., Halpern, B.S., Hazen, L., et al. (2021) 'Harnessing the diversity of small-scale actors is key to the future of aquatic food systems', Nature Food 2021 2:9, 2(9), pp. 733–741.
- Sibly, R.M., Kodric-Brown, A., Luna, S.M. & Brown, J.H. (2018) 'The shark-tuna dichotomy: Why tuna lay tiny eggs but sharks produce large offspring', Royal Society Open Science, 5(8), p. 180453.
- Siegfried, K.I. & Sansó, B. (2006) 'Two Bayesian methods for estimating parameters of the von Bertalanffy growth equation', Special Issue: Age and Growth of Chondrichthyan Fishes: New Methods, Techniques and Analysis, pp. 301–308.
- Simpfendorfer, C. (1999) 'Demographic analysis of the dusky shark fishery in southwestern Australia', American Fisheries Society Symposium, 23pp. 149–160.
- Simpfendorfer, C.A. & Dulvy, N.K. (2017) 'Bright spots of sustainable shark fishing', Current Biology, 27(3), pp. R97–R98.
- Simpfendorfer, C.A., Heithaus, M.R., Heupel, M.R., MacNeil, M.A., Meekan, M., Harvey, E., Sherman, C.S., Currey-Randall, L.M., Goetze, J.S., Kiszka, J.J., Rees, M.J., Speed, C.W., Udyawer, V., Bond, M.E., Flowers, K.I., Clementi, G.M., Valentin-Albanese, J., Adam, M.S., Ali, K., et al. (2023) 'Widespread diversity deficits of coral reef sharks and rays', Science, 380(6650), pp. 1155–1160.
- Simpfendorfer, C.A. & Kyne, P.M. (2009) 'Limited potential to recover from overfishing raises concerns for deep-sea sharks, rays and chimaeras', Environmental Conservation, 36pp. 97–103.
- Smart, J.J., Chin, A., Tobin, A.J. & Simpfendorfer, C.A. (2016) 'Multimodel approaches in shark and ray growth studies: Strengths, weaknesses and the future', Fish and Fisheries, 17(4), pp. 955–971.

- Smart, J.J. & Grammer, G.L. (2021) 'Modernising fish and shark growth curves with Bayesian length-at-age models', PLOS ONE, 16(2), p. e0246734.
- Smith, H., Garcia Lozano, A., Baker, D., Blondin, H., Hamilton, J., Choi, J., Basurto, X. & Silliman, B. (2021) 'Ecology and the science of small-scale fisheries: A synthetic review of research effort for the Anthropocene', Biological Conservation, 254p. 108895.
- Smith, M.W., Then, A.Y., Wor, C., Ralph, G., Pollock, K.H. & Hoenig, J.M. (2012) 'Recommendations for catch-curve analysis', North American Journal of Fisheries Management, 32(5), pp. 956–967.
- Smith, S.E., Au, D.W. & Show, C. (1998) 'Intrinsic rebound potentials of 26 species of Pacific sharks', Marine and Freshwater Research, 49(7), pp. 663–678.
- Smith, W.D., Cailliet, G.M. & Cortés, E. (2008) 'Demography and elasticity of the diamond stingray, Dasyatis dipterura: parameter uncertainty and resilience to fishing pressure', Marine and Freshwater Research, 59(7), p. 575.
- Sparholt, H. (1990) 'Improved estimates of the natural mortality rates of nine commercially important fish species included in the North Sea Multispecies VPA model', Journal du Conseil International pour l' Exploration de la Mer, 46pp. 211–223.
- Stan Development Team (2023) Stan Modeling Language Users Guide and Reference Manual.
- Stawitz, C.C. & Essington, T.E. (2019) 'Somatic growth contributes to population variation in marine fishes', Journal of Animal Ecology, 88(2), pp. 315–329.
- Stein, R.W., Mull, C.G., Kuhn, T.S., Aschliman, N.C., Davidson, L.N.K., Joy, J.B., Smith, G.J., Dulvy, N.K. & Mooers, A.O. (2018) 'Global priorities for conserving the evolutionary history of sharks, rays and chimaeras', Nature Ecology & Evolution 2018 2:2, 2(2), pp. 288–298.
- Stevens, G. (2016) Conservation and population ecology of Manta Rays in the Maldives. PhD thesis. [Online]. University of York.
- Stevens, G., Fernando, D., Dando, M. & Notarbartolo di Sciara, G. (2018) Guide to Manta & Devil Rays of the World. Plymouth: Wild Nature Press.
- Stevens, J.D., Bonfil, R., Dulvy, N.K. & Walker, P.A. (2000) 'The effects of fishing on sharks, rays, and chimaeras (chondrichthyans), and the implications for marine ecosystems', ICES Journal of Marine Science, 57(3), pp. 476–494.
- Sunday, J.M., Bates, A.E. & Dulvy, N.K. (2012) 'Thermal tolerance and the global redistribution of animals', Nature Climate Change, 2pp. 686–690.
- Svarachorn, T., Temple, A.J. & Berggren, P. (2023) 'Marine megafauna catch in Thai small-scale fisheries', Aquatic Conservation: Marine and Freshwater Ecosystems, 33(11), pp. 1245–1262.

- Takeuchi, S. & Tamaki, A. (2014) 'Assessment of benthic disturbance associated with stingray foraging for ghost shrimp by aerial survey over an intertidal sandflat', Continental Shelf Research, 84pp. 139–157.
- Tamburello, N., Côté, I.M. & Dulvy, N.K. (2015) 'Energy and the scaling of animal space use', The American Naturalist, 186(2), pp. 196–211.
- Teh, L.C.L. & Sumaila, U.R. (2013) 'Contribution of marine fisheries to worldwide employment', Fish and Fisheries, 14(1), pp. 77–88.
- Temple, A.J., Berggren, P., Jiddawi, N., Wambiji, N., Poonian, C.N.S., Salmin, Y.N., Berumen, M.L. & Stead, S.M. (2024) 'Linking extinction risk to the economic and nutritional value of sharks in small-scale fisheries', Conservation Biology, e14292pp. 1–14.
- Temple, A.J., Kiszka, J.J., Stead, S.M., Wambiji, N., Brito, A., Poonian, C.N.S., Amir, O.A., Jiddawi, N., Fennessy, S.T., Pérez-Jorge, S. & Berggren, P. (2018) 'Marine megafauna interactions with small-scale fisheries in the southwestern Indian Ocean: A review of status and challenges for research and management'. Reviews in Fish Biology and Fisheries 28 (1) p.pp. 89–115.
- Temple, A.J., Langner, U. & Berumen, M.L. (2024) 'Management and research efforts are failing dolphins, porpoises, and other toothed whales', Scientific Reports 2024 14:1, 14(1), pp. 1–13.
- Temple, A.J., Stead, S.M., Jiddawi, N., Wambiji, N., Dulvy, N.K., Barrowclift, E. & Berggren, P. (2020) 'Life-history, exploitation and extinction risk of the data-poor Baraka's whipray (Maculabatis ambigua) in small-scale tropical fisheries', Journal of Fish Biology, pp. 1–12.
- Temple, A.J., Wambiji, N., Poonian, C.N.S., Jiddawi, N., Stead, S.M., Kiszka, J.J. & Berggren, P. (2019) 'Marine megafauna catch in southwestern Indian Ocean small-scale fisheries from landings data', Biological Conservation, 230pp. 113–121.
- Thorpe, T. & Frierson, D. (2009) 'Bycatch mitigation assessment for sharks caught in coastal anchored gillnets', Fisheries Research, 98(1–3), pp. 102–112.
- Thorson, J.T., Munch, S.B., Cope, J.M. & Gao, J. (2017) 'Predicting life history parameters for all fishes worldwide', Ecological Applications, 27(8), pp. 2262–2276.
- Thorson, J.T. & Simpfendorfer, C.A. (2009) 'Gear selectivity and sample size effects on growth curve selection in shark age and growth studies', Fisheries Research, 98(1–3), pp. 75–84.
- Tickler, D., Meeuwig, J.J., Palomares, M.L., Pauly, D. & Zeller, D. (2018) 'Far from home: Distance patterns of global fishing fleets', Science Advances, 4(8), p. eaar3279.
- Tillett, B.J., Field, I.C., Bradshaw, C.J.A., Johnson, G., Buckworth, R.C., Meekan, M.G. & Ovenden, J.R. (2012) 'Accuracy of species identification by fisheries observers in a north Australian shark fishery', Fisheries Research, 127–128pp. 109–115.

- Tolotti, M.T., Filmalter, J.D., Bach, P., Travassos, P., Seret, B. & Dagorn, L. (2015) 'Banning is not enough: The complexities of oceanic shark management by tuna regional fisheries management organizations', Global Ecology and Conservation, 4pp. 1–7.
- Trinnie, F.I., Walker, T.I., Jones, P.L. & Laurenson, L.J. (2014) 'Regional differences in the reproductive parameters of the sparsely-spotted stingaree, Urolophus paucimaculatus, from south-eastern Australia', Marine and Freshwater Research, 65(11), pp. 943–958.
- Valinassab, T., Daryanabard, R., Dehghani, R. & Pierce, G.J. (2006) 'Abundance of demersal fish resources in the Persian Gulf and Oman Sea', Journal of the Marine Biological Association of the United Kingdom, 86(6), pp. 1455–1462.
- Vaudo, J.J. & Heithaus, M.R. (2011) 'Dietary niche overlap in a nearshore elasmobranch mesopredator community', Marine Ecology Progress Series, 425pp. 247–260.
- Vehtari, A., Gelman, A. & Gabry, J. (2017) 'Practical Bayesian model evaluation using leave-one-out cross-validation and WAIC', Statistics and Computing, 27(5), pp. 1413–1432.
- Venables, S.K., Marshall, A.D., Armstrong, A.J., Tomkins, J.L. & Kennington, W.J. (2020) 'Genome-wide SNPs detect no evidence of genetic population structure for reef manta rays (Mobula alfredi) in southern Mozambique', Heredity, 126(2), pp. 308–319.
- Verity, P.G. & Smetacek, V. (1996) 'Organism life cycles, predation, and the structure of marine pelagic ecosystems', Marine Ecology Progress Series, 130pp. 277–293.
- Vianna, G.M.S., Meekan, M.G., Ruppert, J.L.W., Bornovski, T.H. & Meeuwig, J.J. (2016) 'Indicators of fishing mortality on reef-shark populations in the world's first shark sanctuary: The need for surveillance and enforcement', Coral Reefs, 35(3), pp. 973–977.
- Villavicencio-Garayzar, C.J. (1991) 'Observations on Mobula munkiana (Chondrichthyes: Mobulidae) in the Bajia de la Paz, B.C.S., Mexcio.', Revista Investigaciones Cientifica, 2(2), pp. 78–81.
- Vincent, A.C.J., Sadovy de Mitcheson, Y.J., Fowler, S.L. & Lieberman, S. (2014) 'The role of CITES in the conservation of marine fishes subject to international trade', Fish and Fisheries, 15(4), pp. 563–592.
- Wainwright, B.J., Ip, Y.C.A., Neo, M.L., Chang, J.J.M., Gan, C.Z., Clark-Shen, N., Huang, D. & Rao, M. (2018) 'DNA barcoding of traded shark fins, meat and mobulid gill plates in Singapore uncovers numerous threatened species', Conservation Genetics, 19(6), pp. 1393–1399.
- Waldo, J.L., Altamirano-Nieto, E., Croll, D.A., Palacios, M.D., Lezama-Ochoa, N., Lopez, J., Moreno, G., Rojas-Perea, S. & Cronin, M.R. (2024) 'Bycatch mitigation from the sky: Using helicopter communication for mobulid conservation in tropical tuna fisheries', Frontiers in Marine Science, 11p. 1303324.
- Walker, P.A. & Heessen, H.J.L. (1996) 'Long-term changes in ray populations in the North Sea', ICES Journal of Marine Science, 53(6), pp. 1085–1093.

- Walker, T.I. (2005) 'Reproduction in fisheries science', in W. C. Hamlett (ed.) Reproductive Biology and Phylogeny of Chondrichthyes. [Online]. Enfield, NH: Science Publishers. pp. 81–127.
- Walker, T.I., Taylor, B.L., Hudson, R.J. & Cottier, J.P. (1998) 'The phenomenon of apparent change of growth rate in gummy shark (Mustelus antarcticus) harvested off southern Australia', Fisheries Research, 39(2), pp. 139–163.
- Walls, R.H.L. & Dulvy, N.K. (2020) 'Eliminating the dark matter of data deficiency by predicting the conservation status of Northeast Atlantic and Mediterranean Sea sharks and rays', Biological Conservation, 246p. 108459.
- Ward, P. & Myers, R.A. (2005) 'Shifts in open-ocean fish communities coinciding with the commencement of commercial fishing', Ecology, 86(4), pp. 835–847.
- Ward-Paige, C.A. (2017) 'A global overview of shark sanctuary regulations and their impact on shark fisheries', Marine Policy, 82pp. 87–97.
- Ward-Paige, C.A., Davis, B. & Worm, B. (2013) 'Global population trends and human use patterns of Manta and Mobula rays', PLOS ONE, 8(9), p. e74835.
- Watanabe, M.E. (2017) 'The Nagoya Protocol: Big steps, new problems', BioScience, 67(4), pp. 400–400.
- Watson, F.M., Hepburn, L.J., Cameron, T., Le Quesne, W.J.F. & Codling, E.A. (2019) 'Relative mobility determines the efficacy of MPAs in a two species mixed fishery with conflicting management objectives', Fisheries Research, 219p. 105334.
- Watson, R. & Pauly, D. (2001) 'Systematic distortions in world fisheries catch trends', Nature 2001 414:6863, 414(6863), pp. 534–536.
- Webb, T.J., Dulvy, N.K., Jennings, S. & Polunin, N.V.C. (2011) 'The birds and the seas: Body size reconciles differences in the abundance–occupancy relationship across marine and terrestrial vertebrates', Oikos, 120(4), pp. 537–549.
- Weigmann, S., Gon, O., Leeney, R.H., Barrowclift, E., Berggren, P., Jiddawi, N. & Temple, A.J. (2020) 'Revision of the sixgill sawsharks, genus Pliotrema (Chondrichthyes, Pristiophoriformes), with descriptions of two new species and a redescription of P. Warreni Regan', PLoS ONE, 15(3), p. e0228791.
- White, C.R., Alton, L.A., Bywater, C.L., Lombardi, E.J. & Marshall, D.J. (2022) 'Metabolic scaling is the product of life-history optimization', Science, 377(6608), pp. 834–839.
- White, W.T., Giles, J., Dharmadi & Potter, I.C. (2006) 'Data on the bycatch fishery and reproductive biology of mobulid rays (Myliobatiformes) in Indonesia', Fisheries Research, 82(1–3), pp. 65–73.
- Wilson, K.L., Honsey, A.E., Moe, B. & Venturelli, P. (2018) 'Growing the biphasic framework: Techniques and recommendations for fitting emerging growth models', Methods in Ecology and Evolution, 9(4), pp. 822–833.

- Wong, S., Bigman, J.S. & Dulvy, N.K. (2021) 'The metabolic pace of life histories across fishes', Proceedings of the Royal Society B: Biological Sciences, 288(1953), .
- Worm, B., Davis, B., Kettemer, L., Ward-Paige, C.A., Chapman, D., Heithaus, M.R., Kessel, S.T. & Gruber, S.H. (2013) 'Global catches, exploitation rates, and rebuilding options for sharks', Marine Policy, 40(1), pp. 194–204.
- Worm, B., Orofino, S., Burns, E.S., D'Costa, N.G., Feitosa, L.M., Palomares, M.L.D., Schiller, L. & Bradley, D. (2024) 'Global shark fishing mortality still rising despite widespread regulatory change', Science, 383(6679), pp. 225–230.
- Wourms, J.P. (1977) 'Reproduction and development in chondrichthyan fishes', Integrative and Comparative Biology, 17(2), pp. 379–410.
- Wourms, J.P. (1994) 'The challenges of piscine viviparity', Israel Journal of Ecology and Evolution, 40(3–4), pp. 551–568.
- Wourms, J.P. & Lombardi, J. (1992) 'Reflections on the evolution of piscine viviparity', American Zoologist, 32(2), pp. 276–293.
- Wu, J. (2016) 'Shark fin and mobulid ray gill plate trade in mainland China, Hong Kong and Taiwan'. TRAFFIC
- Yan, H.F., Kyne, P.M., Jabado, R.W., Leeney, R.H., Davidson, L.N.K., Derrick, D.H., Finucci, B., Freckleton, R.P., Fordham, S. V. & Dulvy, N.K. (2021) 'Overfishing and habitat loss drive range contraction of iconic marine fishes to near extinction', Science Advances, 7(7), p. 6026.
- Yulianto, I., Booth, H., Ningtias, P., Kartawijaya, T., Santos, J., Sarmintohadi, Kleinertz, S., Campbell, S.J., Palm, H.W. & Hammer, C. (2018) 'Practical measures for sustainable shark fisheries: Lessons learned from an Indonesian targeted shark fishery', PloS one, 13(11), p. e0206437.
- Zeller, D., Ansell, M., Andreoli, V., Heidrich, K. & Randhawa, H. (2023) 'Trends in Indian Ocean marine fisheries since 1950: Synthesis of reconstructed catch and effort data', Marine and Freshwater Research, 74(4), pp. 301–319.
- Zeller, D., Booth, S. & Pauly, D. (2006) 'Fisheries contributions to the Gross Domestic Product: underestimating small-scale fisheries in the Pacific', Marine Resource Economics, 21(4), pp. 355–374.
- Zeller, D., Harper, S., Zylich, K. & Pauly, D. (2015) 'Synthesis of underreported small-scale fisheries catch in Pacific island waters', Coral Reefs, 34(1), pp. 25–39.
- Zhou, S., Deng, R.A., Dunn, M.R., Hoyle, S.D., Lei, Y. & Williams, A.J. (2021) 'Evaluating methods for estimating shark natural mortality rate and management reference points using life-history parameters', Fish and Fisheries, 23pp. 1264–1281.